Aston University

Some pages of this thesis may have been removed for copyright restrictions.

If you have discovered material in Aston Research Explorer which is unlawful e.g. breaches copyright, (either yours or that of a third party) or any other law, including but not limited to those relating to patent, trademark, confidentiality, data protection, obscenity, defamation, libel, then please read our Takedown policy and contact the service immediately (openaccess@aston.ac.uk)

THE DYNAMICS AND CONTROL OF A

REMOTELY PILOTED PLAN-SYMMETRIC HELICOPTER

ROBERT A DAVIS

A thesis submitted for the degree of Doctor of Philosophy

THE UNIVERSITY OF ASTON IN BIRMINGHAM

October 1986

This copy of the thesis has been supplied on condition that anyone who consults it is understood to recognise that its copyright rests with its author and that no quotation from the thesis and no information derived from it may be published without the author's prior, written consent.

The University of Aston in Birmingham

THE DYNAMICS AND CONTROL OF A REMOTELY PILOTED PLAN-SYMMETRIC HELICOPTER

Robert A Davis

Submitted for the degree of Doctor of Philosophy 1986

SUMMARY

Prior to the development of a production standard control system for ML Aviation's plan-symmetric remotely piloted helicopter system, SPRITE, optimum solutions to technical requirements had yet to be found for some aspects of the work. This thesis describes an industrial project where solutions to real problems have been provided within strict timescale constraints. Use has been made of published material wherever appropriate, new solutions have been contributed where none existed previously.

A lack of clearly defined user requirements from potential Remotely Piloted Air Vehicle (RPAV) system users is identified. A simulation package is defined to enable the RPAV designer to progress with air vehicle and control system design, development and evaluation studies and to assist the user to investigate his applications.

The theoretical basis of this simulation package is developed including Co-axial Contra-rotating Twin Rotor (CCTR), six degrees of freedom motion, fuselage aerodynamics and sensor and control system models. A compatible system of equations is derived for modelling a miniature plan-symmetric helicopter. Rigorous searches revealed a lack of CCTR models, based on closed form expressions to obviate integration along the rotor blade, for stabilisation and navigation studies through simulation. An economic CCTR simulation model is developed and validated by comparison with published work and practical tests. Confusion in published work between attitude and Euler angles is clarified.

The implementation of the theory into a high integrity software package is discussed. Use is made of a novel technique basing the dynamic adjustment of integration time step size on error assessment.

Simulation output for control system stability verification, cross coupling of motion between control channels and air vehicle response to demands and horizontal wind gusts studies are presented.

Contra-Rotating Twin Rotor
Flight Control System
Remotely Piloted Plan-Symmetric Helicopter
Simulation
Six Degrees of Freedom Motion

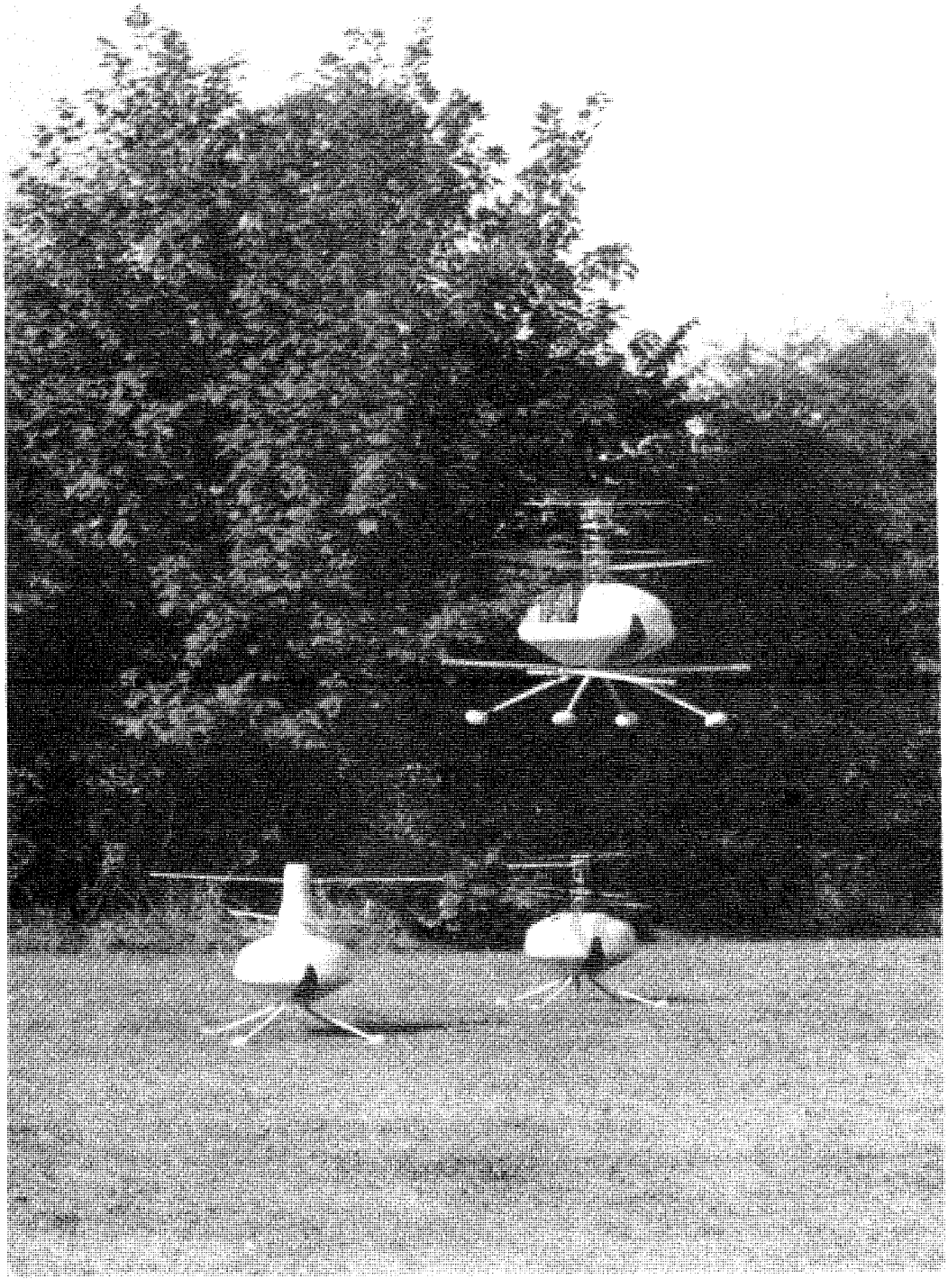

ML Aviation SPRITE Prototype Air Vehicles

ACKNOWLEDGEMENTS

I wish to thank my university supervisors Dr R C Johnson and Dr A J Cochran and my industrial Supervisor Mr C J Roberts for their guidance, support and enthusiasm during this work. I am also grateful to the staff of the IHD Scheme for their assistance.

Many people have been generous with their time and advice which has helped me during this work.

I extend my gratitude to the ML Aviation Publications Department, in particular to Mrs L Warner, for assisting with the production of this thesis.

Financial support for the project was provided by ML Aviation Company Limited and the Science and Engineering Research Council.

CONTENTS

LIST OF TABLES

LIST OF FIGURES

NOTATION

Symbol	Definition	Page
a_0	Blade lift curve slope	145
a_{xB}, a_{yB}, a_{zB}	Blade element acceleration components	278
b	Number of rotor blades	-
c	Blade chord	-
[C]	Direction cosine matrix transform earth to body axes	85
C_I, C_M, C_{M_0}	Matrices in blade flapping equations	283, 284
C_Q	Main rotor torque coefficient	299
C_T	Main rotor thrust coefficient	139
C_X, C_Y, C_Z	Main rotor force coefficients in shaft axes	145
C_{Xsw}, C_{Ysw}, C_{Zsw}	Main rotor force coefficients in shaft-wind axes	142, 143
C_{XF}, C_{YF}, C_{ZF}	Fuselage force functions	175
D_I, D_M, D_{M_0}	Matrices in blade flapping equations	283
d, $\bar{d}$	Drag and normalised drag function acting on blade element	290, 300
E_H	Hysteresis error	189
E_M	Measurement error	189
$F^{(1)}(\psi)$, $F^{(2)}(\psi)$	Integrated blade aerodynamic loads	291
$F_0^{(1)}$, $F_{1c}^{(1)}$, $F_{1s}^{(1)}$, $F_{2c}^{(1)}$, $F_{2s}^{(1)}$, $F_{1c}^{(2)}$, $F_{1s}^{(2)}$	Harmonic components of $F^{(1)}(\psi)$ and $F^{(2)}(\psi)$	143, 144

Symbol	Definition	Page
f_y, f_z	Blade inplane and normal forces	290
f_β, $f_{\dot{\beta}}$, f_λ, $f_{\theta p}$, $f_{\theta tw}$, f_w	Coefficient functions in blade flapping equations	280
g	Gravitational constant	-
g_0	Downwash iteration function	139
g_x, g_y, g_z	Gravitational components	87
G_s	Sensor gain	189
h_j	Downwash iteration increment	139
$\underset{\sim}{i}_B$, $\underset{\sim}{j}_B$, $\underset{\sim}{k}_B$	Unit vectors in blade axes system	270
$\underset{\sim}{i}_s$, $\underset{\sim}{j}_s$, $\underset{\sim}{k}_s$	Unit vectors in shaft axes system	270
I_x, I_y, I_z	Moments of inertia	88
I_{xy}, I_{yz}, I_{zx}	Products of inertia	88
I_β	Blade moment of inertia	279
J	Actuator effective inertia	199
K_β	Blade flapping stiffness - spring constant	279
l, $\bar{l}$	Lift and normalised lift function action on a blade element	290, 300
l_F	Fuselage reference length	175
L, M, N	Overall aircraft rolling, pitching and yawing moments	88
L_F, M_F, N_F	Fuselage aerodynamic rolling, pitching and yawing moments	175
L_s, M_s, N_s	Rotor moments in shaft axes	145, 146
L_R, M_R, N_R	Rotor moments in body axes	146
L_β	Matrix transformation to multi-blade coordinates	283

Symbol	Definition	Page
m	Total mass	87
$m(r_B)$	Blade mass distribution	289
n_β	Blade inertial number (Y/8)	279
p, q, r	Roll, pitch and yaw rates in body axes	90
p_{sw}, q_{sw}, r_{sw}	Roll, pitch and yaw rates of rotor in shaft-wind axes	135
Q_1, Q_2, Q_3	Motion components	189
r_B, $\bar{r}_B$	Blade radial coordinates	277, 289
R	Blade radius	145
s	Rotor solidity = $bc/\pi R$	292
S_p	Fuselage plan area	175
S_s	Fuselage side area	175
S_Q, S	Sensor output	189
S_M, Sc_1, Sc_2	Sensor sensitivities	189
S_β	Stiffness number = $\left(\lambda_\beta^2 - 1\right)/n_\beta$	287
T	Actuator torque	199
$[T1]$	Transformation matrix blade to shaft axes	270
$[T2]$	Transformation matrix body rates to shaft velocity	271
$T2$	Thrust for 2 bladed rotor	160
$[T3]$	Transformation matrix shaft to shaftwind (3x3)	271
$[T4]$	Transformation matrix shaft to shaftwind (2x2)	272

Symbol	Definition	Page
$T4$	Thrust for 4 bladed rotor	160
T_{CCTR}	Thrust for contra-rotating Co-axial twin rotor	160
u, v, w	Velocity components in body axis	89
u_A, v_A, w_A	'Aerodynamic' velocity at cg	133
u_s, v_s, w_s	Velocity components in shaft axes	134
U_T, U_P	Inplane and normal velocities at blade element	290
V_F	Fuselage total velocity	175
V_i	Rotor induced velocity	137
$W_x, W_y, (\bar{W}_x, \bar{W}_y)$	Angular velocities in rotating coordinates (normalised)	277
x, y, z	Body axes	267
x_0, y_0, z_0	Earth axes	267
x_{0L}, y_{0L}, z_{0L}	Local earth axes	268
x_B, y_B, z_B	Blade axes	269
x_{cg}, y_{cg}, z_{cg}	Centre of gravity location with reference to rotor hub	271
x_f, y_f, z_f	Flight path areas	268
x_R	Rotor interaction coefficient	160
x_s, y_s, z_s	Shaft axes (anticlockwise rotor)	268
x_{sc}, y_{sc}, z_{sc}	Shaft axes (clockwise rotor)	268
x_{st}, y_{st}, z_{st}	Stability axes	268
x_{sw}, y_{sw}, z_{sw}	Shaft wind axes	269
X, Y, Z	Overall aircraft force components	87
X_F, Y_F, Z_F	Fuselage aerodynamic forces	175

Symbol	Definition	Page
X_R, Y_R, Z_R	Rotor forces in body reference axes	145
α_F	Fuselage incidence angle	175
α_{ssw}, α_{csw}	Blade incidence functions	144
β, β_i	Blade flapping angles	281
β_0, β_{1c}, β_{1s}	Harmonics of flapping	140, 141
β_{1csw}, β_{1ssw}	Cyclic flapping in shaft-wind axis	294
β_{jc}, β_{js}	Multi-blade coordinates	282
$\underset{\sim}{\beta}_I$, $\underset{\sim}{\beta}_M$	Flapping vectors	283
γ	Actuator motor angle	199
γ	Blade lock number $= \rho c a_0 R^4 / I_\beta (/ I_{\beta_0})$	279
δ	Main rotor blade drag coefficient	290
δ_0	Blade profile drag coefficient	290
δ_2	Blade lift dependent drag coefficient	290
δ_β	Matrix determinant in flapping equations	287
ηa	Rotor loading parameter	138
θ, θ_p	Blade pitch angles	292
θ_0	Main rotor collective pitch at root	135
θ_{1c}, θ_{1s}	Blade cyclic pitch components	135
θ_{1csw}, θ_{1ssw}	Blade cyclic pitch components in shaft wind axes	135
θ_{tw}	Linear blade twist	135

Symbol	Definition	Page
Θ	Inclination attitude angle	79
λ_0, λ_i	Rotor downwash component	137
λ_{1csw}, λ_{1ssw}	Harmonic downwash components in shaft-wind axes	137
λ_β	Rotor blade flap frequency ratio	279
Λ	Total rotor normalised velocity	139
μ_x, μ_y, μ_z	Normalised rotor velocity components	134
$\mu = \mu_{xy}$	Normalised rotor velocity in xy plane	135
ξ	Damping ratio	202
ρ	Air density	145
ρ	Newton iteration constant	139
$\underline{\rho}$	Quaternion of Eulerian parameters	83
τ	Time constant	202
ϕ	Blade angle of attack	290
Φ	Bank attitude angle	79
χ	Wake angle	137
χ, ξ, η, ζ	Euler parameters	83
Ψ, Ψ_i	Blade azimuth angles	270, 289
Ψ_w	Rotor sideslip angle	271
ψ, θ, ϕ	Euler angles	81
Ψ	Azimuth attitude angle	79
Ω	Rotor speed	227
Ω	Intermediate matrix	-

Symbol	Definition	Page
SUBSCRIPTS		
0	Zero	
B	Blade axes	
OL	Local earth axes	
p	Roll channel	
q	Pitch channel	
r	Heading channle	
s	Shaft axes	
sw	Shaftwind axes	
S	Sensor	
z	Altitude channel	
DRESSINGS		
$\dot{}$	Differential with respect to time	
$\bar{}$	Normalised	

ABBREVIATIONS AND ACRONYMS

AHRS	Attitude and Heading Reference System
APRE	Army Personnel Research Establishment
BAe	British Aerospace
CAD	Computer Aided Design
CIS	Cambridge Interactive Systems
FCNS	Flight Control and Navigation System
FR	Flight Refuelling
IAI	Israeli Aircraft Industries
IHD	Interdisciplinary High Degree
ITDU	Infantry Trials and Development Unit
MoD	Ministry of Defence
NACA	National Advisory Committee for Aerodynamics
NASA	National Aeronautics and Space Administration
NK	Not Known
PE	Procurement Executive
plc	public limited company
PSH	Plan Symmetric Helicopter
RAE	Royal Aircraft Establishment
RAM[1]	Radar Absorbing Material
RAM[2]	Random Access Memory
RARDE	Royal Armament Research and Development Establishment
RPAV	Remotely Piloted Air Vehicle
RPH	Remotely Piloted Helicopter
RPV	Remotely Piloted Vehicle
shp	shaft horse power
SRC	Science Research Council
SERC	Science and Engineering Research Council
UK	United Kingdom
US	United States
ZLL	Zero Length Launcher

THESIS PLAN

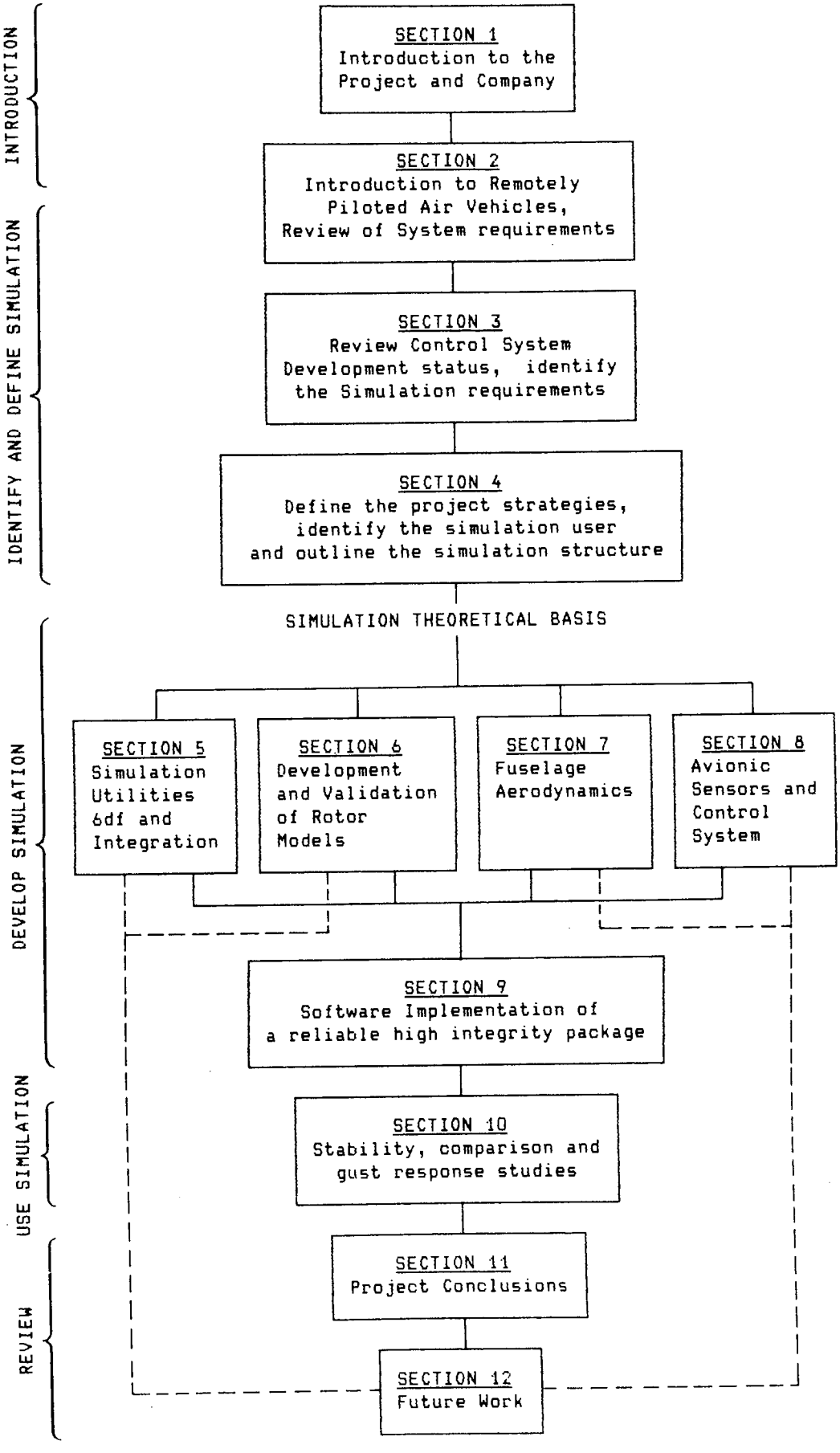
INTRODUCTION
IDENTIFY AND DEFINE SIMULATION
DEVELOP SIMULATION
USE SIMULATION
REVIEW
SECTION 1
Introduction to the Project and Company
SECTION 2
Introduction to Remotely Piloted Air Vehicles, Review of System requirements
SECTION 3
Review Control System Development status, identify the Simulation requirements
SECTION 4
Define the project strategies, identify the simulation user and outline the simulation structure
SIMULATION THEORETICAL BASIS
SECTION 5
Simulation Utilities 6df and Integration
SECTION 6
Development and Validation of Rotor Models
SECTION 7
Fuselage Aerodynamics
SECTION 8
Avionic Sensors and Control System
SECTION 9
Software Implementation of a reliable high integrity package
SECTION 10
Stability, comparison and gust response studies
SECTION 11
Project Conclusions
SECTION 12
Future Work

SECTION 1

INTRODUCTION

1 INTRODUCTION

1.1 Preface

This thesis describes work conducted through the Total Technology higher degree scheme of the University of Aston in Birmingham from October 1983 to September 1986. The work was sponsored by the Science and Engineering Research Council and ML Aviation Company Limited and was conducted substantially at the Company's White Waltham site.

1.2 ML Aviation Company Limited

ML Aviation Company Limited is a wholly owned subsidiary of ML Holdings plc. The present ML Companies originated during the mid 1930's and deal with aerospace support products. Trading names of Wrightson Aircraft Sales and Malcolm and Farquharson were used during the 1930's and 1940's. In 1946 the Companies were renamed ML Aviation (design and development) and ML Engineering (production). Due to considerable expansion an approach was made to the Charterhouse Group for increased funding and the Company went public as ML Holdings in 1958. In 1980 ML Engineering was incorporated into ML Aviation and together they currently contribute at least 60% of the group's turnover. Development activities are presently based at White Waltham and Bristol and production is carried out at several units on the Slough Trading Estate.

Other Companies trading under ML Holdings plc include ML

Engineering (Plymouth) who manufacture railway signalling and data transmission equipment, ML Components who act as agents for MLA's electrical and electronic components and other imported products.

1.3 Company Structure

ML Aviation currently employs approximately 1000 people. A matrix structure is operated with the Engineering Division reporting to the Technical Director and the Production Division reporting to the Production Director. Other departments report either to the Commercial Director or to the Chairman and Managing Director. Resources in the form of either technical expertise or manufacturing and testing facilities report to departmental managers and are drawn upon by each project.

The Quality Assurance Department reports to the board of Directors. Through its quality engineers it is responsible for maintaining the Company quality standards.

A chart showing the matrix organisation of ML Aviation is included in Appendix A.

1.4 Approvals, Facilities and Products

An important measure of the competence of a company operating in the aerospace industry in Britain is the extent of its approval registration. A detailed list is included in Appendix A. The facilities available at ML Aviation are comprehensive,

the major ones are summarised below:

(a) A PRIME 550-II computer with 11 terminals running in BASIC and FORTRAN and 7 CIS CAD workstations.

(b) At White Waltham two separate secure airfield sites contain a Firing Range and a Cartridge Filling area.

(c) A mechanical testing capability which can perform strength, vibration and environmental testing.

(d) An electrical testing facility equipped with a comprehensive range of digital and analog test equipment.

(e) Metallurgy, Plastics and Chemistry Laboratories are equipped to carry out a wide range of testing and treatment services.

The range of ML Aviation's products is diverse and mainly aimed at defence requirements. Weapon carriage and release systems are an important product range. The latest model, the ERU 126 (BRU 36/A American designation) is used on the Harrier GR Mk 5 and the McDonnell Douglas AV8B. Other Aircraft fitted with ML Aviation equipment include the Alpha Jet, Phantom, Jaguar, Buccaneer and Starfighter, Tornado and Lynx.

Aircraft handling systems accomplish a wide range of functions such as allowing one man to manoeuvre a helicopter. Weapon handling systems provide shock isolating storage for missiles. ML Aviation also manufacture aircrew ventilation equipment and a wide variety of test and practice equipment.

During the year ending 31st March 1986 the turnover of ML Holdings plc was £57.2 million which yielded a pre-tax profit of £2.2 million.

1.5 Future Plans

The production and development activities at MLA will continue at their present level, the production capability having been expanded on the basis of recent development work. The Company intends to remain in the defence field but envisaged expansion of the Flight Systems products should encourage interest from civilian customers.

ML Holdings is actively pursuing a policy of acquisition of sound companies complementary to the existing businesses.

1.6 Justification of the Project

Although ML Aviation are committed to support their products, advancing technological and commercial pressures require forward looking companies to continually review their product range. Government policy in the early 1980's has required companies

operating in the defence field to become more competitive to survive.

ML Aviation reviewed it's position and established a Flight Systems Department at the beginning of the decade to pursue new products for both military and commercial customers. One such project is the development of a miniature remotely piloted helicopter.

Moving into a new product area requires the acquisition of development tools, some already available through published work, others requiring tailoring to suit specific Company requirements. This thesis reports on the development of such a tool, drawing on available knowledge wherever possible and contributing new solutions where none existed previously.

1.7 Description of the Project

This research reviews the analytical requirements of the Company in the field of remotely piloted helicopter control system design and development. Pursuing studies by simulation is identified as an optimum method and the pre-requisite simulation package is defined.

This thesis reports how this 'real' industrial requirement is satisfied by the design, development and validation of a simulation package to realise the required capability within strict timescale limits. Considerable effort is directed to

the areas of co-axial rotor, six degrees of freedom motion and control system modelling. However, the entire air vehicle is simulated.

A contribution is made in the areas of the co-axial rotor simulation techniques and confusion arising from publications discussing six degrees of freedom motion is clarified. A novel dynamically adjusted integrating time step size technique permits high accuracy to be achieved for minimum simulation run time. The Company is provided with a custom designed simulation software package within a timescale appropriate to its application to product development.

1.8 Review

This section has described the Company sponsoring this project. The background to the work is given and there is an outline description of the information which the reader can expect from this thesis.

SECTION 2

BACKGROUND

2 BACKGROUND

2.1 Introduction

An introduction, including a brief history, of Remotely Piloted Air Vehicles (RPAVs) is presented in this section. Examples of RPAV applications are discussed and the development status reviewed.

ML Aviation's SPRITE miniature Remotely Piloted Helicopter RPH project is introduced and its history, recent development and future plans are discussed.

Information required by RPAV system designers and potential users is surveyed and deficiencies are identified.

2.2 Remotely Piloted Air Vehicle Systems

In performing a variety of duties including passenger and freight transport, aerial surveys and supporting military roles, aircraft are normally flown by onboard pilots. Under certain situations, however, it may be desirable to use aircraft with the pilot remote from the air vehicle, either based on the ground or in an accompanying aircraft. RPVs have proved useful tools when the risks to the pilot are unacceptably high, in research programmes and on certain military missions (1)(2)(3)(4)(5). The main two categories of this type of vehicle are Remotely Piloted Air Vehicles (RPAVs) which can be controlled in real time from a remote control unit and Drones

which follow a pre-programmed flight plan. Alternative techniques using satellites have been investigated for some applications (6).

Remotely Piloted Air Vehicles can be traced back to before the second world war, examples include the Queen Bee. During the 1940's the Germans had success with the V1 and V2 weapons. RPAVs have been the subject of much interest resulting in the development of many types (7) and speculation as to whether manned flight is 'a thing of the past' (1)(8)(9).

New technology allows compact packaging of sophisticated equipment. The cost, however, of transferring contemporary technology to the battlefield is inevitably high because performance is a dominating factor and quantities in production are not large. However it has been asserted (10)(11) that by using miniature RPAVs cost effectiveness can be demonstrated.

2.3 Miniature Remotely Piloted Air Vehicle Development Status

Many potential capabilities of RPAV systems have been put forward and some of these included in developers and manufacturers literature (11)(12)(13)(14)(15)(16) are presented below:

Military

(a) reconnaissance and surveillance,

(b) target acquisition and fire control,

(c) target designation/illumination,

(d) autonomous ground target attack,

(e) electronic intelligence and countermeasures,

(f) missile detection,

(g) anti-missile defence,

(h) communications,

Civil

(i) aerial photography,

(j) monitoring crop diseases,

(k) crop spraying,

(l) geophysical surveys,

(m) pollution monitoring,

(n) fire control,

(o) security surveillance,

(p) powerline and pipeline inspection,

(q) search for missing persons,

(r) shipping lanes patrol,

(s) fisheries protection,

(t) incident illumination,

(u) emergency communications.

This is not intended as a complete list and in fact it is suggested (17) that the US Government have 170 possible RPAV applications. Until information on the capabilities and economics of RPAV systems becomes generally available many

potential users will not consider them. The question of public acceptability may prove overriding even when compared to cost and technical arguments (18). It is important for companies developing the technology to present the required information in its most favourable, but realistic, form. Serious development of miniature RPAV systems was accelerated in the early 1970s throughout the world, especially in Canada, Europe, Israel and the United States of America (19)(20)(21)(22)(23)(24)(25). In the UK the Royal Aircraft Establishment (RAE), Farnborough (26) initiated this work.

A miniature RPAV system generally comprises the following sub-systems:

(a) payload,
(b) ground control unit,
(c) tracking unit,
(d) two way communications,
(e) air vehicle(s),
(f) ground support equipment,
(g) transport system,
(f) interface to the outside world.

The payload is of primary importance. The concept behind the use of RPAV systems is that the payload is positioned at desired positions in space in order to perform its function. The payload may be a video camera, radio communications relay, target decoy

etc. Initial developments of miniature RPAV systems have been based around a video or camera payload. These capture the imagination of potential users and provide useful information during development flights.

2.4 Miniature Fixed Wing RPAV Development Status

The following paragraphs give a brief summary of development of fixed wing RPAV systems with particular reference to major contributors in UK based systems. UK military RPAV projects are summarised in Table 2.1. European, Israeli and US developments are briefly cited to indicate the status of development world wide.

British Aerospace (BAe) initiated development in the early 1970s with the FLYBAC programme. Funded jointly by BAe and RAE the programme commenced with experimentation using novel sensors and control systems but these proved generally inappropriate (27). RPAV research progressed into the STABILEYE series of air vehicles using more conventional sensors. In parallel a lightweight (less than 5 kg) 'model' category airframe was used during development satisfying less stringent Ordnance Board requirements. A 'pusher' engine/propeller unit left the nose available for payloads.

Launching of the most recent air vehicle, the STABILEYE Mk III, is performed using a modified Short Bros (Belfast) SKEET launcher which accelerates the air vehicle to 55 knots in 4.5 m.

Organisation	Air Vehicle	MoD Project	Activity
APRE Farnborough		SUPERVISOR PHOENIX	Operator simulations and recommendations
British Aerospace	FLYBAC STABILEYE 1 STABILEYE 2 STABILEYE 3		Fixed wing air vehicle development funded jointly by RAE
Ferranti	NK	PHOENIX	Competed for UK prime-contract (lost)
Flight Refuelling	ASAT RAVEN		Target air vehicle Production development of X-RAE 1
Marconi Avionics	WIDEYE ASAT MACHAN NK	SUPERVISOR PHOENIX	Ground station Control system Fixed wing development especially control systems Won UK prime-contract
ML Aviation	SPRITE		Rotary wing air vehicle and RPH System development
RAE Farnborough	X-RAE 1 X-RAE 2	 SUPERVISOR PHOENIX	Air vehicle and ground station development Technical support/ assessment
RARDE Fort Halstead		SUPERVISOR PHOENIX	Requirement evaluation
Smiths Industries			Control system development
Westland Helicopters	MOTE WISP WIDEYE	 SUPERVISOR	Rotary wing air vehicle development

Table 2.1 Summary of Major UK Miniature RPAV Projects 1970-1986

NK = Not Known

Recovery is performed by the use of a parachute. The development programme involved experimenting with different engine and airframe options and landing and recovery techniques, during which, reliance was placed on an RAE designed ground station and tracking system. A variety of payloads have been considered including night IR cameras (28).

The operational team envisaged would consist of 2/3 operators and two 3 ton, or equivalent, vehicles. One would contain up to 3 air vehicles and payloads and would tow the launcher. The second vehicle would contain the ground station and tow a tracking radar. Normally 3 air vehicles would be operated by one ground station although the 4 bit vehicle identification code used would allow up to 15 (Code 0000 is reserved to indicate a system failure). A typical operating configuration would be for the 3 air vehicles to be deployed as follows:

(a) one on the launcher,

(b) one conducting surveillance or other duties,

(c) one inbound for recovery.

Further details can be found in references (15)(27)(29).

Flight Refuelling (FR) have been involved with RPVs, air, land and sea based, for several years. In 1982 they formed an RPV Systems Department. Their interest lies primarily in the sales of RPVs and research and development work is aimed to this end.

They adopt a policy of doing little funded research without the firm promise of production orders.

RAVEN is a 'productionised' version of the X-RAE 1 RPAV developed by RAE Farnborough. It is a small air vehicle with 2.7 m wingspan and a mass of 18 kg. The first FR RAVEN successfully flew in August 1983 and was released (30) in February 1984. The usual payloads carried are a solid state video TV camera or a vertical panoramic camera. A D-band telemetry system allows real time pictures to be returned to the ground station. Launching is via an elastically assisted rail launcher and vehicle recovery by landing on a fuselage skid or flying into previously deployed nets. Onboard sensors and associated processing stabilize the air vehicle. An operational team of six crew and two vehicles is planned. The ground station is being engineered into a container suitable for installation to a range of flat bed vehicles.

One vehicle will carry the ground station and tow a radar and the other will carry associated support equipment and tow a launcher which will house 2 RAVENS in modular form. A contract for 10 units was received from the MoD in December 1983.

An Advanced Subsonic Aerial Target (ASAT) vehicle has been developed as a target for surface to air missiles (31). Powered by an AMES TRS18-075 turbojet engine, ASAT has a take off speed

of 110 knots and a full speed capability of 400 knots. As it is designed as a target, costs are minimised.

Commercial quality die-castings and foam filled skin techniques are used. The air vehicle is being offered as a surveillance and target acquisition RPAV with a selection of payloads. The payload capability is 15 kg. A Marconi Avionics control system stabilizes the air vehicle and a radar tracking navigation system similar to that used on RAVEN is under development. Launching is currently via a circular runway called a 'Carousel' where the air vehicle is tethered to a central pylon and released when it is airborne. A 'Zero Length Launcher' (ZLL) using rocket boosters is under development. Recovery is by a parachute with ASAT landing on a replaceable crushable nose section. Further details can be found in references (14)(32).

FR also carry out conversions on full scale aircraft allowing them to be remotely controlled. These aircraft are expensive and larger than the miniature RPAV's which are the subject of this document.

Ferranti entered RPAV development recently in a competitive situation seeking to obtain the current UK MoD RPAV PHOENIX Contract. They were unsuccessful and have not published in this field.

Marconi Avionics develop control systems and optical sensors for many civil and military applications including RPAV systems. They collaborated with Westland Helicopters on the SUPERVISOR project in the mid 1970's. Marconi Avionics assert (33) that the ground station is the most vulnerable part of any RPAV system and concentrate their effort to protect it. Using techniques such as highly directional transmitting and receiving antennae, minimum communications from the ground station and low mark/space ratio transmissions reduces the possibility of detection.

During the late 1970's and early 1980's Marconi Avionics MACHAN miniature RPAV was used to develop and gain experience in the use of microprocessors in the control system. The knowledge is commercially useful and hence not published in detail although general progress reports (34)(35) have been made available.

Based on this experience, now renamed GEC Avionics having been taken over, they competed for and won the contract for the UK Government PHOENIX RPV system, in competition with Ferranti. The contract, worth £80 million, was awarded in February 1985 for delivery in the early 1990's (36). Although engineering details are not made available of this MoD classified project progress reports have been published showing that the development system is now flying (37).

RPAV research work at RAE has been aimed towards demonstrating

technology and to the development of an air vehicle as a suitable platform for payload development and assessment (21)(26)(38). RAE supported BAe's FLYBAC and STABILEYE programmes and developed a ground control and display station (39) and their own X-RAE 1 and X-RAE 2 air vehicles. The rights for X-RAE 1 have been sold to Flight Refuelling as the basis of RAVEN. X-RAE 2 is a linear scaled up version of X-RAE 1 having a wing span of 3.4 m and an all up mass of 45 kg. Recent work has been carried out in conjunction with GEC (Marconi) Avionics on the MACHAN programme.

RAE have developed a telemetry command system (40) for RPAV use and this has been adopted by the majority of UK RPAV projects whilst they are in the development stage.

Within the UK other companies are experimenting with small RPAV systems including Thorn EMI who are developing a 'low cost' lightweight battery powered RPAV (41) and Vinten who are developing their Autogyro for military applications in both manned and unmanned forms (42)(43)(44).

In Europe VFW a wholly owned subsidiary of MBB have been developing TUCAN and K20, both 100 kg RPVs, which have over 3 hours endurance capabilities (45). Some funding from the German Ministry of Defence and the Federal German Defence Technology and Procurement Agency has been received since 1979 to support these programmes.

Canadair, in conjunction with Dornier Gmbh, have developed a fixed wing RPAV system CL289 designed as a Reconnaissance, Surveillance and Target Acquisition System (46). The CL289 is a high speed air vehicle which is designed to reach the target area as quickly as possible.

Launch is rocket assisted from a rail launcher and recovery via a two stage parachute. The CL289 System is intermediate between the miniature and large RPAVs.

A simple miniature RPAV has been developed by British Columbia Research (Vancouver) for use by Resource Management staff (47)(48)(49).

The SKYEYE development programme initiated in 1972 by Development Sciences Inc (USA) has produced four generations of air vehicles (50). Over 300 flights have been conducted and payloads have been carried internally and externally. The air vehicle has a wingspan of 5.36 m and a gross mass of 200 kg. Due to the success of the project the SKYEYE was selected as a basis for AQUILA (25)(51) the RPAV system for the US Army. Payloads used include a real time video system and a 35 mm camera.

A programme has been carried out at the Airforce Flight Dynamics Laboratory (AFFDL) to develop low cost RPAVs (52). Work was initiated in 1971 and development of several air vehicles has

been carried out. In the mini RPAV category is the XBQM-106 with launch masses of between 50 to 105 kg. Techniques such as the use of foamed plastics have aided lightweight and low cost manufacturing.

Israel Aircraft Industries (IAI) developed the SCOUT mini RPAV system to satisfy operational 'real time' requirements. The system is outlined in refs (53)(54) and (16). The importance of high reliability, due to the high costs of payloads carried, is stressed. It has been in active service for some time and development is continuing. An operational crew consists of 8 personnel and four vehicles. The hardware comprises 4-6 air vehicles, 1 ground station, 1 launcher, and 1 recovery mechanism.

A system similar to SCOUT has been developed by Tadiran Israel Electronics Industries Ltd. Named Mastiff this mini RPV has been purchased by the US Marine Corps in its Mk 3 form (55).

Other developments have been reported in reviews e.g. (56), books e.g. (57) and conference proceedings e.g. (58) have been published listing many RPAV variants. Intermediate size RPAVs outside the scope of this document have included the AERODYNE (59) Hawker Siddeley Dynamics/Dornier Gmbh, and SKYSPY (60) Short Bros Belfast.

Generally whilst the existence of RPAV systems is publicised in

an attempt to attract potential customers, little is published pertaining to engineering detail as this is usually commercially sensitive information. It must be acknowledged that despite the extensive publicity given to RPAV development in the middle 1970's e.g. (61) there is little evidence available ten years later to show that significant advances have been made.

Speculation for the future continues with proposals publicised for future projects such as the Scicon SOARFLY (62) which is expected to be produced by the year 2000.

2.5 The Remotely Piloted Helicopter

Remotely Piloted Helicopters (RPHs) have been in existence for three decades varying in size from models to full scale aircraft. An early example is the Gyrodyne Co QH-50D for which contracts were placed in 1958. It was an insect like device supported by a pair of 20ft co-axial rotors driven by a 365 shp Boeing Turboshaft engine. Since that time interest has been shown in several other RPH systems (63). Rotary wing tethered platforms have been developed for reconnaissance and other purposes such as the Dornier KIEBITZ. Currently available full size RPHs include a range from HYNES Aviation (64).

Early work on RPAV systems was carried out by RAE Farnborough (26)(38)(63). A miniature helicopter was also used in research in Germany (19). In both cases a model was used to take

advantage of both low cost technology and readily available hardware.

In the late 1960's Westland Helicopters carried out studies to consider replacements for manned surveillance helicopters. The Head of Experimental Projects, Mr R G Austin, considered:

(a) a means of reducing the vulnerability of reconnaissance aircraft over the battlefield,

(b) alternative methods of obtaining accurate up-to-date battlefield information.

Solutions considered were:

(a) high speed low altitude fixed wing aircraft,

(b) camouflaged balloons,

(c) various types of rotorcraft,

(d) shell launched parachuted systems.

It soon became apparent that the man-carrying aircraft would always be detectable and vulnerable, due, largely to the presence and support requirements of its human payload (65). An RPAV system became the favoured option and the RPH offered advantages of small size, and required little take off and recovery support equipment. In contrast fixed wing vehicles require cumbersome launchers and recovery systems such as rail launchers and nets retarders e.g. (66)(67).

The Plan-Symmetric Helicopter (PSH) is symmetrical about the rotor axis using two contra-rotating rotors. It has several potential advantages over the conventional helicopter layout (68) including:

(a) compact size,

(b) no aerodynamically preferred direction of flight,

(c) minimum of cross coupling between axes,

(d) optimum configuration for minimum radar signature from all directions.

This configuration was selected for further development.

Following the decision to opt for a PSH air vehicle doubt was cast by some parties as to its controllability. To demonstrate the controllability of a RPH Westlands Helicopters built and tested MOTE (69). This used model aeroplane engines and a model aeroplane radio control system. The results of the tests proved conclusively that stable flight and a good heading hold capability was possible.

Following the successful trials using MOTE, Westland Helicopters designed WISP (70)(71) a larger air vehicle. WISP used a similar rotor system to MOTE but was powered by two larger engines via centrifugal clutches and a belt drive. Designed to fulfil an 'over the hill' capability WISP carried a daylight TV. It had no tracking facility and was flown visually

by a pilot from the ground.

WISP suffered from engineering problems and development was hampered by interference from the motor ignition system. Nevertheless 4 WISP air vehicles were manufactured and several successful flights were carried out. Considerable interest was shown in an RPAV system based on WISP from Japan, the Middle East and USA.

At that time, in the mid 1970's more stringent army requirements became known. Long range guns and missile systems were being ordered with no means of sighting over their full range (17) (72). The solution was thought to lie in a longer range and more sophisticated RPAV. With limited resources available the decision was made to terminate WISP development in favour of the larger WIDEYE (12).

Developed jointly by Marconi Avionics and Westland Helicopters WIDEYE used a similar plan-symmetric configuration to MOTE and WISP. It was designed as the air vehicle for the Army RPAV system SUPERVISOR to carry payloads of 15 kg over a 50 km range for sorties in excess of 2 hours. A low radar signature was sought and the body was fitted with a retractable undercarriage and coated with Radar Absorbing Material (RAM). The complexity of the SUPERVISOR programme demanded increasingly high levels of resources and in 1979 the contract was terminated by the Treasury as part of a general cutback.

Westland Helicopters broke away from Marconi Avionics and continued development supported by RAE until,in 1981, the resources were diverted to other company projects.

In competition with the Westlands development Canadair have been developing a small RPH air vehicle with contra-rotating rotors, the CL227 (73). It was designed to a similar requirement that of operating over a 50km range to perform surveillance and target acquisition roles. Testing using tethered air vehicles has been carried out and free flights totalling 100 minutes had been performed by 1982. However, since the early publications little evidence of successful progress has been found, although references appear in recent articles (9).

2.6 ML Aviation SPRITE

Following the decision at Westland Helicopters to withdraw from RPAV development Mr Austin moved to ML Aviation where he set up a Flight Systems Department. ML Aviation soon became convinced of the potential advantages of an RPH system and in 1981 development of a second generation miniature PSH, SPRITE (13) (74), similar in concept to Westland Helicopter's WISP, was started. Designed as a low cost system, SPRITE was successfully flown in 1983. It is envisaged that it will be operated by a crew of two using a Landrover or similar vehicle. A range of payloads is under consideration, the initial one being a real time video system.

In 1981 ML Aviation submitted a proposal for the PHOENIX project but it was not accepted by the MoD. This was probably due to the MoD policy decision to opt for fixed wing air vehicles at a time when RPH development was not considered sufficiently mature (17). Nevertheless studies carried out into the human interface with RPAV systems show that a RPH vehicle is preferred (75).

The major reasons being that:

(a) The air vehicle can be positioned in sheltered locations and return continuous data from a hover position when sustained observation is required. In contrast a fixed wing air vehicle would have to maintain a sensibly circular loiter around the observation area. This would return rotating images and may cause the air vehicle to overfly a hostile area thus reducing the probability of it remaining undetected.

(b) The PSH air vehicle is small and compact which makes transportation easy and its vertical take off and landing capabilities mean that a minimum of support equipment and deployment space is required.

In view of these advantages RPH development is continuing at ML Aviation.

Following the first flights using the experimental air vehicle three further air vehicles have been built. They are dedicated to the following tasks:

(a) ground endurance testing,

(b) continued development,

(c) flight demonstrations.

Endurance ground testing using air vehicle 01 is being used to improve component and sub-assembly reliability and to verify the life of components previously predicted through fatigue analysis. Air vehicles 02 and 03 are currently used to evaluate experimental sensors and sub-systems and to provide pilot flight training including demonstrations to customers.

In parallel with this experimental programme five further air vehicles are under manufacture for further development, performance trials and for customer evaluation. Included in the latter category is weapon evaluation by foreign countries. The development programme is scheduled to be completed by the year 1987 when, subject to customer orders, tooling will begin for full scale production.

2.7 User Performance Requirements

Much has been said regarding the operational requirements of RPAV systems by many people e.g. (76)(77) including the Army (78), Navy (79) and Air Force (80). However with changing

environments and new technologies, requirements soon date. Inevitably, funding for research and development activities is most readily available for projects aimed to satisfy military requirements with the consequence that military requirements are dominant. All aspects (81) of an RPAV system have to be developed to an acceptable stage before a viable RPAV system is suitable for a user. Many alternative techniques of employing RPAV systems such as 'A Philosophy for the Tactical use of RPH's on the Battlefield' (82) have been put forward. The scope of this document however is restricted to the performance of the miniature RPAV control system and those aspects of the control system which affect the user/system interface.

Constraints will be particular to the payload (and its intended use) so it is important that the constraints are defined prior to the RPAV system being designed.

UK Military RPAV requirements are assessed by the Royal Armament Research and Development Establishment (RARDE), Fort Halstead, using a wide range of techniques (83)(84) and comparisons between expendable and recoverable air vehicles have been made (85). They have appeared as the basis of project MRUASTAS (Medium Range Unmanned Airborne Surveillance and Target Acquisitions System) and later SUPERVISOR.

The current Military requirement is Project PHOENIX (86). Information relating to PHOENIX is subject to the Official

Secrets Act 1939, but ML Aviation have been privileged to have discussions regarding the project with RARDE (17). However, this information is classified and may not be published.

Further data has been collected from the Infantry Trials and Development Unit (ITDU) Warminster (87). They have identified a major lack of quantitative data being available for the potential RPAV system user. They argue that qualitative data and general performance predictions from manufacturers are prevalent but techniques such as simulation, where specific tasks could be modelled are not available to them. Infantry and other units who have not been identified as potential users by MoD studies lack the capability to assess potential RPAV applications which they have identified. A commercial organisation providing this service may generate customer interest in these new areas.

2.8 Review

An introduction to remotely piloted air vehicle systems and their history has been given in this section. Their development is discussed and suggested uses of RPAV systems are presented. The remotely piloted helicopter is introduced and the background to the ML Aviation SPRITE project presented. Finally the lack of specified requirements is blamed on the dearth of RPAV performance data available to enable potential users to evaluate their proposed applications.

SECTION 3

IDENTIFYING THE SIMULATION

3 IDENTIFYING THE SIMULATION

3.1 Introduction

This section of the thesis describes the research which resulted in the identification of the requirement for a detailed air vehicle simulation model for a variety of evaluation tasks.

A general review of air vehicle control systems is given together with a summary of control systems specifically for miniature RPAV applications. Following an introduction to helicopter control systems the requirements of SPRITE are discussed. The status of prototype control systems for experimental air vehicles is summarised and the development aims are identified.

In order to achieve these aims certain development aspects have to be pursued, the tools and their required capabilities are discussed and a simulation model is identified in a form which will assist the RPAV designers. Example applications of simulation are introduced for discussion later in the thesis.

Strategies adopted when designing the simulation model to satisfy the requirements stated here are the subject of Section 4 of the thesis. The theoretical development of the model is contained in sections 5 to 8 inclusive and the computer implementation is discussed in Section 9. The degree of success achieved in meeting the requirements stated in this section is

the main measure of the success and value of this project to the Company and is reviewed in Section 11.

3.2 Project Identification

During mid 1983 when the Remotely Piloted Helicopter System (SPRITE) was under development optimum solutions to technical requirements had yet to be found for some aspects of the work. Amongst these were requirements for the control system combining stabilisation and navigation functions. It was desirable that use be made of novel technology and the latest user requirements so that new compromises could be drawn between performance, costs, mass and size.

The original aim of the project was stated in reference (88) as 'to make recommendations to assist with the development of an optimum control system in terms of performance, cost, mass, and size constraints to satisfy specific customer requirements'. It was asserted that a means of evaluating and comparing sensors and processing both by ML Aviation and the Aerospace Industry at large was required so that improvements could be compared to the current status of control systems. A longer term SPRITE project aim was to identify equipment to satisfy the needs of future production units taking into account new sensors which are being developed both outside and more specifically within ML Aviation.

In order to satisfy the SPRITE project requirements the following pre-requisite tasks were identified:

(a) identify a means of evaluating and comparing control systems and sensors,

(b) review mini RPAV control systems,

(c) review stand alone mini RPAV control systems available for purchase,

(d) review available sensors,

(e) review sensors under development.

Unless ML Aviation possess, or at the very least have the use of, a reliable and dependable means of comparing different sensors and processing techniques they will have no satisfactory method of evaluating and comparing alternative design options for the particular SPRITE applications. Task (a) is singularly important for the design and development of an optimum standard control system. This tool would provide the system designer with an understanding of how individual elements within the control system contribute to, and eventually limit, the performance of a control system.

Moreover, if the Company had to rely on data and design guidance supplied by sensor and control system manufacturers they would be extremely vulnerable to unscrupulous third party organisations. It would be an onerous task to select from

alternative sensors with no means of technical evaluation as this would amount to little more than guesswork.

Through rigorous reviews of literature and through discussions with RPAV developers and national bodies providing development financial support, such as the RAE, it was concluded that a means of analysing control systems for remotely piloted helicopters was not readily available. The Company has proceeded using simplified single axis linear transfer function stability analyses to the flight control system. These techniques relied on three main assumptions:

(a) that the system was linear,

(b) that there was no cross coupling between channels and axes,

(c) that theoretically derived rotor transfer functions based on four bladed rotor theory were invariant over small velocity ranges.

Due to constraints on resources it was not possible for the Company to develop the necessary expertise to evaluate in greater depth the stabilisation or navigation functions of the control system.

In view of these circumstances the aims of the IHD project were clearly identified as:

(a) to briefly survey existing mini RPAV control systems and sensors,

(b) to develop a means of evaluating sensor and control system variants.

The survey task was carried out in advance of the more important evaluation model development for several reasons:

(a) to provide data on competitive organisations,

(b) to provide data on current and new sensors and control systems,

(c) to ensure that the evaluation tool could be developed appropriate to the available input data and required output data,

(d) to provide useful background knowledge both to the SPRITE project team and to the author.

A review of mini RPAV control systems comparing the prototype SPRITE unit with other development RPAVs would ensure that any outstanding sensors used by competitive organisations would not be overlooked by ML Aviation. However, account would have to be taken of the differing air vehicle configurations, especially when comparing control systems for fixed and rotary wing air vehicles.

An important parallel activity is to review the flight control system packages that are available. Some companies, e.g. GEC

(Marconi) Avionics, sell stand alone control systems designed as part of development programmes such as MoD funded missile research.

3.3 Review Technique - Sensors, Control Systems and User Requirements

The research was initiated by reviewing published literature pertaining to control systems. Much of the published literature concerning miniature RPAV development tends to be of a generalised nature. The main reason for this is that RPAV systems are current and future commercial products and are as such subject to normal 'Commercial in Confidence' policy. The general nature of papers presented in journals and conferences e.g. (89)(90) suggests that they are being used as ways of generating publicity in an attempt to attract interest from customers.

In addition to reviewing available literature, privileged discussions with organisations involved in RPAV development were held, where detailed information was more readily presented. Visits were restricted to organisations within the UK for logistic and cost reasons however overseas developers were approached when they visited the UK for conferences etc e.g. (48). The review of existing development is reported in Sections 3.4 to 3.6.

User requirements within the UK were investigated using a similar technique of reviewing published data and organising meetings and discussions with interested parties. It soon became apparent that whilst many organisations found the idea of RPAV systems attractive, they lacked information pertaining to RPAV system performances or costs. This lack of information, or realistic estimates, restricted users from deciding on their requirements from an educated position. All they have available are generalisations, which, whilst they give guidance, do not suffice when detailed applications are under consideration. This is one area a detailed simulation should address.

When identifying sensors for consideration for alternative sensor packages the original intention was to investigate:

(a) available sensors,

(b) sensors under development within the industry in general,

(c) sensors under development within ML Aviation.

A literature search seeking to identify sensors within the scope of (b) above was initiated e.g. (91). In parallel over 150 sensor manufacturers and distributors world wide were located, by the aid of trade directories e.g. (92) and from other sources such as recommendations, and asked to provide data within broad guidelines of sensors which they could supply.

One lesson which was soon learnt by comparing the literature with available hardware was that novel sensors which were either the subject of articles or patents may take years to, or may in fact never, be produced in sufficient numbers to be considered economic for RPAV applications. One example of such a development is a technique patented by Bendix in 1948 (93) for a means of determining air speed by charging the air and measuring the time taken for it to travel between two electrodes. An article appeared (94) in 1983 describing a similar technique but there is still no indication that the sensor will become available. As SPRITE development is restricted in timescale it is considered important to give priority to available sensors and then to sensors under development within ML Aviation where more accurate status reports may be available. However, novel development in industry at large should not be ignored.

3.4 Introduction to Control Systems

A control system consists of the following sub-systems:

(a) motion sensors,) Flight Control System
(b) actuators,)
(c) stability processing,) Control Laws
(d) command processing and mixing,)
(e) command and display unit,
(f) telemetry link (specific to RPVs).

The telemetry link is likely to be influenced by specific user requirements and may therefore, vary greatly depending on the degree of security required. For this reason the telemetry link will not be considered here. During later developments telemetry system constraints imposed on the operations of RPAV systems will need to be borne in mind. The limited data rates of commonly encountered hardware and the desirability of maintaining radio silence during certain periods of operation, are two examples. These constraints may affect updating procedures or general operating philosophies.

The command and display unit is also highly dependant on other aspects of the RPAV systems such as control modes desired and motion sensors employed. The interface between the operator and control station has been extensively studied by APRE (75) and the interface between the control stations and the users existing communication network will be specific to each requirement. Consequently, attention turns to the flight control and navigation systems in particular to the motion sensors.

The functions of a control system are twofold. It has to provide the air vehicle with:

(a) short term stability

and

(b) long term navigation.

The sensors employed in such systems may be common or specific to each sub-system. In general, if high accuracy is required, integration of long term navigation data from the stabilisation system sensors will not suffice without periodic updating. To provide airborne vehicles with a means of stabilisation and navigation the usual starting point is a device to detect body motion. Both angular and linear accelerations need to be integrated with respect to a Newtonian reference frame (95). Early systems maintained such a reference through the use of conventional gimballed platforms. Mounted on these stabilised platforms were gyroscopes and accelerometers. Many high performance systems of this type have been developed between 1950-1970.

A 'strapdown' system (96)(97) can replace a gimballed platform. The instruments are mounted directly to the air vehicle. The inertial reference frame is established by the use of computed mathematical transformations. Potential advantages of the strapdown technique have been recognised and debated over many years (97). These include:

(a) lower cost,

(b) reduced mass,

(c) lower power consumption,

(d) increased reliability,

(e) greater ease of manufacture and maintenance.

With the great advances in computerised techniques and hardware miniaturisation it became practical to realise these advantages in the mid 1960's. Honeywell used a strapdown system for the PRIME re-entry vehicle in 1966 and in 1969 a strapdown system received man-rated operational status for the Apollo abort guidance system. Much work has been carried out in this field as is testified by Garg's 'Strapdown Navigation Technology: A Literature Survey' (98) which provides a further 328 references. To complement 'on-board' systems there are many alternative navigation systems (99), some using the receiving and transmitting of signals and others relying on natural phenomena such as stars.

Many factors influence the choice of a navigation and control system for any application, these include:

(a) accuracy,
(b) cost,
(c) reliability,
(d) size,
(e) mass,
(f) safety,
(g) availability,
(h) adaptability.

It is asserted that cost and performance (in terms of accuracy, size and mass) are the two overriding factors. This is

supported by the great deal of work which is carried out to improve the performance/cost ratio. 'Low cost' implies a reduced cost compared to currently accepted systems for given applications. 'Low cost' systems have included a 1 nautical mile/hour accuracy strapdown system (89)(100) at US $35000 (1974) each for 500 units and the 'Low Cost Inertial Guidance System' of reference (101) was $10,000 (1976) each for 2000 units for the processing unit alone. These prices would not be considered as 'low cost' for RPAV control systems.

3.5 Miniature Remotely Piloted Air Vehicle Control Systems

Concepts for miniature RPAV control systems vary from manual flying via a radio link to automatic navigation. Information pertaining to detailed system design and cost is not generally available for company confidentiality reasons. Furthermore basic RPAV systems are not found on the market place with published performance figures. More usual, is the practice to tailor the RPAV system to the specific requirements of each customer. However, the avionic sensors employed in the control system are readily available and cost, performance and mass data are published. A simple method of comparing control systems is to collate information regarding the avionics sensors and use this information as 'a measure' to compare different techniques.

Comprehensive full scale control systems such as those used on HIMAT (102) and JINDIVIC (90) are considered outside the scope

of this thesis. Instead less sophisticated low cost systems, similar to those already under development for use on miniature RPAVs, are taken as a basis for comparison.

Early work in the UK was carried out by RAE and BAe using low cost novel sensor systems (29). Amongst those tested were electrostatic autopilots and low cost fluidic sensors. These proved unsatisfactory due to environmental effects i.e., varying electrostatic potential due to weather changes and temperature range effects and work graduated to the use of more conventional sensors. RAE have supported the development of sensors especially for use on RPAVs and the resulting products include a low cost Smiths Industries 900 series rate gyroscope (103).

Several variants of on-board stabilisation and ground based tracking systems have been developed for use on the following current RPAVs:

(a) X-RAE (RAE),

(b) STABILEYE (BAe),

(c) RAVEN (FR).

The RAE on-board system (26)(104)(105) was developed for use on the FLYBAC programme. It is an analog system providing the air vehicle with stabilisation, given external demands. One rate gyroscope operates in the pitch axis to provide suitable damping and another rate gyroscope is mounted such that it is sensitive

in both yaw and roll planes. This gyroscope enables the air vehicle to be stable in the yaw and roll axes. A barometric altitude sensor and an incidence angle sensor provide signals for operating the throttle and elevators respectively. This system is also used on the FR RAVEN.

The BAe on board system (27) used on STABILEYE consists of a 2 axis position gyroscope in the pitch and roll axes supplemented by a rate gyroscope which provides pitch damping. A barometric altitude sensor provides the inputs for an altitude lock system, control being via the elevators. The system is at present in analog form but a digital version based on the Texas 9900 series microprocessor is under development. Table 3.1 shows the RAE and BAe System avionic sensors and details their cost at January 1984 prices and mass.

Sensors	No off	Mass (kg) each/total	Cost £ (1984) each total
RAE System			
Smiths Industries: Rate Gyroscope, 900 series	2	.15/.30	465/930
Rosemount: Barometric Altitude Sensor, 1241 M1 B2	1	.17	1100
EMI: Angular Sensor	1	-	-
BAe System			
Humphrey: Two Axis Vertical Gyroscope, VG-24 421-1	1	.565	4020
Smiths Industries: Rate Gyroscope, 900 Series	1	.15	465
Rosemount: Barometric Altitude Sensor, 1241M	1	.17	1100

Table 3.1 RAE and BAe Stabilisation System Avionic Sensors

The ground based tracking system is common to the three RPAV systems. Developed by RAE (106)(107) the navigation system comprises a tracking radar and a desk top micro-computer. Control demands are transmitted back to the air vehicle via the telemetry link. The engineered system will use a portable radar which tracks the air vehicle. This data will be processed by the ground station and used to drive a moving map display. A micro-computer, an HP85, will process the positional data using a program written in BASIC and new commands will be generated and transmitted to the air vehicle. Various versions of the software have been written. A typical control program will support the use of 99 waypoints entered in polar or Cartesian co-ordinate form.

There are disadvantages to this navigation system:

(a) the tracking radar is expensive (approx £100 k)

(b) continuous or frequent ground to air communications facilitates detection by an enemy.

Two on board Flight Control and Navigation Systems (FCNS) are currently under development. GEC (Marconi) Avionics developed a system for use on MACHAN to generate expertise for the PHOENIX programme. Smiths Industries have produced a system which is undergoing initial tests on BAe's STABILEYE. Table 3.2 shows the avionic sensor cost and weight breakdown for both systems.

Sensors	No Off	Mass (kg) each/total	Cost £ (1984) each/total
Smiths Industries FCNS			
Smiths Industries: Rate Gyroscopes, 900 series	3	.15/.45	465/1395
Schaevitz: Linear Accelerometer, LSM ± 5g	2	-	575/1150
Domain Microsystems: Fluxgate Magnetometer, A4/81 - 026 (3 axis)	1	.28	1180
Rosemount: Barometric Altitude Sensor, 1241 N	1	.17	1100
Rosemount: Air Speed Indicator, 12210	1	.17	1500
Philips Research: 4 Channel Switched Doppler	1	-	-
Marconi Avionic FCNS			
Marconi Avionics: Rate Integrating Gyroscopes, GIG6	3	-	1800/5400
Marconi Avionics: Linear Accelerometers, AP6G	3	-	1450/4350
Rosemount: Barometric Altitude Sensor, 1241 M	1	.17	1100
Proser: Cooled Thermistor Air Speed Indicator	1	-	-

Table 3.2 Smiths Industries and Marconi Avionics FCNS Avionic Sensors

In 1978 a development programme funded 50% by RAE commenced using the MACHAN fixed wing experimental air vehicle to enable experience to be gained on microprocessor applications to RPAV control and navigation systems (108). Based on three rate

integrating gyroscopes and three accelerometers mounted in an orthogonal triad the system provides stabilisation and is a dead reckoning navigator.

The first prototype was based on GRH4 gyroscopes but it failed to meet the self imposed requirements for a 2-3°/hr system. The second generation system is based around three GIG6 gyroscopes (£2000 each 1984) and three APG6 accelerometers. The construction of the accelerometers and gyroscopes is similar except that in the accelerometer the rotating mass is replaced by a static mass. This has the advantage of the six inputs to the processor being similar but the cost penalty is that the accelerometers are approximately twice the price of comparable performance units at £1600 (1984) each.

During development trials the system demonstrated that it can achieve 2°/hr in heading and would therefore require infrequent updates. By characterising the gyroscope errors and storing this data in RAM onboard, designers are confident that the system will operate over a wide (90°C) temperature range. The prototype onboard hardware measures approximately 0.3m x 0.3m x 0.5m.

Updating from sources other than the ground station (r, θ_1, θ_2 from telemetry system) is not considered necessary at this stage of development but investigations into the following updating techniques are continuing:

(a) fluxgate heading compass,

(b) terrain matching (using linescan camera sensor),

(c) doppler (velocity correction).

There is at present no intention to market an RPAV control system in this form. However, GCE (Marconi) Avionics have been awarded the MoD PHOENIX project and the control system proposed for this system is similar to that developed on MACHAN using 3 x GIG6 gyroscopes and 3 x APG6 accelerometers.

Derived from Marconi Avionics previous work on control systems, the most recent Attitude and Heading Reference System (AHRS), designed for use on a British Navy torpedo, adopts the same sensor configuration as that on MACHAN. The AHRS system configured for RPAV applications can be purchased for £35000 (1984) each for one off or £15000 (1984) each in production quantities (50-100 off). Development and adaptation of the torpedo AHRS system to specific user requirements can be carried out at additional cost.

The GIG6 gyroscopes have been incorporated in many control systems including NASA's control system used in the first space shuttle Columbia. The cost of the GIG6 gyroscopes range typically between £1800 to £5000 (1984). APG6 accelerometers are approximately 20% less. The gyroscopes suitable for RPAV applications are approximately £2000 (1984). Marconi also

claimed that they supplied GIG6 gyroscopes to Ferranti for use in their early PHOENIX experimental programme.

Smiths FCNS (26)(109) has been under development since 1980. Rate gyroscopes provide stabilisation whilst navigation is performed using two accelerometers and a doppler velocity measuring system. A ground control unit enables full control to be exerted over the air vehicle. An initialisation routine performs functional tests on each sensor and the operator is given a visual indication of the system condition through lights on the display. Joysticks are provided for manual flying and way-point navigation can be programmed prior to, or during, flight. The system was first flown in 1984. The controller package is a 0.3m cube and the mass breakdown is tabulated in table 3.3.

Unit	Mass (kg)
FCNS Controller	4.4
Avionics Sensors	2.8
Battery	2.6
Total	9.8kg

Table 3.3 Mass Breakdown for Smiths Industries FCNS and Accessories

Smiths Industries have announced an Attitude and Heading Reference System (AHRS) (110) based on three 900 series gyroscopes and three 800 series servoed accelerometers. Prices

quoted start from £8500 (1984) for production quantities (20-50 off). For custom versions and single units the prices will be higher.

Control system development for European based RPAVs has not been discussed in open publications. Work carried out in the US is often inappropriate due to the large size of even their miniature RPAVs. The only relevant work being that carried out at the Wright Patterson Air Force Base in the Air Force Institute of Technology. The XBQM-106 mini RPAV which has a 10ft wingspan is the subject of a control system development programme (111); an analog system has been proven and a digital version is under development.

3.6 Miniature RPH Control System History

Rotary wing air vehicles are inherently unstable (112) whereas fixed wing aircraft may be made stable depending on the geometry. Full scale helicopter control systems are designed such that the time constants of the instability are large enough to permit control by a pilot. However, a recent CAA review of helicopter airworthiness (113) reports that 60-65% of helicopter accidents are due to '"human error", in general "pilot error"', which suggests that this is not an acceptable situation. The report recommends that a special study takes place to 'see where technology might contribute to useful improvement'.

On reduced scale rotary wing vehicles the time constants of the

instability are reduced, making control by the average human operator extremely difficult (114). Two paths lay open to a designer to ensure that the miniature RPH is 'controllable':

(a) the time constant of the instability is increased to an acceptable value,

or

(b) an automatic onboard Control System with feedback from motion sensors is fitted.

In order to achieve a more damped response, the control demands to the rotor blades may be fed via a control rotor system. Two basic versions are available. The Bell System invented by Young, circa 1940, is in effect a rate gyroscope and itself requires some form of damping. This may be supplied on full scale helicopters by hydraulic dampers similar to those used in the suspension of passenger cars. The alternative type invented by Hiller in 1943, using similar principles, employs weighted aerofoil blades which obtain the necessary damping from their aerofoil section. Both systems aim to provide a 'following rate' of the main rotor appropriate to human and servo response times. The 'following rate' is defined as the time for the main rotor to move from one extreme angular position to the other for a maximum step input whilst the rotors are running at full speed. Reference (114) asserts that for a total rotor travel of approximately 1/2 radian (30°) the 'following rate' should be between 1/4 and 2 seconds to permit human control.

Alternatively, to provide automatic stabilisation, motion sensors are required, usually gyroscopes, whose outputs are suitably processed and fed back to control the rotor. It is possible to combine both systems to allow slower response sensors and servos to be used.

Model helicopter enthusiasts had, until the mid 1980's, adopted the Hiller system due to its simpler damping arrangements. Modellers enjoy the challenge of manual flying and only recently have complex mixing linkage systems been used in any numbers. The cost of comprehensive autopilots would be prohibitive for amateur use, consequently only crude gyroscopes have been developed for model applications and these are not widely used.

Development of a control system for the miniature PSH was carried out by Westland Helicopters during the mid 1970's. Successful flights were achieved with the MOTE air vehicle using control rotor stabilisation in June 1975 (65). The control rotor was an adapted Bell type using aerodynamic paddles to provide damping. During the following year gyroscope based stabilisation in pitch, roll and yaw was added.

Due to increases in the control system mass a larger air vehicle, WISP, was designed. Westlands continued development of the attitude demand system until 1981. They considered that an RPH system required the following three control modes for satisfactory operation (115):

(a) the hover mode (including take off, landing, hover and low speed flight within visual range of the operator),

(b) the navigation mode (flight between waypoints outside the operator's visual range),

(c) the remote hover mode (holding station outside visual range of the operator).

Results of these developments and engineering details have not been published.

3.7 SPRITE Control System Requirements

A flight control system is required to perform two main functions. The air vehicle, which is inherently unstable, requires short term stabilisation in pitch, roll and yaw and long term positional control in space.

The operating regime and philosophy of RPAV Systems has been discussed widely (17)(68)(76)(77)(78)(79)(80)(83)(84)(85)(87)(116) but have yet to be finalised and refined. Nevertheless it is likely that modes such as those introduced in 3.6 (115) will be considered for evaluation and development in SPRITE.

3.8 SPRITE Control System Development Status

The prototype SPRITE air vehicles are fitted with experimental attitude demand and stabilisation systems to allow development flight testing. The analog system performs roll, yaw and pitch stabilisation. A range of equipment is under consideration including a simple 2 axis navigator using two accelerometers

and altitude and magnetic heading sensors. Details of the Avionics sensors used in the experimental control system are given in table 3.4.

Investigations into the performance and effectiveness of the above arrangements with recommendations for enhanced cost effectiveness by the use of alternative techniques, configurations or sensors is required before production SPRITE systems are finalised.

Sensors	No Off	Mass (kg) each/total	Cost £ (1984) each/total
Humphrey: 2 axis Position Gyroscope, Model VG-34-0301-1 (Pitch/Yaw axes)	1	.565	4020
Humphrey: North Seeking Gyroscope, Model BG-60-0201-1	1	.575	5280
Smiths Industries: Rate Gyroscope, Model IP 902-RGS-1	1	.15	465
Smiths: Linear Accelerometer, Type 2P 801-ADA/S	2	.120/.24	565/1695

Table 3.4 Prototype SPRITE RPAV Avonics Sensors

3.9 Avionics Sensors Review Summary

At the present time several sensors have been identified which warrant further investigation. Amongst those are the examples listed below:

(a) sensors in use by RPAV developers,

(b) Watson Industries angular sensors which use coriolis force sensing

e.g. Angular rate sensor ARS-C131-1A 110g US$425 (1984)

Angular position (Indicator) and rate sensor ADS-C121-1A 450g US$965 (1984),

(c) Japanese Electronics Industry (Nichimen Corporation) Low cost copies of available devices e.g. Sunstrand Q Flex accelerometer copy,

(d) Domain Micro-systems fluxgate magnetometers

e.g. (3 axis System £6000 (1984)).

Of the many novel sensors under development many are subject to commercial restriction and even their existence is not publicised. However, the development of the following sensors which may be available by 1990 should be monitored and consideration given to their use in future control system variants.

Under Development in Industry

(a) STC (Harlow) surface acoustic wave accelerometer (117) (118).

Under Development Within ML Aviation

(a) Single axis electro-magnetic rate sensor*,

(b) Altitude sensor using the telemetry RF link**,

---

* Recently assessed by Imperial College London as part of UK MoD LAW Rocket development programme.

** ML Aviation development number G06264.

(c) Radio frequency vertical reference.

An issue worthy of future discussion is the desirability, or otherwise, of using non-UK manufactured sensors. This point should be borne in mind for later consideration but it is outside the scope of this work.

3.10 Identifying the Simulation Requirements

In view of the circumstances and constraints prevailing in 1984, namely that:

(a) no means of evaluating control systems and sensors for the SPRITE application was available,

(b) lack of RPAV system performance data available to potential users was identified,

(c) motion sensor data were widely available.

It was concluded that ML Aviation would benefit from a means of providing control system performance estimates for the purpose of modelling alternative sensor packages and for supplying data to users. A comprehensive computer simulation of the air vehicle would allow the performance of sensors to be estimated prior to costly implementation in hardware. It would allow a wider range of sensors to be evaluated at a lower cost, in a shorter time period and updating techniques could be evaluated and refined without risk to the air vehicle. It was proposed

that efforts be channelled into the development of a six degree of freedom simulation to provide data which could be relied upon.

It is asserted that to meet the requirements imposed upon the simulation it should be capable of performing the following functions:

(a) model short term stability,

(b) model long term navigation,

and possess the following features:

(c) model avionics sensor mechanism and performance,

(d) model different control processing regimes,

(e) model control laws,

(f) account for 6 df motion,

(g) model co-axial rotor performance,

(h) model fuselage aerodynamics,

(i) allow air vehicle parameters to be input as variables,

The following sections of this thesis show how the simulation was developed to satisfy these requirements.

3.11 Review

Fixed and rotory wing air vehicle control systems and avionics sensors have been reviewed. The need to evaluate sensor, flight system processing, and navigation techniques including alternative updating philosophies has been discussed and the lack of a facility to compare alternative control system configurations and sensors has been identified. The capabilities required of a model to provide these design capabilities have been proposed.

SECTION 4

PROBLEM DEFINITION AND SOLUTION STRATEGIES

4 PROBLEM DEFINITION AND SOLUTION STRATEGIES

4.1 Introduction

Sections 2 and 3 have reviewed the status of RPV development and identified a need for a further tool which an RPV design team require. This section identifies the RPV design team and seeks to define the tool, or RPV simulation, and discusses the limits of the proposed simulation and its design uses. Conflicting arguments for simple and detailed analyses are presented and a compromise solution is identified. This solution is expanded and the structure of the simulation is developed.

4.2 Simulation User

It is important to precisely identify the user of the proposed RPH simulation prior to its development in order that it may be tailored accordingly. It is also important that the simulation be designed to give the best advantage to the user.

A project such as SPRITE, the PSH designed by ML Aviation, requires a multi-disciplined team of engineers for its successful development. This team, headed by a technical manager, has representation from the fields of aerodynamics, structures, avionics and control engineering both at a theoretical level and more practically for development hardware trials. Each sub-team is led by an engineer of chartered status or equivalent. Inevitably in smaller companies some of these

roles are combined but it is unlikely that any one member of the team will have a detailed knowledge in all fields. Time alone would preclude this unless the development is to proceed at an unacceptably slow pace.

It is these sub-team leaders who were identified as the potential users of the simulation, specialists in their own fields with a good background understanding in engineering, but not expert in all disciplines.

In comparing alternative approaches it is useful to use the term 'visibility' defined as a measure of how readily available design information is from within a simulation. As examples, the following two extremes are presented; a quantity directly used within the simulation in a form readily meaningful to the designer, such as overall force, is said to be 'highly visible'. Whereas, a required quantity which has to be extracted from a normalised form and, perhaps, undergo several axes transformations until it is available in usual units with respect to a usual axes system is said to be of 'low visibility'.

Furthermore, practical engineers prefer to be able to verify simulation output with measurements taken during tests on hardware (119). It is therefore more helpful to present results with reference to physical parameters such as 'flapping angle of 6° with reference to the rotor shaft datum; rotational rate of 20°/second about the shaft axis' rather than 'combined rotation

in azimuth, roll and pitch about the plane of no feathering; forward velocity of 3 m/s with reference to stability axes'.

It is these two points, namely:

(a) high visibility,

(b) high practical application,

which are borne in mind during both the design and development of the system of equations and during the computer implementation of the simulation software package. Success in these areas would be a measure of achievement of the project. It is the opinion of the author that the more simple and readily usable the design tools are, then the more of his intellectual capacity and enthusiasm a designer or development engineer can apply to solving the problems in hand, thus enabling development to progress at a faster overall rate. Whether the simulation is adopted and used widely as a tool may depend on these factors, but only experience and time will tell. This is not to say that 'the more trivial the simulation is, the better' as the value of the solution is important. Perhaps the value of a design tool could be measured by an algorithm of the form:

$$\text{Design Tool Value} = \frac{\text{Confidence in Solution}}{\text{Time and Effort Required by User}}$$

These points are not intended to be rigorous intellectual arguments merely to attempt to 'set the scene' for design and development of the simulation.

4.3 Requirements of a Simulation

It has already been stated that the simulation is aimed at providing an analysis aid for assessing sensor performance contributing towards maximising control system value. As a by-product it is seen that it also provides the design team with enhanced analysis capabilities.

Early analysis work carried out by ML Aviation was at a simple level (120)(121)(122) using single axis linear transfer functions both for rotor and control system performance. As will be seen in Section 10 these techniques may give inaccurate solutions due to the inapplicability of the 'linear' assumption and they are certainly too crude for optimising components within the control system.

The simulation has to be designed at a technical level appropriate to the solutions being sought. However there is a conflict between two competing requirements, namely:

(a) adequate depth and visibility of solution,

(b) acceptably quick run times.

If recourse is made to very detailed analysis the quality and quantity of output data will increase and the understanding provided and the range of application offered by the simulation would be substantial. However, as the degree of complexity increases so does the simulation development timescale and the computer power and runtime required. There would also be an increased burden of verifying and disseminating the available data placed on the user. Development timescale constraints were placed upon the project by the sponsoring Company. This is where an interdisciplinary sandwich project differs from traditional research. Whereas it might be argued that the traditional University requirement is primarily for academic excellence the IHD approach tempers this with the need to provide solutions to real problems within pre-determined timescales. The IHD scheme, which was set up in response to the Swann Report*, is described in reference (123) in more detail. The following extracts from this reference give a flavour of the scheme; the first is an extract from a letter to the Vice-chancellor of the University of Aston from SERC and the second extract taken from reference (123) gives the aims of the IHD scheme:

'.... a new system might also make it possible to develop an environment for the study which is more in line with that attaching to industrial and commercial operations (and come to

---

* The flow into Employment of Scientists, Engineers and Technologists. HMSO Cmnd 3760. 1968.

that in local and national Governments, etc., employment). For example, one might realise the need to work to a tight timetable, to take a decision on open-ended problems with only limited data available, to work with and control the work of others, to give status to material things rather than those that appeal mainly as an intellectual challenge.'

'To equip postgraduate students for positions of responsibility in industry and publicly financed organisations by providing training in practical, real world problem-solving: more specifically in:

- application of existing knowledge
- generation of new knowledge needed
- appreciation of academic disciplines different from those of students' first degrees
- implementation of solutions'

In order to be of use to the Company the simulation needed to be available and running on their PRIME 550 Computer in a 'debugged' form within timescales early enough to influence control system design and development for second generation prototype air vehicles. In practice this was within 24-36 months of identifying the requirements of the simulation.

Furthermore, at the commencement of the IHD Project ML Aviation had entered into a three year agreement with SERC and the

University of Aston (124) and was anticipating results within that timescale.

A further timescale requirement, that of computer simulation runtime had not been defined explicitly. However, by reference to two proposed uses of the simulation, stability and navigation analysis, acceptable upper limits may be proposed. Short term stability analysis should be carried out for real times of, say, 20 or 30 seconds following input demands, allowing the air vehicle response to be modelled. Navigation analyses runs would be extended to real times of flight of 10 to 20 minutes. It would be considered acceptable for stability cases to be run overnight with perhaps several days being considered acceptable for the navigation runs. The Company has previously had experience with programs with long runtimes of up to 120 hours for a dynamic response software package, the value of the solution justifying the duration. Summarising these requirements, guidelines for the maximum desirable runtimes were placed as follows:

(a) stability runs (30 sec real time) 12 hours,

(b) navigation runs (10-20 min real time) 120 hours.

The two tasks to be performed by the simulation can be briefly summarised within the two following categories:

ASTON UNIVERSITY LIBRARY

(a) stability analysis,

(b) navigation analysis.

The former being of use for the design and development of RPV systems where alternative sensors and techniques may be compared and the latter for predicting optimum performance for a given air vehicle configuration. Examples of these studies include:

Design and Development

(a) stability verification;

(b) demand response - step inputs,
- impulse inputs;

(c) cross coupling evaluation,
roll, pitch, yaw, altitude;

(d) gust response;

(e) sensor error effect;

(f) navigation system evaluation;

(g) component failure effect;

(h) effect of: aerodynamic changes to rotors,
aerodynamic changes to fuselage,
mass changes,
cg position changes;

Operational Assessment

(i) economic flight envelope determination,

(j) flight envelope extreme condition determination,

(k) navigation updating frequency

vs

error analysis comparison,

(l) waypoint navigation evaluation.

4.4 Simulation Development Strategy

The requirements of this research project are stated in Sections 2 and 3, the objectives here are to present the strategy adopted to realise these aims. It is clearly necessary to define the interface between the Company project and this IHD project so that logical arguments can be presented in support of the strategies which were adopted.

The SPRITE system development is a Company funded project, and it was made clear that this work should make use of data available from trials being carried out as part of normal development. As a consequence of the quality and quantity of data that was available on SPRITE performance; namely that there was only little data, mostly of a subjective nature; it was decided from the outset that it was important to draw heavily from published material, both of a theoretical and practical nature, during the development of the simulation.

Furthermore, as some, perhaps the more financially promising, potential applications of the SPRITE system are military, it would be of advantage to make full use of work carried out by

government supported bodies in addition to work by educational establishments. These include the National Advisory Committee for Aerodynamics, NACA, the National Aeronautics and Space Administration, NASA, in the US and the Royal Aircraft Establishment, RAE, in the UK. An inevitable result of this policy is the burden of hand calculation and detailed checking required when adopting for use previously validated material. Verification may only be achieved by meticulous and logical checking. Repeating published runs to verify correct implementation of proven theoretical work is usually not possible as input data is infrequently made available.

With regard to the philosophy for simulation software design (125)(126) and documentation (127)(128) texts were considered and salient points were drawn out and adopted. In particular, top down development was considered to be particularly appropriate with new modules being added one at a time in the approved fashion (125). During development of the software 'debugging' techniques were given similar consideration (125) (129). The documentation aspects are not discussed in this document but are proceeding to satisfy Company requirements (130).

During software design and development three points were given a high priority. These are introduced in this section and the actual implementation is discussed within the appropriate technical sections and in Section 9. The three criteria which

were borne in mind from the outset of development are:

(a) modular program design,

(b) high emphasis on traceability and repeatability,

(c) good visibility of results.

Modular development (131) was considered important, not only as it is considered good practice (125) but, because it would give the simulation more flexibility. Once a skeletal package has been developed to satisfy the initial requirements, specialists in their own field may choose to develop further one particular module to extend the useful range of the model to cover specific applications. An example of this is the development of a sophisticated rotor model which aerodynamicists require for rotor or blade optimisation or stress engineers could use for component strength analysis. A scenario is envisaged where a library of modules is developed and simulation programs selected on a 'mix and match' basis appropriate to the required depth of solution and other constraints.

The simulation was designed with the following skeletal structure:

(a) data input file handler,

(b) simulation control and module caller,

(c) data output file handler,

with the following air vehicle specific modules:

(d) co-axial rotors,

(e) flight control system,

(f) fuselage aerodynamics,

(g) control laws,

and the following utility modules:

(h) six degrees of freedom motion,

(i) integration,

(j) axes systems transformations,

all called as subroutines.

Traceability of the program standard and repeatability of individual runs contributed significantly to confidence in the software package. Importance was placed on specifying the standard of:

(a) all module subroutines,

(b) the simulation calling program,

(c) input data files,

(d) output data files.

Further consideration was given to two methods of running the simulation:

(a) interactive,

(b) batch queue,

with a dual capability desirable.

The strategies outlined in this section are reflected in the development of the air vehicle performance and utility modules described in Sections 5 to 8 and the techniques employed during the implementation into software code are described in Section 9.

4.5 Review

This section defining the project strategies has identified the proposed simulation user and the requirements of the simulation. Practical constraints typical to IHD projects have been introduced and example cases for simulation presented. The strategies have been developed and the software structure has been outlined.

SECTION 5

SIX DEGREES OF FREEDOM MOTION

5 SIX DEGREES OF FREEDOM MOTION

5.1 Introduction

The motion of a body can be quantified and measured with reference to any point which may itself be stationary or in motion. It is normal practice to resolve the angular and linear motion about three mutually perpendicular axes. Six degrees of freedom motion is the term commonly used to describe the three linear and three angular motions with reference to an orthogonal triad axis system.

Additionally the choice of axes systems and the techniques of transformation between the axes systems has implications of both computational speed and the users' understanding of the simulation. This section reviews 6 degrees of freedom motion modelling, introduces the assumptions and presents the underlying theory with reference to other work. The implementation within the simulation is also described. Axis system definitions and transformations not given in the main text may be found in Appendix B.

5.2 Six Degrees of Freedom Motion - Theory

To reduce the problems of simulating the six degrees of freedom motion of the air vehicle in the simulation to a practical level it is useful to make certain assumptions regarding the motions and the air vehicle configuration.

To determine the air vehicle six degrees of freedom motion several alternative axes systems have been used by previous researchers. Two popular combinations being body axes/earth axes (132) and flight path axes/earth axes (133). Fogarty and Howe (134) discuss the relationship between axes systems and computational speed and accuracy. They recommend the decoupling of translational and rotational motions, solving translational motion through the use of flight path axes and rotational motion through the use of body axes. The advantages of flight path axes are greater where the aircraft has a high speed capability resulting in the magnitude of cross coupling acceleration terms in body axes, such as uq, to be in the region of two orders of magnitude greater than the physical accelerations.

This, as Forgarty and Howe indicate, may lead to scaling difficulties resulting in poorer solution accuracies for a given computer precision. Flight path axes do not have these scaling difficulties and thus alleviate this problem.

For the SPRITE application however, the forward speed capability is low compared to fixed wing aircraft, thus reducing the magnitude of any cross coupling terms. There are two arguments against adopting the Fogarty/Howe approach. Firstly, there would be an increased complexity which would inevitably be required to include separate linear and rotational motion solution techniques. Secondly, perhaps more importantly, there would be a reduction in visibility of the air vehicle

motion resultant from the inclusion of another system of axes and the associated transformations which require the definition of further axes (stability axes). Consequently it was concluded that both linear and rotational motion would be determined using body/earth axes. If simulation runs are to be carried out involving a considerable proportion of high speed motion and the computational accuracy and speed is not adequate, then, it may be advantageous to re-consider this choice of method. However, at present the flight programmes involve a substantial degree of low speed manoeuvring (135).

Moreover, flight path axes have their own disadvantages, such as the difficulty of introducing wind direction (132) and acceleration term errors which are introduced if the simulation progresses to include a spherical rotating earth (134).

A flat earth model is appropriate for short flight segment simulations of low speed vehicles. Simulations of extended flight cases or high speed vehicles should use a spherical earth kinematic model (136) which includes the curvature effects and the rotation of the earth. To aid computational speed the flat earth model is included in the simulation. However, the effects of earth rotation may need to be considered at the sensor input stage to account for earth rate effects which depend on the mechanism of operation of the sensor.

The angular orientation of the vehicle can be described by three

rotations starting from the local earth axes. Two sets of rotations are in common use, these give rise to Euler angles (137) and attitude angles (138). It should be noted that the order of rotations is important and expressions derived for one set of rotations are not transferable to different orders of rotations (e.g. they are non-commutative).

There is confusion amongst users of these sets of rotations, Tomlinson (132) in a technical paper, on which the RAE simulation work is based, discusses the angular orientation of the aircraft with reference to a 'conventional trio of Euler angles' but then he quotes results for attitude angles. Upon closer examination of his work it can be seen that he uses expressions appropriate to attitude angles taken from other published work and in his discussion he incorrectly refers to Euler angles. McFarland (136) also uses the term Euler angles to describe attitude angles. Fortunately he derives the transformation matrices from first principles and obtains the correct solution. Upon further investigation, other texts, especially those from the US (139), appear to use the term 'Euler angles' to describe attitude angles. It appears that this 'corruption' is widely used and is unfortunate.

Because of the confusion found in the reference texts which come from establishments such as RAE and NASA, whose scientists base a considerable proportion of modelling on previous work, it was felt justified to restate definitions and results for both Euler

and attitude angle systems. Especially as will be seen later in this section, both have a place in this simulation.

Attitude Angles

The attitude angle orientation system is described by ESDU (138). The air vehicle orientation can be measured from the earth axes by the three attitude angles, Φ, bank angle, Θ, inclination angle and Ψ, azimuth angle. It is important that the order of rotations is specified. The order of rotations which give rise to the familiar direction cosine matrix [C] are (see figure 5.1):

(a) a rotation about the z_0 axis, Ψ, $(x_0, y_0, z_0) \rightarrow (x^1, y^1, z_0)$,

(b) followed by a rotation about the intermediate y axis, y^1, Θ, $(x^1, y^1, z_0) \rightarrow (x^1, y^1, z^{11})$,

(c) finally a rotation about the intermediate x axis, x, Φ $(x, y^1, z^{11}) \rightarrow (x, y, z)$.

The directional cosine matrix can be written:

	x_0	y_0	z_0
x	$l_1=\cos\Theta\cos\Psi$	$l_2=\cos\Theta\sin\Psi$	$l_3=-\sin\Theta$
y	$m_1=\sin\Phi\sin\Theta\cos\Psi$ $-\cos\Phi\sin\Psi$	$m_2=\sin\Phi\sin\Theta\sin\Psi$ $+\cos\Phi\cos\Psi$	$m_3=\sin\Phi\cos\Theta$
z	$n_1=\cos\Phi\sin\Theta\cos\Psi$ $+\sin\Phi\sin\Psi$	$n_2=\cos\Phi\sin\Theta\sin\Psi$ $-\sin\Phi\cos\Psi$	$n_3=\cos\Phi\cos\Theta$

(138)

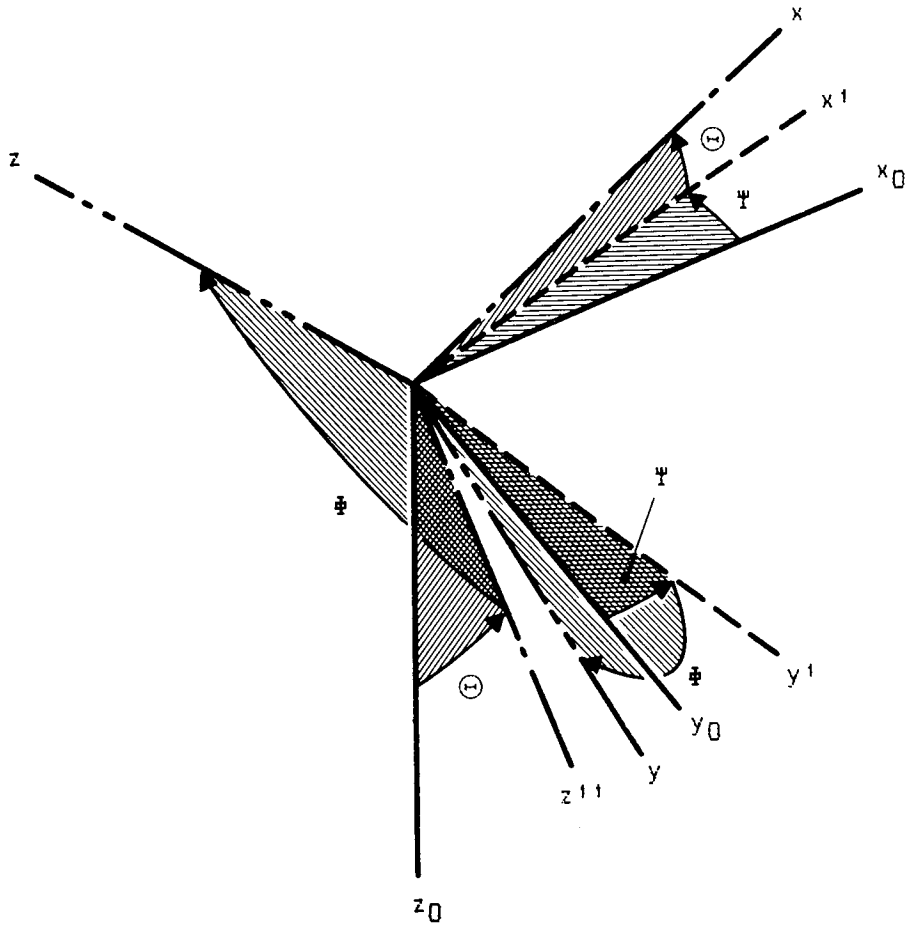

Figure 5.1 Attitude Angles

Euler Angles

Euler angles θ, ϕ, ψ are defined more clearly by construction than by rotation (137) and are stated with reference to figure 5.2.

By construction of a k axis perpendicular to the z_0 and z axes it is shown in figure 5.2 that:

the angle between the z_0 and z axes is θ,

the angle between the y_0 and k axes is ϕ,

the angle between the y and k axes is ψ.

The associated direction cosine matrix for the Euler angles is:

	x_0	y_0	z_0
x	$\cos\phi\cos\theta\cos\psi-\sin\phi\sin\psi$	$\sin\phi\cos\theta\cos\psi+\cos\phi\sin\psi$	$-\sin\theta\cos\psi$
y	$-\cos\phi\cos\theta\sin\psi-\sin\phi\cos\psi$	$-\sin\phi\cos\theta\sin\psi+\cos\phi\cos\psi$	$\sin\theta\sin\psi$
z	$\cos\phi\ \sin\theta$	$\sin\phi\ \sin\theta$	$\cos\theta$

(137)

It should be noted that the numerical values of all corresponding elements of the direction cosine matrix are identical, as is implicit in the definition that the matrix transforms between two axes systems.

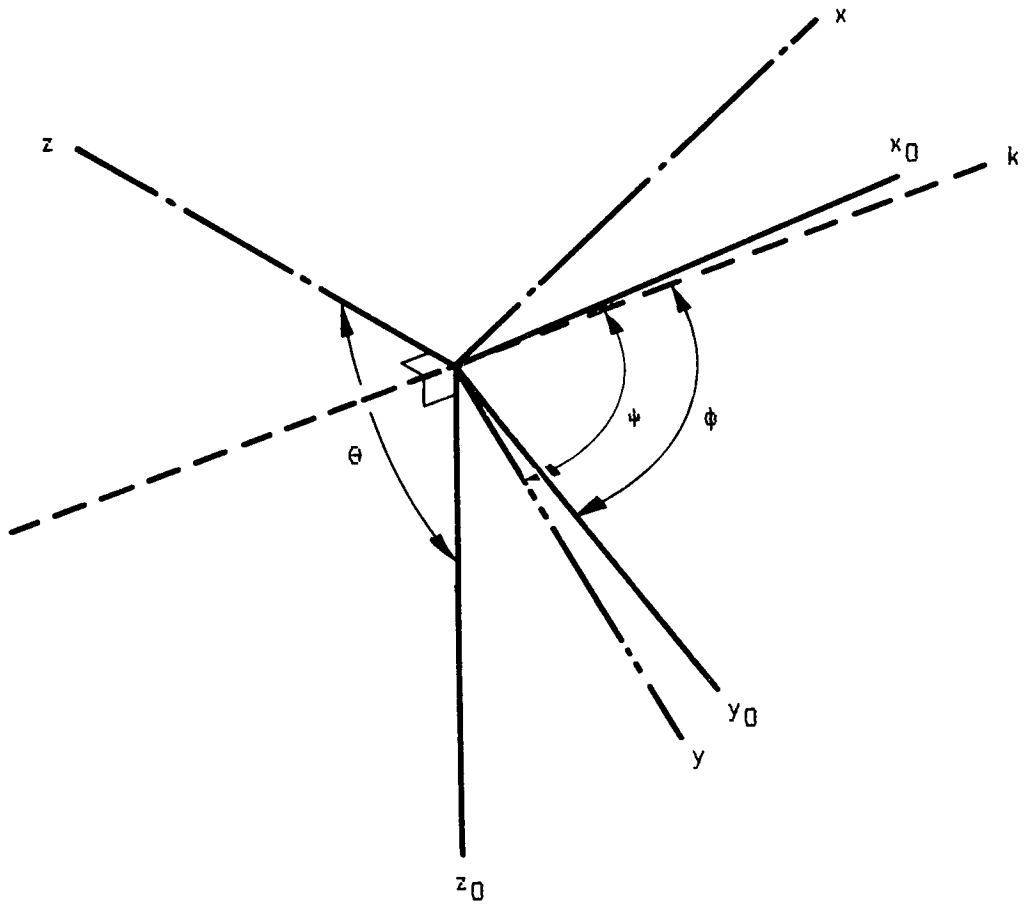

Figure 5.2 Euler Angles

Transformations

The usual implementation of the transformations between body and local earth axes is to directly integrate a set of differential equations solving for Euler or attitude angles (132). This scheme is suitable for most flight cases, however, a singularity occurs for vertical flight conditions and for continual rotations the computed angles may lie outside the range $\pm \Pi$. Whilst this may be useful when monitoring the flight history it tends to obscure the actual orientation of the air vehicle.

Mortensen (140) carried out a comparison of the accuracies of two transformation techniques, one based on the use of attitude or Euler angles and the other which uses the Euler parameter quaternion to obtain the direction cosine matrix. Scale, skew and drift errors were defined and the susceptability of the two schemes to these types of error examined. Mortenson concluded that the quaternion approach is superior as it intrinsically yields zero skew errors. The quaternion approach has additional advantages. It does not suffer from singularities so it is valid for all flight conditions and the numerical value of the terms within the quaternion remain in the range ± 1 giving greater visibility to quantities aiding user understanding. Mortensen's method was selected for the transformations between body and local earth axes. The technique is summarised below.

The transformations from the body axes vehicle state to the local ground axes state is accomplished through the use of the quaternion $\underline{\varrho}$ of Eulerian parameters χ, ξ, η, ζ:

$$\underline{\varrho} = \begin{bmatrix} \chi \\ \xi \\ \eta \\ \zeta \end{bmatrix}$$

Where the Euler parameters are defined (137) in terms of the Euler angles θ, ϕ, ψ as follows:

$$\xi = \sin 1/2\ \theta \sin 1/2\ (\psi - \phi)$$

$$\eta = \sin 1/2\ \theta \cos 1/2\ (\psi - \phi)$$

$$\zeta = \cos 1/2\ \theta \sin 1/2\ (\psi + \phi)$$

$$\chi = \cos 1/2\ \theta \cos 1/2\ (\psi + \phi)$$

The system dynamics embodied in the vector are given by (140):

$$\begin{bmatrix} \\ \dot{\underset{\sim}{\rho}} \\ \\ \end{bmatrix} = 1/2 \begin{bmatrix} 0 & -p & -q & -r \\ p & 0 & r & -q \\ q & -r & 0 & p \\ r & q & -p & 0 \end{bmatrix} \begin{bmatrix} \\ \underset{\sim}{\rho} \\ \\ \end{bmatrix}$$

The technique for obtaining the direction cosine matrix makes use of the intrinsic properties of quaternions and two matrices CY, CZ which are given by Mortenson (140). The inherent structure of these matrices results in a commutative relationship. The solution is:

$$[CY]\ [CZ] = [CZ]\ [CY] = \begin{bmatrix} 1 & 0 & 0 & 0 \\ 0 & & & \\ 0 & & C & \\ 0 & & & \end{bmatrix} \qquad (140)$$

where

$$[CY] = \begin{bmatrix} \chi & \xi & \eta & \zeta \\ -\xi & \chi & \zeta & -\eta \\ -\eta & -\zeta & \chi & \xi \\ -\zeta & \eta & -\xi & \chi \end{bmatrix} \qquad (140)$$

and

$$[CZ] = \begin{bmatrix} \chi & -\xi & -\eta & -\zeta \\ \xi & \chi & \zeta & -\eta \\ \eta & -\zeta & \chi & \xi \\ \zeta & \eta & -\xi & \chi \end{bmatrix} \quad (140)$$

Transformation of a vector of local earth axes quantities to body axes is accomplished by pre-multiplying the earth axes vector by the direction cosine matrix.

This can be written in matrix notation:

$$\underset{\sim}{x} = [C] \; \underset{\sim}{x}_0$$

The inverse of the direction cosine matrix is equal to its transpose hence:

$$\underset{\sim}{x}_0 = [C]^{-1} \; \underset{\sim}{x} = [C]^T \; \underset{\sim}{x}$$

Rutherford (141) gives the general expression for the gross translational velocity $\dot{\underset{\sim}{x}}'$ of a point with radius of gyration $\underset{\sim}{r}$ in the body axis system as:

$$\dot{\underset{\sim}{x}}' = \dot{\underset{\sim}{x}} + \Omega \, \underset{\sim}{r}$$

The velocities in the instantaneous x, y or z directions can be written (137):

$$\dot{x}' = \dot{x} + zq - yr \qquad \text{(along x axis)}$$

$$\dot{y}' = \dot{y} - zp + xr \qquad \text{(along y axis)}$$

$$\dot{z}' = \dot{z} + yp - xq \qquad \text{(along z axis)}$$

The matrix Ω can be determined by inspection:

$$\Omega = \begin{bmatrix} 0 & -r & q \\ r & 0 & -p \\ -q & p & 0 \end{bmatrix}$$

This form of expressing the ground velocities is used by McFarland (136).

The definition of body axes requires the origin to be coincident with the cg, this gives an implicit value for the radius of gyration vector $\underset{\sim}{r}$ of zero hence:

$$\dot{\underset{\sim}{x}}_0 = [C]^T \dot{\underset{\sim}{x}}$$

This result for the cg position gives the instantaneous velocities in local earth axes. By definition the local axes translate with the air vehicle, the origins being coincident, but the local earth axes remain parallel with the earth axes, this implies that the linear motion of the air vehicle in flight can be determined as follows:

$$\underset{\sim}{x}_0 = \int \dot{\underset{\sim}{x}}_0 \, dt = \int \dot{\underset{\sim}{x}}_{0L} \, dt$$

5.3 Rigid Body Motion

This section is concerned with the rigid body motion of the air vehicle induced by the action of the resultant forces and

moments acting upon it (wrt body axes). Instantaneous accelerations are determined and integrated to define the position and instantaneous motion of the air vehicle. References are cited where the expressions are quoted from authoritative sources.

The instantaneous linear acceleration equations may be written:

$$\dot{u} = \frac{X}{m} - qw + rv + g_x \tag{138}$$

$$\dot{v} = \frac{Y}{m} - ru + pw + g_y \tag{138}$$

$$\dot{w} = \frac{Z}{m} - pv + qu + g_z \tag{138}$$

where the gravity components are:

$$g_x = - g \sin\Theta$$

$$g_y = g \sin\Phi \cos\Theta$$

$$g_z = g \cos\Phi \cos\Theta$$

and the external forces acting on the air vehicle may be written as:

$$X = X_{RU} + X_{RL} + X_F$$

$$Y = Y_{RU} + Y_{RL} + Y_F$$

$$Z = Z_{RU} + Z_{RL} + Z_F$$

The instantaneous angular acceleration equations may be written:

$$L = I_x\dot{p} - I_{yz}\,(q^2-r^2) - I_{zx}\,(\dot{r}+pq) - I_{xy}\,(\dot{q}-rp) - (I_y-I_z)\,qr + J_z q - J_y r \qquad (138)$$

$$M = I_y\dot{q} - I_{zx}\,(r^2-p^2) - I_{xy}\,(\dot{p}+qr) - I_{yz}\,(\dot{r}-pq) - (I_z-I_x)\,rp + J_x r - J_z p \qquad (138)$$

$$N = I_z\dot{r} - I_{xy}\,(p^2-q^2) - I_{yz}\,(\dot{q}+rp) - I_{zx}\,(\dot{p}-qr) - (I_x-I_y)\,pq + J_y p - J_x q \qquad (138)$$

The external moments acting on the air vehicle may be written:

$$L = L_{RU} + L_{RL} + L_F$$

$$M = M_{RU} + M_{RL} + M_F$$

$$N = N_{RU} + N_{RL} + N_F$$

where

$$L_{RU} = L_{sU} + Y_{sU}\,z_{cgU} - Z_{sU}\,y_{cgU}$$

$$M_{RU} = M_{sU} + X_{sU}\,z_{cgU} - Z_{sU}\,x_{cgU}$$

$$N_{RU} = N_{sU} + X_{sU}\,y_{cgU} - Y_{sU}\,x_{cgU}$$

and similarly,

$$L_{RL} = L_{sL} + Y_{sL}\,z_{cgL} - Z_{sL}\,y_{cgL}$$

$$M_{RL} = M_{sL} + X_{sL}\,z_{cgL} - Z_{sL}\,x_{cgL}$$

$$N_{RL} = N_{sL} + X_{sL}\,y_{cgL} - Y_{sL}\,x_{cgL}$$

A simplification is possible because of the symmetrical design of the air vehicle. It is asserted that the body axes, which lie through the cg position, are coincident with the principle axes of inertia of the air vehicle. Hence:

$$I_{xy} = 0$$

$$I_{yz} = 0$$

$$I_{zx} = 0$$

The equations for the angular accelerations may be simplified and rearranged as:

$$\dot{p} = \frac{1}{I_x} \left(L + (I_y - I_z)\, qr \right)$$

$$\dot{q} = \frac{1}{I_y} \left(M + (I_z - I_x)\, rp \right)$$

$$\dot{r} = \frac{1}{I_z} \left(N + (I_x - I_y)\, pq \right)$$

The linear velocities with respect to the instantaneous body axes are found by integrating the instantaneous rates:

$$\begin{bmatrix} u \\ v \\ w \end{bmatrix} = \int \begin{bmatrix} \dot{u} \\ \dot{v} \\ \dot{w} \end{bmatrix} dt$$

Similarly for rotational rates:

$$\begin{bmatrix} p \\ q \\ r \end{bmatrix} = \int \begin{bmatrix} \dot{p} \\ \dot{q} \\ \dot{r} \end{bmatrix} dt$$

5.4 Implementation of Air Vehicle Motion

The desire to provide the facility of having simulation inputs and outputs in units most appropriate to the user, giving the best visibility of the simulation, has already been emphasised. Initial displacements are input in earth reference axes using x_0, y_0 and z_0 linear displacements and Φ, Θ and Ψ the attitude angles for the angular orientation. Initial linear and angular velocities are input in the instantaneous body axes.

The attitude angles at initialisation are converted to Euler angles which are used to determine the quaternion of Euler parameters and henceforth the Euler parameter vector is updated using the technique described in Section 5.2. The direction cosine matrix is evaluated when required for transformations between instantaneous body and local earth axes.

The simulation outputs are in the same format as the inputs, the orientation is presented in attitude angles and the linear displacement measured in the reference earth axes and the angular and linear velocities given relative to instantaneous body axes. This is summarised in figure 5.3.

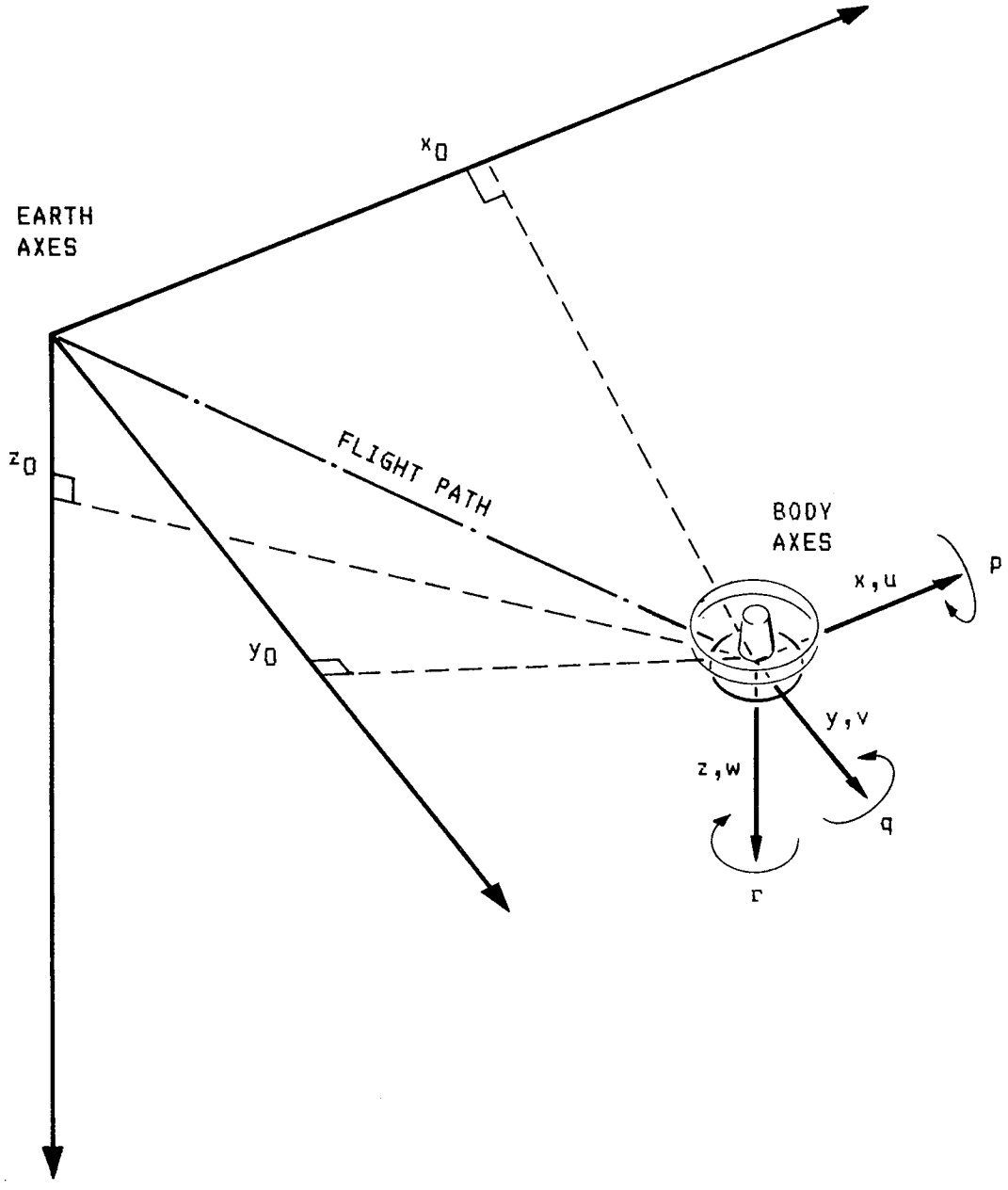

Figure 5.3 Air Vehicle Position and Motion

The units used for inputs to and outputs from the simulation are SI throughout, with angular data in degrees or radians selectable by the individual user.

5.5 Variable Integration Interval

This simulation uses the Runge Kutta order 4 integration process to determine the state vector at time t + Δt from the state vector and its derivatives at time t. By consideration of typical air vehicle motion and required simulation run times it was concluded that using fixed integration time step sizes would require unacceptable compromises to be made. To optimise the trade off between high accuracy results and long run times it is sensible to dynamically adjust the integration time step size to suit differing rates of change of the integrated variables. When rates of change are high the desirable integration interval is smaller compared to that required when rates of change are lower.

In addition to the Runge Kutta order 4 integration the values of selectable elements of the state vector at t + Δt are computed by the Runge Kutta order 2 integration process. On the basis that Runge Kutta order 4 is more accurate than Runge Kutta order 2 the difference between these two integration techniques is used to control the integration time step size.

This technique has been implemented by specifying the elements in the state vector to be used for monitoring the integration process (these would most sensibly be the elements undergoing the greatest rate of change) and the allowable differences between Runge Kutta order 2 and 4 integration processes. If these errors are exceeded on any selected element of the state

vector the new values are not accepted, the integration interval is halved and the integration process repeated. If the differences are below those specified then the integration result is accepted and the state vector is updated. Furthermore if the differences between the order 2 and order 4 integrations is less than a second test value then the integration time interval is doubled. This is summarised in Figure 5.4.

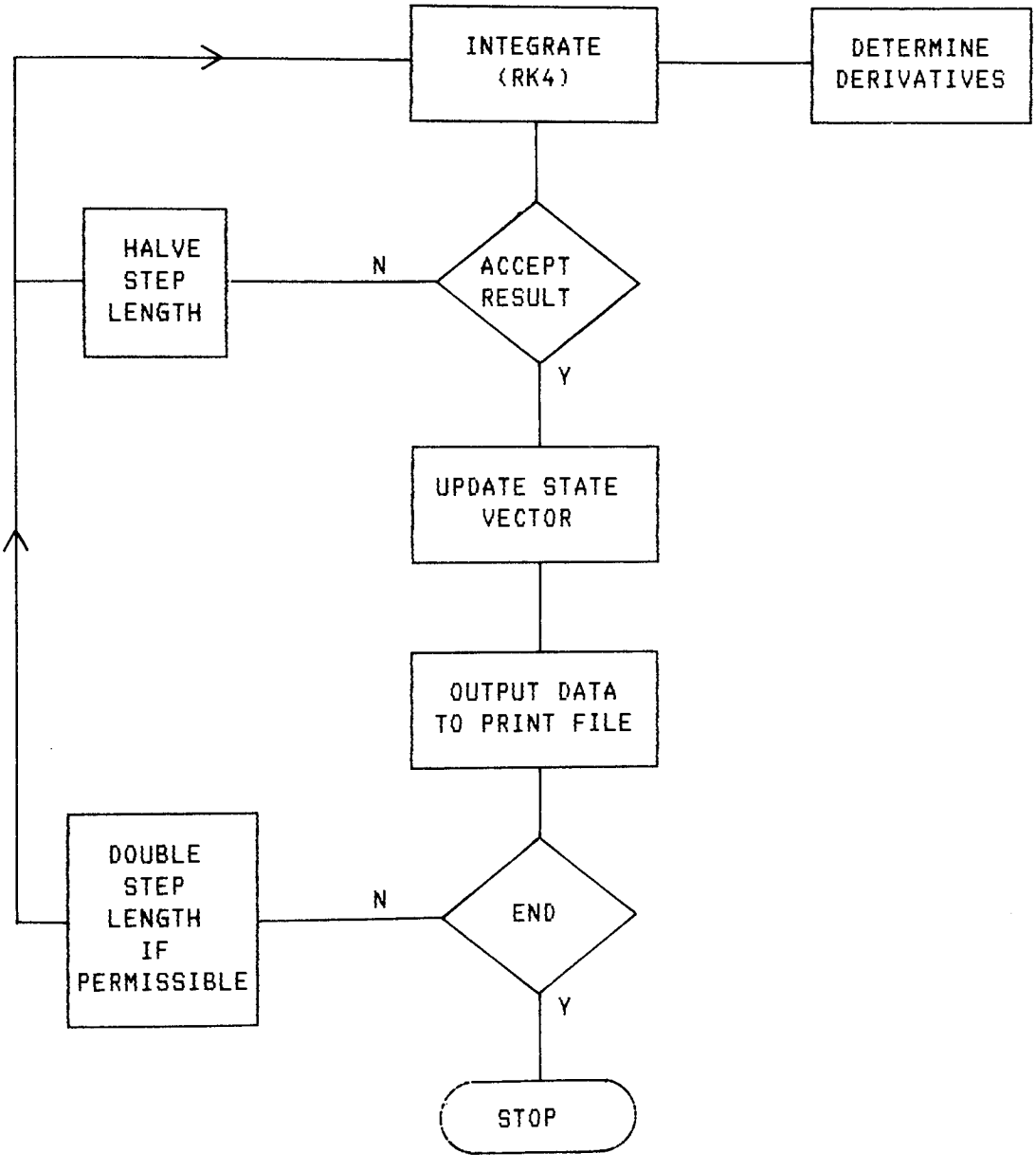

Figure 5.4 - Simulation Flow Chart - Integration Process

5.6 Accuracy Testing

The six degrees of freedom motion module was tested in 'single' and 'double' precision form. Due to the accuracy required the 'single' precision variant used double precision Euler parameters, the other variables all being single precision.

Initial testing was performed by applying single x axis forces as a function of time as detailed in table 5.1 to a 50kg* air vehicle. The theoretical body velocities and ground displacements were calculated and compared to the simulation output. The results included in this thesis are restricted in number of decimals for reasons of clarity. Inputs and outputs used the full precision available (single 7 decimals, double 14 decimals).

Time s	Force N	Velocity at (end of period) m/s	Displacement (end of period) m
0-5	0.000000	0.000000	0.000000
5-10	10.000000	1.000000	2.500000
10-15	0.000000	1.000000	7.500000
15-20	-10.000000	0.000000	10.000000
20-25	0.000000	0.000000	10.000000

Table 5.1 Initial Validation Force Inputs and dynamics

*Validation mass value

The results from the program runs indicated an initial misalignment error causing 'cross coupling' between the x_0, y_0, and z_0 axes. The errors for the single precision model are shown in table 5.2 and those for the double precision model in table 5.3.

The single and double precision models share double precision Euler parameter subroutines, the 'single' and 'double' precision names referring to the kinematics including the integration and force models.

In both cases the displacement errors are similar in direction, the different magnitudes reflecting the difference in variable precision. The cross coupling errors between axes were similar in both magnitude and direction implying an error in the direction cosine matrix at initialisation.

In order to investigate the cross-coupling error in axes transformations a family of programs were written which call the relevant subroutines and print out results at each stage. Table 5.4 outlines these operations which are carried out by the test programs. Runs were carried out with inputs 'forced' at each stage of the transformation. The results are shown in figures 5.5, 5.6, and 5.7.

RUNFL Name	Int Int sec	Login Time min	CPU Time sec	Displacement at 25 sec			Overall Distance m	Resultant Velocity u m/s	Non Zero Attitude Angle
				X_0 m	Y_0 m	Z_0 m			
THEORY	-	-	-	10.000000	0.000000	0.000000	10.000000	0.000000	-
RUNFL20	1.0	< 1.0	6.0	9.999984	0.7543E-6	-0.7543E-6	9.999984	-0.4601E-6	0
RUNFL21	0.125	16	22.0	9.999870	0.7543E-6	-0.7543E-6	9.999870	-0.3602E-5	0
RUNFL22	0.0125	91	106.0	9.998705	0.7543E-6	-0.7543E-6	9.998705	-0.3470E-4	0
THEORY	-	-	-	0.000000	10.000000	0.000000	10.000000	0.000000	
RUNFL23	0.125	17	22.0	0.7644E-6	9.999870	-0.7543E-6	9.999870	-0.3602E-5	90° Heading
THEORY	-	-	-	7.071068	0.000000	-7.071068	10.000000	0.000000	
RUNFL24	0.125	-	-	7.070979	0.000000	-7.071103	9.999962	-0.3602E-5	45° Inclination
RUNFL25	0.125	50	81.0					N/A	DIST 1.25 VEL 0.125

Table 5.2 Summary of Validation Runs on 6df Module - Single Precision Module

DRUNFL Name	Int Int sec	Login Time min	CPU Time sec	Displacement at 25 sec			Overall Distance m	Resultant Velocity u m/s	Non Zero Attitude Angle
				X_0 m	Y_0 m	Z_0 m			
THEORY	-	-	-	10.000000	0.000000	0.000000	10.000000	0.000000	-
DRUNFL20	1.0	< 1.0	14.0	10.000000	0.7543E-6	-0.7543E-6	10.000000	-0.2128E-12	0
DRUNFL21	0.125	1.0	79.0	10.000000	0.7543E-6	-0.7543E-6	10.000000	-0.2153E-12	0
DRUNFL22	0.0125	2.0	104.0	10.000000	0.7543E-6	-0.7543E-6	10.000000	-0.2078E-11	0
THEORY	-	-	-	0.000000	10.000000	0.000000	10.000000	0.000000	90° Heading
DRUNFL23	0.125	4.0	23.0	0.6073E-9	10.000000	-0.7543E-6	10.000000	-0.2153E-12	90° Heading
THEORY	-	-	-	7.071068	0.000000	-7.071068	10.000000	0.000000	45° Inclination
DRUNFL24	0.125	-	-	7.071068	0.000000	-7.071068	10.000000	-0.2153E-12	45° Inclination

Table 5.3 Summary of Validation Runs on 6df Module - Double Precision Module

Simulation Program Section	Procedure	Program/ Subroutine
Input	Input attitude angles	Main Program
Initialisation	Form direction cosine matrix and Euler angle from attitude angles	DRATCV
Initialisation	Form Euler parameters from Euler angles	DRATCV
Main Loop	Convert Euler parameters to direction cosine matrix	DDCMP

Table 5.4 Axis Transformation Test Program Summary

ATTITUDE ANGLES

0.00000000000000

0.00000000000000 (ZERO AT INPUT)

0.00000000000000

EULER ANGLES

0.75437128543853E-07

0.75437128543853E-07 (1st STAGE ERROR SHOULD ALL BE ZERO)

0.00000000000000

DIRECTION COSINE MATRIX

0.99999999999997	0.00000000000000	0.00000000000000	(SHOULD BE
0.00000000000000	0.99999999999997	0.00000000000000	IDENTITY
0.00000000000000	0.00000000000000	0.99999999999997	MATRIX)

EULER PARAMETERS

0.99999999999995		SHOULD BE
-0.14226900907354E-14		1
0.37718564271926E-07	(2nd STAGE ERROR)	0
0.37718564271926E-07		0
		0

Table 5.5 Axis Transformation Program Results - Zero Input at Attitude Angles

EULER ANGLES		
0.00000000000000		
0.00000000000000	ZERO AT INPUT	
0.00000000000000		
EULER PARAMETERS		
0.99999999999997		
0.00000000000000		
0.00000000000000	1st STAGE ERROR	
0.00000000000000		
RESULTANT DIRECTION COSINE MATRIX		
0.99999999999994	0.00000000000000	0.00000000000000
0.00000000000000	0.99999999999994	0.00000000000000
0.00000000000000	0.00000000000000	0.99999999999994

Table 5.6 Axis Transformation Program Results - Zero Input at Euler Angles

EULER PARAMETERS		
0.99999999999999	1.0 forced at input	
0.00000000000000		
0.00000000000000		
0.00000000000000		
RESULTANT DIRECTION COSINE MATRIX		
0.99999999999999	0.00000000000000	0.00000000000000
0.00000000000000	0.99999999999999	0.00000000000000
0.00000000000000	0.00000000000000	0.99999999999999

Table 5.7 Axis Transformation Program Results - Unity and Zero Input at Euler Parameters

By making use of the trace function the program could be monitored at each operation. Unfortunately the PRIME trace facility is unnecessarily restrictive only printing out eleven places of fourteen figure numbers. Consequently the small cross coupling errors which were then the subject of the investigation were difficult to identify without temporarily modifying the main programs.

However, it soon became apparent that the major reasons for the errors lay in the inaccuracy of the trigonometric functions and their inverses which were in the PRIME and Company generated libraries. In particular the inverse cosine function was only accurate to 6 to 7 significant places. Furthermore there were occasions where the results were irritating to the reader, for instance $\cos(0) = 0.\dot{9}$.

Fortunately Roberts (142) had reason to investigate techniques for obtaining approximation to the trigonometric functions.

Trigonometric Approximation Techniques

Based on the theory and program listing of reference (142) the sine, cosine and tangent functions were generated through the use of a 6th order Thiele approximations. The input range is unrestricted but is reduced to lie in the range $\pm\Pi/4$ by the first part of the program. The results have found to be accurate to within 2 in 10^{14} compared to reference (143).

To investigate whether these accuracies were machine or method restricted a higher order Theile algorithm was used in an attempt to improve accuracy in the last place but without success. It was concluded that the errors were caused by truncation and rounding errors rather than limitations of the method.

As a comparison, functions for obtaining Taylor Series sine, cosine and tangent functions were also written. These included terms to 10^{-26} in magnitude.

A technique using iterative square root functions to generate inverse sine, cosine and tangent functions designed by Roberts was also adopted. These functions were sign validated in each octant and accuracy evaluated over the range $\pm$ 10 radians in step sizes of 0.1 radian. The techniques used were compared to reference (143) and found to be consistently accurate to 1 in 10^{14}.

The functions were loaded into special programs to be timed using loops stepping the function inputs over the range 0-10 radians in 10^{5} increments and the inverse function between 0-1 in 10^{5} increments. The results are given in table 5.8.

When comparing the techniques for operational speed it must be borne in mind that the PRIME functions are written in machine code and the Roberts/Theile and Taylor function are written in

Function Under Test		Login Time (min)	CPU Total (sec)	Function Run time (CPU sec)
Sine:	Prime	0	20	13.78
	Roberts/Thiele	1	68	61.79
	Taylor	5	279	272.96
Cosine:	Prime	0	20	14.35
	Roberts/Thiele	1	66	60.07
	Taylor	5	276	269.82
Tangent:	Prime	0	47	41.00
	Roberts/Thiele	1	67	60.88
	Taylor	5	277	270.79
Arcsin:	Prime	1	53	46.91
	Roberts	22	1237	1231.17
Arccos:	Prime	1	84	77.62
	Roberts	23	1324	1317.78
Arctan:	Prime	1	19	12.81
	Roberts	21	1199	1192.90

Table 5.8 Trigonometric Function Run Times

Trig functions 10^5 cycles 0-10 rad step size 10^{-4}

Inverse trig functions 10^5 cycles 0-1 step size 10^{-5}

Fortran IV, which is slower. Nevertheless the immediate speed advantage of the non-iterative Roberts/Thiele method can be seen when compared to the Taylor method. The Roberts/Thiele method has an added advantage that both sine and cosine values are available after one pass, if both are required the function needs only to be called once.

The high precision trigonometric functions were used to repeat the cosine matrix transformation described earlier. The results in table 5.9 shown the improved results.

ATTITUDE ANGLES
0.00000000000000
0.00000000000000 (ZERO AT INPUT)
0.00000000000000

EULER ANGLES
0.00000000000000
0.00000000000000 (1st STAGE ERROR)
0.00000000000000

DIRECTION COSINE MATRIX

1.0000000000000	0.00000000000000	0.00000000000000
0.00000000000000	1.0000000000000	0.00000000000000
0.00000000000000	0.00000000000000	1.0000000000000

EULER PARAMETERS
1.0000000000000
0.00000000000000 (2nd STAGE ERROR)
0.00000000000000
0.00000000000000

Table 5.9 Axis Transformation Program Results
Attitude Angle Inputs are all Zero

The Roberts/Thiele trigonometric techniques were adopted for use in the simulation where high accuracy is important. It is not claimed that this is necessarily the optimum technique however it is an attractive solution offering the following advantages:

(a) available and proven,

(b) quick to program (simple coding only),

(c) faster than the Taylor Series techniques,

(d) validated over the working range to full variable length.

Final testing and evaluation of the axis transformation subroutines was accomplished through the following technique:

(a) input attitude angles (range $\pm$ Π rad),

(b) form direction cosine matrix,

(c) decompose to attitude angles,

(d) form second direction cosine matrix from decomposed attitude angles,

(e) subtract the second direction cosine matrix from the initial direction cosine matrix,

(f) calculate the residual (sum of the absolute values of all terms) of the resulting matrix.

The results for each computational precision are given below:

PRECISION	RESIDUAL
SINGLE	<5.0 E-3
DOUBLE	<1.0 E-4
HIGH	<2.0 E-6

Table 5.10 Cosine Matrix Decomposition Accuracy Summary

The angular validation was conducted in two phases. The initial approach was to apply a single moment, in body axis, about each axis in turn on the air vehicle and to ensure that the torque causes the appropriate angular velocity and that this integrates correctly to give the appropriate attitude angle. Further, inputs were selected so that the angular motion was large enough to demonstrate that more than one revolution about any axis of the air vehicle could be modelled without discontinuities occurring (particularly at the 180 and 360 degree positions).

Once the initial correct sign and sense was demonstrated, single moments as functions of time, were input to produce angular accelerations and velocities of both signs such that the resultant final angles and velocities should be zero. The theoretical motion is shown in Table 5.11.

Time sec	Input Torque Nm	Angular Acceleration rad/s^2	Angular Velocity at end of period rad/s	Angular Displacement at end of period rad
0-5	0.000	0.000	0.000	0.000
5-10	1.040	0.520	2.600	6.500
10-15	0.000	0.000	2.600	19.500
15-20	-1.040	-0.520	0.000	26.000
20-25	0.000	0.000	0.000	26.000
25-30	-1.040	-0.520	-2.600	19.500
30-35	0.000	0.000	-2.600	6.500
35-46	1.040	0.520	0.000	0.000
40-45	0.000	0.000	0.000	0.000

Table 5.11 Angular Validation Motion for Air Vehicle with Moment of Inertia = 2.0 kgm^2

Using a fixed integration interval of 1 millisecond results given in table 5.12 were achieved.

Finally moments of 1.040 Nm and forces of 10 N were applied simultaneously in accordance with the signs and time periods of table 5.11. The resultant errors are shown in table 5.13. This run was again carried out using an integration interval of 1 milli second.

The accuracy testing of the six degrees of freedom module showed that angular accuracies of considerably better than 1 micro-radian and linear accuracies within 10 nanometres were achieved using typical velocities for durations of 45 seconds.

Simulation File	Input Axis Torque	Angular Resultant Error			Resultant Angular Velocity		
		Bank rad	Azimuth rad	Inclination rad	p rad/s	q rad/s	r rad/s
DRUNFL46	L	-0.603E-5	0.000	0.603E-5	-0.139E-9	0.000	0.000
DRUNFL47	M	0.603E-5	0.157E-8	0.603E-5	0.000	-0.139E-9	0.000
DRUNFL48	N	0.603E-5	0.000	-0.603E-5	0.000	0.000	-0.139E-9

Table 5.12 Angular Validation Results

Simulation File	Simulation Data Files	Input Force/ Torque	Angular Resultant Error		Resultant Linear Errors	
			Angle (rad)	Velocity (rad/s)	Displacement	Velocity
			Bank	p	x_0	u
			Azimuth	q	y_0	v
			Inclination	r	z_0	w
DRUNFL49	DRP12D	XYZ	-0.155E-8	-0.139E-9	-0.259E-8	-0.474E-10
	DSICN11	LMN	-0.155E-8	-0.139E-9	-0.259E-8	-0.474E-10
	DCOND4		-0.155E-8	-0.139E-9	-0.259E-8	-0.474E-10

Table 5.13 Linear and Angular Combined Validation

5.7 Variable Integration Interval Testing

The variable integration internal function was validated by carrying out tests to verify the following:

(a) that the permissible error is not exceeded at any point during the run*,

(b) that the integration time period was adjusted in accordance with design aims.

As a further exercise the influence of the permissible error and maximum integration interval on run time was investigated.

Linear and angular validation was conducted in four phases. Firstly a maximum run time of 50 seconds real time was selected. During this period an X force of peak value 10 Newtons was injected at a frequency of 1 Hertz as specified in table 5.14. The motion of the air vehicle is shown in figures 5.5 and 5.6.

Time Period (sec)	X Force (N)
0-20	10 sin 2πt
20-25	0.0
25-45	-10 sin 2πt
45-50	0.0

Table 5.14 Variable Integration Interval Validation - Simulation Program 1 Hertz Force Input

* The author ensured that the smallest integration step size was sufficiently low to obviate any influence on these results.

The second phase of the validation was to use a maximum run time of 500 seconds real time and inject a force at 0.1 hertz with a peak value of 10 Newtons as specified in table 5.15. Figures 5.7 and 5.8 show the air vehicle motion.

The third and fourth phases, similar to the first and second, were carried out using an input torque of 1.040 Nm at frequencies of 1.0 and 0.1 Hertz.

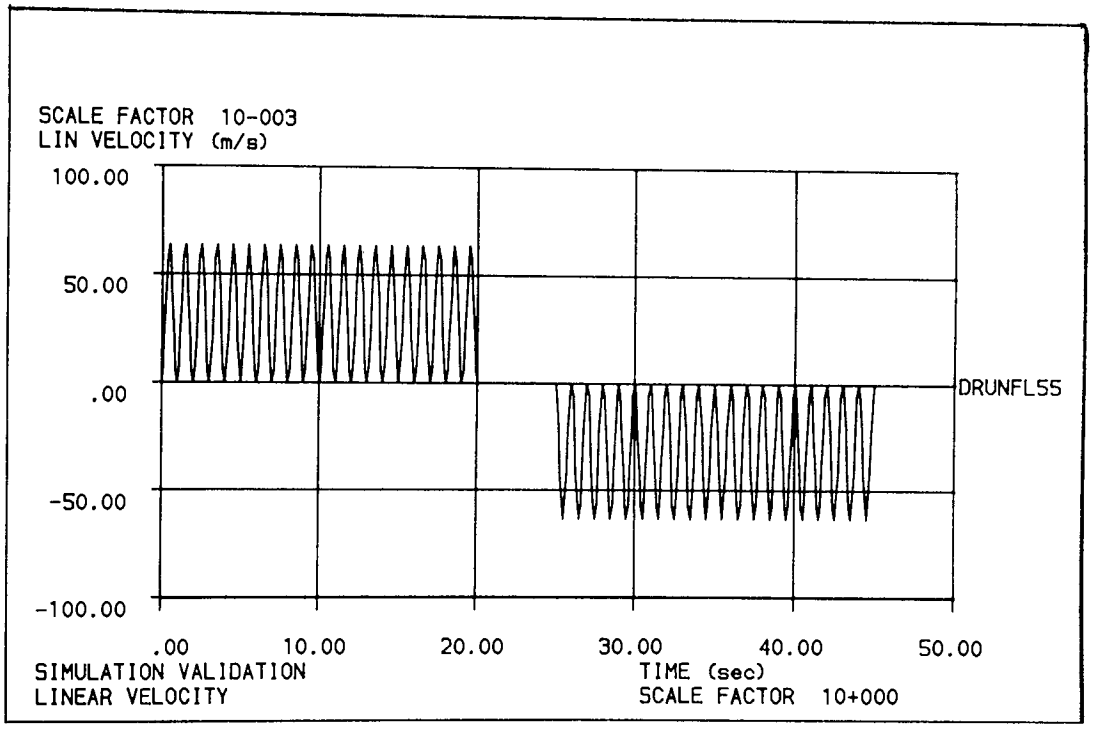

Figure 5.5 Phase 1 Validation Velocity

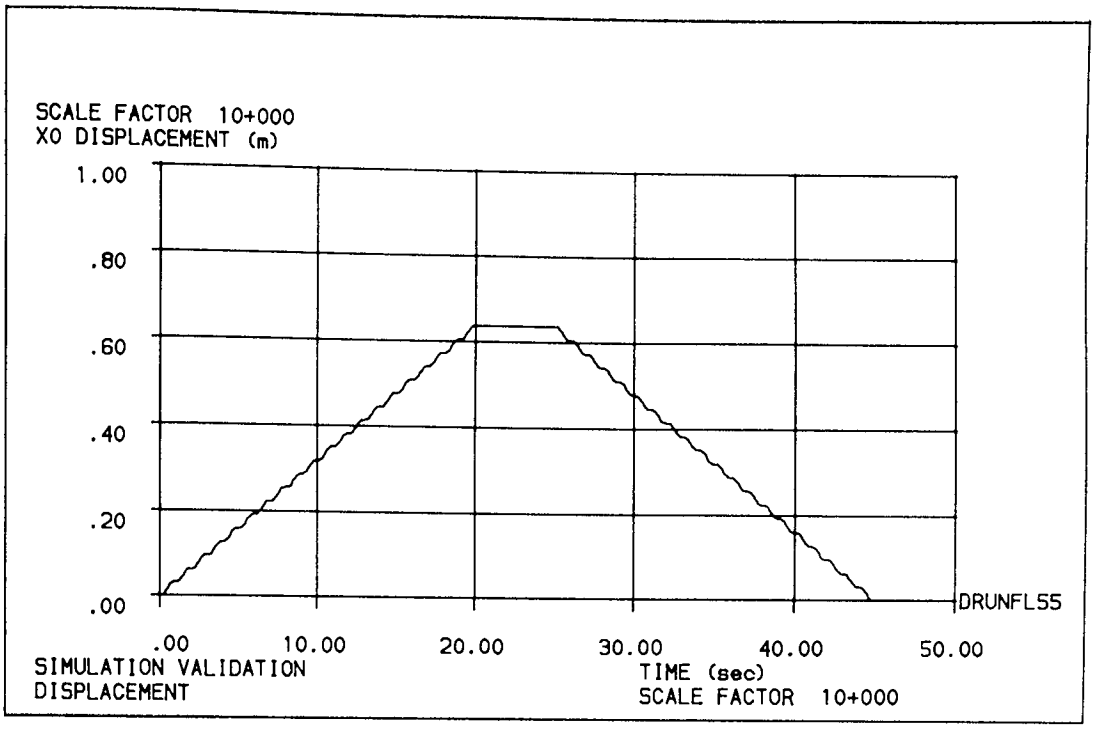

Figure 5.6 Phase 1 Validation Displacement

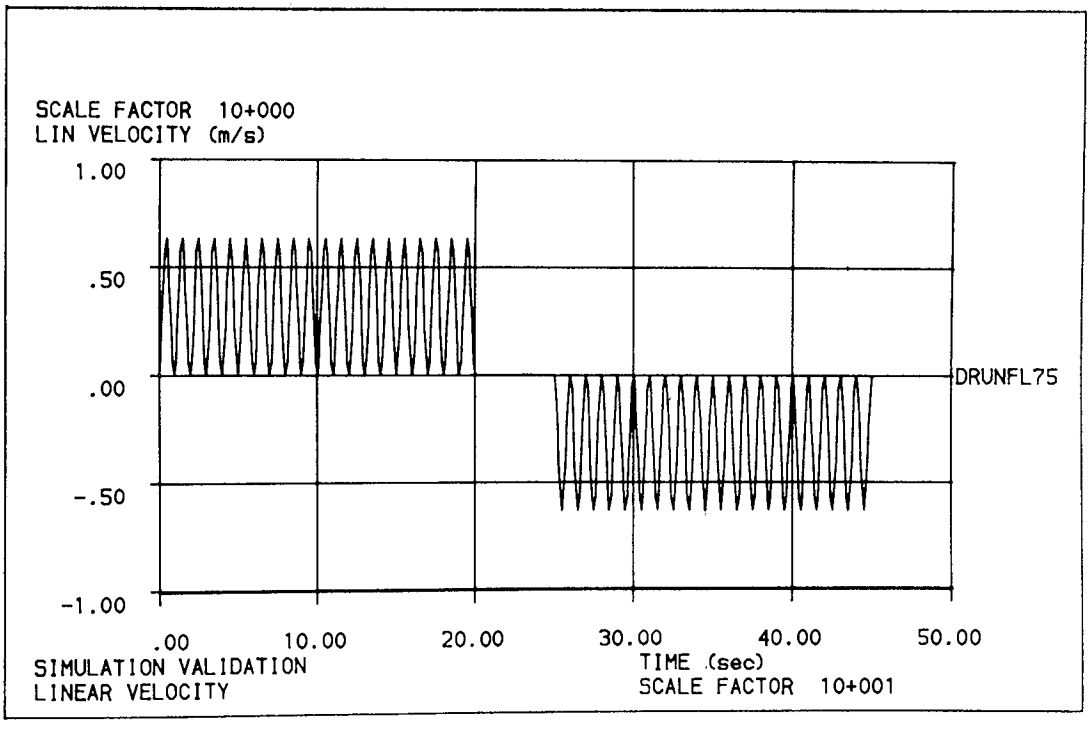

Figure 5.7 Phase 2 Validation Velocity

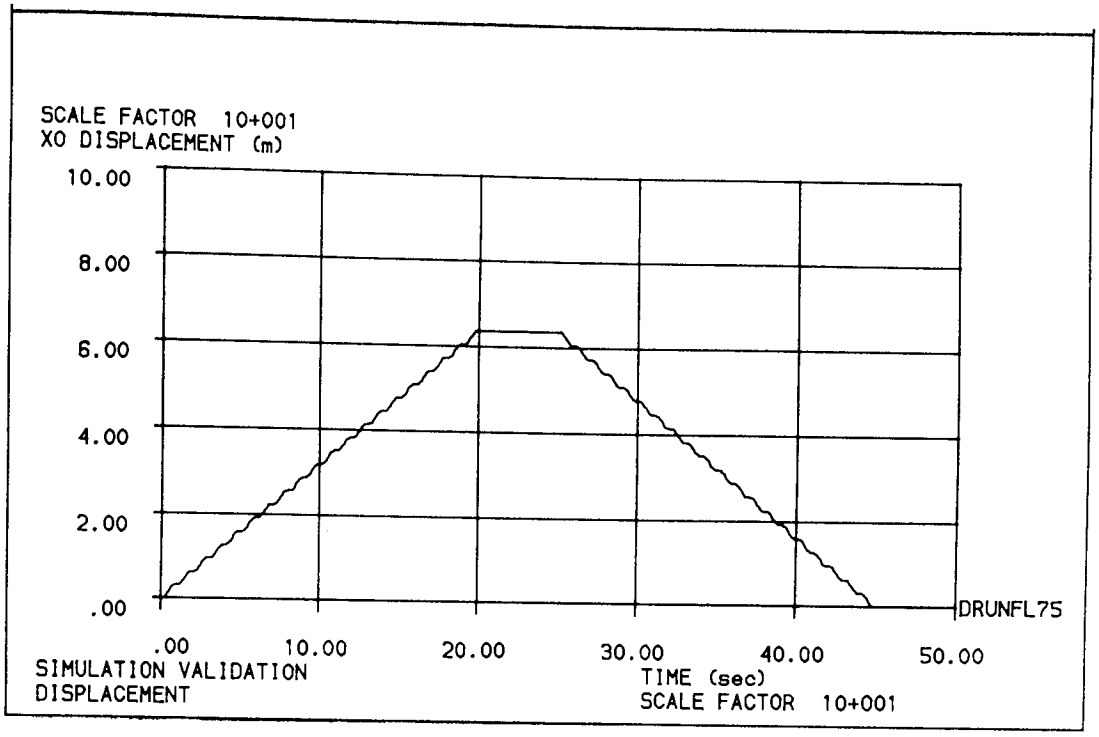

Figure 5.8 Phase 2 Validation Displacement

Time Period (sec)	X Force (N)
0-200	10 sin 0.2 πt
200-250	0.0
250-450	-10 sin 0.2πt
450-500	0.0

Table 5.15 Variable Integration Interval Validation - Simulation Program 0.1 Hertz Input

Validation runs were carried out limiting the maximum integrations step size within the range 1 x 10^{-2} to 10 seconds and limiting the maximum error between order 2 and order 4 integration within the range 1 x 10^{-10} to 1 x 10^{-2}.

Sample graphical output from phases one and two are shown in figures 5.9 to 5.12. Tables 5.16 to 5.19 show the overall resultant errors and the simulation run time.

Phases one and two were controlled using one appropriate element of the state vector and phases three and four were controlled using six elements of the state vector. This technique was adopted to prove the single and multi-element integration monitoring facilities.

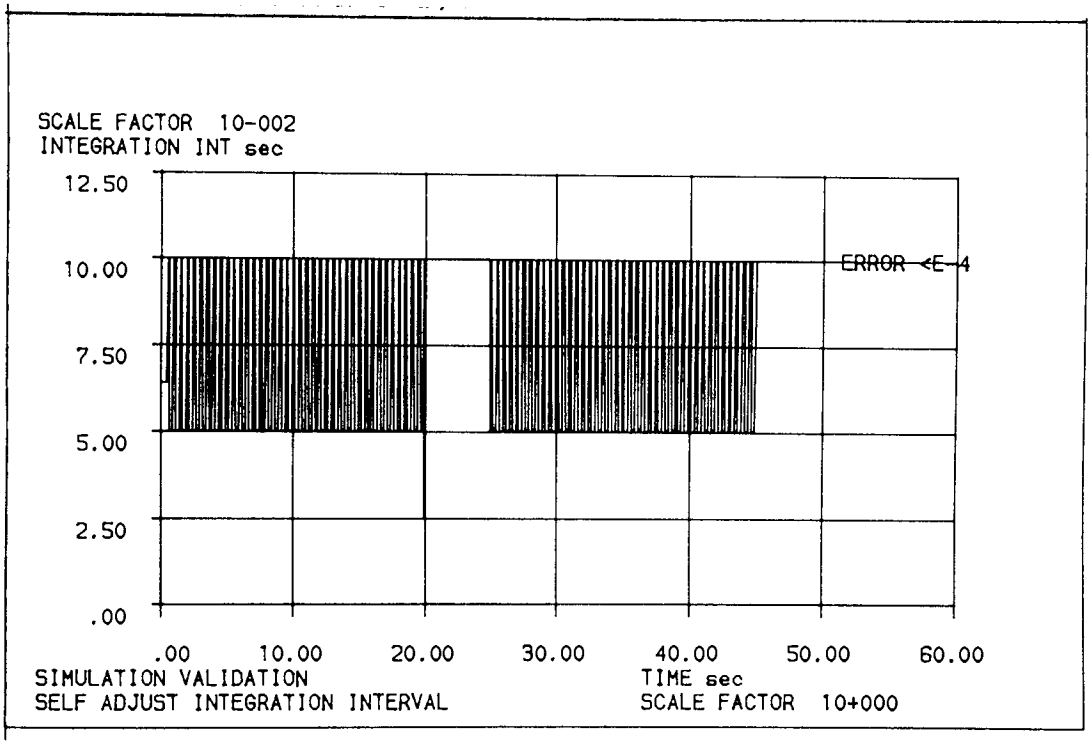

Figure 5.9 Example Output - Integration Interval Vs Time (DRUNFL57)

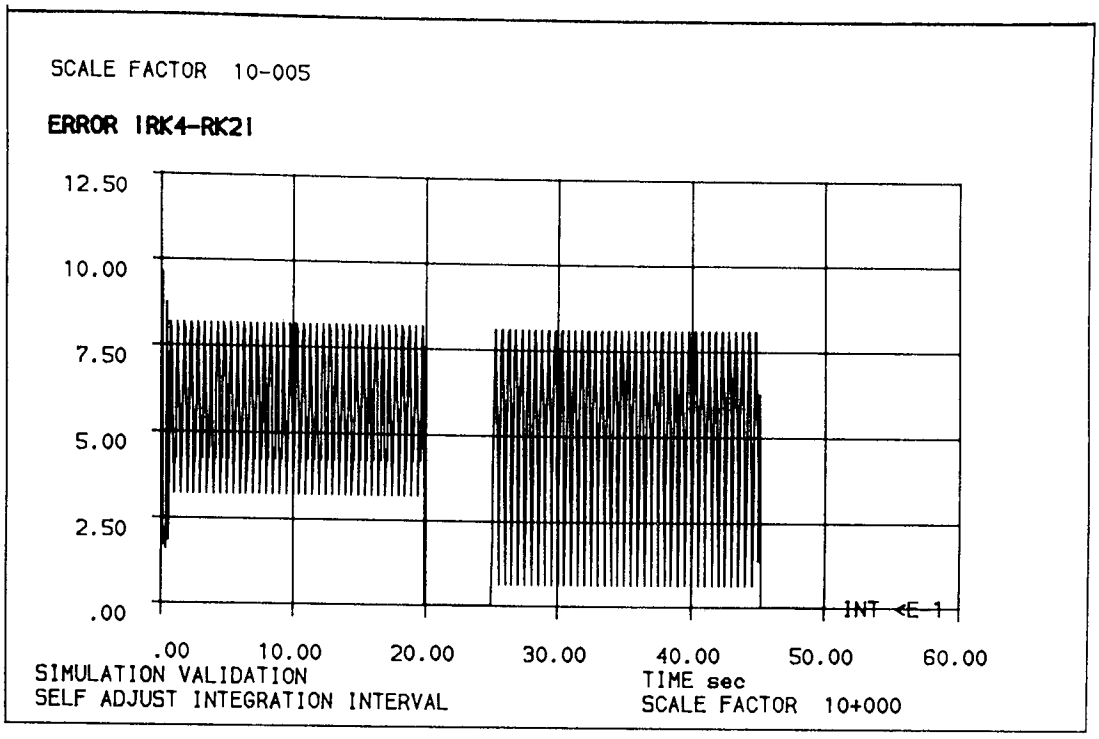

Figure 5.10 Example output - Error between Runge Kutta Orders 2 and 4 Vs Time (DRUNFL57)

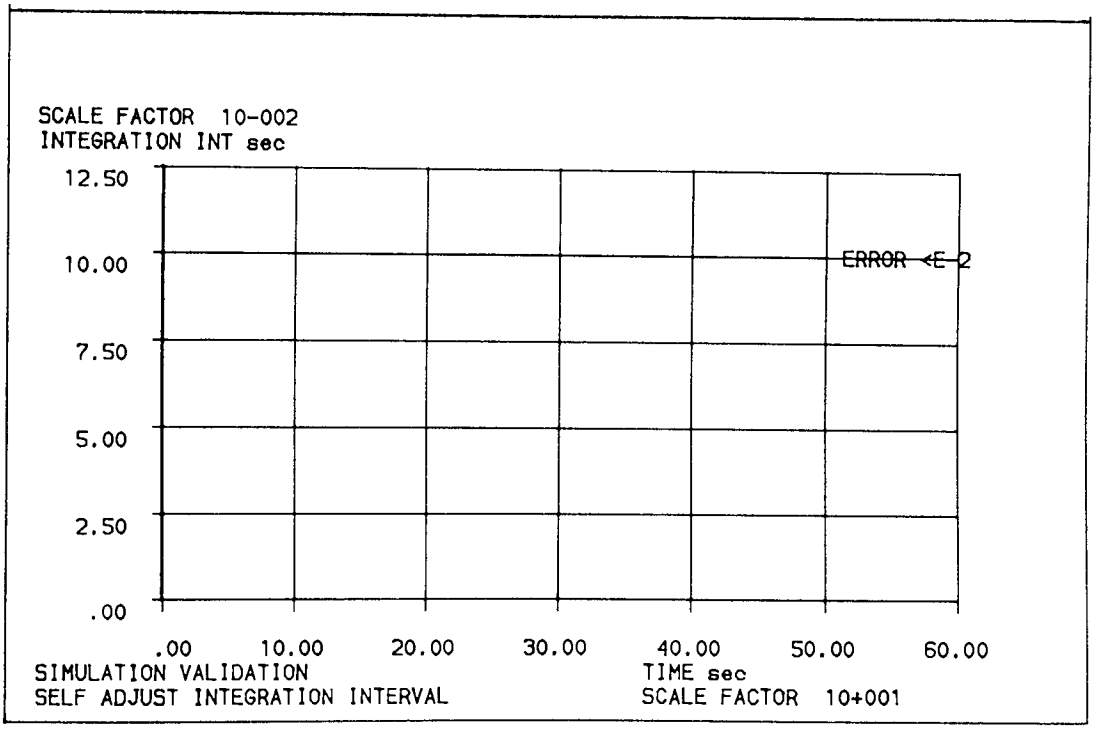

Figure 5.11 Example output - Integration Interval Vs Time (DRUNFL71)

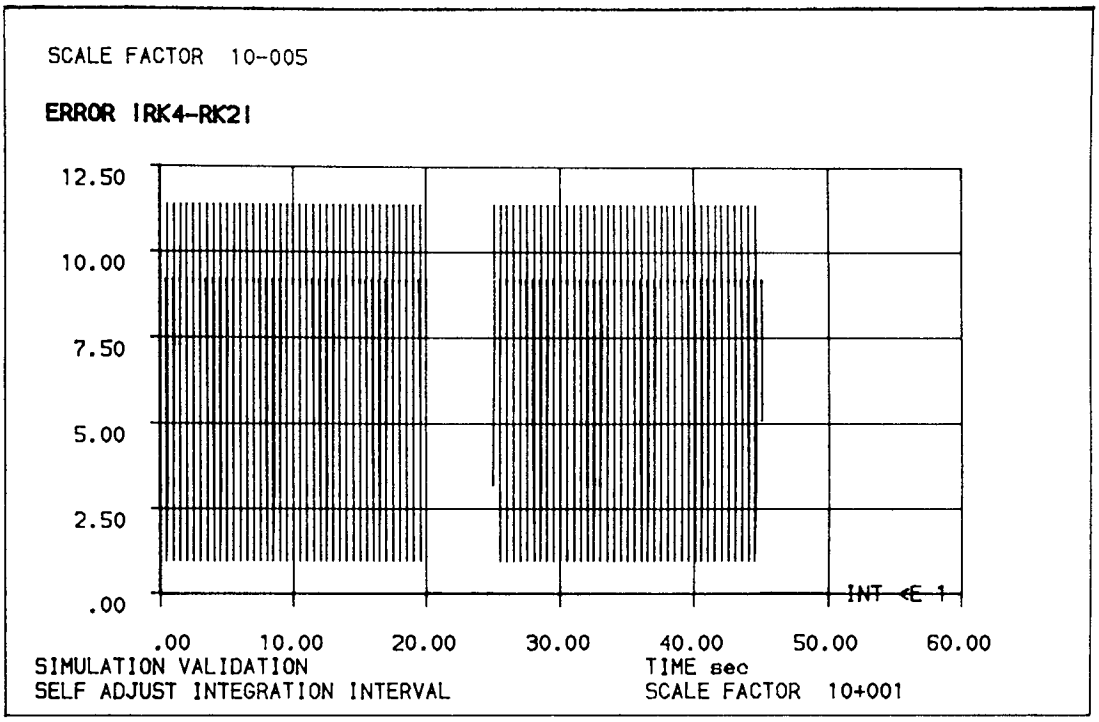

Figure 5.12 Example output - Error between Runge Kutta Orders 2 and 4 Vs Time (DRUNFL71)

Run	Integration Interval max (sec)	Error |RK4-RK2| max	Velocity @ 22 sec m/s	Displacement @ 22 sec m	Velocity @ 50 sec m/s	Displacement @ 50 sec m	Login Time min	CPU Usage se
DRUNFL51	1E-2	1E-2	0.524E-5	0.6366	0.524E-5	0.262E-3	6	352
DRUNFL52	1E-2	1E-4	0.524E-5	0.6366	0.524E-5	0.262E-3	6	352
DRUNFL53	1E-2	1E-6	-0.840E-12	0.6366	-0.542E-12	-0.821E-10	6	351
DRUNFL54	1E-2	1E-8	-0.166E-11	0.6366	-0.323E-11	-0.330E-7	27	1507
DRUNFL55	1E-2	1E-10	-0.667E-11	0.6366	-0.138E-10	-0.107E-8	120	6739
DRUNFL56	0.1	1E-2	-0.106E-3	0.6364	-0.106E-3	-0.531E-2	1	60
DRUNFL57	0.1	1E-4	-0.649E-5	0.6366	0.921E-5	-0.401E-3	1	89
DRUNFL58	0.1	1E-6	0.207E-6	0.6366	0.350E-6	0.649E-5	8	485
DRUNFL59	0.1	1E-8	-0.166E-11	0.6366	0.995E-9	-0.768E-8	31	1771
DRUNFL60	0.1	1E-10	-0.667E-11	0.6366	-0.135E-10	-0.148E-8	117	6546
DRUNFL61	1.0	1E-2	-0.106E-2	0.6347	-0.133E-2	-0.484E-1	0	21
DRUNFL62	1.0	1E-4	-0.260E-4	0.6366	-0.190E-5	-0.459E-3	2	130
DRUNFL63	1.0	1E-6	-0.207E-6	0.6366	-0.207E-6	0.166E-5	8	486
DRUNFL64	1.0	1E-8	-0.166E-11	0.6366	-0.312E-11	-0.466E-7	30	1689
DRUNFL65	1.0	1E-10	-0.667E-11	0.6366	-0.336E-11	-0.327E-9	88	4960
DRUNFL66	10	1E-2	-0.106E-2	0.6336	-0.358E-3	-0.373E-1	0	26
DRUNFL67	10	1E-4	-0.260E-4	0.6366	-0.225E-3	-0.632E-2	2	132
DRUNFL68	10	1E-6	-0.207E-6	0.6366	0.209E-6	0.111E-4	8	485
DRUNFL69	10	1E-8	-0.166E-11	0.6366	-0.188E-11	-0.130E-9	28	1571
DRUNFL70	10	1E-10	-0.667E-11	0.6366	-0.108E-10	-0.111E-8	87	4859

Table 5.16 Phase 1 Variable Integration Validation Results (Linear)

Run	Integration Interval max (sec)	Error |RK4-RK2| max	Velocity @ 22 sec m/s	Displace-ment @ 22 sec m	Velocity @ 50 sec m/s	Displace-ment @ 50 sec m	Login Time min	CPU Usage
DRUNFL71	0.1	1E-2	-0.107E-4	63.662	-0.107E-4	-0.537E-2	6	351
DRUNFL72	0.1	1E-4	-0.149E-4	63.662	-0.149E-4	-0.747E-2	6	351
DRUNFL73	0.1	1E-6	-0.105E-7	63.662	-0.105E-7	-0.524E-5	11	634
DRUNFL74	0.1	1E-8	-0.484E-10	63.662	-0.602E-10	-0.167E-6	70	3913
DRUNFL75	0.1	1E-10	-0.399E-9	63.662	0.408E-10	-0.170E-6	418	16725
DRUNFL76	1.0	1E-2	-0.452E-3	63.662	-0.452E-3	-0.226	3	62
DRUNFL77	1.0	1E-4	-0.211E-4	63.662	-0.212E-4	-0.106E-1	67	208
DRUNFL78	1.0	1E-6	-0.272E-6	63.662	-0.129E-6	-0.101E-3	57	1003
DRUNFL79	1.0	1E-8	-0.484E-10	63.662	0.193E-9	-0.620E-7	283	4065
DRUNFL80	1.0	1E-10	-0.399E-9	63.662	-0.560E-9	-0.172E-6	320	15978
DRUNFL81	10	1E-2	0.307E-3	63.679	0.316E-3	-0.217	1	61
DRUNFL82	10	1E-4	-0.256E-5	63.662	-0.256E-5	-0.702E-2	4	226
DRUNFL83	10	1E-6	-0.272E-6	63.662	-0.153E-6	-0.841E-4	18	949
DRUNFL84	10	1E-8	-0.484E-10	63.662	-0.813E-10	-0.530E-6	65	3411
DRUNFL85	10	1E-10	-0.399E-9	63.662	-0.535E-9	-0.179E-6	229	12211

Table 5.17 Phase 2 Variable Integration Validation Results (Linear)

Run	Integration Interval max (sec)	Error |RK4-RK2| max	No state Variables Monitored	Velocity @ 22 sec rad/s	Displacement @ 22 sec rad	Velocity @ 50 sec rad/s	Displacement @ 50 sec rad	Login Time min	CPU Usage sec
DRUNFL91	0.1	1E-2	6	0.2093E-2	0.1540	0.2093E-2	0.1048	1	98
DRUNFL92	0.1	1E-4	6	-0.6142E-4	0.1651	-0.5261E-4	-0.2290E-2	9	517
DRUNFL93	0.1	1E-6	6	-0.4265E-10	0.1655	0.1580E-10	0.1073E-4	46	2550
DRUNFL94	0.1	1E-8	6	-0.1347E-10	0.1655	-0.1565E-10	-0.2089E-4	216	11912
DRUNFL95	0.1	1E-10	6	-0.4861E-10	0.1655	-0.5777E-10	-0.4633E-4	1345*	58682
DRUNFL96	1.0	1E-2	6	-0.1410	-1.735	-0.1229	0.8938	1	98
DRUNFL97	1.0	1E-4	6	-0.6142E-4	0.1651	-0.6152E-4	-0.2653E-2	8	467
DRUNFL98	1.0	1E-6	6	-0.4265E-10	0.1655	0.1037E-6	-0.1049E-4	50	2772
DRUNFL99	1.0	1E-8	6	-0.1347E-10	0.1655	0.4963E-9	-0.2190E-4	239	13192
DRUNFL100	1.0	1E-10	6	-0.4861E-10	0.1655	-0.6084E-10	-0.4536E-4	1295*	57014
DRUNFL101	10	1E-2	6	-0.1410	-1.886	0.8031E-2	2.8310	1	87
DRUNFL102	10	1E-4	6	-0.6142E-4	0.1651	-0.2722E-4	-0.2301E-2	8	465
DRUNFL103	10	1E-6	6	-0.4265E-10	0.1655	-0.2097E-12	-0.9828E-5	50	2763
DRUNFL104	10	1E-8	6	-0.4861E-10	0.1655	-0.6574E-10	-0.4519E-4	238	13135
DRUNFL105	10	1E-10	6	-0.4861E-10	0.1655	-0.6574E-10	-0.4519E-4	1021*	56328

* These runs were partially performed with other users on the computer

Figure 5.18 Phase 3 Variable Integration Validation Results (Angular)

Run	Integration Interval max (sec)	Error |RK4-RK2| max	No state Variables Monitored	Velocity @ 220 sec rad/s	Displacement @ 220 sec rad	Velocity @ 500 sec rad/s	Displacement @ 500 sec rad	Login Time min	CPU Usage sec
DRUNFL106	0.1	1E-2	6	2.1577	-0.2793E-4	-0.1416E-1	-0.2793E-4	6	320
DRUNFL107	0.1	1E-4	6	2.1583	-0.2069E-5	0.2423E-2	0.3376E-5	6	320
DRUNFL108	0.1	1E-6	6	2.1583	-0.1762E-6	-0.5030E-3	-0.1761E-6	26	1434
DRUNFL109	0.1	1E-8	6	2.1583	-0.1256E-9	-0.1374E-4	-0.2406E-9	96	5305
DRUNFL110	0.1	1E-10	6	2.1583	-0.1714E-8	-0.4396E-5	-0.4810E-9	474	26265
DRUNFL111	1.0	1E-2	6	*	*	*	*	0	9
DRUNFL112	1.0	1E-4	6	*	*	*	*	1	59
DRUNFL113	1.0	1E-6	6	2.1583	-0.2720E-6	-0.7123E-3	-0.2721E-6	22	1124
DRUNFL114	1.0	1E-8	6	2.1583	-0.1256E-9	-0.1503E-4	0.5006E-9	89	4827
DRUNFL115	1.0	1E-10	6	2.1583	-0.1714E-8	-0.4216E-5	-0.2293E-8	516	28438
DRUNFL116	10	1E-2	6	*	*	*	*	0	6
DRUNFL117	10	1E-4	6	*	*	*	*	3	163
DRUNFL118	10	1E-6	6	2.1583	-0.2720E-6	-0.5887E-3	-0.2071E-6	21	1185
DRUNFL119	10	1E-8	6	2.1583	-0.1256E-9	-0.1256E-9	-0.2610E-9	100	5530
DRUNFL120	10	1E-10	6	2.1583	-0.1714E-8	-0.1714E-9	-0.2298E-8	512	28265

Fatal error halt due to non-orthogonal direction cosine matrix

Table 5.19 Phase 4 Variable Integration Validation Results (Angular)

Throughout the validation tests the maximum error between Runge Kutta orders 2 and 4 integration techniques was controlled to below the specified value at all times. The Integration step size was adjusted continually, if necessary, to achieve this and it can be observed that minimum and maximum permitted integration step size values for each run are selected at twice the exciting frequency. This would be expected because the minimum and maximum rates of change occur twice (with opposite signs) during each cycle. The only exception to this occurred when the maximum permitted integration step size gave satisfactory error results throughout the run.

The effects of integration step size and using the difference between Runge Kutta order 2 and order 4 processes as an integration time step controller on simulation run time, run cost and accuracy have been thoroughly investigated. These results may be used to select appropriate inputs for future simulation runs to ensure that a required accuracy is achieved for optimum run time and cost.

The policy of adopting dynamically adjusted integration time step size gave savings of up to one order of magnitude for typical simulation runs. Moreover, prior knowledge of air vehicle motion, which would be required for fixed time step integration, was not a pre-requisite for successful simulation runs.

5.8 Review

This section has presented the theoretical basis for the six degrees of freedom motion module. Confusion between attitude and Euler angles was identified in the literature. Basic definitions and transformations were re-stated to alleviate the confusion. Axes transformations based on the quaternion of Euler Parameters were identified and adopted for use in this work. A technique for varying the integration time step size was proposed and validation results presented.

SECTION 6

CO-AXIAL CONTRA-ROTATING TWIN ROTOR MODELS

6 CO-AXIAL CONTRA-ROTATING TWIN ROTOR MODELS

6.1 Introduction

The development of a system of equations describing the dynamics and aerodynamics of the SPRITE rotor system is discussed in this section making use of existing work wherever possible. Gaps in the knowledge base are identified and modelling techniques are proposed.

Previous researchers into rotor systems have concentrated on one of the following two separate but related fields. Firstly, detailed analyses of air flows, allowing knowledge to be gained of component strength requirements and the performance of specific elements of the individual rotor blades. Secondly, analyses yielding the overall performance of single rotor systems in terms of total rotor moments and forces as a function of blade conditions, vehicle motion and environmental conditions. The author identified a distinct lack of simulation models within the second category for multiple rotor systems, more specifically for the Co-axial Contra-Rotating Twin Rotor (CCTR) System.

It is important that whilst the model to be employed gives adequate visibility of component performance the overriding consideration of acceptably short run times must be borne in mind. In this section a new CCTR model is presented for a miniature plan symmetric helicopter. Axes system definitions

and transformations not given in the main text may be found in Appendix B.

6.2 Rotor Analysis Technique

Single rotor system analysis began early this century (144) and accelerated in the war years (145). A wide range of literature is available covering a variety of detailed analyses which have been carried out to determine the operational envelopes of rotor systems (112)(146)(147)(148). There are also simplified texts adopting pragmatic approaches drawing out the essential elements for model rotorcraft design (114).

The level of detail sought for simulation should account for the dynamics and aerodynamics of a rotor in sufficient depth to allow rotor coning and flapping angles to be estimated and should be sufficiently detailed to allow the physical characteristics of the rotor to be used to determine rotor performance in terms of total forces and moments. Additional detail which would impose a substantial iterative and computational burden was not required. It has already been shown in Section 5 (6df) that a likely integration time step size of 1 millisecond is of the order required to obtain the desired navigation accuracies.

Reports detailing this depth of simulation have been identified for single main rotor helicopters (149)(150)(151). Mathematical models similar to these have been used for real and slow time

simulation. Despite rigorous searches through published literature no suitable simulation models could be identified for twin rotor helicopters of either co-axial or side by side configuration of any physical size.

One model has been identified which Cranfield Institute have used for simulating Westland's Wideye air vehicle as part of the SUPERVISOR project (152), but this is a simplistic model used for human factor investigations concerned with the work load of RPV operators at the ground station and is inappropriate for control system development.

Until recently little work had been published on the complex aerodynamics of multi-rotors in a co-axial configuration, although earlier research investigated helicopters with tandem rotors (153). A fundamental approach to model a CCTR is to represent it as a single rotor with the same radius and number of blades as the twin rotor (154). This has the disadvantage of not estimating rotor shaft drag torque.

During the last decade work has been carried out to analyse the interactive effects of a CCTR using vortex strip theory (155) and local momentum theory (156)(157). However, whilst giving good results, both of these techniques require substantial computer power, typically up to 4 minutes (156) to solve at each time step.

The aim of this part of the work is not to provide a tool suitable for the optimisation of the rotors or to identify the operational limits of the rotor system. Previous work (158) has investigated the performance of multi-rotor systems and the optimisation of the design of such systems including the effects of the complex air flows resulting from the interactions of one rotor upon another.

In the absence of an appropriate model it was proposed that a system of equations for defining the performance of a co-axial contra-rotating twin rotor system would be developed based on equations for a full size single rotor model. This work is original in two major areas:

(a) applying a single rotor model developed for a full size helicopter to a miniature rotor,

(b) using single rotor modelling as a basis for simulating a CCTR by use of an empirical interaction coefficient.

The following sections describe in detail the single rotor model which is used as a basis for the simulation and the techniques used to extend this model for use when simulating a miniature Plan-Symmetric Helicopter (PSH).

6.3 Single Rotor Model

Analysis of rotor systems has been the subject of much work by individuals and government and commercial organisations (112)

(147)(146)(151)(159). The individual researcher's work is often limited by the amount of data available for validation of his theory. Work by commercial organisations is usually unpublished as the design techniques are closely guarded from competitors. The greatest source of validated knowledge is supplied by government sponsored bodies, such as the Royal Aircraft Establishment (RAE) in the UK and the National Advisory Committee for Aeronautics (NACA) in the US who have a combination of technical capability and adequate resources to commission testing work from manufacturers for validation and verification of theoretical work. This has resulted in the development of some useful validated models (149)(150)(151)(159).

It would be of little value to attempt to derive another system of equations here due to the disproportionate time which would be required and could be better spent on other aspects of simulation. Indeed, by developing a model around a core of a previously validated system of equations from a major authority such as the RAE, acceptance of data generated by such a model will be more readily attainable.

When deciding which of the existing single rotor models to use the following points were considered:

(a) the model must be a complete and compatible set of equations (including any assumptions),

(b) the axes systems and variables used should allow access to physical quantities,

(c) validation data should be published,

(d) the level of detail should not be so fine as to require integration along the rotor blades, but should otherwise be as detailed as possible.

It was considered that the set of equations should be complete and compatible so that assumptions and approximations follow through the work. It is important that the complete model is published in order that one can be confident that the validation and conclusions published are applicable to the system of equations programmed for simulation.

There are many axes systems used throughout rotor work, some have a physical basis such as body axes which are aligned in the air vehicle whereas others are chosen to simplify analysis such as axes based on the plane of no feathering. So that data may be supplied which is more readily understood and useful for the system designer, preference is given to equations using axes systems related closely and simply to the air vehicle.

Although this simulation model will be validated against available data there are two reasons why independent validation and assessment data are important. Firstly, the original assessment of the work may indicate a major flaw in the model, which if used may also show up here. Secondly, there is only

limited accurate quantitative data available from the SPRITE rotor test programme, so the basis of the model should be already proven.

Conflicting with the desire for a simple model for fast computational running there is the inevitable requirement for detailed data such as blade coning and flapping motion. The major divide in rotor models which has a considerable impact on the run times are the detailed models which require integration along the blade itself and models which, through the use of approximations, include a closed form expression for the determination of overall force and moment performance of the rotor. Consequently, as microscopic data was not being sought for rotor component design and stress analysis, a model which did not require integration along the blade was adopted.

Several single rotor models have been identified as satisfying the majority of the stated requirements (149)(150)(151)(159). Models such as those used by Price (160) were rejected as they adopted a detailed approach demanding integration along the blade. References such as (150) and (159) were rejected as they did not give adequate detail of the modelling equations and their derivation. Two full size helicopter models by RAE (149)(151) were identified as adopting the required depth of detail and they had also been validated with full size helicopters. The final choice was that of Padfield (151) in preference to Wilcock (149) for two reasons. Firstly Wilcock

(149) uses no-feathering axes as recommended by Bramwell (112) which are not fixed with reference to the air vehicle body. In contrast Padfield (151) uses shaft wind axes which have a simple relationship to body axes and as a result any data generated from this model such as flapping angles will be more readily useful to the system designer. If required they could be measured during trials, perhaps photographically, with reference to the air vehicle body. The second argument for selecting Padfield's model is that it is chronologically later and has made use of Wilcock's work.

Once the basis of the single rotor model has been selected it remains to state the equations in the form in which they have been implemented and indicate where they have been extended from the original work for this simulation model.

SINGLE ROTOR MODEL BASIS

The basis of the single rotor model is that developed by Padfield (151) at RAE for a single anti-clockwise rotating rotor. The rotor consists of rigid constant chord blades hinged to allow flapping motion; the method allows stiffness of the hinge to be incorporated. Lag freedom is not included in the model and this would appear to be a reasonable assumption as SPRITE has no lag hinge, any lag motion would be due to bending of the blade and as a consequence is assumed to be of second order. Linearly varying blade twist can be defined. Blade twist due to washout, as a function of thrust, has not been

incorporated as there is no empirical data for SPRITE available for modelling this effect. However, adding an interative loop to provide this feature would be a relatively simple matter, but would increase simulation run time.

The blade pitch angle, collective and cyclic components, are updated once per rotor cycle. The collective angle input to the rotor model as used in this dual rotor simulation contains components of common collective and differential control angles. The blade flapping angles are assumed small in the analysis so that linearity and small angle assumptions can be invoked. Overall fuselage accelerations are assumed small compared to blade accelerations and are neglected in the analysis. Similarly blade weight effects are assumed small compared to other forces acting on the blade and are neglected.

Further assumptions are made regarding the aerodynamics of the rotor so that closed form expressions for the rotor force and moment coefficients can be derived by analytical integration of the aerodynamic loading. Blade stall and reversed flow effects can only be incorporated by integrating along each blade and are hence ignored. Span wise variation in lift curve slope from Mach number and three dimensional effects also require individual blade integration so a constant two dimensional lift curve slope approach is adopted. Up to moderate Mach numbers, lift curve slope variation can be included by the use of a Prandtl-Glauert correction factor (161). Unsteady aerodynamic

effects and complex induced velocity distribution would also necessitate a more detailed approach so the former are neglected and the latter incorporated as a mean velocity distribution normal to the rotor disc satisfying momentum considerations with linear longitudinal variations. Ground effects are also neglected as the majority of the flight envelope falls outside the effected region.

Padfield (151) has developed a centre hinge model which can also be used to model hingeless and small offset articulated rotors through stiffness and inertia matching. He shows that the precision is adequate for generating overall loads by comparison with a full modal analysis. Coupling from blade pitch and lag dynamics into flapping motion are ignored and the interaction of disc tilt modes with fuselage modes is neglected.

In summary the following assumptions are embodied in the analysis:

(a) Flapping angles are assumed small so that linearity and small angle assumptions can be invoked.

(b) Overall fuselage accelerations and blade weight effects are assumed small compared to other accelerations and forces and are hence neglected in the rotor analysis.

(c) Yaw and side slip rates are assumed small compared to the rotor rotation rate.

(d) The rotor speed controller is assumed to govern the rotor at a constant speed.

(e) Unsteady and transient aerodynamic effects are ignored.

(f) Stall and reverse flow effects are ignored.

(g) The induced velocity distribution, normal to the rotor disc, includes linear longitudinal and lateral variations. The flow is described as a uniform flow added to a linearly varying distribution produced by the wake. (The flow at the centre satisfies simple momentum considerations).

(h) A constant, two dimensional, lift curve slope is assumed.

(i) Compressibility effects are ignored.

(j) Coupling from blade pitch and lag dynamics into flapping motion are ignored.

(k) Quasi-steady flapping and coning are assumed in calculating the forces and moments on the fuselage. This implies that the interaction of disc tilt modes with fuselage modes is neglected.

(l) Ground effects are ignored.

AERODYNAMIC VELOCITIES

The aerodynamic velocity is the velocity of the air vehicle relative to the air, it therefore includes body and wind velocities. In its existing form the model used by Padfield (151) required wind velocities to be input in inverted body axes. This meant that if the instantaneous body axis is

pointing north, a 10 m/s wind blowing north would require to be input as -10 m/s, following meteorological practice of denoting a wind direction from its source. This approach was thought to be inappropriate for the modelling work. Firstly, it is clear that average wind conditions will generally be constant in fixed earth axes and not in moving body axes. Secondly, in order to simplify the use of the simulation, which is designed for engineers, it is of assistance to reduce the number of axes systems to a minimum, at least those of which the user needs to be aware. The two main axes systems for inputs and outputs are fixed earth reference and instantaneous body axes. If users require to monitor variables within the rotor model such as flapping angles and harmonic components the data will be quantified relative to the appropriate axes, but for general force, moment velocity and displacement outputs the axes are those of fixed earth reference and instantaneous body.

Taking these points into account the simulation allows any wind to be entered in fixed earth axes such that a 10 m/s wind blowing north would be entered as +10 m/s. The following transformation allows the shaft wind vector to be determined:

$$\begin{bmatrix} u_A \\ v_A \\ w_A \end{bmatrix} = \begin{bmatrix} u - u_w \\ v - v_w \\ w - w_w \end{bmatrix}$$

and

$$\begin{bmatrix} u_s \\ v_s \\ w_s \end{bmatrix} = \begin{bmatrix} u_A \\ v_A \\ w_A \end{bmatrix} + \begin{bmatrix} 0 & -z_{cg} & +y_{cg} \\ z_{cg} & 0 & -x_{cg} \\ -y_{cg} & x_{cg} & 0 \end{bmatrix} \begin{bmatrix} p \\ q \\ r \end{bmatrix}$$

NORMALISED ROTOR VELOCITIES AND ACCELERATIONS

The rotor velocities and accelerations are used in normalised form to simplify the expressions for rotor coning and flapping. These are defined as:

$$\mu_x = \frac{u_s}{\Omega R} \qquad \dot{\mu}_x = \frac{\dot{u}_s}{\Omega R}$$

$$\mu_y = \frac{v_s}{\Omega R} \qquad \dot{\mu}_y = \frac{\dot{v}_s}{\Omega R}$$

$$\mu_z = \frac{w_s}{\Omega R}$$

The shaft wind axes are defined as sharing the z_s axis with the shaft axes with the x_{sw} and y_{sw} axes rotated about the z_s axis such that the x_{sw} axis is aligned with the resultant aerodynamic velocity in the x_s y_s plane. Hence there will be a zero v_{sw} velocity component.

The angle through which the shaft wind axes are rotated is defined such that:

$$\sin \psi_w = \frac{\mu_y}{\mu} \quad \text{and} \quad \cos \psi_w = \frac{\mu_x}{\mu}$$

Where the normalised resultant velocity $\mu = \sqrt{\left(\mu_x^2 + \mu_y^2 \right)}$

and $$\dot{\psi}_w = \frac{\left(\dot{\mu}_y \cos \psi_w - \dot{\mu}_x \sin \psi_w \right)}{\mu} \qquad (151)$$

it may be noted that $\mu_z = \frac{w_s}{\Omega R} = \frac{w_{sw}}{\Omega R}$

BLADE PITCH IN SHAFT WIND AXES

The rotor blade pitch angle is defined as having a common collective component θ_0 a linear twist component as θ_{tw} and sine and cosine cyclic components. The blade pitch vector in shaft wind axes is:

$$\begin{bmatrix} \theta_0 \\ \theta_{tw} \\ \theta_{1ssw} \\ \theta_{1csw} \end{bmatrix}$$

where $$\begin{bmatrix} \theta_{1ssw} \\ \theta_{1csw} \end{bmatrix} = \begin{bmatrix} T4 \end{bmatrix} \begin{bmatrix} \theta_{1s} \\ \theta_{1c} \end{bmatrix}$$

NORMALISED BODY RATES AND ACCELERATIONS

The vector of normalised instantaneous body rates and accelerations is defined as:

$$\begin{bmatrix} \dot{p}_{sw} \\ \dot{q}_{sw} \\ p_{sw} \\ q_{sw} \end{bmatrix}$$

where

$$\begin{bmatrix} \dot{p}_{sw} \\ \dot{q}_{sw} \end{bmatrix} = \begin{bmatrix} T4 \end{bmatrix} \begin{bmatrix} \dot{p} + \dot{\psi}_w q \\ \dot{q} - \dot{\psi}_w p \end{bmatrix}$$

and

$$\begin{bmatrix} p_{sw} \\ q_{sw} \end{bmatrix} = \begin{bmatrix} T4 \end{bmatrix} \begin{bmatrix} p \\ q \end{bmatrix}$$

It also follows that:

$$r_{sw} = r + \dot{\psi}_w$$

ROTOR AIR FLOW

Many attempts at modelling the air flow through the rotor have been made over the years, from relatively simplistic approaches where uniform flow is assumed (162) to more complex theories (163) where an account for non-uniform flow is made. Due to the complexity of non-uniform modelling there is a need to have detailed specific knowledge of the interaction between the air vehicle body and rotor system for a very wide range of air flow conditions. This knowledge is not available for this PSH configuration and attempts to estimate it could lead to errors which would negate any advantage obtained by adopting a complex analysis. Therefore it has been decided that a relatively simple model of the rotor airflow will be adopted.

The airflow through the rotor is assumed to be approximated by a uniform distribution with a longitudinal variation produced by the rotor wake. In normalised form the downwash distribution can be written as:

$$\lambda_i = \frac{V_i}{\Omega R} = \lambda_0 + \frac{r_B}{R} \left(\lambda_{1csw} \cos \psi + \lambda_{1ssw} \sin \psi\right) \qquad (151)$$

The uniform component, λ_0, is derived from momentum theory (144) and can be written as:

$$\lambda_0 = \frac{C_T}{2\sqrt{(\mu^2 + (\mu_z - \lambda_0)^2)}} \qquad (151)$$

Padfield acknowledges that this theory applies only to the rotor when it is operated in the helicopter or windmill modes. The vortex ring state between the other two states has been the subject of further investigations with attempts being made to fit correction factors to the theory (151)(164)(165). It has been observed that in the vortex ring state that large power and thrust changes accompany changes in rotor disk incidence.

Padfield (151) recommends the use of expressions developed by Coleman et al (145) to describe the fore and aft variation by recourse to a model of continuously shed circular vortex rings given by:

$$\lambda_{1csw} = \lambda_0 \tan\left(\frac{\chi}{2}\right) \qquad \chi < \frac{\pi}{2} \qquad (151)$$

$$\lambda_{1csw} = \lambda_0 \cot\left(\frac{\chi}{2}\right) \qquad \chi > \frac{\pi}{2} \qquad (151)$$

where $$\chi = \tan^{-1}\left(\frac{\mu}{(\lambda_0 - \mu_z)}\right) \qquad (151)$$

The lateral component is assumed to be zero ie:

$$\lambda_{1ssw} = 0 \qquad (151)$$

Corrections to this simplified approach have been investigated (151) through the use of the parameter ηa where:

$$\eta_a = \frac{1}{1 + (16/a_0 s)\lambda_0} = \frac{\left(\frac{\theta_0}{3(2C_T/a_0 s)} \right) - 1}{\left(\frac{\theta_0}{3(2C_T/a_0 s)} \right) + 1} \qquad (151)$$

Changes in ηa cause variations in flapping derivatives of up to 70% in some cases, but in teetering rotors Padfield (151) asserts that a practical cancellation occurs between this and an effect where a reduction in C_X and C_Y, the force coefficients from the thrust tilt value, causes the increased flapping to be reduced.

This model is appropriate to SPRITE's teetering rotor configuration.

Any of the usual iteration techniques can be employed to solve the downwash equations. However, successful convergence was achieved with Padfield's recommended technique employing the use of Newton's method with the addition of a correction factor, here denoted by ρ, which is set to a value of 0.6 to aid convergence. The equations used to solve for downwash can then be written as:

$$g_0 = \lambda_0 - \left(\frac{C_T}{\sqrt{2\Lambda}} \right) \qquad (151)$$

where

$$\Lambda = \mu^2 + (\mu_z - \lambda_0)^2 \qquad (151)$$

and

$$C_T = \frac{a_0 s}{2} \left(\theta_0 \left(\frac{1}{3} + \frac{\mu^2}{2} \right) + \frac{\mu}{2} \left(\theta_{1ssw} + \frac{\bar{p}_{sw}}{2} \right) \right. \qquad (151)$$

$$\left. + \left(\frac{\mu_z - \lambda_0}{2} \right) + \frac{1}{4} (1 + \mu^2) \theta_{tw} \right) \qquad (151)$$

Newton's method can then be expressed in the form,

$$\lambda_{0j+1} = \lambda_{0j} + \rho h_j (\lambda_{0j}) \qquad (151)$$

where

$$h_j = -\left(\frac{g_0}{(dg_0/d\lambda_0)} \right)_{\lambda = \lambda_{0j}} \qquad (151)$$

therefore

$$h_j = - \frac{\left(2\lambda_{0j} \Lambda^{1/2} - C_T \right) \Lambda}{2\Lambda^{\frac{3}{2}} + (a_0 s/4)\Lambda - C_T(\mu_z - \lambda_{0j})} \qquad (151)$$

Padfield (151) investigated areas where the solution may become unstable. However, when running the simulation, success was achieved using an initial estimate of λ_0 of unity for the first iteration and thereafter using the value from the preceding time step. The only conditions where convergence failed were where $\lambda_0 = 0$. These conditions are coincident with zero rotor thrust

i.e. when no downwash is generated. In practice this occurs at rotor blade angles of less than one degree from the line of no lift in still air.

ROTOR BLADE CONING AND FLAPPING

Flapping and coning equations as derived by Padfield based on a simplified central spring model are used for the single rotor simulation. Terms up to and including the first harmonic only are retained and these are transformed into multi-blade coordinates (166) and then reduced to a quasi-steady form (151). Coupling from blade pitch and lag dynamics is ignored. A synopsis of the derivations followed by Padfield (151) appears in Appendix D. The resultant expressions used to calculate the coning and sine and cosine cyclic flapping terms are quoted:

$$\beta_0 = \frac{n_\beta}{\lambda_\beta^2} \left[\left[1 + \mu^2 \;,\; \frac{4}{5} + \frac{2}{3}\mu^2 \;,\; \frac{4}{3}\mu \;,\; 0 \right] \begin{bmatrix} \theta_0 \\ \theta_{tw} \\ \theta_{1ssw} \\ \theta_{1csw} \end{bmatrix} + \left[\frac{4}{3}, \frac{-2}{3}\mu \;,\; 0 \right] \begin{bmatrix} \mu_z - \lambda_0 \\ \lambda_{1ssw} \\ \lambda_{1csw} \end{bmatrix} + \left[0 \quad 0 \quad \frac{2}{3}\mu \;,\; 0 \right] \begin{bmatrix} \bar{p}'_{sw} \\ \bar{q}'_{sw} \\ \bar{p}_{sw} \\ \bar{q}_{sw} \end{bmatrix} \right] \qquad (151)$$

$$\begin{bmatrix} \beta_{1csw} \\ \beta_{1ssw} \end{bmatrix} = \frac{-n_\beta}{\lambda_\beta^2\left(1+S_\beta^2\right)} \left\{ \begin{bmatrix} \frac{4}{3}\mu\left(S_\beta + \frac{2\lambda_\beta^2}{n_\beta}\right), & 2\mu\left(\frac{\lambda_\beta^2}{n_\beta} + \frac{8}{15}S_\beta\right), & \left(1+2\mu^2\right)\frac{\lambda_\beta^2}{n_\beta} + \left(\frac{4}{3}\mu\right)^2 S_\beta, & -\frac{\lambda_\beta^2}{n_\beta}S_\beta\left(1+\frac{\mu^2}{2}\right) \\ \frac{4}{3}\mu\left(1-2S_\beta\frac{\lambda_\beta^2}{n_\beta}\right), & 2\mu\left(\frac{8}{15}-S_\beta\frac{\lambda_\beta^2}{n_\beta}\right), & \left(\frac{4}{3}\mu\right)^2 - S_\beta\frac{\lambda_\beta^2}{n_\beta}\left(1+\frac{3}{2}\mu^2\right), & -\frac{\lambda_\beta^2}{n_\beta} \end{bmatrix} \begin{bmatrix} \theta_0 \\ \theta_{tw} \\ \theta_{1ssw} \\ \theta_{1csw} \end{bmatrix} \right.$$

$$+ \begin{bmatrix} \mu\left(\left(\frac{4}{3}\right)^2 S_\beta + \frac{2\lambda_\beta^2}{n_\beta}\right), & -\left(\frac{\lambda_\beta^2}{n_\beta}\left(1+\frac{\mu^2}{2}\right) + \frac{S_\beta}{2}\left(\frac{4}{3}\mu\right)^2\right), & \frac{\lambda_\beta^2}{n_\beta}S_\beta \\ \mu\left(\left(\frac{4}{3}\right)^2 - 2S_\beta\frac{\lambda_\beta^2}{n_\beta}\right), & -\frac{1}{2}\left(\frac{4}{3}\mu\right)^2 + \frac{\lambda_\beta^2}{n_\beta}S_\beta, & -\frac{\lambda_\beta^2}{n_\beta}\left(\frac{\mu^2}{2}-1\right) \end{bmatrix} \begin{bmatrix} \mu_z - \lambda_0 \\ \lambda_{1ssw} \\ \lambda_{1csw} \end{bmatrix}$$

$$\left. + \begin{bmatrix} \left(\frac{\lambda_\beta}{n_\beta}\right)^2\left(1+\frac{\mu^2}{2}\right), & -\left(\frac{\lambda_\beta}{n_\beta}\right)^2 S_\beta, & \frac{\lambda_\beta^2}{n_\beta}\left(1+\frac{\mu^2}{2}-\frac{2S_\beta}{n_\beta}\right) + \frac{S_\beta}{2}\left(\frac{4}{3}\mu\right)^2, & -\frac{\lambda_\beta^2}{n_\beta}\left(S_\beta + \frac{2}{n_\beta}\left(1+\frac{\mu^2}{2}\right)\right) \\ -\left(\frac{\lambda_\beta}{n_\beta}\right)^2 S_\beta, & \left(\frac{\lambda_\beta}{n_\beta}\right)^2\left(\frac{\mu^2}{2}-1\right), & \frac{\lambda_\beta^2}{n_\beta}\left(\frac{2}{n_\beta}\left(\frac{\mu^2}{2}-1\right) - S_\beta\right) + \frac{1}{2}\left(\frac{4}{3}\mu\right)^2, & \frac{\lambda_\beta^2}{n_\beta}\left(\frac{2S_\beta}{n_\beta} + \frac{\mu^2}{2} - 1\right) \end{bmatrix} \begin{bmatrix} \bar{p}'_{sw} \\ \bar{q}'_{sw} \\ \bar{p}_{sw} \\ \bar{q}_{sw} \end{bmatrix} \right\}$$

ROTOR FORCES AND MOMENTS

Expressions are developed by Padfield (151) for the force and moment coefficients by making the necessary assumptions to allow analytic integration to produce expressions which do not require individual integration along each blade. This, as previously discussed, is important to minimise simulation speed. The assumptions include:

(a) constant, 2D, lift curve slope,

(b) compressibility effects ignored (M=0),

(c) unsteady aerodynamic effect ignored,

(d) stall and reverse flow ignored.

A spanwise variation of curve slope from either Mach number or 3D effects and the inclusion of stall or reversed flow effects would require integration along each blade.

The expression developed by Padfield for the three force coefficients in shaft wind axes are given below (a summary of the derivation is included in Appendix D).

$$\left(\frac{2C_{Xsw}}{a_0 s}\right) = \left(\frac{F_0^{(1)}}{2} + \frac{F_{2c}^{(1)}}{4}\right) \beta_{1csw} + \frac{F_{1c}^{(1)}}{2} \beta_0 + \frac{F_{2s}^{(1)}}{4} \beta_{1ssw} + \frac{F_{1s}^{(2)}}{2} \qquad (151)$$

$$\left(\frac{2C_{Ysw}}{a_0 s} \right) = \left(- \frac{F_0^{(1)}}{2} + \frac{F_{2c}^{(1)}}{4} \right) \beta_{1ssw} + \frac{F_{1s}^{(1)}}{2} \beta_0$$

$$- \frac{F_{2s}^{(1)}}{4} \beta_{1csw} + \frac{F_{1c}^{(2)}}{2} \qquad (151)$$

$$\left(\frac{2C_{Zsw}}{a_0 s} \right) = - \left(\frac{2C_T}{a_0 s} \right) = - F_0^{(1)} \qquad (151)$$

where:

$$F_0^{(1)} = \theta_0 \left(\frac{1}{3} + \frac{\mu^2}{2} \right) + \frac{\mu^2}{2} \left(\theta_{1ssw} + \frac{\bar{p}_{sw}}{2} \right)$$

$$+ \left(\frac{\mu_z - \lambda_0}{2} \right) + 1/4 \ (1 + \mu^2) \ \theta_{tw}, \qquad (151)$$

$$F_{1s}^{(1)} = \frac{\alpha_{ssw} + \theta_{1ssw}}{3} + \mu \ (\theta_0 + \mu_z - \lambda_0 + \frac{2}{3} \theta_{tw}), \qquad (151)$$

$$F_{1c}^{(1)} = \frac{\alpha_{csw} + \theta_{1csw}}{3} - \mu \frac{\beta_0}{2} ,$$

$$F_{2s}^{(1)} = \frac{\mu}{2} \left\{ \theta_{1csw} - \beta_{1ssw} + \frac{\bar{q}_{sw} - \lambda_{1csw}}{2} - \mu\beta_0 \right\} \qquad (151)$$

$$F_{2c}^{(1)} = - \frac{\mu}{2} \left\{ \theta_{1ssw} - \beta_{1csw} + \frac{\bar{p}_{sw} - \lambda_{1ssw}}{2} \right.$$

$$\left. + \mu \left(\theta_0 + \frac{\theta_{tw}}{2} \right) \right\} ,$$

$$F_{1s}^{(2)} = \frac{\mu^2}{2}\ \beta_0\ \beta_{1ssw} + \left(u_z - \lambda_0 - \frac{\mu}{4}\ \beta_{1csw} \right) \alpha_{ssw}$$

$$- \frac{\mu}{4}\ \beta_{1ssw}\ \alpha_{csw} + \theta_0 \left(\frac{\alpha_{ssw}}{3} + \mu\ (\mu_z - \lambda_0)\ \frac{\mu^2}{4}\ \beta_{1csw} \right)$$

$$+ \left(\frac{\alpha_{ssw}}{4} + \frac{\mu}{2} \left(\mu_z - \lambda_0 - \frac{\beta_{1csw}\ \mu}{4} \right) \right) \theta_{tw}$$

$$+ \theta_{1ssw} \left(\frac{\mu_z - \lambda_0}{2} + \mu \left(\frac{3}{8}\ (\bar{p}_{sw} - \lambda_{1ssw}) + \frac{\beta_{1csw}}{4} \right) \right)$$

$$+ \frac{\mu}{4}\ \theta_{1csw} \left(\frac{\bar{q}_{sw} - \lambda_{1csw}}{2} - \beta_{1ssw} - \mu\ \beta_0 \right) - \frac{\delta\mu}{a_0} \qquad (151)$$

$$F_{1c}^{(2)} = - 2\beta_0\ \mu\ (\mu_z - \lambda_0 - \frac{3}{4}\ \mu\ \beta_{1csw})$$

$$+ (\mu_z - \lambda_0 - \frac{3}{4}\ \beta_{1csw}\mu)\ \alpha_{csw} - \frac{\mu}{4}\ \beta_{1ssw}\alpha_{ssw}$$

$$+ \theta_0 \left(\frac{\alpha_{csw}}{3} - \frac{\mu}{2} \left(\beta_0 + \frac{\mu}{2}\ \beta_{1ssw} \right) \right)$$

$$+ \theta_{tw} \left(\frac{\alpha_{csw}}{4} - \mu \left(\frac{\beta_0}{3} + \frac{\mu}{8}\ \beta_{1ssw} \right) \right)$$

$$+ \theta_{1csw} \left(\frac{\mu_z - \lambda_0}{2} + \frac{\mu}{4} \left(\frac{\bar{p}_w - \lambda_{1ssw}}{2} - \beta_{1csw} \right) \right)$$

$$+ \frac{\mu}{4}\ \theta_{1ssw} \left(\frac{\bar{q}_w - \lambda_{1csw}}{2} - \beta_{1ssw} - \mu\ \beta_0 \right) \qquad (151)$$

$$\alpha_{ssw} = \bar{p}_{sw} - \lambda_{1ssw} + \beta_{1csw}\ ,$$

$$\alpha_{csw} = \bar{q}_{sw} - \lambda_{1csw} - \beta_{1ssw}\ .$$

The force coefficients are converted into air vehicle shaft axes

by means of the inverse of the shaft to shaft wind transformation matrix:

$$\begin{bmatrix} C_X \\ C_Y \end{bmatrix} = \begin{bmatrix} T2 \end{bmatrix}^T \begin{bmatrix} C_{Xsw} \\ C_{Ysw} \end{bmatrix}$$

$$C_Z = C_{Zsw}$$

The shaft axes forces are then determined:

$$X_s = \frac{1}{2} \rho \pi R^2 (\Omega R)^2 a_0 s \begin{bmatrix} \frac{2C_X}{a_0 s} \end{bmatrix}$$

$$Y_s = \frac{1}{2} \rho \pi R^2 (\Omega R)^2 a_0 s \begin{bmatrix} \frac{2C_Y}{a_0 s} \end{bmatrix}$$

$$Z_s = \frac{1}{2} \rho \pi R^2 (\Omega R)^2 a_0 s \begin{bmatrix} \frac{2C_Z}{a_0 s} \end{bmatrix}$$

and then transformed into body axes (vertical rotor shaft)

$$\begin{bmatrix} X_R \\ Y_R \\ Z_R \end{bmatrix} = \begin{bmatrix} 1 & 0 & 0 \\ 0 & 1 & 0 \\ 0 & 0 & 1 \end{bmatrix} \begin{bmatrix} X_s \\ Y_s \\ Z_s \end{bmatrix}$$

Similarly the expressions for the moments are presented, writing the roll and pitch moments as functions of flapping angles and spring stiffness. The expression for the yaw moment coefficient includes a term for rotor accelerations should variable rotor speed be introduced at a later date. Again the derivation of the following function is outlined in Appendix D:

$$L_s = \frac{-b}{2} K_\beta \beta_{1s}$$

$$M_s = \frac{-b}{2} K_\beta \beta_{1c}$$

$$N_s = \frac{1\rho}{2} \left(\Omega R \right)^2 \pi R^3 \, a_0 s \left(\frac{2 \, C_Q}{a_0 s} + \left(\frac{2 I_\beta}{b I_\beta} \right) \frac{\bar{\Omega}'}{\gamma} \right)$$

where $\bar{\Omega}' = \frac{\dot{\Omega}}{\Omega^2}$

and

$$\left(\frac{2C_Q}{a_0 s} \right) \simeq - (\mu_z - \lambda_0) \left(\frac{2C_T}{a_0 s} \right) + \mu \left(\frac{2C_{Xsw}}{a_0 s} \right)$$

$$+ \frac{\delta}{4a_0} \left(1 + 2 \mu^2\right)$$

The effects of the rotor forces acting about a moment arm (the distance from the shaft hub to the cg) are included to determine the overall rotor moments in instantaneous body axes:

$$L_R = L_s + Y_s \, z_{cg} - Z_s \, y_{cg}$$

$$M_R = M_s + Z_s \, x_{cg} - X_s \, z_{cg}$$

$$N_R = N_s + X_s \, y_{cg} - Y_s \, x_{cg}$$

CLOCKWISE ROTOR ROTATION

The rotor model developed by Padfield (151) is explicitly for an anti-clockwise rotating rotor. The effects of the rotor direction are included in expressions such as those which account for the interaction of body rates when determining the harmonic components and the N_R torque coefficient or where allowing for the effects of rotor assembly accelerations. In preference to developing a second system of equations for a clockwise rotor, or indeed a system of equations which included

the rotor velocity rather than its speed of rotation it was considered more efficient both in development time and computational speed to apply the appropriate transformations to the single rotor model input and output data to allow use of the model, based on that of Padfield (151), developed in the previous sections. In effect the clockwise rotor can be modelled as an anti-clockwise rotor flying in an inverted mode. This is accomplished by applying a rotation of π radians about the x_s axis of the anti-clockwise rotor shaft axes to give a clockwise rotor axes system based at the rotor hub with the x_{sc} axis pointing forward coincident with the x_s axis and the y_{sc} pointing port and the z_{sc} axis pointing upwards.

Body rate and linear aerodynamic velocities are simply transformed to the revised axes:

$$\begin{bmatrix} p_{sc} \\ q_{sc} \\ r_{sc} \end{bmatrix} = \begin{bmatrix} 1 & 0 & 0 \\ 0 & -1 & 0 \\ 0 & 0 & -1 \end{bmatrix} \begin{bmatrix} p_s \\ q_s \\ r_s \end{bmatrix}$$

and

$$\begin{bmatrix} u_{Ac} \\ v_{Ac} \\ w_{Ac} \end{bmatrix} \begin{bmatrix} 1 & 0 & 0 \\ 0 & -1 & 0 \\ 0 & 0 & -1 \end{bmatrix} \begin{bmatrix} u_A \\ v_A \\ w_A \end{bmatrix}$$

The blade incidence angles also require transformation. These are input to the existing rotor model in blade axes and not shaft axes as used for the other inputs and outputs from the model. By inspection it can be deduced that in order to achieve

a downwards rotor airflow (positive in body axes, negative in clockwise rotor shaft axes) that the common angular inputs require inverting:

$$\theta_{0c} = -\theta_0$$

$$\theta_{twc} = -\theta_{tw}$$

Intuitively it can be stated that the X force coefficient C_X (which is a function of θ_s due to the 90° phase lag associated with the rotor motion) should remain unchanged whilst the Y force coefficient (which is a function of θ_c) should be inverted due to the fact that the y_s and y_{sc} axes are inverted. However, it must also be noted that both C_X and C_Y are a function of the downwash which is in turn a function of θ_0 (and implicitly θ_{tw}) hence:

$$\theta_{1sc} = -\theta_{1s}$$

$$\theta_{1cc} = \theta_{1c}$$

INPUT-OUTPUT AXES SIMPLIFICATION

Throughout the original analysis of the single rotor system Padfield (151) used the various axes systems which he considered most appropriate for each stage of the model. This is quite acceptable for researchers who have a detailed knowledge and understanding of the analysis and who are proficient with the necessarily complex notations which distinguish between the axes systems. However, as simulation programs are to be used by

engineers who will be involved in tasks which will be taxing enough in their own right and often not requiring outputs other than air vehicle motions, it was considered important to allow data inputs and outputs to be in axes systems which are most appropriate.

Therefore ground displacements, wind velocities and vehicle attitude angles are input and output in earth axes. Air vehicle instantaneous velocities, body rates and swashplate angles are input and output in body axes. The transformation between swashplate angles and blade angles in blade axes will be different for each air vehicle and will depend on the geometry of the linkage system. This will usually be optimised for the operating conditions (i.e. operational blade angle range, rotor rotation direction etc.). For this reason a unique sub-routine may be required to transform the swashplate angles to blade incident angles for each air vehicle configuration.

6.4 Single Rotor Model Results

As has been previously stated the single anti-clockwise rotor model has been validated by Padfield against full size rotors. The aims of the validation carried out as part of this work were to:

(a) confirm correct implementation of the model,

(b) confirm that changes to the model give results of correct sign,

(c) compare model output to small rotor data.

This was carried out by adopting the following techniques:

(a) verification by hand calculation,

(b) full simulation runs.

Several cases were selected to exercise the various parts of the model when it was in subroutine form to ensure correct functioning of all logical program paths thus testing 100% of the code in isolated tests. This follows recommended practice (125). Once debugging at this stage had been completed satisfactorily a few test cases were selected to be the subject of full hand calculation verification of the single model performance, these were:

(a) hover,

(b) $\pm$ sine cyclic,

(c) $\pm$ cosine cyclic,

(d) x_0, y_0 and z_0 winds

The hand calculations confirmed that the simulation output was in fact that which would be expected by use of the system of equations described in 6.3. The next stage was to confirm correct operation of the clockwise rotor transformations. This

was performed using a sign validation technique. Clockwise and anti-clockwise rotor models were run and outputs of the principal forces and moments were compared to the hover case. Swashplate inputs were expected to have similar effects as this is a swashplate and linkage design criterion but certain wind cross couplings were expected to have second order and opposite effects. The results are given in table 6.1 with changes denoted by '+' and '-' symbols and second order effects indicated by '(+)' and '(-)' symbols and are as expected.

Case	Rotor Forces and Moments											
	Anti-Clockwise Rotor						Clockwise Rotor					
	X	Y	Z	L	M	N	X	Y	Z	L	M	N
Hover	0	0	0	0	0	0	0	0	0	0	0	0
Sine swashplate +	0	+	0	+	0	0	0	+	0	+	0	0
Sine swashplate -	0	-	0	-	0	0	0	-	0	-	0	0
Cosine swashplate +	-	0	0	0	+	0	-	0	0	0	+	0
Cosine swashplate -	+	0	0	0	-	0	+	0	0	0	-	0
X_0 Wind	+	(-)	-	(-)	-	-	+	(+)	-	(+)	-	+
Y_0 Wind	(+)	+	-	+	(-)	-	(-)	+	-	+	(+)	+
Z_0 Wind	0	0	+	0	0	-	0	0	+	0	0	+

Table 6.1 Sign Validation of Clockwise Rotor Model

In parallel with this work a ground rotor test rig has been designed by Company staff and was under development to obtain practical data for rotor and blade configuration. The device named the 'spin rig' encountered severe technical and instrumentation problems. Some rotor data was made available on a provisional basis by project staff. It must be noted that practical tests use a geometric blade angle relative to the flat base of the aerofoil section, whereas simulation runs use the line of zero lift as the datum. Simulation output is quoted with reference to the line of no lift and practical tests quoted using the geometric blade angle, unless otherwise stated.

Work carried out by Company design staff (167) gave estimates of blade washout at hover as 0.1047 radians (6°) and the geometric angle for zero lift as -0.0899 radians (-5.15°). The latter figure was computed using reference (168) and agreement is good being within 0.0175 radians (1°). However, it must be borne in mind that blade torsional stiffness variations have been measured of between -30% to +66% (167) so the performance of rotors under test may vary considerably. The simulation was run using the above washout and compared to test results. The simulation output giving geometric blade angle on this occasion for easy comparison with practical test data. The blade twist was defined such that a value of -0.1047 radians (6°) occurred coincident with a common collective angle of 0.1920 radians (11°) which is the nominal hover common collective angle. The results showing good agreement appear in figure 6.1.

It is important that reliable practical tests should be implemented to confirm this relationship between these geometric and line of no lift blade angle datum quantities. There are additional uncertainties of blade angles in practical tests caused by backlash of linkage systems of up to ± 0.0175 radians (± 1°) which must be allowed for when assessing results.

Simulation outputs giving lateral thrust versus cyclic blade angle are shown in figure 6.2 for zero blade twist.

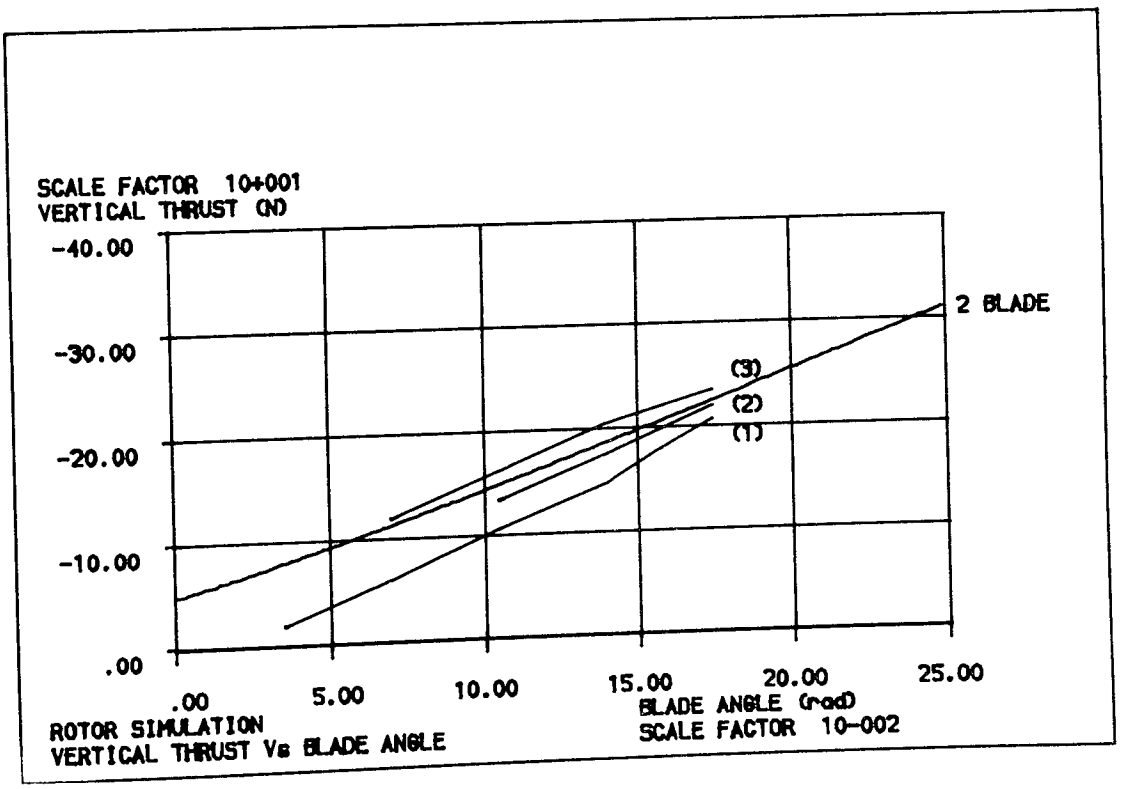

Figure 6.1 Simulation output and test data (171) - two bladed single rotor thrust Vs geometric common collective blade angle

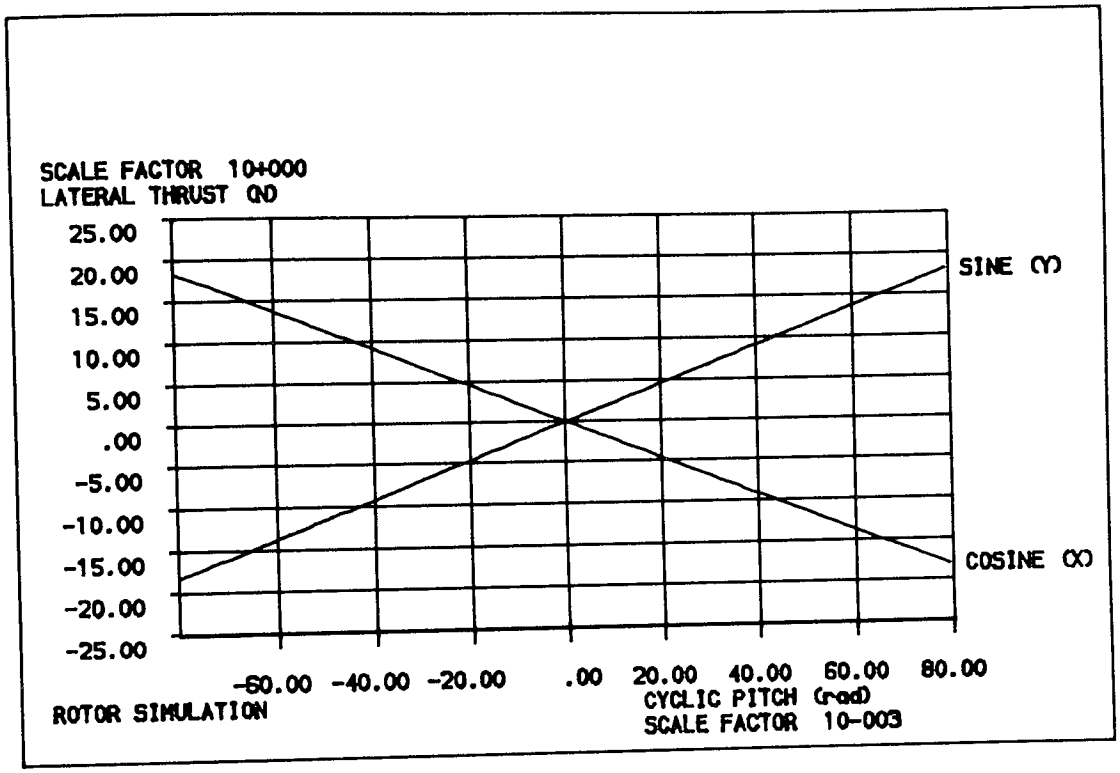

Figure 6.2 Simulation output - two bladed single rotor lateral thrust Vs cyclic blade angle (common collective 0.1920 radians)

Further limited sensitivity studies were carried out and these results are given in Tables 6.2 to 6.6

The results are as expected, after allowing for the 1 decimal place displayed accuracy, from inspection of the equations confirming satisfactory operation of the single rotor simulation module.

Lift Curve Slope	% of Datum Value	Thrust N	% of Datum Value	Moment Nm	% of Datum Value
5.1300	90	-186.4	92.4	9.4	91.3
5.4150	95	-194.1	96.2	9.8	95.2
5.7000	100	-201.7	100.0	10.3	100.0
5.9850	105	-209.0	104.6	10.7	103.9
6.2700	110	-216.3	107.2	11.1	107.8

Table 6.2 Single Rotor Simulation
Lift Curve Slope Sensitivity

Rotor Rate rad/s	% of Datum Value	Thrust N	% of Datum Value	Moment Nm	% of Datum Value
151.650	90	-163.4	81.0	8.3	80.6
160.075	95	-182.0	90.2	9.3	90.3
168.500	100	-201.7	100.0	10.3	100.0
176.925	105	-222.4	110.3	11.3	109.7
185.350	110	-244.0	121.0	12.4	120.4

Table 6.3 Single Rotor Simulation
Rotor Rate Sensitivity

Air Density kg/m^3	% of Datum Value	Thrust N	% of Datum Value	Moment Nm	% of Datum Value
1.0710	90	-181.5	90.0	9.2	89.3
1.1305	95	-191.6	95.0	9.7	94.2
1.1900	100	-201.7	100.0	10.3	100.0
1.2495	105	-211.8	105.0	10.8	104.9
1.3090	110	-221.8	110.0	11.3	109.7

Table 6.4 Single Rotor Simulation
Air Density Sensitivity

Downwash Iteration Tolerance	Thrust N	% of Datum Value	Moment Nm	% of Datum Value
10^{-10}	-201.7	100.0	10.3	100.0
10^{-8}	-201.7	100.0	10.3	100.0
10^{-6}	-201.7	100.0	10.3	100.0
10^{-4}	-201.7	100.0	10.3	100.0
10^{-2}	-195.5*	96.9	9.9*	96.1

*First value - Subsequent values 100%

Table 6.5 Single Rotor Simulation
Downwash Iteration Tolerance Sensitivity

x_0 wind Velocity m/s	X Thrust N	Y Thrust N	Z Thrust N	% of Datum	L Moment Nm	M Moment Nm	N Moment Nm	% of Datum
0	0	0	-201.7	100.0	0	0	10.3	100.0
1	+0.6	-0.4	-202.3	100.3	-0.1	-0.15	10.2	99.0
2	+1.3	-0.8	-204.2	101.2	-0.2	-0.32	10.2	99.0
3	+2.0	-1.2	-207.3	102.8	-0.3	-0.50	10.1	98.1
4	+2.8	-1.6	-211.3	104.8	-0.4	-0.69	10.0	97.1
5	+3.6	-2.0	-216.2	107.2	-0.5	-0.91	9.9	96.1

Table 6.6 Single Rotor Simulation Tail Wing Sensitivity

6.5 CCTR Models

Having identified a model suitable for simulating a single rotor in section 6.3 it requires extending to simulate the properties of a CCTR. Results such as those published in reference (157) show that the performance of the upper rotor of a CCTR is within 5% of a single rotor of the same dimensions. It seems reasonable therefore to model the upper rotor of the CCTR as a single free rotor.

Paglino (169) experimented with a simple model for a co-axial rotor in forward flight. He suggested increasing the induced velocity of the lower rotor by the average downwash from the upper rotor. He has also proposed that the induced velocity should be increased by a value equal to 50% of the upper rotor downwash, arguing that when the rotor flow is fully developed the outer 50% of the rotor draws in clean air. However, none of his models covered more than a limited part of the flight envelope. Other approaches have adopted an empirical coefficient used to factor rotor performance calculations in a variety of ways (170).

As a first attempt the components of the downwash from the upper rotor would be added to the aerodynamic velocities of the lower rotor, (known as the A-Model). This permits the minimum of changes to the single rotor model, only modifying the aerodynamic wind velocities which are already an input to that model. Figure 6.3 shows the vertical thrust Vs collective blade

angle for the A-model co-axial rotor simulation. Adopting the usual practice co-axial rotor results are given for torque balance between the upper and lower rotors.

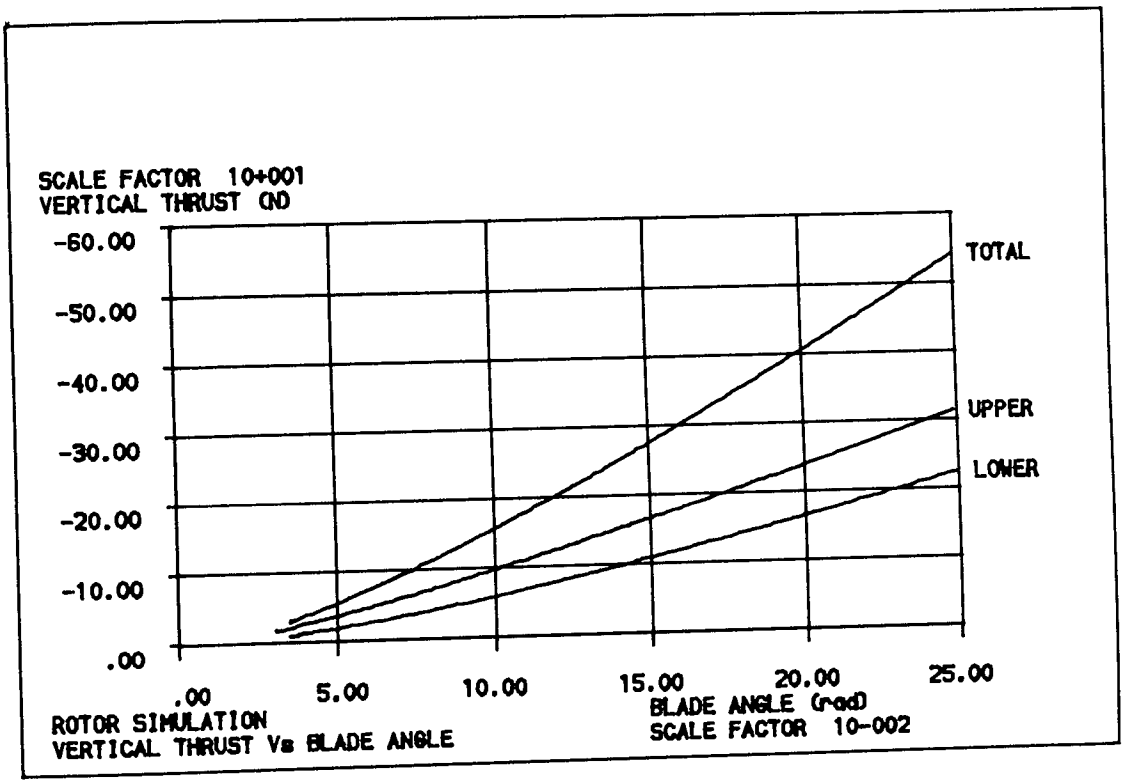

Figure 6.3 Simulation output - Coaxial rotor A-Model vertical thrust Vs blade common collective angle - upper and lower rotor contributions and total thrust

In order to increase the accuracy of the rotor model it was proposed that use should be made of existing published wind tunnel and detailed analysis data. Saito (157) shows results for a detailed miniature co-axial rotor model which has been validated against wind tunnel trials for both hover and

cruise conditions. It was considered that an interaction coefficient should be defined to combine the advantages of using published data and yet retain fast running of the model. In the interests of computational speed it was decided to avoid the use of empirical coefficients to describe the air flow as a function of the position at the lower rotor such as that used by Azuma (170) because this would require a more complex aerodynamic model and integration along each blade. Instead it was proposed that the upper rotor be modelled as a free rotor, as in the A-model, and that the downwash from this rotor be fed into the lower rotor as an aerodynamic velocity. In addition the thrust performance of the lower rotor would be factored by an interaction coefficient. This is the B-Model. The coefficient would account for swirl and other interference effects occurring between the two rotors.

Performance of two and four bladed rotors has been measured and reported upon. Recent work (157) compares the performance of a miniature CCTR (157 figure 9) to both a two and four bladed rotor, (157 figure 7). This work is of particular importance as it has been carried out for a d/r ratio of 0.26 which is identical to that of SPRITE. Table 6.7 below shows this data extracted from reference (157). A coefficient, x_R, can be used as a measure of co-axial rotor performance based on the performance of 2 and 4 bladed rotors:

$$T_{CCTR} = T_4 + x_R (T_2 - T_4)$$

Figures 7 and 9 of reference (157) show that this definition is accurate to within 2%. The mean value for x_R from table 6.7 is 0.350.

$C_{Q/s}$ x 10^{-3}	$C_{T/s}$ x 10^{-2}		
	2 Blade	CCTR	4 Blade
2.000	1.943	1.457	1.143
3.000	3.400	2.743	2.429
4.000	4.386	3.686	3.329
5.000	5.229	4.500	4.143
6.000	6.000	5.214	4.857
7.000	6.714	5.929	5.500
8.000	7.286	6.571	6.086

Table 6.7 Torque Coefficient Vs Thrust Coefficient for Hovering Flight
(from Reference S2 figures 7 and 9)

Under cruise conditions the behaviour of the CCTR moves away from that of a four bladed rotor towards that of a two bladed rotor. Over the SPRITE operational envelope of $\mu = 0$ to $\mu = 0.2$ figure 13 of reference (156) shows that for a constant blade pitch angle the rotor torque coefficient remains sensibly constant whilst the value of the thrust coefficient increases. Over this restricted range the experimental data of reference (156) indicates that a straight line variation is justified. Based on figure 14 of reference (156) table 6.8 shows the comparison of a CCTR at $\mu = 0.16$ to two and four bladed rotors. The mean value for x_R in table 6.8 is 0.735.

$C_{Q/s}$ x 10^{-3}	$C_{T/s}$ x 10^{-2}		
	2 Blade	CCTR	4 Blade
2.000	2.400	2.216	1.707
3.000	4.512	4.160	3.200
4.000	5.867	5.483	4.245
5.000	6.944	6.427	5.013
6.000	7.904	7.269	5.707
7.000	8.640	8.022	6.315

Table 6.8 Torque Coefficient Vs Thrust Coefficient for μ = 0.16 (from Reference A2 figure 14)

The single rotor model described in section 6.3 was used to carry out simulation runs of two and four bladed rotors at flight conditions of μ = 0 and μ = 0.2. Similar runs were carried out using the dual rotor A-model described earlier in this section. Figure 6.4 shows the vertical thrust performance for these three runs at hover and figure 6.5 shows similar results for μ =0.2.

Figures 6.6 and 6.7 show thrust and torque coefficient divided by solidity versus blade collective angle and figure 6.8 shows the plots of the thrust versus torque coefficient divided by solidity. Similar plots were obtained for μ = 0.2.

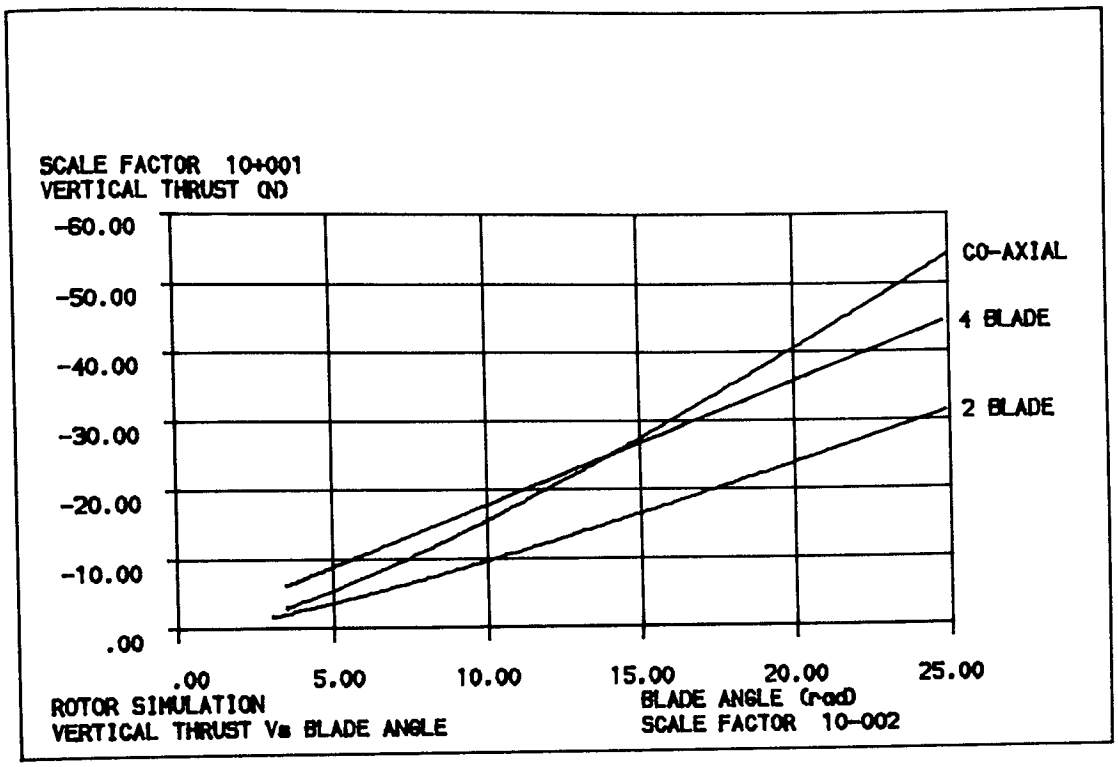

Figure 6.4 Simulation output - Co-axial rotor A-Model and single 2 and 4 bladed rotors - Vertical thrust Vs blade collective angle at hover

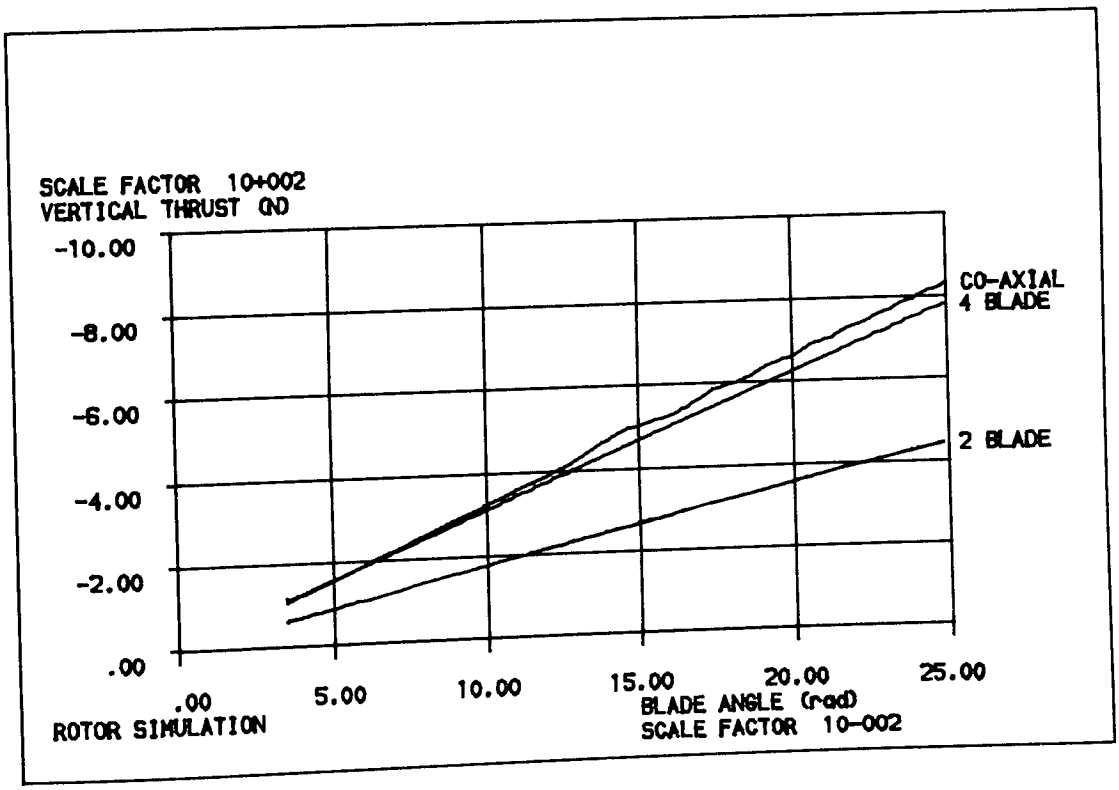

Figure 6.5 Simulation output - Co-axial rotor A-Model and single 2 and 4 bladed rotors - Vertical thrust Vs blade collective angle at $\mu = 0.2$

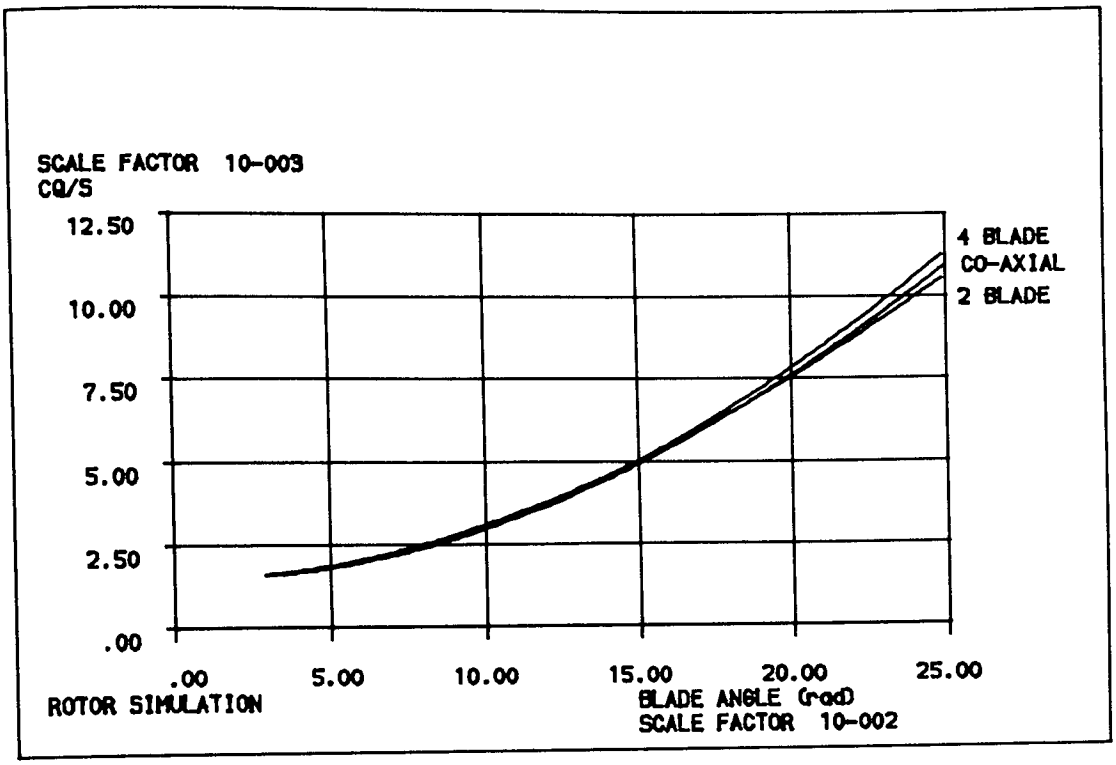

Figure 6.6 Simulation output - Co-axial rotor A-Model and single 2 and 4 bladed rotors - Torque coefficient divided by solidity Vs blade angle

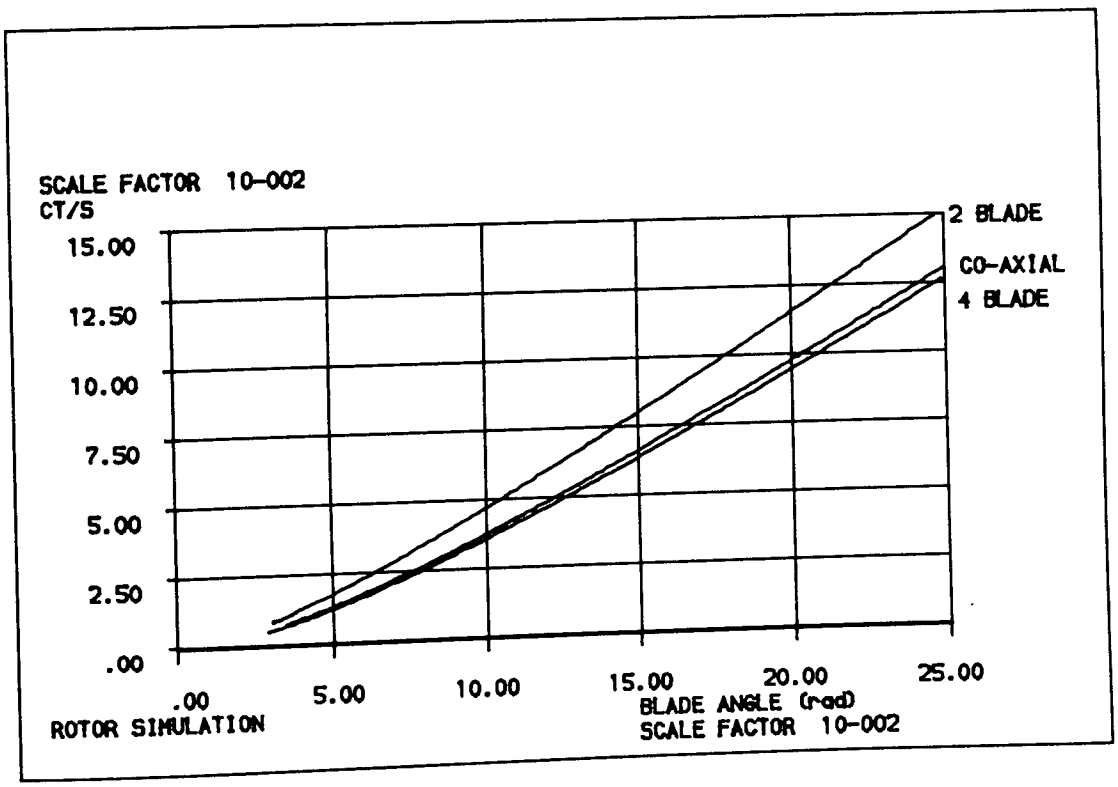

Figure 6.7 Simulation output - Co-axial rotor A-Model and single 2 and 4 bladed rotors - Thrust coefficient divided by solidity Vs blade angle

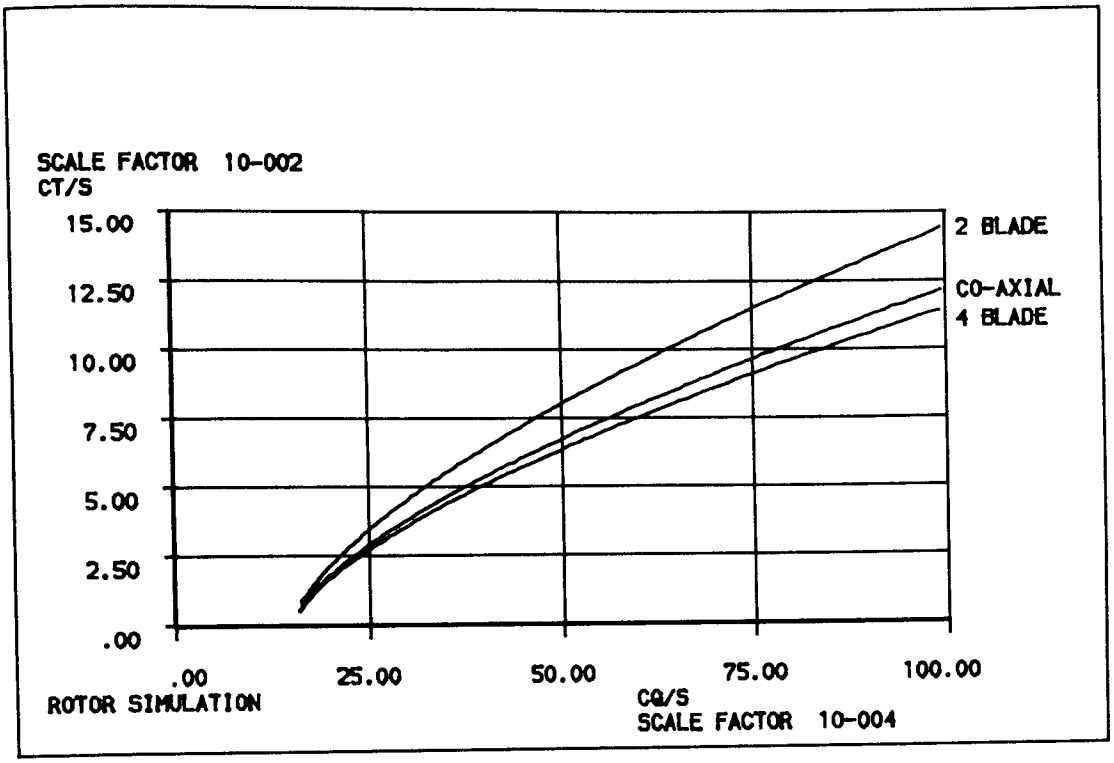

Figure 6.8 Simulation output - Co-axial rotor A-Model and single 2 and 4 bladed rotors - Thrust coefficient divided by solidity Vs torque coefficient divided by solidity

From these results the interaction coefficient, C, which is used to factor the thrust of the lower rotor was determined for the hover condition and at cruise, $\mu = 0.2$.

The interaction coefficient is defined as:

$$C = A + \mu B$$

where the values of A and B have been evaluated as:

$$A = 1.084$$

$$B = 0.148$$

6.6 CCTR Model Results

The comments in section 6.4 regarding the differences between the blade incidence angles (line of no lift for simulation runs, relative to blade lower face for practical tests), blade backlash in practical tests and zero simulation blade twist angles also apply here. B-Model simulation runs are presented for μ=0.

A B-model rotor simulation run was carried out with blade twist similar to that used in figure 6.1. The results shown in figure 6.9 show good agreement to 'spin rig' (171) and endurance (172) air vehicle data.

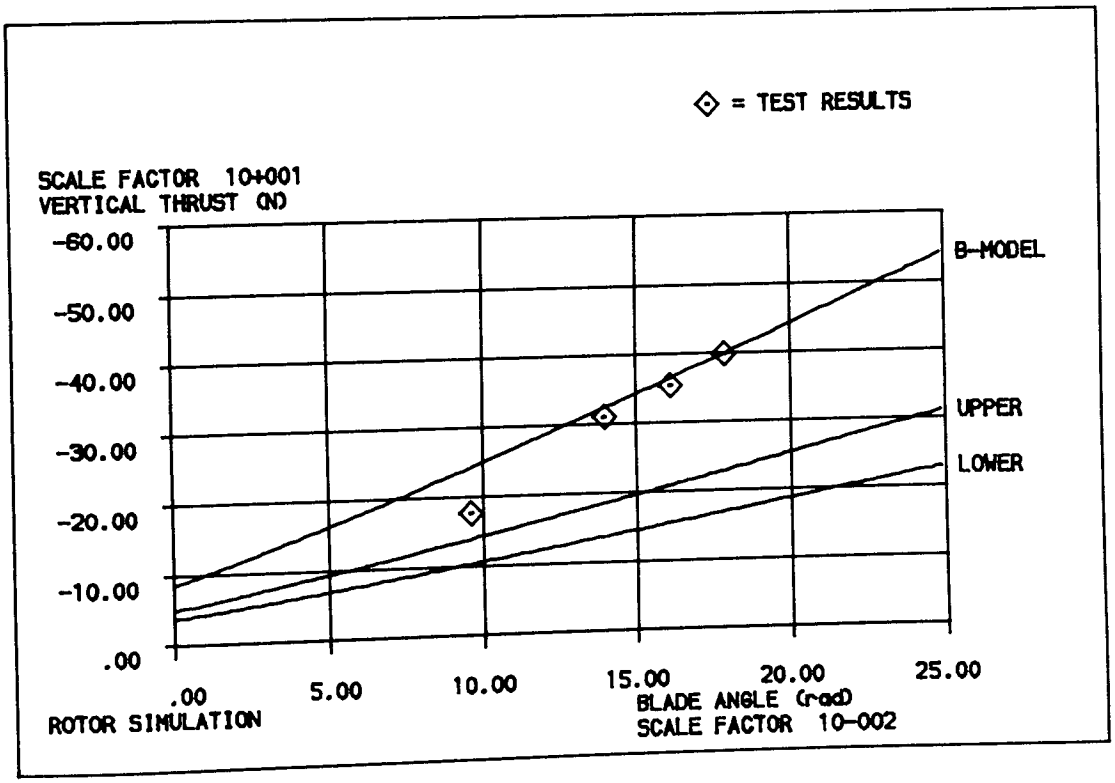

Figure 6.9 Simulation output - Co-axial rotor B-Model and test data (171)(172) - Vertical thrust Vs common geometric blade collective angle

The differential collective angle (positive for increased lower blade incidence compared to upper blade incidence) required for torque balance between rotors is shown plotted versus common collective angle is shown in figure 6.10.

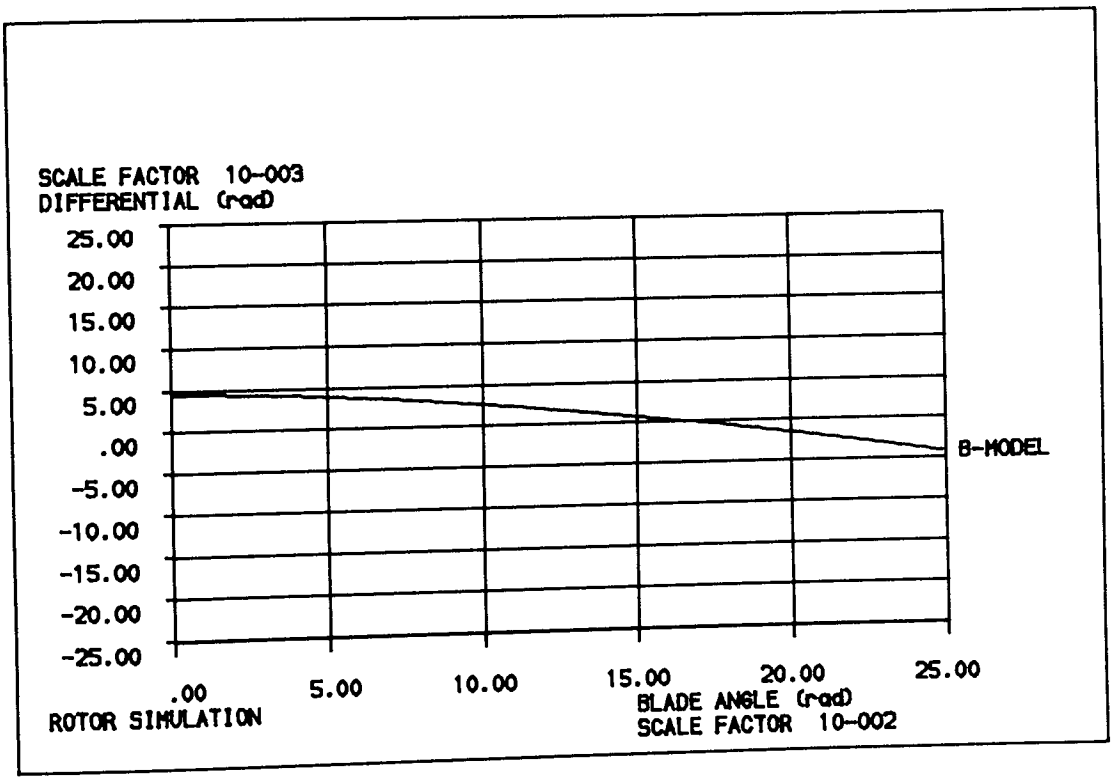

Figure 6.10 Simulation output - Co-axial rotor B-Model - Differential collective angle for torque balance between rotor Vs common geometric blade collective

The major importance of this result is to note that the differential collective angle is always small. The reducing trend can be seen in other published work (173) but published literature has not been located showing a negative value. Perhaps if the published work of (173) was extended to include the higher incidence angles of figure 6.10 this effect may be observed. In any case the assumptions that twist varies linearly with collective angle may not be accurate, and it could be asserted that the twist should be related to thrust, however, to include this in the simulation would require a further iterative loop thus reducing simulation speed. Practical results (172) show that the magnitude of the differential angle is always small (<0.02 radians) for rotor torque balance. Recent practical tests (174) show that a negative differential may occur under certain circumstances but the accuracy of this data has yet to be verified.

It is asserted that for vehicle motion and stability simulation the model is more than adequate but further work in this area may be of interest to aerodynamicists.

Figure 6.11 shows the rotor thrust for zero blade twist and figure 6.12 compares this to 2 and 4 bladed rotors.

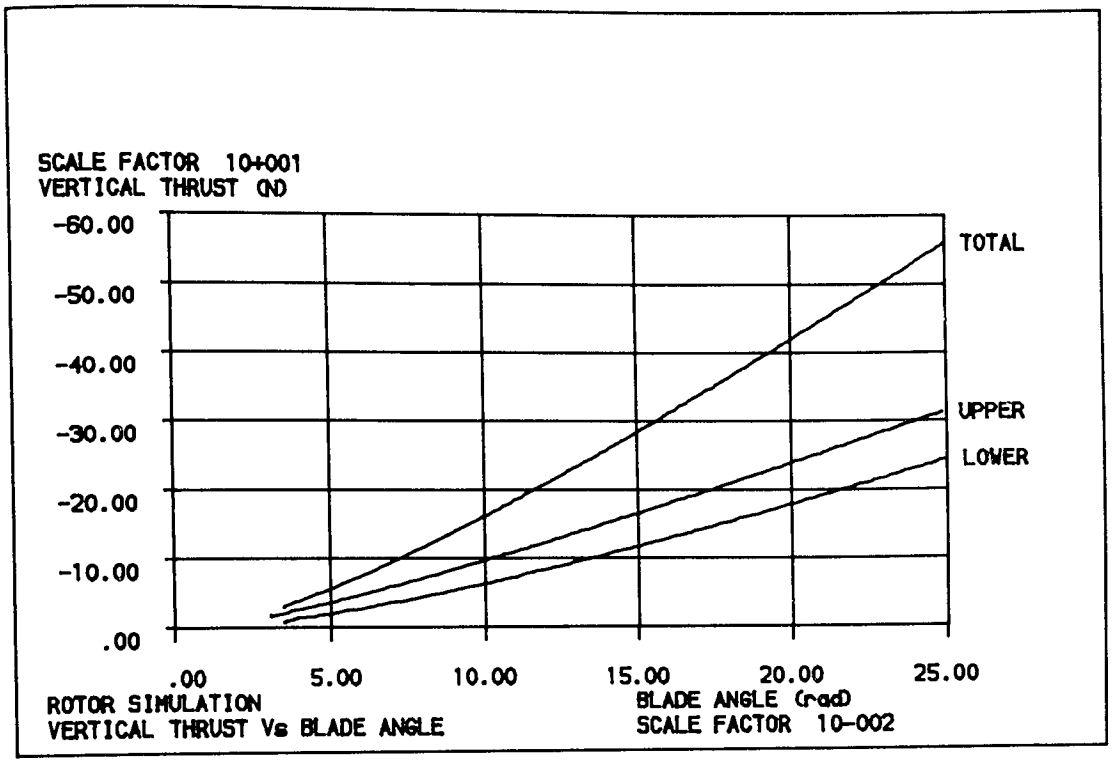

Figure 6.11 Simulation output - Co-axial rotor B-Model - vertical thrust Vs blade angle - upper and lower rotor contributions and total thrust

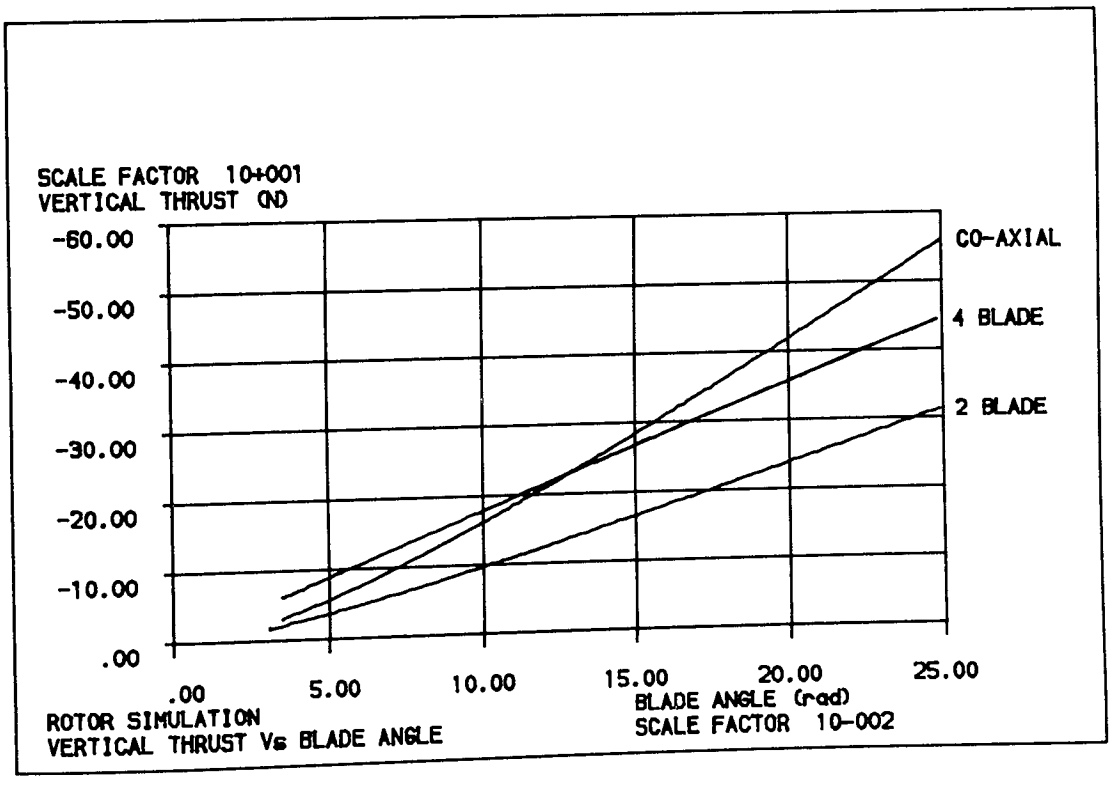

Figure 6.12 Simulation output - Co-axial rotor B-Model and 2 and 4 bladed rotors - Vertical thrust Vs blade incidence angle

Figures 6.13 to 6.14 show B-model rotor torque coefficient divided by solidity and rotor thrust coefficient divided by solidity plotted Vs blade incidence angles and figure 6.15 show these quantities plotted together where good agreement with Azumas work (156) is seen.

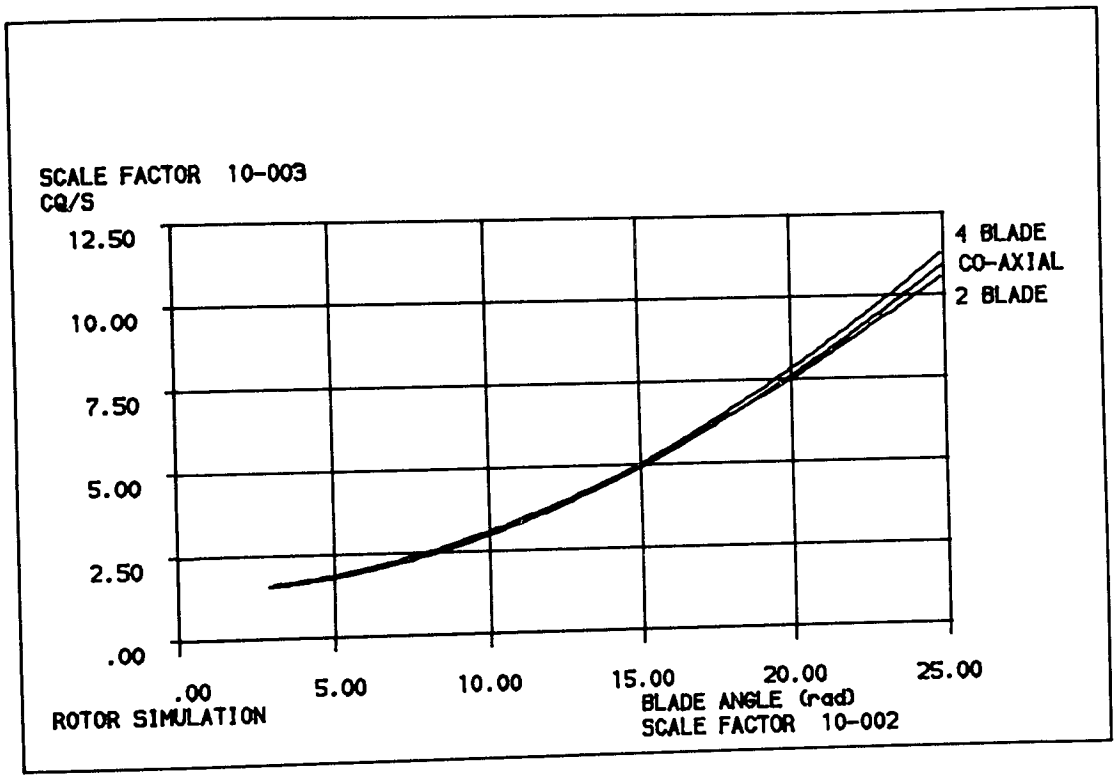

Figure 6.13 Simulation output - Co-axial B-Model torque coefficient divided by solidity Vs blade incidence angle

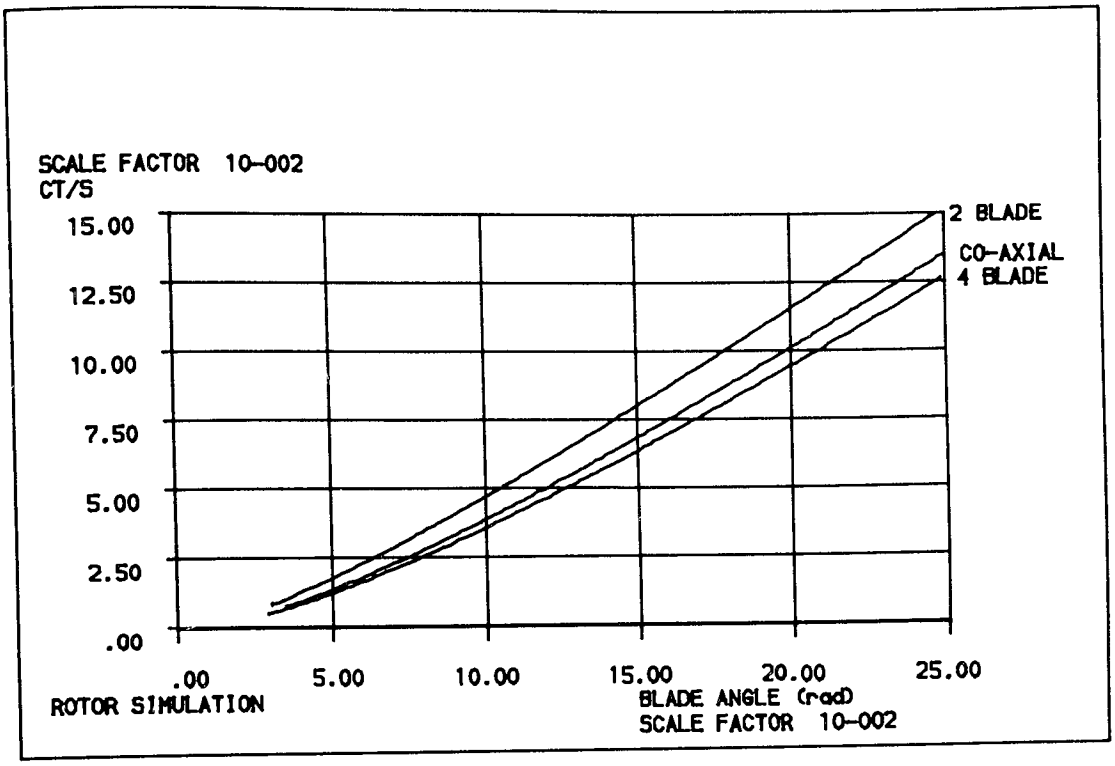

Figure 6.14 Simulation output - Co-axial B-Model thrust coefficient divided by solidity Vs blade incidence angle

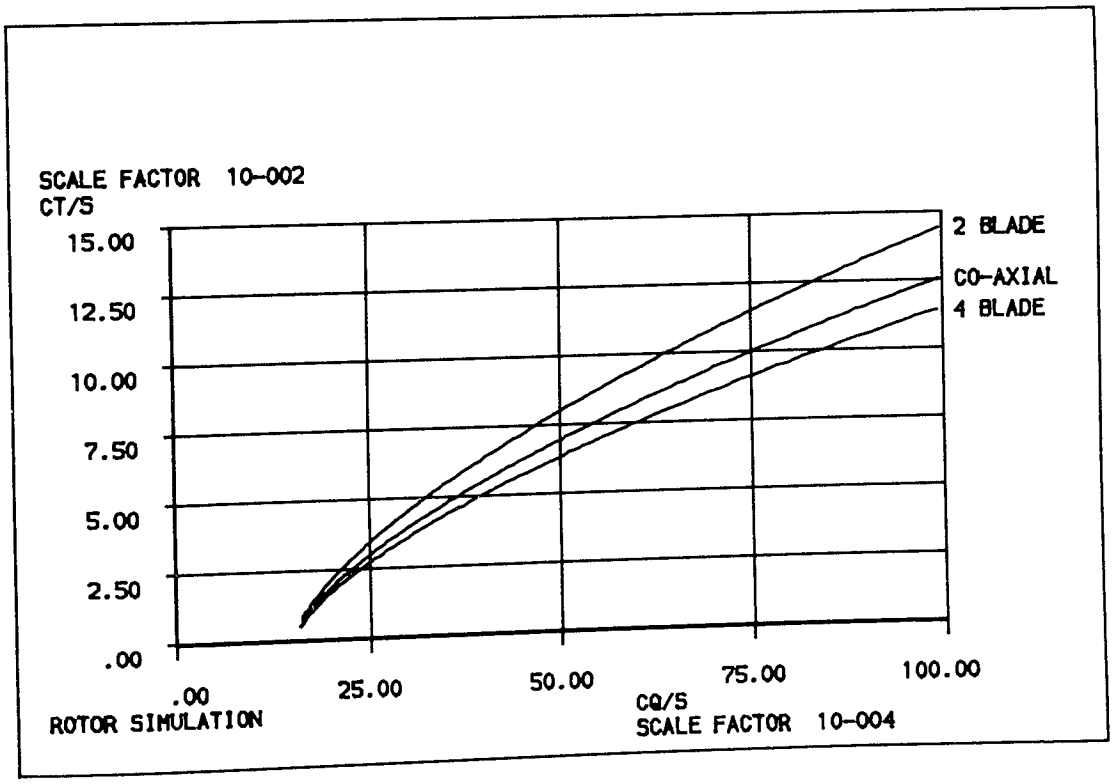

Figure 6.15 Simulation output - Co-axial B-Model thrust coefficient divided by solidity Vs torque coefficient divided by solidity

Figure 6.16 shows lateral thrust for the B-model simulation verses cyclic blade angle.

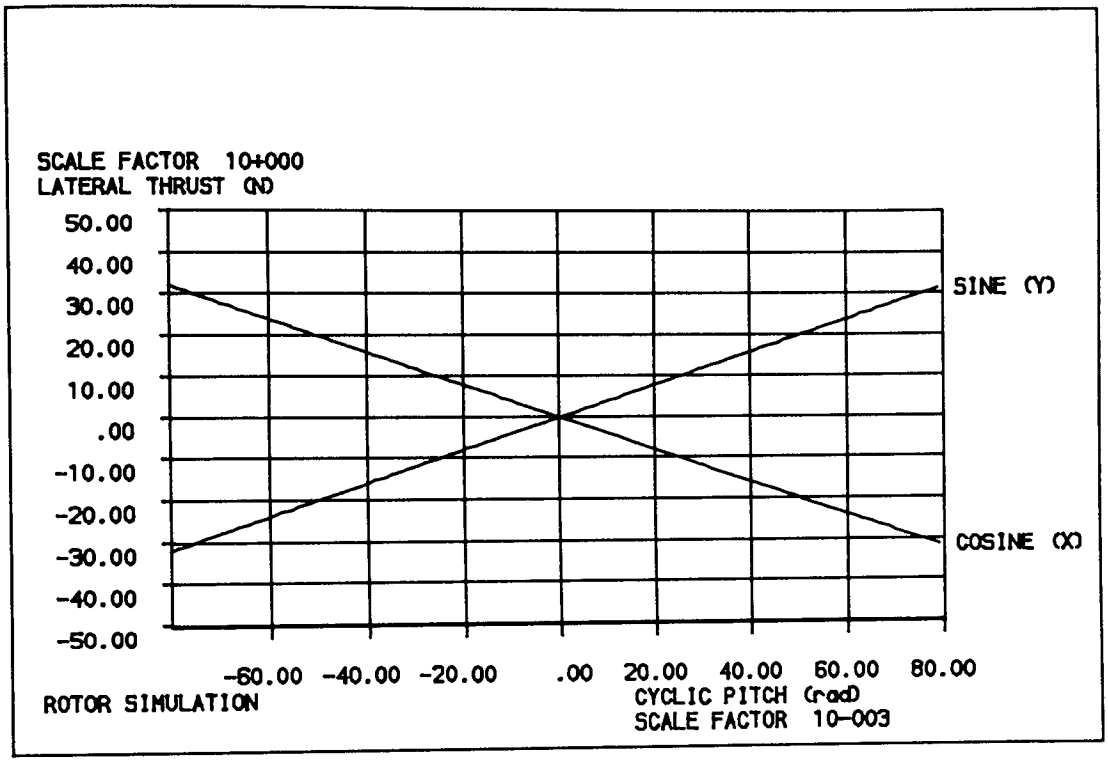

Figure 6.16 Simulation output - Co-axial B-model - lateral thrust Vs cyclic blade angle

This rotor model provides results which compare favourably with test data and published work. The performance is acceptably fast and in fact the whole simulation including this model runs at 1000 times real time which is 240 times faster than the detailed models requiring blade and rotor disc integration.

6.7 Review

Section 6 has described the development of the rotor module of the simulation. A validated single rotor model, employing a closed form solution, was selected as the basis simulation. This work was extended to form the nucleus of a simple co-axial model (A-model) which in turn was improved using results from other published work (B-model). The result was an economic to run rotor model which demonstrated good performance compared to both published papers and practical tests.

SECTION 7

AIR VEHICLE AERODYNAMICS

7 AIR VEHICLE AERODYNAMICS

7.1 Introduction

The forces acting on the air vehicle are considered in three categories in this simulation. These are the gravitational forces included in Section 5, the forces resulting from the upper and lower rotors which are discussed in Section 6 and the forces due to the air resistance of the fuselage which are the subject of this section.

The requirement placed upon this section is to evaluate the three fuselage forces X_F, Y_F, and Z_F and moments L_F, M_F and N_F for given air vehicle conditions. One solution practice (175) is to determine force and moment coefficients, which are a function of the wind/fuselage pitch angle α_F and the wind/fuselage sideslip angle β_F, often through the use of 'look up' tables. The aerodynamic forces and moments can then be evaluated using the usual equations:

$$X_F = \tfrac{1}{2}\rho\,(\Omega R)^2\, S_p\, \bar{V}_F^{\,2}\, C_{XF}(\alpha_F, \beta_F)$$

$$Y_F = \tfrac{1}{2}\rho\,(\Omega R)^2\, S_s\, \bar{V}_F^{\,2}\, C_{YF}(\alpha_F, \beta_F)$$

$$Z_F = \tfrac{1}{2}\rho\,(\Omega R)^2\, S_p\, \bar{V}_F^{\,2}\, C_{ZF}(\alpha_F, \beta_F)$$

and

$$L_F = \tfrac{1}{2}\rho\,(\Omega R)^2\, S_p\, l_F\, \bar{V}_F^{\,2}\, C_{LF}(\alpha_F, \beta_F)$$

$$M_F = \tfrac{1}{2}\rho\,(\Omega R)^2\, S_p\, l_F\, \bar{V}_F^{\,2}\, C_{MF}(\alpha_F, \beta_F)$$

$$N_F = \tfrac{1}{2}\rho\,(\Omega R)^2\, S_s\, l_F\, \bar{V}_F^{\,2}\, C_{NF}(\alpha_F, \beta_F)$$

Different reference lengths and areas are adopted by various researchers, however, so long as the definition of the force or moment coefficient is clearly related to a given length or area no confusion should arise.

7.2 Aerodynamic Data

Aerodynamic force and moment coefficient can be determined either theoretically or practically through wind tunnel or flight trials. Limited aerodynamic data for the SPRITE configuration is available for wind tunnel tests carried out on models supplied by ML Aviation (176) and Westland Helicopters (177). Unfortunately both of these programmes considered only limited portions of the flight envelope, $\pm$ 20° about the x_0 axis and $\pm$ 5° about the z_0 axis, with the wind velocities in the direction of the z_0 axes.

In an attempt to supplement these results for application to the whole flight envelope, theoretical data for simplistic solids of rotation was reviewed. ESDU publish aerodynamic coefficients for ellipsoidals of rotation (178) and blunt forebodies (179). The comparison of the ESDU literature with the wind tunnel data showed that it was not the main fuselage shape which dominates the airflow, but the interaction of the rotor shaft cowling and the landing legs and other excrescences. This conclusion is supported by reference (177) which presents pressure distribution plots both for the bare fuselage which

approximates to an ellipsoidal of rotation and the fuselage with rotor cowling fitted.

It was clear that in order to rectify this lack of information for the total flight envelope one of the following paths would have to be followed:

(a) develop a detailed aerodynamic model,

(b) perform wind tunnel tests using a small scale or full scale model,

(c) adopt a simple empirical solution.

In the interests of theoretical completeness paths (a) and (b) could be followed in parallel. Practically, however, there are major reasons why these options were not pursued further. Firstly, having already briefly compared simple published data with the wind tunnel results it was clear that substantial resources would be required to develop a model adequate to account for the interactive effects of the protuberances added to the basic fuselage shape. Techniques such as finite element analysis, similar to those used for stressing and dynamic analyses, would be applicable.

It was concluded that this would be a large programme in its own right and it did not warrant the effort required. We shall see later that a more simple solution is obtainable for a very much reduced effort.

Wind tunnel trials are, in the opinion of the author, the most appropriate technical solution, as the fuselage with its antennae, cooling cutouts and other features could be mounted in a wind tunnel and data obtained which, after correction for scale and other wind tunnel effects such as Reynolds number variation, would be obtained for a particular fuselage configuration. This could be fed into the simulation from look up tables. At this stage of development of the SPRITE system, the Company did not plan to commit the resources for comprehensive wind tunnel trials.

Having discounted the two 'preferred' options it remained to devise a simple empirical solution to determine the aerodynamic loadings on the fuselage.

The SPRITE flight envelope was considered and available data generated by the rotor model taken into account. At hover, the rotor downwash over the fuselage was in the range of 9 m/s and at a full forward speed of 30 m/s (μ = 0.2) the downwash reduced to approximately 2.5 m/s. Simple calculations show that the available wind tunnel data is applicable over approximately the range 50% - 100% full speed and at close to hover conditions. In the absence of other information the wind tunnel results, which had been carried out at a constant velocity of 30 m/s, were extended using a blend of common sense and 'poetic licence' to fill in lift and drag force curves.

Figure 7.1 shows the actual and estimated data. Greater confidence is placed in the lift curve as it does not seem too unreasonable for it to become asymptotic to the zero lift point

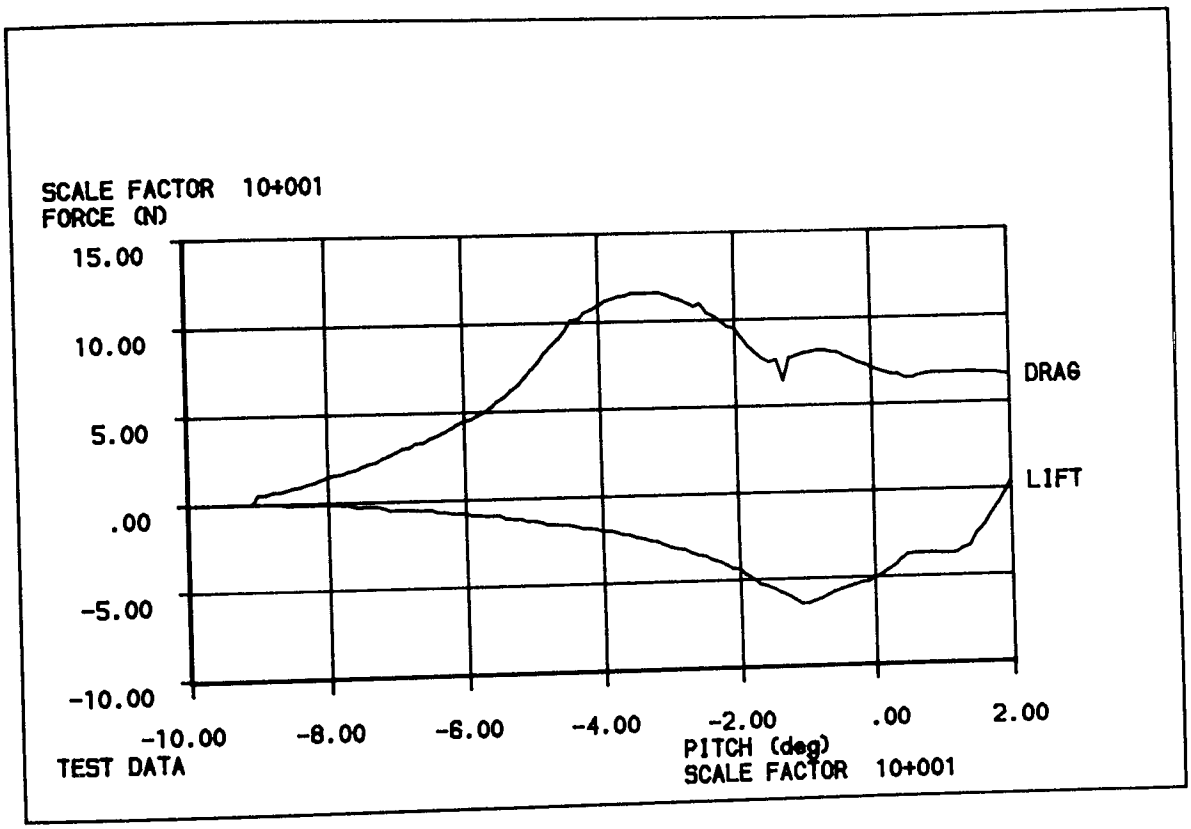

Figure 7.1 Actual and estimated aerodynamic force data Vs fuselage pitch angle (30 m/s wind)

at -90 degrees. The drag data, perhaps, is open to greater criticism but there is no better information readily available to influence the shape of the curve. In defence of this pragmatic solution three supportive arguments can be presented. These are:

(a) That data, as shown, is for a 30 m/s velocity; when the reduced actual aerodynamic velocities are considered the predicted fuselage forces are small in comparison with gravity and rotor aerodynamic forces and hence do not dominate the air vehicle motion.

(b) Actual data is available at the extreme conditions in the flight envelope which may be argued to be of greater interest to the designer, for instance, when evaluating stability at hovering or fuselage attitude angles at full speed.

(c) The solution is available in the required financial and time constraints.

The caveat with regard to the validity of the assumptions made in obtaining the aerodynamic data must be borne in mind when making use of simulation generated output. The wind tunnel tests show the moment coefficients to be negligible; these are therefore entered as zero into the simulation.

7.3 Simulation Aerodynamic Coefficients

The simulation aerodynamic coefficients are obtained by converting the wind tunnel fuselage lift and drag forces, which are presented in earth axes, into body axes and factorising by the reference area and velocity squared terms.

A look up table was generated with values for the lift and drag coefficients being determined at incidence angles of between -90 to +20 degrees at one degree increments. Between these values simple linear interpolation is carried out. Figure 7.2 shows the lift and moment coefficients, in body axes, used in the simulation.

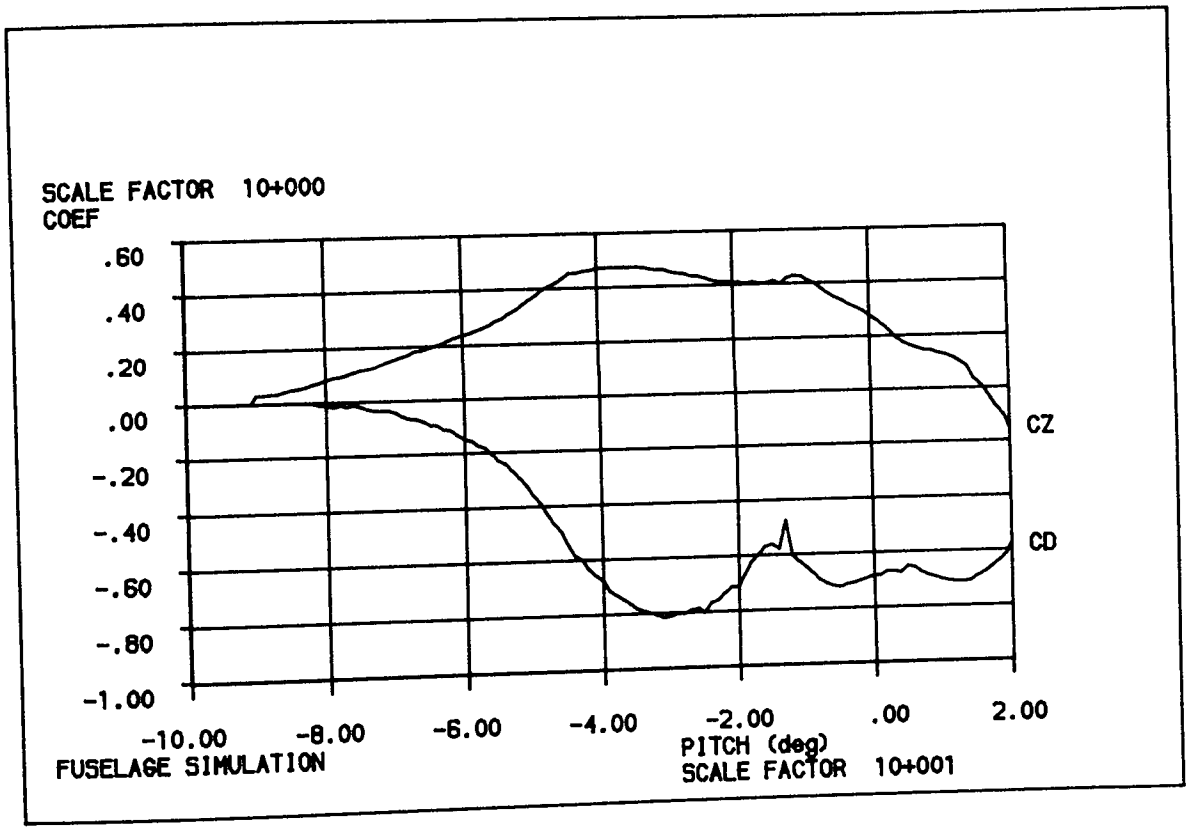

Figure 7.2 Simulation lift and drag coefficients Vs fuselage pitch angle

7.4 Review

Techniques for determining the aerodynamic forces due to wind action on the fuselage have been discussed. Rigorous analytical and wind tunnel approaches were not available due to financial and timescale restrictions. A simple approach based on limited wind tunnel data is proposed and lift and drag coefficients, evaluated for use in the simulation, were presented.

SECTION 8

CONTROL SYSTEM AND SENSORS

8 CONTROL SYSTEM AND SENSORS

8.1 Introduction

The air vehicle control system model used in the simulation is described here. The term control system in this context is taken to describe the following elements:

(a) flight control system,

(b) control laws.

The flight control system is defined as the on-board sub-systems required for stability and navigation. The control laws govern the mix of actuator movements resulting from control demands. They are optimised to provide smooth and well behaved motion of the air vehicle. Usually requirements such as minimal cross coupling are prime considerations when developing the control laws.

The control laws for SPRITE have yet to be designed. At present demands for individual channels are selected by the pilot, with no mixing or pre-processing being performed. It is intended that simulation will aid the development of the control laws. This point is discussed in Section 3 and developed in Section 12.

The SPRITE flight control system consists of four discrete stabilisation loops for the control of roll, pitch and heading

angle and altitude displacement. The terms roll, pitch, heading and altitude in this context must be recognised as descriptive terms for the control channels, the actual quantities measured are not necessarily synonymous with the attitude angles and earth reference displacements defined earlier. These quantities are defined in terms of the reference schemes used in the simulation in the sensor section, as it is the mechanism of the sensor and its mounting arrangements that define the measured quantity.

8.2 Flight Control System

It is outside of the scope of this project to perform stability analysis on the stabilisation loops of the air vehicle, this has already been performed at a simple linear level by the project team (120)(121)(122). The requirement placed upon this project is to model the present control system within the air vehicle simulation. This section describes the existing control system and, in particular, how it is modelled. It is the intention to design and develop the model as a tool for use by the system designer in the development of the flight control system within the many constraints imposed upon him, some of which are discussed in Section 4.

Control of the roll (bank) and pitch (inclination) angles is accomplished by comparing the demanded angle to the outputs of a two axis vertical gyroscope. Rate damping is synthesised in the signal processing via a differentiator and summing this with the

position signal with appropriate gains. Roll and pitch moments are generated by varying the blade angle cyclically once per rotor revolution in both the sine and cosine planes. This generates precession of the rotor disc giving rise to moments which causes angular acceleration of the air vehicle in the roll and pitch axes. When the rotor disc thrust vector is non-vertical there are horizontal components giving the air vehicle accelerations in the translational x and y directions. This is the mechanism of translational flight.

The air vehicle is controlled in the heading (azimuth) plane by comparing a demanded heading angle to the output of an azimuth (north seeking) gyroscope. Rate damping is provided from a rate gyroscope also mounted in the azimuth plane. Torque is generated by simultaneously adjusting the collective pitch angle of the upper and lower rotors, one increasing and one decreasing, such that the net rotor system drag torque causes the air vehicle to accelerate about the z axis.

The altitude of the air vehicle is maintained by adjusting the common collective angle of both rotors to increase and decrease the magnitude of the rotor thrust vector. This is performed as a result of comparing a demanded altitude to the sensed altitude, either absolute or line of sight depending upon the sensor. Early SPRITE prototype air vehicles relied purely on position feedback in the altitude loop, but the revised design

altitude processing circuits allow a synthesised rate damping term to be included to reduce overshoot.

The following sub-sections describe the types of sensors used in the flight control system and discusses the quantities which they measure. The associated errors are introduced and modelling methods discussed. A general form of the closed loop stabilisation processing is introduced, shown in figures 8.1 and 8.2 the same form being used for roll, pitch and altitude loops and a second form used for the heading loops which uses sensors with trigonometric function outputs. The actuator model, including its

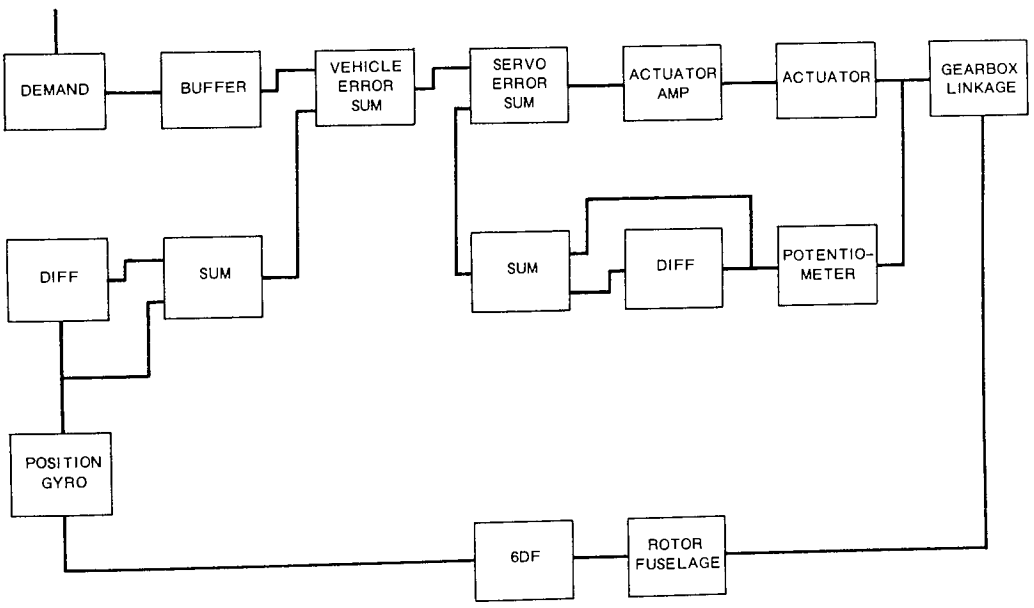

Figure 8.1 Roll, pitch and altitude flight control system block diagram

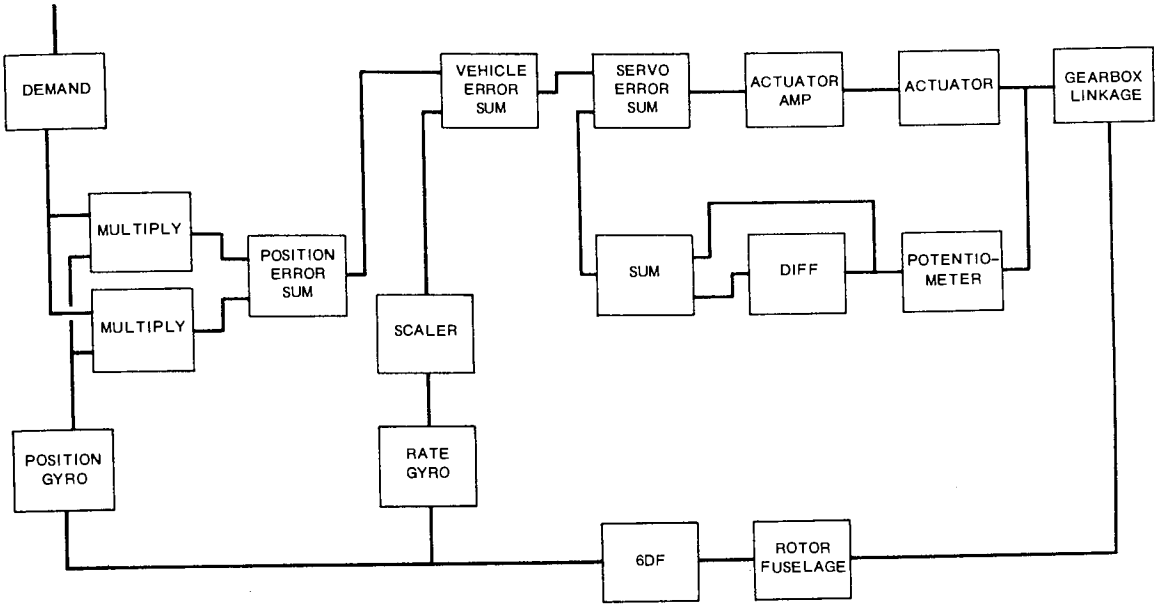

Figure 8.2 Heading flight control system block diagram

driving electronics, and the linkage systems is proposed. Finally the implementation of this part of the model is discussed and results for open and closed loop actuator responses are presented.

The elements of each stabilisation loop fall neatly into three sub-sections; sensors, processing and actuators. The flight control system models are discussed below under these headings.

8.3 Sensors

There are two aspects of sensor performance included in the model. The first part is to determine which angular rate, linear rate angle or distance the sensor is designed and installed to measure, these clearly need not be attitude angles and earth displacements

used elsewhere. The second aspect is to include the errors associated with the sensors themselves due to practical performance limitations. The error is considered as containing two components as defined below:

(a) threshold, (b) resolution, (c) non linearity, (d) scale factor accuracy, (e) scale factor temperature variation, (f) noise,	Measurement Errors (E_M)
(g) hysteresis, (h) zero bias, (i) zero bias temperature variation,	Hysteresis Errors (E_H)

The alignment of the sensor in both its own fixture and when it is mounted to the air vehicle results in the sensor having a main axis of sensitivity (S_M) of less than unity and cross axis sensitivities (S_C) in the other two orthogonal planes of greater than zero.

A sensor of gain, in volts/unit, of G_S will give an output S_O when mounted with its main axis of sensitivity measuring component Q_1 and the two perpendicular components are Q_2 and Q_3 such that:

$$S_O = G_S \left[(S_M Q_1 + S_{C1} Q_2 + S_{C2} Q_3) \ (1 + E_M + E_H) \right]$$

For the initial simulation runs the sensors will be included as 'perfect' blocks such that:

$$S_M = 1.0$$

$$S_{C1} = S_{C2} = 0.0$$

$$E_M = E_H = 0.0$$

Roll Position Angle

Figure 8.3 shows the three attitude angles. Also shown is the angle which a vertical (roll) gyroscope measures, Φ_S, this is the angle between the y axis and the line yz_0 on figure 8.3. Clearly Φ_S is only equal to the bank attitude angle Φ for zero pitch angles, Θ. With reference to figure 8.3 the general solution can be determined:

$$\sin \Phi_S = \frac{0z_0}{0y_0} \qquad \text{(i)}$$

$$\sin \Phi = \frac{01}{0y} \qquad \text{(ii)}$$

$$01 = \frac{0z_0}{\cos\Theta} \qquad \text{(iii)}$$

Substituting (ii) and (iii) into (i)

$$\sin \Phi_S = 01 \cos\Theta \frac{\sin \Phi}{01}$$

$$\therefore \Phi_S = \sin^{-1} (\cos\Theta \sin\Phi) \qquad \text{(iv)}$$

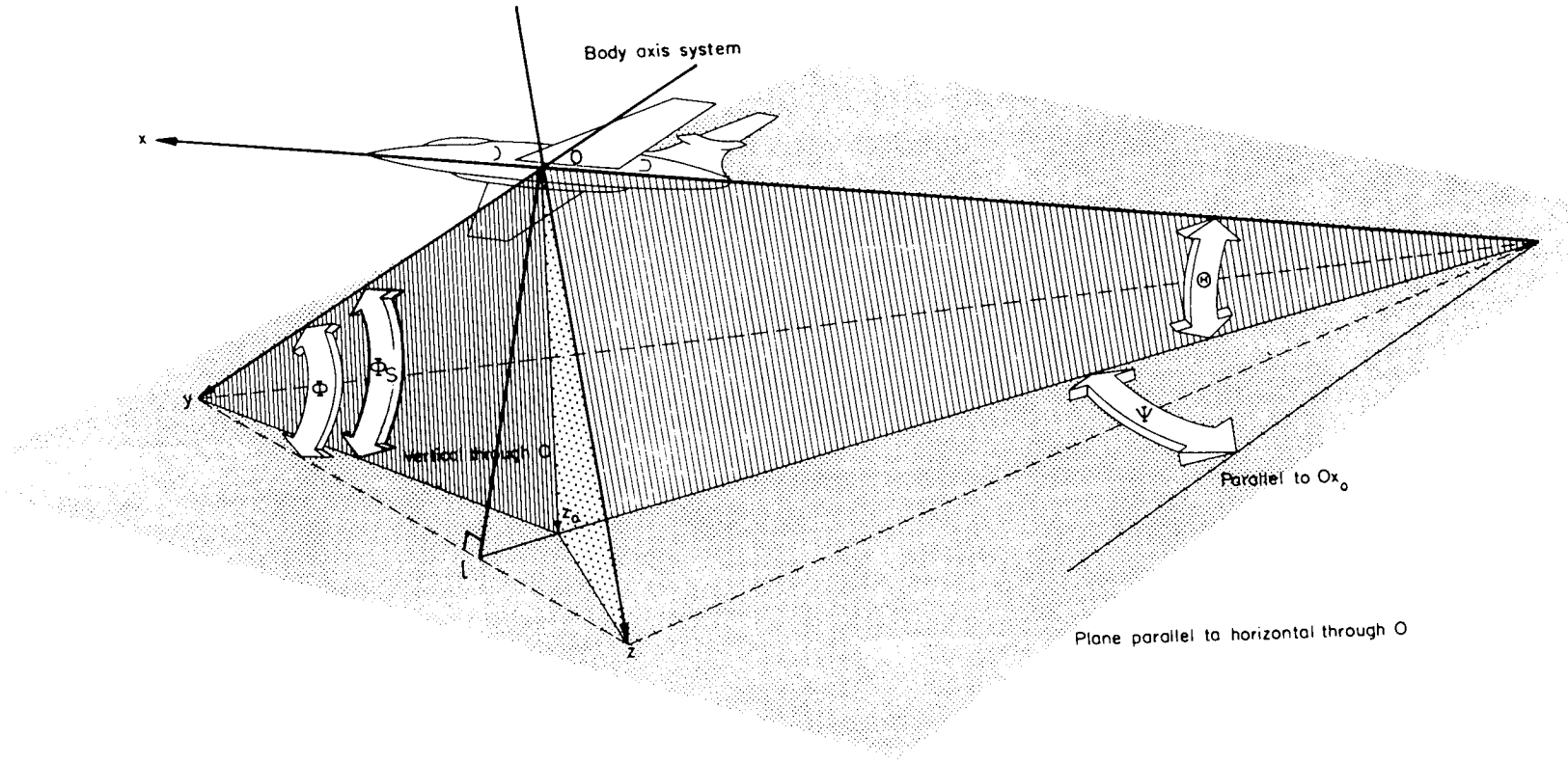

Figure 8.3 Air vehicle measured angles

Roll Position Gyroscope

The roll position gyroscope is modelled as a pure gain such that:

$$S_p = K_{pS} \Phi_S$$

Pitch Position Angle

Clearly from figure 8.3 the pitch angle measured by a vertical gyroscope is identical with the inclination attitude angle Θ. This can be stated as:

$$\Theta_S = \Theta$$

Pitch Position Gyroscope

The pitch position gyroscope is modelled as a pure gain such that

$$S_q = K_{qS} \Theta_S$$

Heading Position Angle Measured

Due to the fact that the gyroscope is mounted directly on the air vehicle the angle measured need not be the azimuth attitude angle Ψ. In fact the angle measured is simply:

$$\Psi_S = \int r \, dt$$

The measured angle Ψ_S is only identical with the attitude angle Ψ for flight cases where the bank and inclination angles, Φ and Θ respectively, are zero.

Heading Angular Rate

The rate gyroscope in the yaw plane is mounted directly to the air vehicle structure with its sensitive axis measuring rotational rate about the z axis. Therefore this sensor detects the body rate r.

Heading Position Gyroscope

The position gyroscope gives sine and cosine outputs and is modelled as a pure gain such that:

$$S_{r1} = K_{rS1} \sin \Psi_S$$

$$S_{r2} = K_{rS1} \cos \Psi_S$$

Heading Rate Gyroscope

The rate gyroscope is modelled as a pure gain such that:

$$S_{r3} = K_{rS2}\, r$$

Altitude Distance Measured

Two types of altitude sensors have been under consideration. One type is a line of sight sensor. The distance measured by this sensor is given as Oz in figure 8.3 and is related to the true altitude as follows:

$$Oz_0 = Ol \cos \Theta \qquad \text{(i)}$$

$$Oz = \frac{Ol}{\cos \Phi} \qquad \text{(ii)}$$

Substituting (ii) into (i)

$$Oz = \frac{Oz_0}{\cos\Theta \cos\Phi} \qquad \text{(iii)}$$

The second type of attitude sensor measures barometric pressure which can be approximated to some function of z_0 directly.

Line of Sight Altitude Sensor

The line of sight sensor can be modelled as a pure gain such that:

$$S_z = K_{zS1}\, Oz$$

Pressure Sensor

The baromeric sensor measures true altitude and can be modelled as:

$$S_z = K_{zS2}\, Oz_0$$

8.4 Processing

Three levels of analysis of the flight control loops were considered:

(a) linear transfer functions,

(b) op-amps (as gains, differentiators summers) + limiters,

(c) full component level simulation.

Using a simple transfer function is the most trivial technique where all non-linear effects are neglected. This would be a simple approach to implement and would run quickly. If necessary only the dominant roots could be included to further simplify the model.

Modelling each operational amplifier as a simple gain, summer differentiator etc followed by a limiter, which could be the result of either a diode clipping network or limiting caused by the rail voltage, would allow the effects of block diagram level non-linearities implicit in the design to be included without recourse to component level simulation.

A component level analysis based on the specific operational amplifiers could be carried out with reference to standard texts (180) or using computer packages such as SPICE* on a PRIME computer.

A simple analysis of the flight control system indicated that the performance is dominated by the slow actuator response, the time constants of individual components being several orders of magnitude faster. At realistic perturbations of the control system, simple hand calculations showed that several points in

---

*SPICE Circuit Simulation Program Dept Electrical Engineering and Computer Science, University of California US.

the circuit, amplifiers would reach their maximum voltage levels, thus causing the circuit to operate in a non-linear mode.

From these simplistic check calculations the most appropriate level at which to model the control system became clear. Obviously the non-linear effects could not be neglected as operating in this regime was common during normal flight conditions. This assertion rules out the simple linear transfer function approach. Adopting the in-depth component level technique would not significantly provide improved modelling of the actuator dominated system, and more advanced techniques require substantial computational power. It might at first sight appear to be more efficient to use a detailed proprietary software package, but, after allowing for the time required to interface the package with RPAV simulation, a disproportionate level of resources would be required for little gain in simulation capability.

Therefore in the interests of development and run time efficiency it was concluded that modelling the processing circuits as pure gains etc with post limiters was the most appropriate solution. Consequently this approach has been adopted and included in the model in a form shown in figures 8.1 and 8.2.

8.5 Actuator and Linkage Model

The 'actuator' consists of a driving amplifier and an electric motor; the 'linkage' consists of a reduction gearbox and a linkage system including bars, pivots, swashplates and sliding tubes designed to convert the rotary motion of the actuator motor to rotation of the rotor blade along its long axis, thus controlling the blade angle of attack.

The actuator driving electronics consists of an SGS L292 amplifier and supporting passive components configured by the designer, in accordance with manufacturers recommendations (181)(182), as a transconductance amplifier (183). In effect the output of the amplifier is a current, which flows through the motor armature, proportional to the input voltage. The amplifier in this configuration automatically compensates for armature resistance and back EMF within the limits of the supply voltages. The user is also able to specify a maximum current level (up to 1 amp) to avoid damage occurring to the actuator motor. Figure 8.4 shows the calculations performed in the simulation of the actuator amplifier.

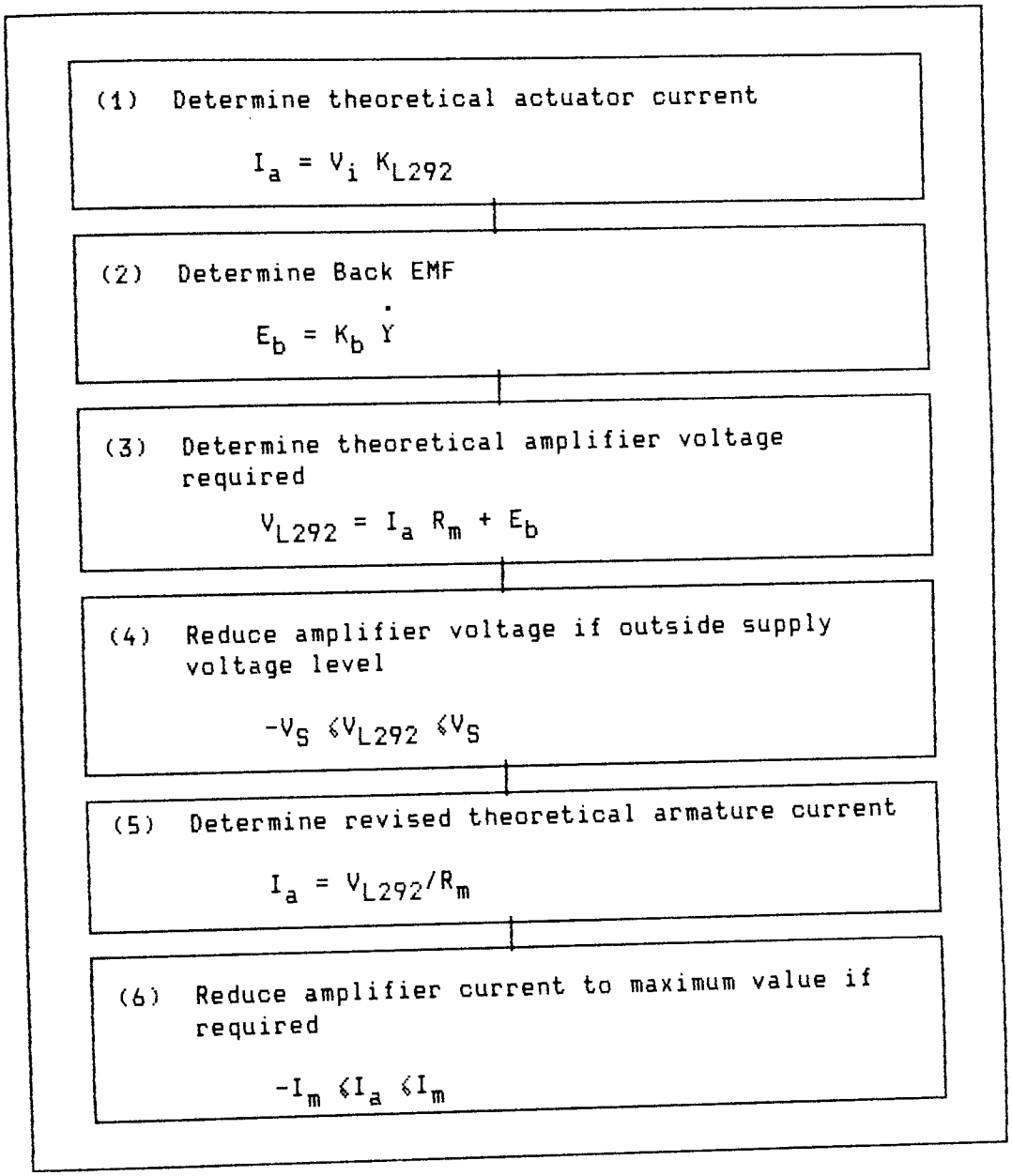

Figure 8.4 Actuator Amplifier Model

The equations used for modelling the motor element of the actuator are based on reference (184). The motor electrical time constant is small (at 0.27 ms) when compared to the mechanical time constant (34 ms) (121) and is hence neglected. Results from laboratory tests carried out at ML Aviation have enabled the effective inertia of the motor and its load to be determined.

The effects of viscous friction are not included in the model but are, to some extent, embodied in the motor and load time constant, which was obtained experimentally (121). The simulation equations are presented below:

armature torque

$$T = K_T \, I_a$$

armature acceleration

$$\ddot{Y} = \frac{T}{J} \qquad \left(J = \frac{K_T \; K_b \; \tau_m}{R_a} \right)$$

armature velocity

$$\dot{Y} = \int \ddot{Y} \; dt$$

$$Y = \int \dot{Y} \; dt$$

The motor armature position is converted to blade angle by representing the actuator gearbox as a simple gain plus offset, hence the blade angle is given by:

$$\theta_b = K_{B1} \, Y + K_{B2}$$

Four common effects are not included in the actuator model to date, basically through the lack of empirical data available. These are:

(a) motor load torque,

(b) linkage and gearbox flexibility,

(c) load direction dependant hysteresis (blacklash) (estimated at ± 1 degree (185)),

(d) actuator direction dependant hysteresis (feedback potentiometer wiper stiction).

Upon assessment of techniques which could be employed to include these effects in the model it became clear that the poor quality of the input data available would negate any advantages gained by a more detailed approach.

It is proposed that these could be considered for inclusion as part of the future work, at the very least a comprehensive practical programme is required to give good quality input data.

8.6 Actuator Results

The control system was simulated to give both open and closed loop responses for a step input demand. The open loop run, was monitored to verify that non-linear clipping occurred at the correct levels and to confirm that the motor time constant is in the region of 34 ms (183). The position and velocity responses are shown in figure 8.5.

Figure 8.6 shows the closed loop position and velocity responses.

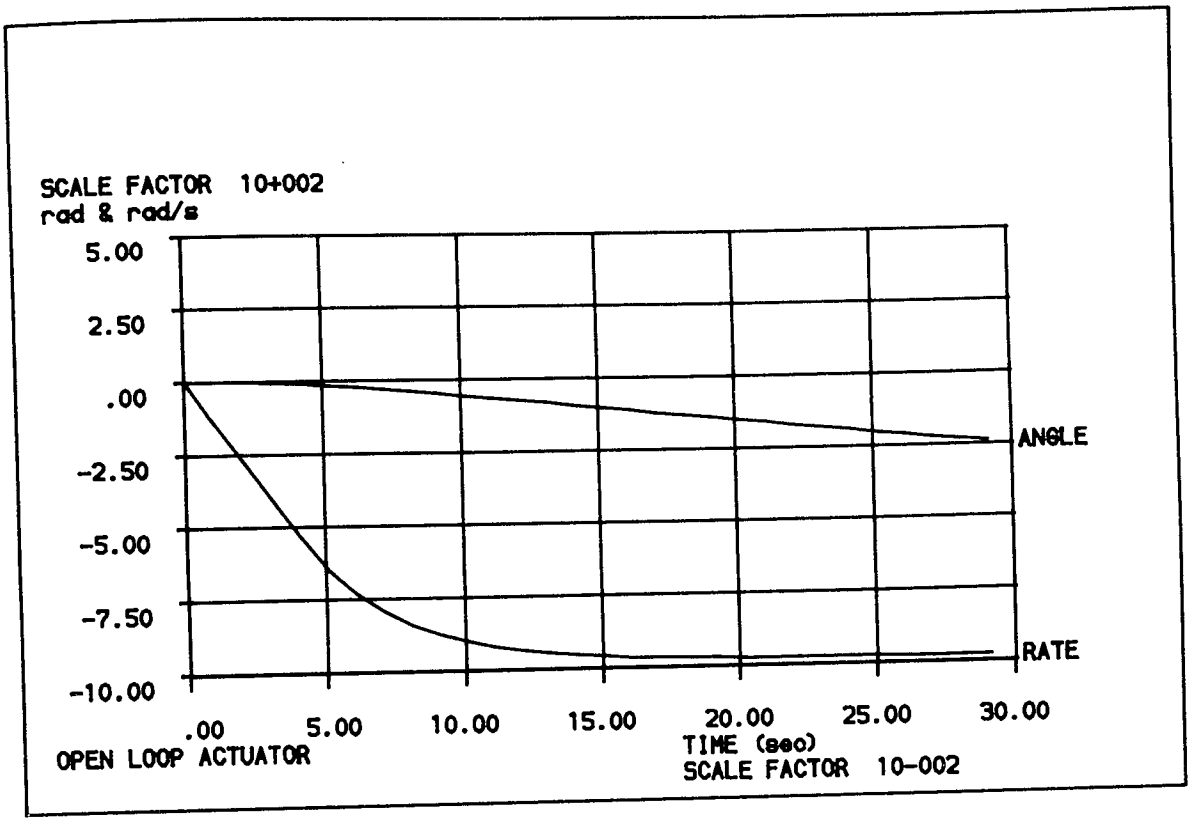

Figure 8.5 Simulation output - Open loop actuator response

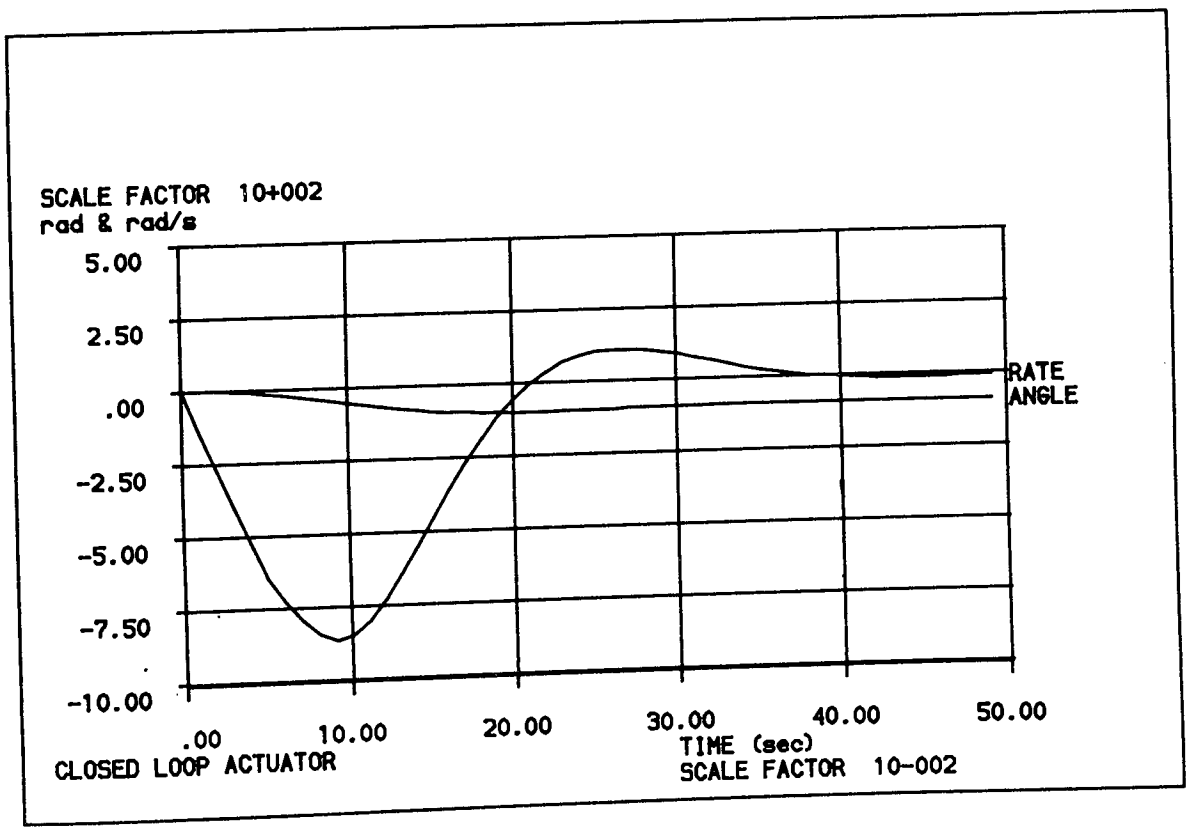

Figure 8.6 Simulation output - Closed loop actuator response

The closed loop response, was measured for similar input voltage levels to those used in laboratory tests (122). The computer simulation response shows an overshoot of approximately 12% which can be interpreted as a relative damping ratio, ξ, of 0.55 (186) and a time constant of 102 ms. (This value being obtained for a value of 4τ at the end of the first cycle of overshoot).

For ξ = 0.55 the end of the first overshoot cycle corresponds to a value for 4τ when compared to the curve for ξ = 1.0 in reference (186)).

Practical data presented in reference (122) showed that a time constant of 0.114 seconds was measured, but the system response is claimed to be of first order with no apparent overshoot. The time constant of the simulation is considered acceptably close to that of the practical tests. After discussions with the test organisers it is the opinion of the author that the friction and hysteresis in the linkage system disguised and contributed to the damping of the closed loop response. In view of the close time constant agreement it was concluded that the actuator model was acceptable in performance in its basic form, however, several items of future work worthy of consideration include re-evaluation of the assumptions implicit in the model, see Section 8.5, and perhaps the inclusion of some of these effects in a more comprehensive model. Consideration could be also given to a well planned test programme to provide the necessary input data which would be required in a more comprehensive model and

to provide more detailed practical data against which to validate the model. These points are discussed in Section 12.

8.7 Review

This section has presented a control system model. Actuator and sensor models have been discussed in some detail. An approach of modelling the processing electronics as a series of gains and summers with post limiters was considered optimum for this simulation.

SECTION 9

SIMULATION IMPLEMENTATION CONTROL AND RUNNING PRACTICE

9 SIMULATION IMPLEMENTATION CONTROL AND RUNNING PRACTICE

9.1 Introduction

The implementation of the theory into a simulation software package for use by Company engineers is discussed here. The strategies of Section 4 requiring traceability, repeatability and visibility have been designed into the package. This section describes these techniques and the way in which they have been implemented. Section 5 described the dynamically adjustable time step integration process and Sections 6 to 8 described the theoretical basis for specific modules of the simulation. Attention is now concentrated on how the simulation is controlled, in particular, where and how data is fed into and taken out from the main program and how results are stored and prepared for the simulation user.

9.2 Software Development

The simulation was designed for use on the ML Aviation PRIME 550-II computer in Fortran IV. This language was chosen in preference to unsupported Basic, which was the only other language available, for reasons including the following:

(a) to take advantage of existing utilities in Fortran IV (187),

(b) more suitable for modular development through the use of subroutine and function libraries,

(c) faster running from compiled code,

(d) six character variable names allow the use of more explicit terms (PRIME Basic supports only single characters),

(e) software portability.

There is no intention to discuss the relative merits of alternative computer languages here. This topic is merely raised to illustrate the fact that there was no practical alternative to using Fortran IV. Assembly languages, had any been available, would be dismissed as requiring excessive development effort which would detract from the main aims of the project which are to provide to the Company, within timescale limits, a working air vehicle simulation.

The software design reflected the requirement, introduced in Section 4, for a modular structure. A simple skeletal control program was designed which could be easily expanded to include additional air vehicle modules as required. The flow chart for the simulation program is given in figure 9.1.

In-built to this part of the program are the following features:

(a) input and output files selectable at runtime,

(b) list of selected datafiles recorded in a run file,

(c) initialisation of state vector and other variables,

(d) integration with expandable module caller,

(e) error verification with result accept/reject capability,

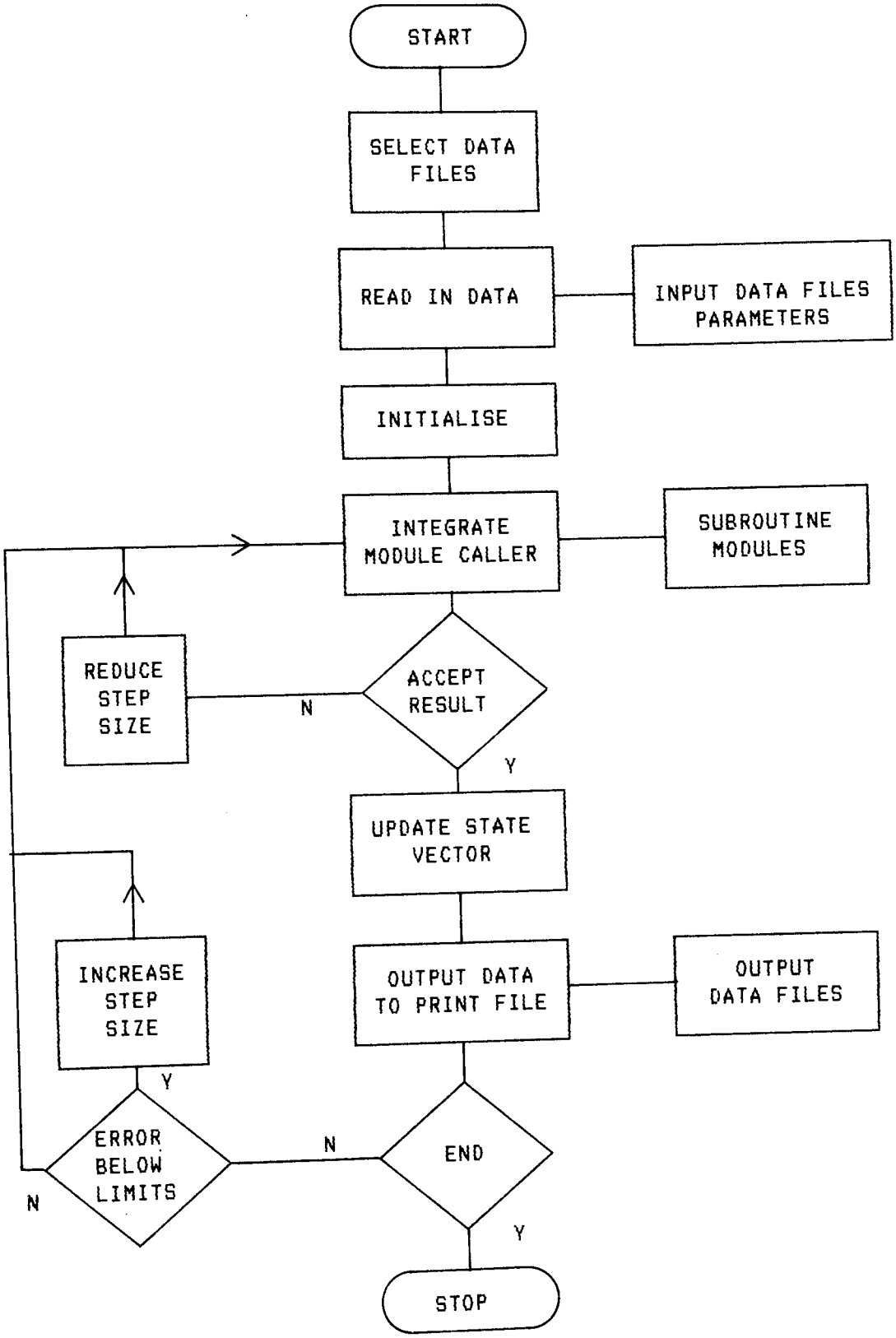

Figure 9.1 - Simulation Flow Chart

(f) controlled dynamically variable time step size feature,

(g) selectable output data frequency,

(h) user definable run time,

(i) current values stored in state vector for ease of identification.

These features are discussed below in the form in which they appear in the final simulation program. It was found that the philosophy of adopting a simple skeletal calling program with expandable module caller was most successful, the basic structure is little changed in the final simulation program to that first used.

As additional modules were required in the simulation they were developed as subroutines and validated in their own right. Once satisfactory, they were introduced into the simulation package, one at a time in the approved manner (125), and the following validation steps performed:

(a) sign validation for all branches of code,

(b) quantitative validation for all branches of code (verified by hand calculation),

(c) further limited test cases as appropriate.

During the development of new subroutines they were attached to the bottom of the calling program and recompiled as required. Upon completion of the validation process non-air vehicle

specific subroutines were transferred into software libraries which had been developed by ML Aviation (187), so that they could be made available to other users.

As development proceeded it appeared that at some time in the future the company may benefit from faster running of the simulation at reduced accuracies. In addition to the PRIME single (7 decimal) and double (14 decimal) precisions there is also, as explained in Section 5, high precision which uses the alternative trigonometric functions. In order to achieve flexibility the existing, to some extent inconsistent (187), company program naming notation was adopted and rationalised whereby the first letter of a function or subroutine name was reserved to describe the degree of precision and the remaining five characters used to describe the operation. Double and high precision are denoted by D and H prefixes respectively but due to the inconsistencies referred to above, where no initial policy had been adopted by the Company during early development of utilities, single precision subroutines were prefixed by a blank or R, E or S. During simulation development single precision subroutines and functions were prefixed by a blank adopting PRIME practice and program names were prefixed by S.

To increase flexibility nine codes were used to replace these prefix letters, and the technique was extended to include variable declaration and exponents. A title of 'Master Code' was awarded to these codes which are shown in table 9.1. This

MASTER	CONVERTED TO:			EXAMPLE	COMMENT
CODE	SINGLE	DOUBLE	HIGH		
#1	4	8	8	REAL*#1	Variable declaration
#2		D	D	#2ABS	Double versions used in High Precision
#3	R	D	D	INP#3	Some subroutine names
#4		D	H	#4COS	Function names
#5	R	D	H	#5BUNTY	Some program names
#6	E	D	D	#6+2	Exponent
#7	E	D	H	#7RATCV	Some Dynamics subroutine names
#8	S	D	D	#8SIM.COM	Some insert file names
#9	S	D	H	#9RPV2D	Generated Program/ subroutine names

Table 9.1 Program Precision Conversion Master Code

technique had the advantage of allowing a global edit program to be written in PRIME Command Programming Language (CPL) allowing configuration of a program written using master code to single, double or high precision by simply typing in one command line:

CP filename P Q

where CP is the utility command name, filename is the name of the master code program, P, a code for the required precision; S, D or H and Q is the name of the job queue upon which the conversion is run. These utility files are included in Appendix E with an example of source master code. The change precision

utility generated a new set of code of the required precision saved under the source code filename with an S, D or H prefix denoting the precision. A further file is also generated containing screen messages which are generated during the global edit to record errors should they occur.

Adopting the use of the master code practice obviated the need for the parallel time consuming development and maintenance of programs of differing precisions providing similar functions.

Program standard and traceability was assured by using the master code practice described above and by adopting and recording specific names for the development software which indicated which modules were called. Issue numbers were allocated and updated during development. The program code was preceded by comment lines using master code where required giving the following information in all functions, subroutines and programs developed as part of the simulation suite:

(a) program name,

(b) program issue,

(c) date of issue,

(d) author,

(e) list of changes at each issue revision,

(f) description of function,

(g) summary of theoretic basis,

(h) source of theory,

(i) definition of each variable name.

These details were aimed at aiding understanding of the following groups:

(a) program author,

(b) project supervisors,

(c) program users (company staff).

For economy of development time and the reliability of the software product use was made of insert files (files containing commonly used code loaded at compilation time) wherever possible for documentation, data, variable declaration and other repeated areas of code common to more than one function, subroutine or program. This reduced larger programs into more manageable units. A typical example of the latter category being the print units which were written as insert files for easy identification as they were frequently modified during debugging.

Further utilities written to aid software development enabled subroutines to be coded and stored individually. Simulation program builders then simply created the simulation programs by loading the skeletal program followed by the necessary subroutines. An example builder is included in Appendix E. These were then passed to the precision conversion program. The

stages of building up a simulation program are summarised below:

(a) develop individual skeletal program, functions and subroutines,
(b) use loader to build program,
(c) select required precision,
(d) load insert files and compile program,
(e) load previously compiled library routines,
(f) run simulation.

The simulation was designed to be run interactively, with input and output data file names being requested from the operator. However, as the input required was minimal, only data file names and edit responses, simple command files could be written to run the simulation on the more economical batch service* job queues or via phantoms.

The simulation program builders and precision conversion utilities and command run files were a major contribution to economic software development, in the opinion of the author, resulting in major timescale savings of up to 50% overall, with increased quality of software assured by obviating the need for parallel program development.

---

* ML Aviation charge batch Service CPU time at 10% of interactive CPU time rates

9.3 Simulation Data Units

The simulation input and output data and all internal calculations use SI units throughout. One choice is, however, given to the operator which is to specify angular quantities in either radians or degrees. Whilst radians are the preferred units which are used internally, degrees are still widely used within the Company especially for measuring small quantities.

9.4 Simulation Data Files

To ensure traceability of data, to aid detection of data entry errors and to ensure repeatability, a policy of transferring data using data files was adopted from the outset. Input data is segregated into files, where, broadly speaking, one input file serves one module.

In the complete simulation program the following files are used for data entry:

(a) simulation control,

(b) air vehicle parameters,

(c) flight control system,

(d) initial conditions,

(e) flight plan,

(f) wind velocities,

and the following output data files are generated:

(g) record of input and output filenames,

(h) summary output and error messages,

(i) detailed output.

The simulation data flow is summarised in figure 9.2.

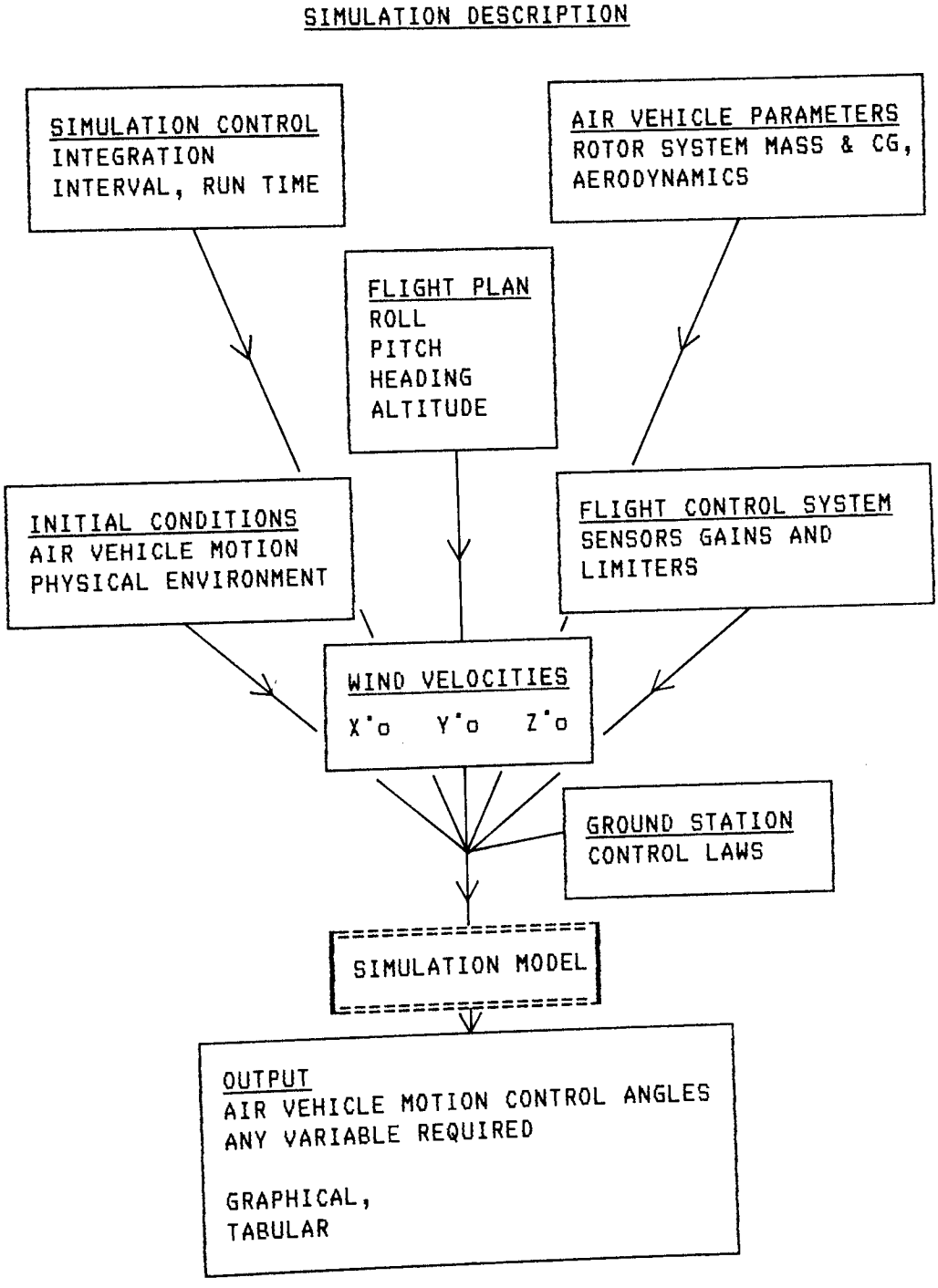

Figure 9.2 Simulation Data Flow

Individual stand alone programs were designed and developed to allow the creation and editing of each of the input data files. Using these programs standard development files were created and updated, so that they could be called up as required. Consistent systems of filenames were developed so that the data filenames identified the file type. As a further effort to ensure traceability a backup paper record system was also adopted.

Proformas were prepared for recording the contents of input data files, examples are included in Appendix E. These proformas show all data required and the following examples illustrate the data types in each file.

Simulation Control File

The data stored in this file is used to actually control the running of the skeletal program. Items entered here include maximum runtime, integration control data, output data frequency and angular units.

Air Vehicle Parameters

This file describes the physical aspects of the specific air vehicle under consideration. Examples include rotor data such as blade radius, chord and lift curve slope and overall air vehicle parameters such as mass, cg position and moments of inertia. These parameters are used by the rotor and six degrees of freedom motion modules.

Flight Control System

The mechanism of operation of sensors and gains, control processing electronics gains, clipping voltages and actuator gains are included in this file. The control system subroutine uses this data.

Initial Conditions

The values of variables are initialised using data from this file. Parameters include air vehicle motion (velocities and displacements) rotor speed and initial values for physical quantities such as gravity and air density.

Flight Plan

This file gives control demands in roll, pitch and heading angle and altitude distance as a function of time. Up to one hundred inputs allow the response to ramp, step, impulse or other demands to be observed. This is the file which will include waypoint coordinates when navigation packages are developed.

Wind Velocities

The wind velocities file allows air vehicle response to steady state wind conditions or ramp, impulse or other profile gusts to be modelled. Up to 100 wind vectors are available for any simulation run.

Filename Record

When the simulation is run the user is either given the

opportunity to repeat a previous run by calling up an existing record of filenames or invited to input filenames for a new run which are stored for future reference. This facility aids traceability and ensures that a record is kept of all data required to repeat simulation runs. Further, by using a philosophy of 'pick and mix' a great variety of runs can be performed for minimal keyboard data entry by the user.

Summary Output File

The summary output file contains the data which is also displayed on the screen when the simulation is run interactively. All user responses, data file names and general headings showing the simulation program version number and date and time of run are found here. In addition to low frequency simulation output, showing the trend of the run, there are also all error and warning messages. During the writing of the software, fault detection routines were included which cause error or warning messages to be printed out, the name of the subroutine where this occurred and the name and value of the variable triggering the message. Dependent upon the degree of error occurring several courses may be followed:

(a) fatal error - value outside acceptable range - halt program and print error message,

(b) correctable error - value in error but lies inside acceptable range and information available to correct value - continue running, amend variable value, print warning message, variable name and previous and revised value,

(c) minor error - value in error but lies inside acceptable range, but information not available for correction - continue running, print warning message, variable name and value.

An example of a fatal error is where a potential divide by zero is detected in advance; a correctable error where a variable lies outside an expected range, this could occur as a result of rounding errors causing the evaluation of an inverse sine of a variable whose absolute value is slightly greater than unity. In this case the absolute value can be rounded to unity. A further test is carried out, where, if the variable absolute value is above a second tolerance a fatal error is declared. An example of the third class or error is where a matrix is found to be non-orthogonal, when it should be, but the specific cause is not certain. Again a large error here is treated as a fatal error.

Detailed Output File

This is the file where the major output appears at user definable frequencies. Normally air vehicle forces, moments and dynamics are output, but any variable can be transferred into

this file. A 'Result' matrix has been provided so that any intermediate values or subroutine variables can be output if required.

9.5 Presentation of Results

It was appreciated during the design phase that there would be copious output from the simulation and it was important that it should be presented to the simulation user in its most useful form. Tabular output is the most simple to generate and requires minimal programming time, however if fine detail is required the printout becomes unwieldy in size and a great deal of time is required to interpret the results. However, absolute accuracy for specific points during the simulation can easily be identified and accuracies up to the maximum 14 places displayed.

Presenting the data graphically gives an immediate visual impression of the trend with minimal user effort. This facility would be useful when discussing preliminary results with senior company staff whose available time is restricted due to project commitments. Furthermore, there is an economy of output, one graph can be plotted including all data which may otherwise take several hundred pages of printout in tabular form.

Depending upon the application is was apparent that a requirement existed for both forms of output. During the development phase of the project it was predicted that the following output types would be required.

Predominant Output Type	Development phase example
(a) Tabular	6df
(b) Tabular and Graphical	Stability checks
(c) Graphical	Full simulation runs

Prior to this project several 'in house' graphics software utilities had been written for the PRIME 550-II/MEDUSA CAD System (187) by Company staff. As part of this project these utilities were amalgamated and a program developed which would read ASCII and binary data files to provide graphical outputs on terminal screens. These may be converted to hard copies by using the terminal screen dump facility. High resolution quality plots can be obtained by transferring the output to the CAD System pen plotter. The graphical results within this thesis have been produced in this manner.

If only graphical outputs are required the output can be stored in the inherently more economical binary form so as to reduce the disc space absorbed by each run.

These facilities which provide both 'quick working quality' and 'report quality' outputs have contributed to the efficient development of the simulation and this thesis.

9.6 Review

Section 9 has discussed the detailed implementation of the

simulation software package. The specific needs of the sponsoring Company have been of particular importance during this aspect of the work. Techniques to optimise software development timescales and reliability have been presented and techniques for handling the input and output data are described.

SECTION 10

A SELECTION OF SIMULATION OUTPUT

10 A SELECTION OF SIMULATION OUTPUT

10.1 Introduction

Previous sections of this thesis have described work which identified a need for a comprehensive air vehicle simulation. The simulation development strategies have been discussed and the theoretical basis of a simulation presented. This work has been implemented in software and the individual subroutines have been validated. This section of the thesis presents a few example cases where the simulation has been used to assist the RPAV designer.

Arguably this section may be the most important in the thesis as its very presence gives evidence that the main objective of this project has been achieved. A full air vehicle simulation package has been written and is already available to the sponsoring Company. Before an accurate assessment of the performance of this package can be conducted the SPRITE project itself needs to progress to a point where reliable flight data is available for validation purposes. The Company have always realised the importance of recording flight data and work on the necessary instrumentation is advancing well. The section on future work takes up this discussion and proposes test flight cases which should be considered as part of a comprehensive validation programme.

Nevertheless, the validation work already carried out on the individual modules of the simulation provides confidence for the user. The following brief investigations carried out with the aid of this simulation package are 'real studies' which the Company had identified as important tasks but lacked the analysis tools to complete this work other than at a simple level using gross approximations.

The three studies were to investigate:

(a) whether the air vehicle would be stable or unstable without the use of the 'control rotor',

(b) whether proposed alternative control system gain settings would reduce steady state errors and how air vehicle response would be affected,

(c) the effects of horizontal wind gusts.

10.2 Air Vehicle Stability

When the prototype air vehicles were designed for development purposes control rotors were incorporated into the co-axial rotor system so that the air vehicle could be flown manually without stabilisation loops in all channels and also to reduce the response speed required of prototype actuators. As explained in Section 6 the control rotor effectively reduces the overall air vehicle speed of response to a level appropriate to a human pilot (114).

It was always intended that the control rotor should be replaced at the earliest opportunity to simplify the rotor system thus reducing production costs. However, successful development flights were achieved using this configuration.

Although simple single axis linear analysis indicated that the air vehicle should be stable without the control rotor, project staff were not confident enough to pursue this design change.

As part of this project simulation runs were performed to investigate the stability of the control loops. Runs were performed for step input control demands initially using single axis, 2 degrees of freedom motion and finally a full simulation run was carried out using the full six degrees of freedom motion facility. Table 10.1 shows the input demands and axes under investigation.

Figure	Control Channel	Demand
10.1	Roll	0.1 rad
10.2	Pitch	0.1 rad
10.3	Heading	1.0 rad
10.4	Altitude	-10.0m
10.5-10.8	All axes (6df)	All above simultaneously

Table 10.1 Stability Investigation Simulation Runs

Graphical output showing the air vehicle motion, control system voltages and currents and control surface deflection was output from the simulation and made available to the project team. However, for reasons of space economy only the vehicle motion plots are included in this thesis. Figures 10.1 to 10.4 show the two degrees of freedom responses as detailed in table 10.1 and figures 10.5 to 10.8 show the overall six degrees of freedom responses when all demands are made simultaneously.

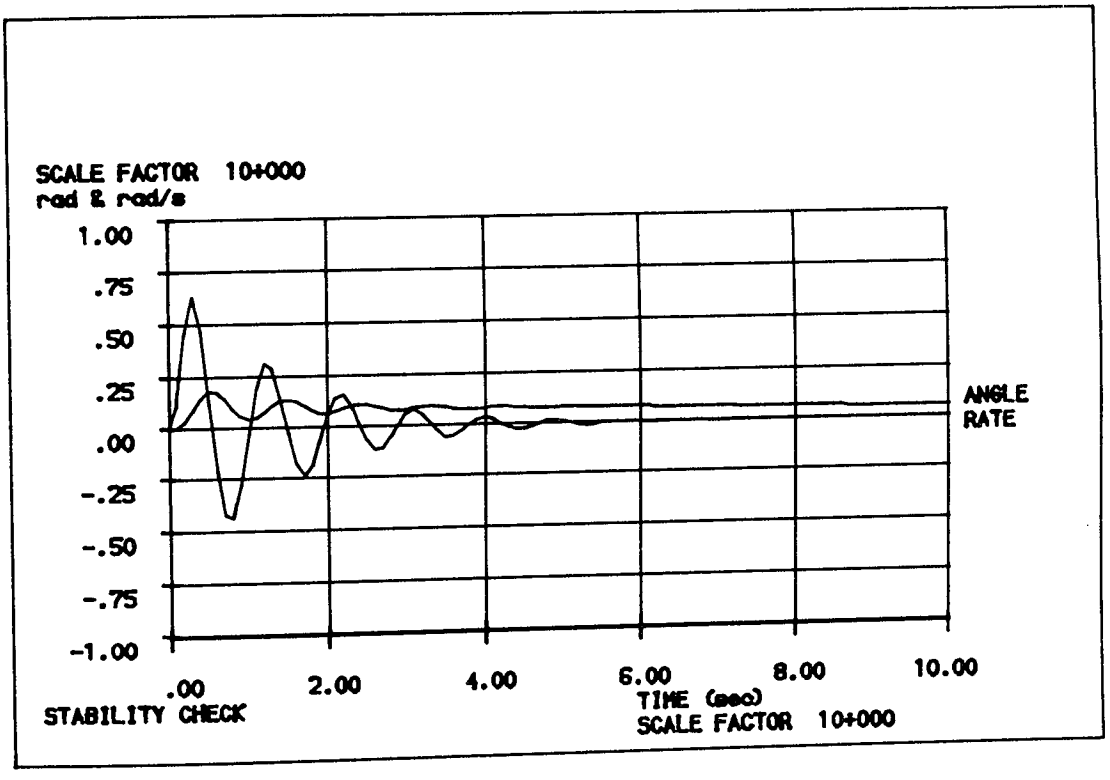

Figure 10.1 Simulation output (2df) - Roll axis response to 0.1 rad demand

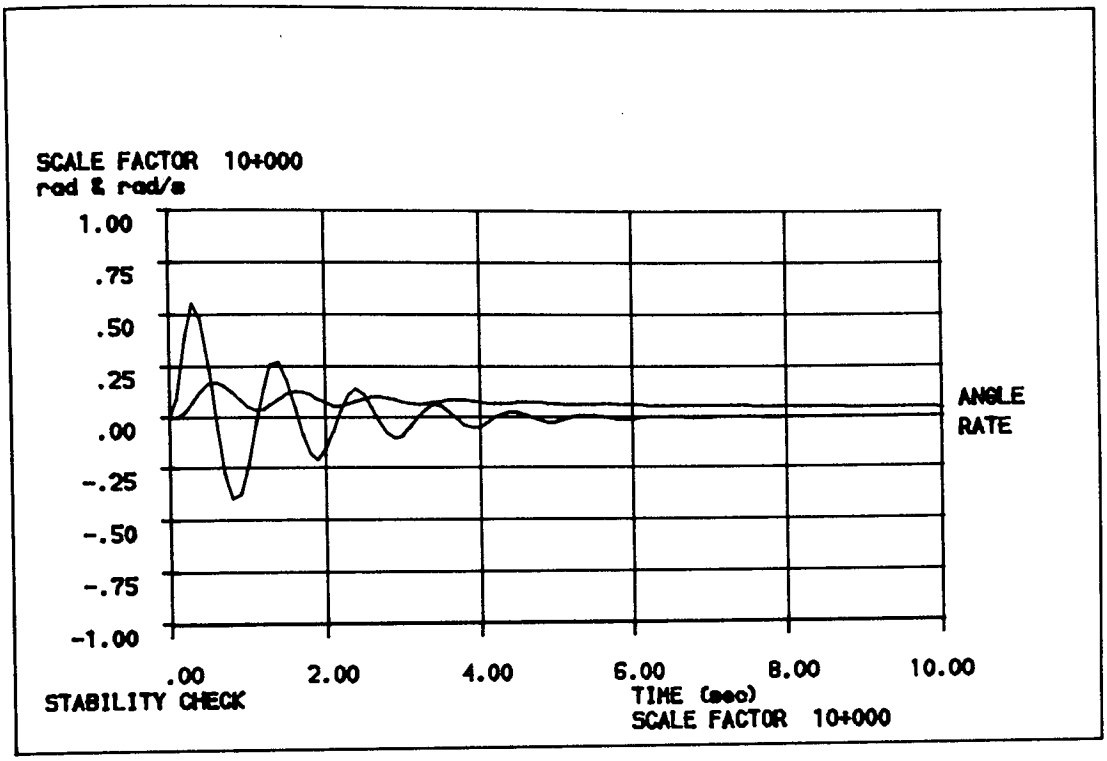

Figure 10.2 Simulation output (2df) - Pitch axis response to 0.1 rad demand

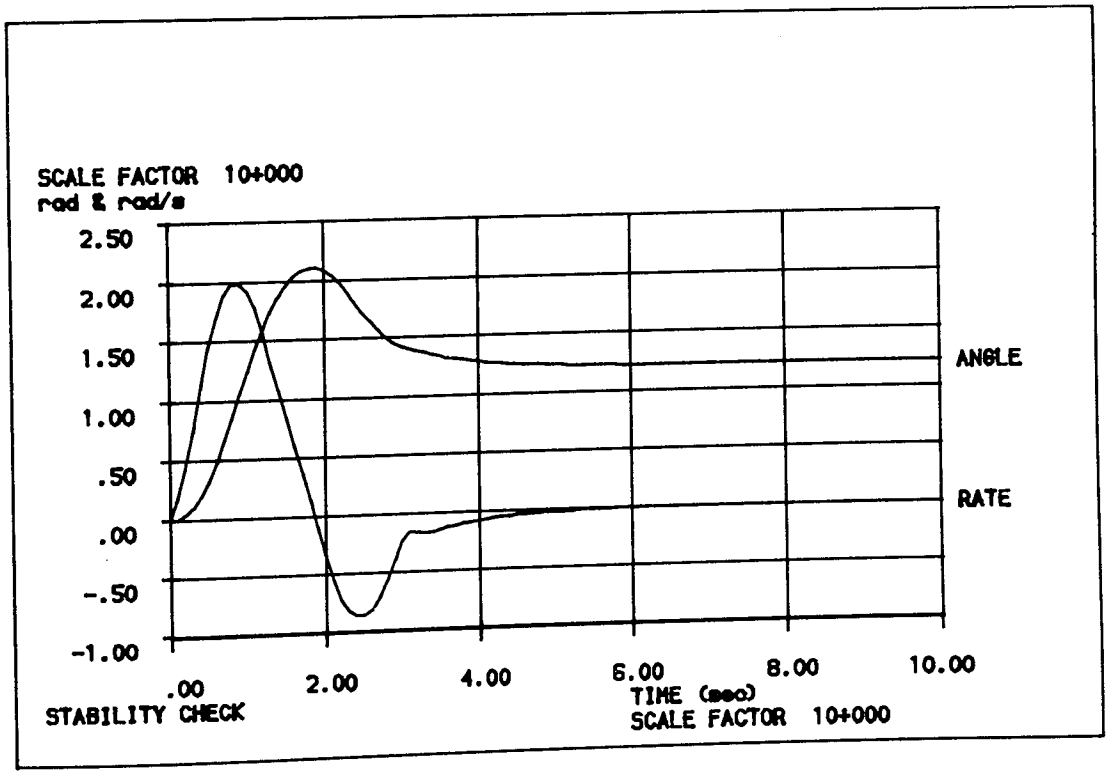

Figure 10.3 Simulation output (2df) - Heading response to 1.0 rad demand

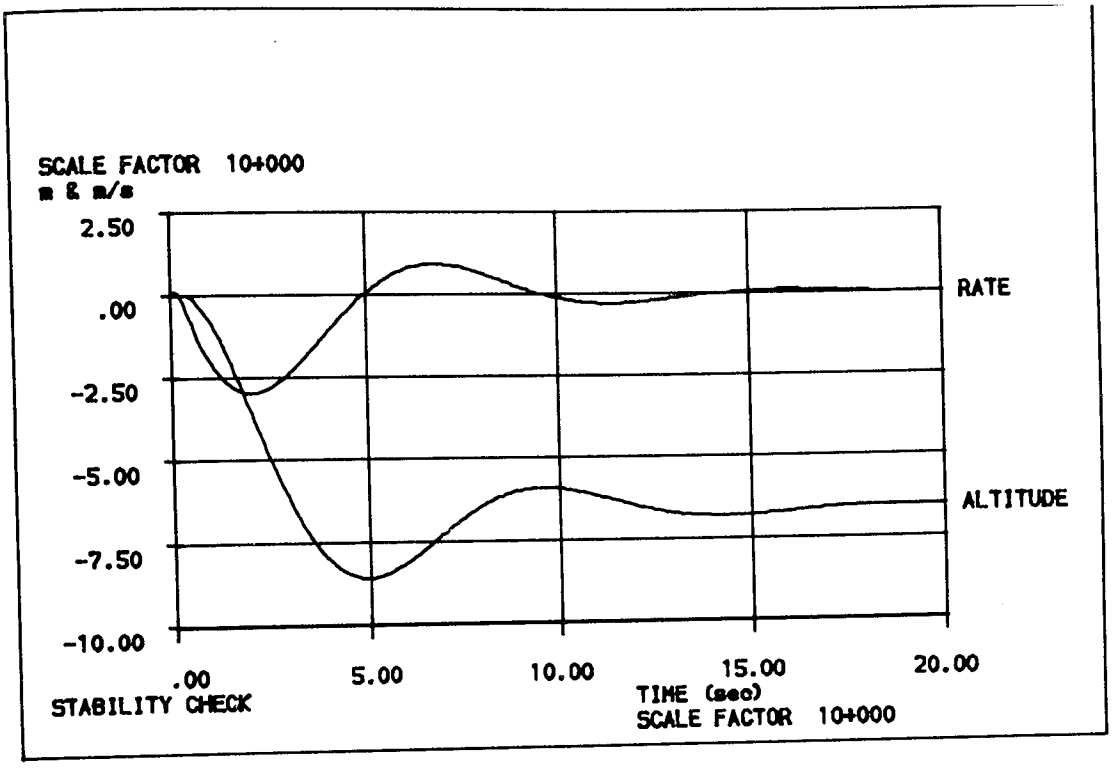

Figure 10.4 Simulation output (2df) - Altitude response to -10.0m demand

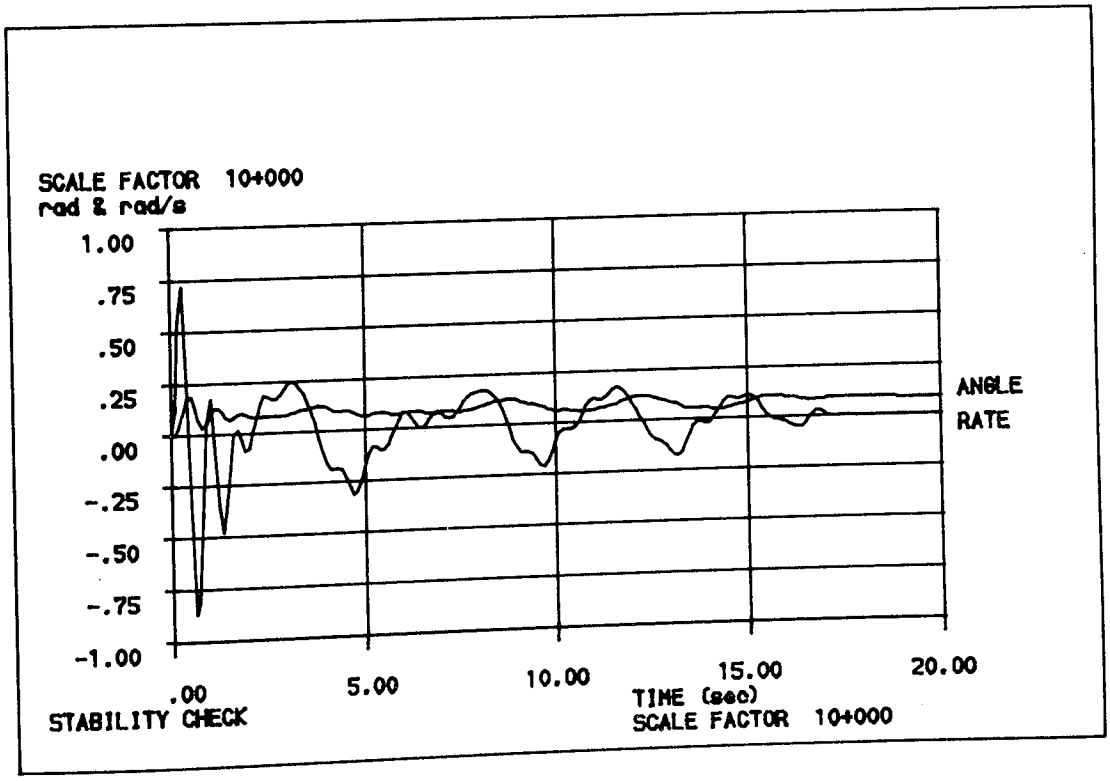

Figure 10.5 Simulation output (6df) - Roll response to roll, pitch, heading and altitude demands

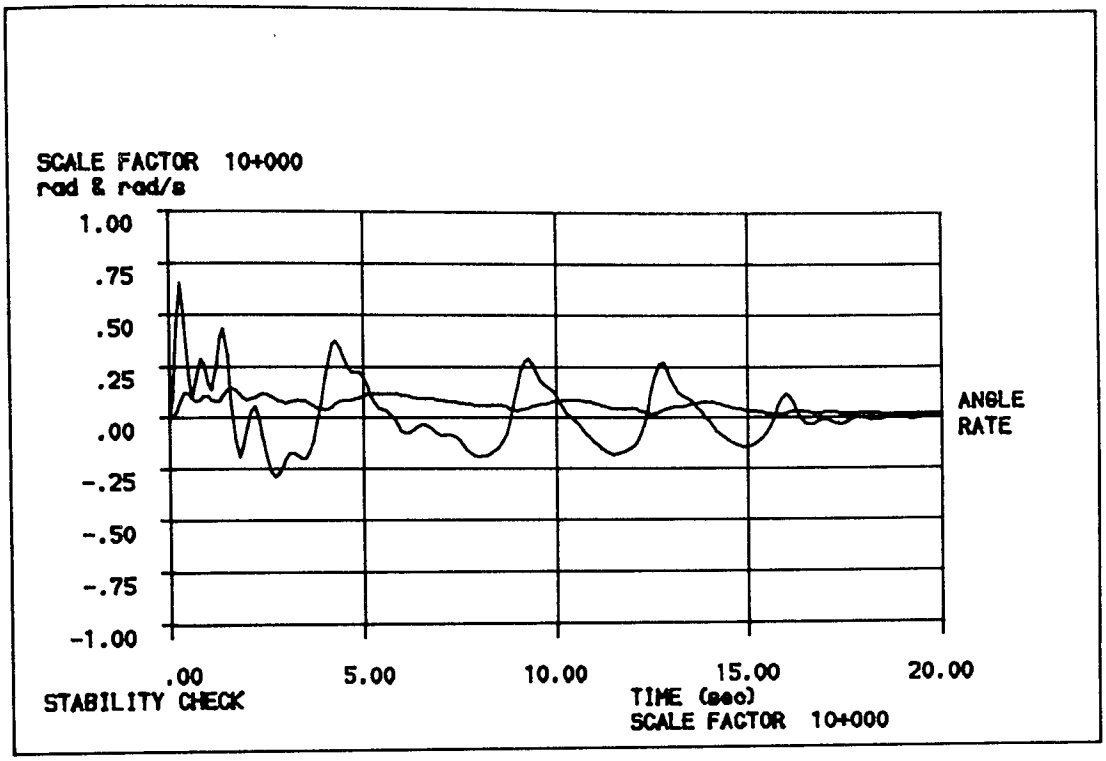

Figure 10.6 Simulation output (6df) - Pitch response to roll, pitch, heading and altitude demands

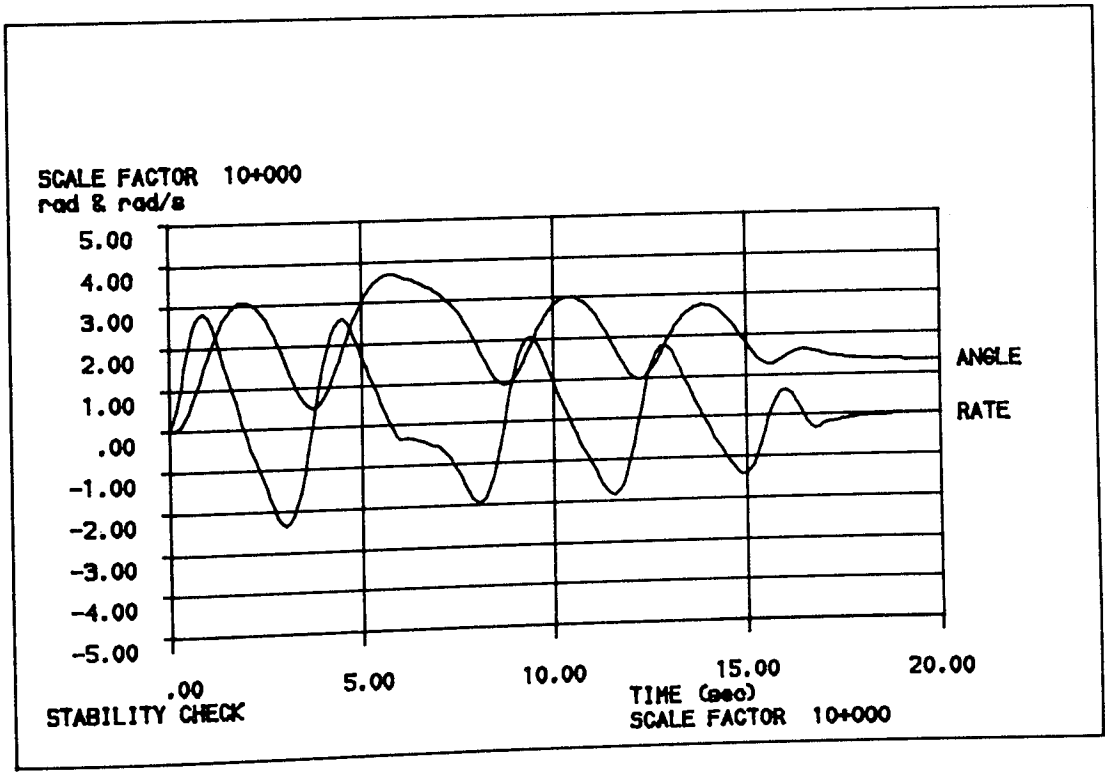

Figure 10.7 Simulation output (6df) - Heading response to roll, pitch, heading and altitude demands

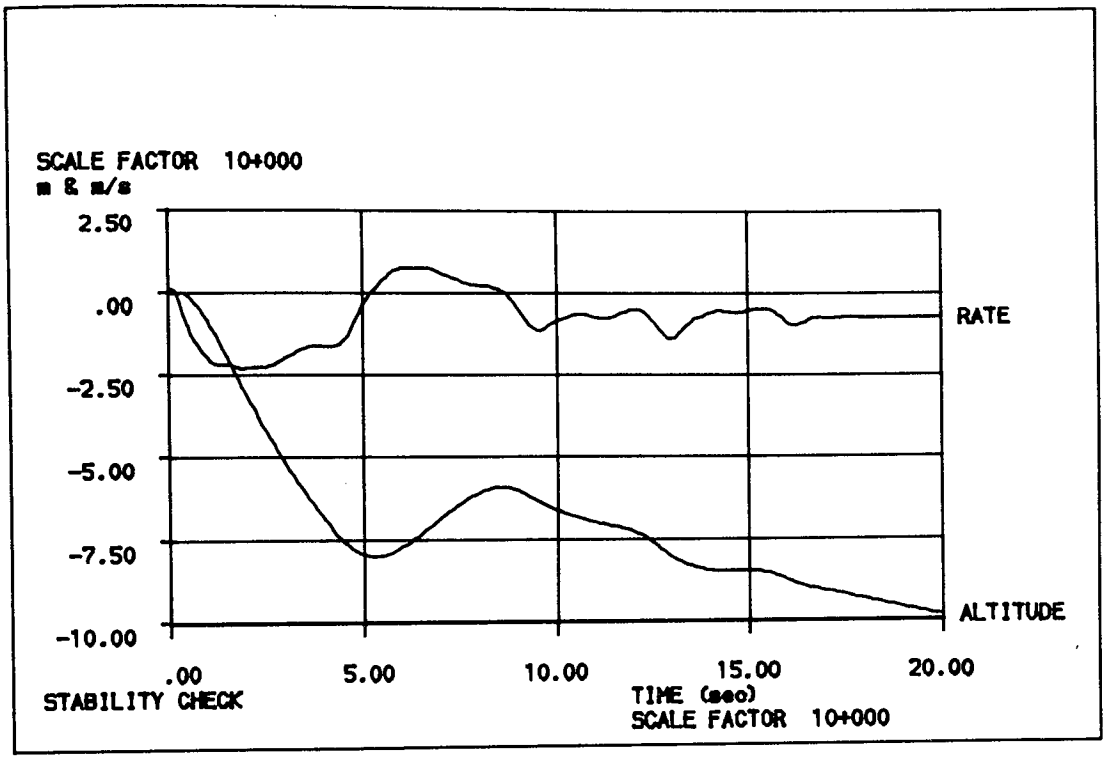

Figure 10.8 Simulation output (6df) - Altitude response to roll, pitch, heading and altitude demands

Figures 10.1 to 10.4 show that when modelled in isolation, stable but highly oscillatory responses to step demands on each of the four control channels occurred. On comparison of figures 10.1 to 10.4 to 10.5 to 10.8 the cross-coupling effects between channels can be noted. The performance, however, is still stable but oscillatory. The air vehicle motion settles after approximately 17 seconds. Figures 10.9 and 10.10 show intermediate control system voltages for the 2 degrees of freedom heading axis run demonstrating that the system performance is far from linear. Section 8 has already shown that the actuator and processing electronics are non-linear by design, as limits are imposed on driving voltages and currents.

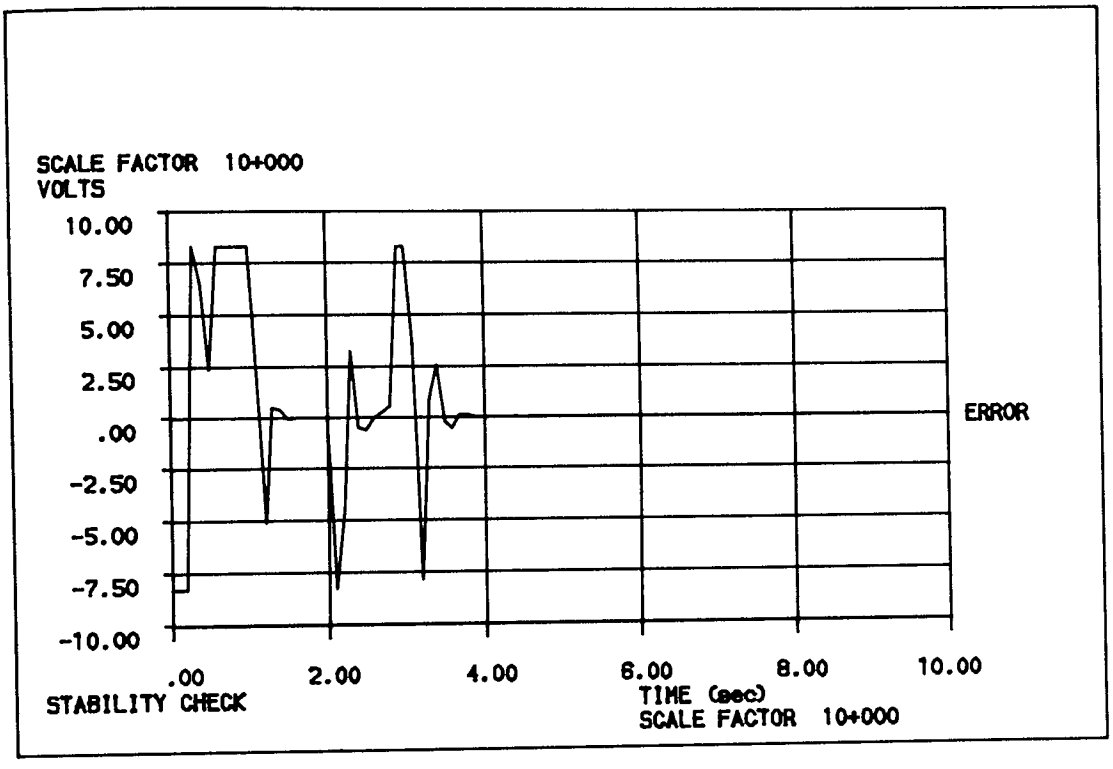

Figure 10.9 Simulation output - Actuator error voltage Vs time for 1.0 rad heading demand

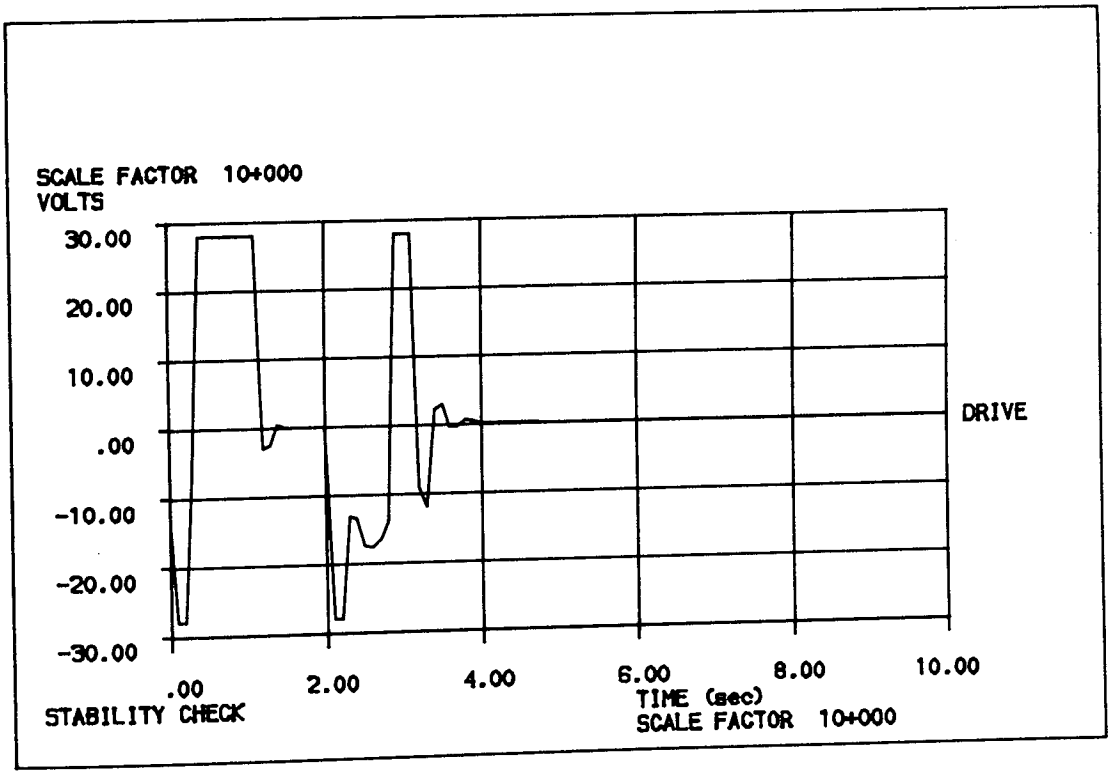

Figure 10.10 Simulation output - Acuator driving voltage Vs time for 1.0 rad heading demand

These simulation runs indicate to the designer that the control system in its present form is predicted to provide stable, but perhaps far from optimum performance, when the air vehicle is flown with the control rotors removed.

Large steady state errors can be observed. These have been verified by hand calculation and are due to the low overall forward gain of the control system. In particular the actuator reduction gearbox gain contributes significantly to these errors.

10.3 Simulation of Alternative Control System Gain Settings

The control system engineer had identified the large steady state errors shown in Section 10.2 and had designed alternative control system gain settings in an attempt to alleviate these errors and to reduce the oscillatory motion in the roll and pitch channels. Quite independently some alternative gain settings were selected as part of this project in an attempt to reduce the oscillatory motion in the roll and pitch planes. These were performed by simply doubling the rate feedback terms at the appropriate part of the circuit. Simulation runs using the alternative control systems are summarised in table 10.2.

Figure	Axis	Comment
10.1	Roll	Existing Control System
10.2	Pitch	Existing Control System
10.11	Roll	Revised Control System (high) gains
10.12	Pitch	Revised Control System (high) gains
10.13	Roll	IHD Selected alternative gains
10.14	Pitch	IHD Selected alternative gains

Table 10.2 Alternative Control Systems Simulation Runs

By comparison of figures 10.11 and 10.12 showing alternative gain setting with the existing control system performance shown in figures 10.1 and 10.2 a large change in performance can be

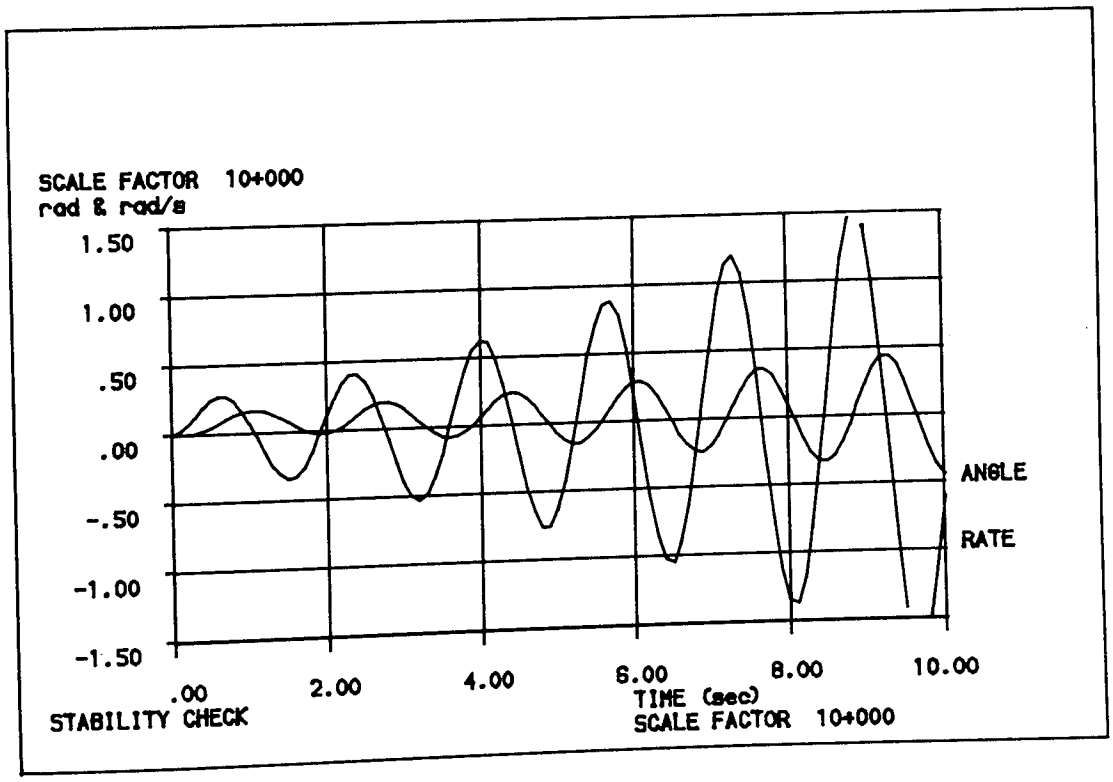

Figure 10.11 Simulation output - Roll angle and rate Vs time - revised (high) control system gains 0.1 rad roll demand

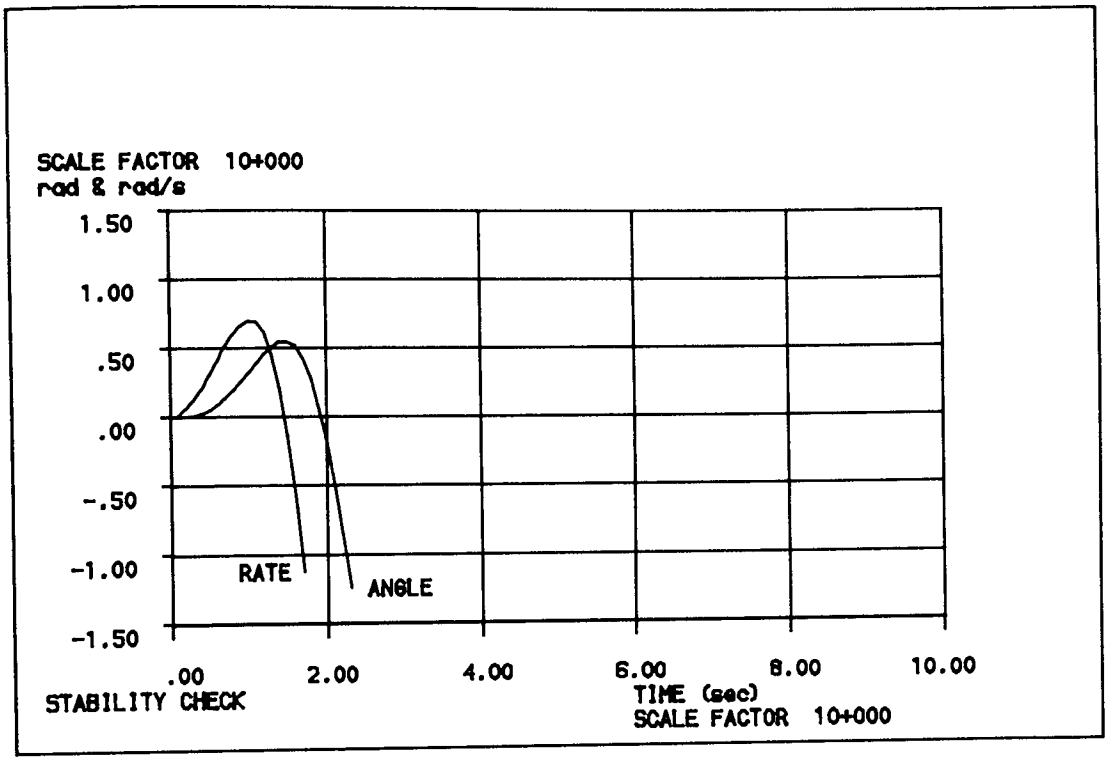

Figure 10.12 Simulation output - Pitch angle and rate Vs time - revised (high) control system gains 0.1 rad pitch demand

observed. The high gains of the alternative control system reduce the oscillatory frequency of response and also reduce the excursion of the first cycle. Unfortunately, however, they modify a previously stable response to an unstable divergent one. In practice this implies that should the air vehicle be flown with the alternative control system fitted, with no control rotors, it would go out of control.

A previous linear analysis (121) predicted that the alternative control system gain would impart on the control system a stable, low error performance. With the benefit of the simulation the

processing circuit voltages and currents were observed to be far from linear.

Assumptions that the system was linear were clearly in error. Conclusions drawn from a too simplified analysis approach can give false confidence and endanger air vehicles if design changes are implemented in hardware.

Figures 10.13 and 10.14 show improved roll and pitch responses, the oscillatory element of the motion settling after 1.5 seconds. The steady state errors are similar to those of figures 10.1 and 10.2 as the position gains are unchanged.

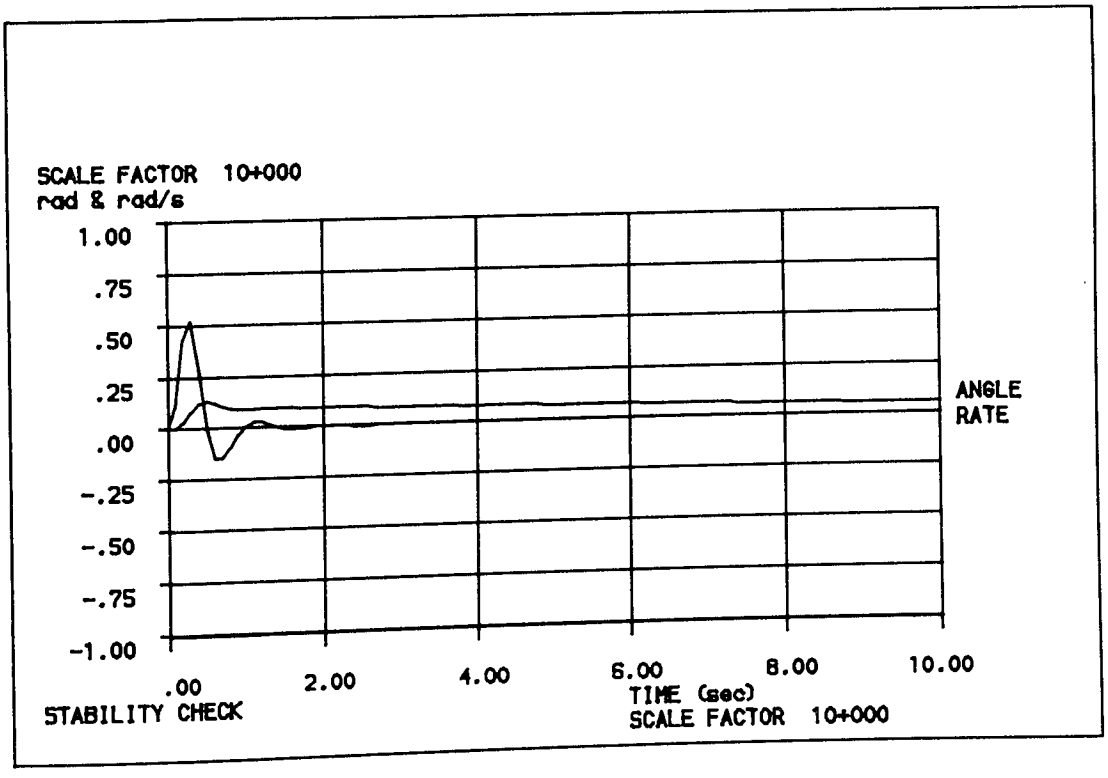

Figure 10.13 Simulation output - Roll angle and rate Vs time IHD control system gains, 0.1 rad roll demand

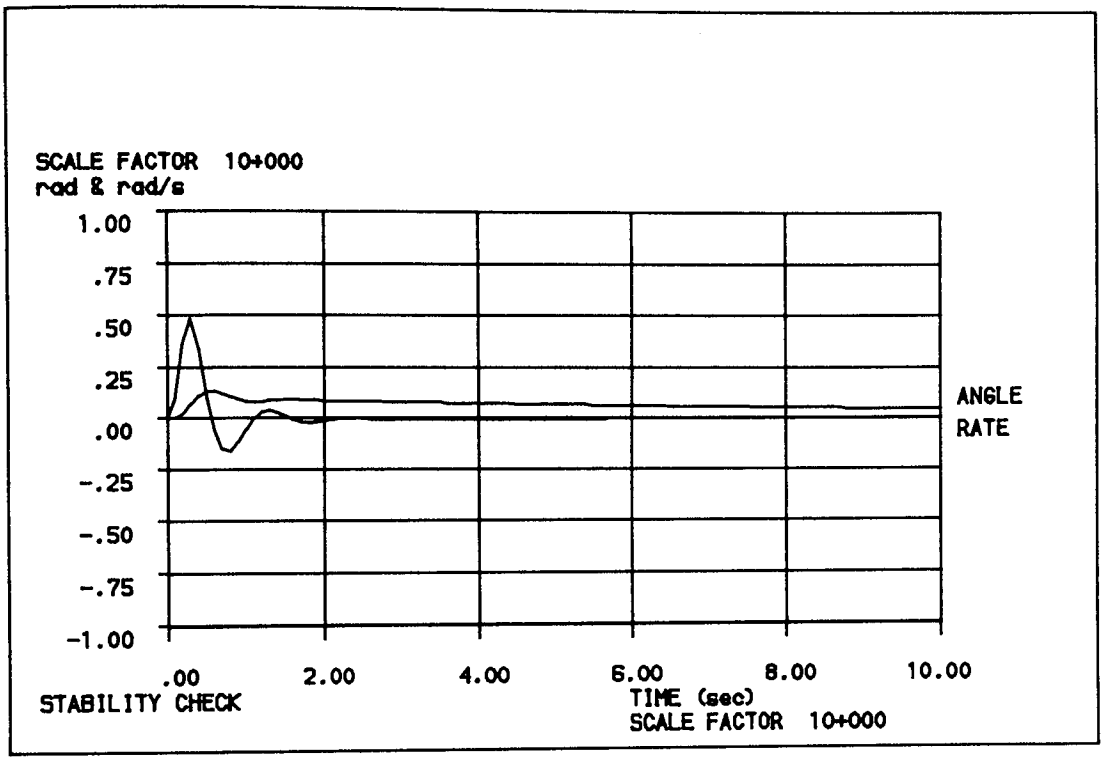

Figure 10.14 Simulation output - Pitch angle and rate Vs time IHD control system gains, 0.1 rad pitch demand

10.4 Air Vehicle Response to Wind Gusts

The simulation software package was used to model the effect of horizontal wind gusts on the air vehicle whilst it was hovering. The wind velocity was input as a square wave, the duration of the input being short in relation to the speed of response of the air vehicle so that it may be assumed to be an impulse function with unity area. Different duration impulses were used to confirm this approach.

A simulation run was carried out with an initial altitude demand of 10 metres. After the air vehicle had settled the wind gust, along the x_0 axis, of 10 m/s was applied at t = 15 seconds for a duration of 0.1 seconds. The responses of the air vehicle can be seen in figures 10.15 to 10.22. The initial heading response of the vehicle was again the result of the inbuilt differential angle of one degree.

As would be expected the dominant motion was in the pitch plane, with the air vehicle being 'blown' by the wind in the x direction. Responses due to cross coupling in the roll and azimuth planes of a smaller magnitude can be observed.

No perceptible response in the vertical plane can be seen. Upon closer investigation it was found that, as expected, a large increase in vertical thrust did occur when the wind gust was applied, but the speed of response of the vertical stability loop together with the mass of the air vehicle masked the effect of this thrust change almost completely.

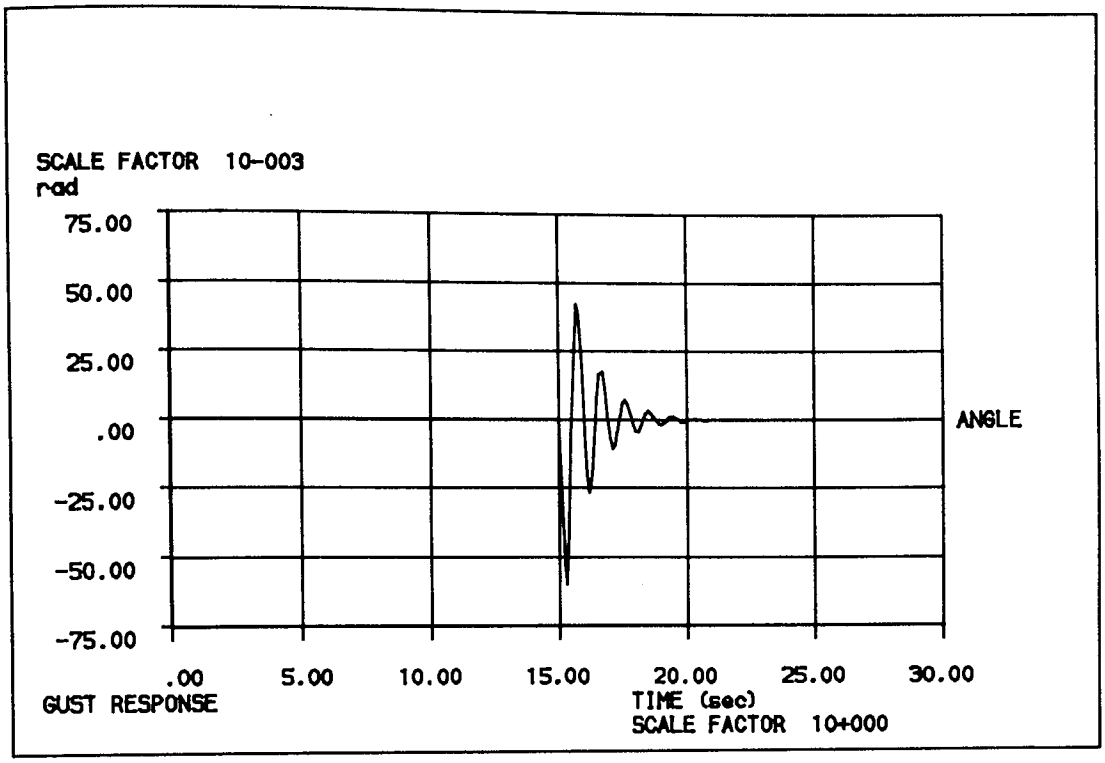

Figure 10.15 Simulation output - Pitch position response to an x_0 wind gust of 10 m/s applied for 0.1 second duration at t = 15 seconds

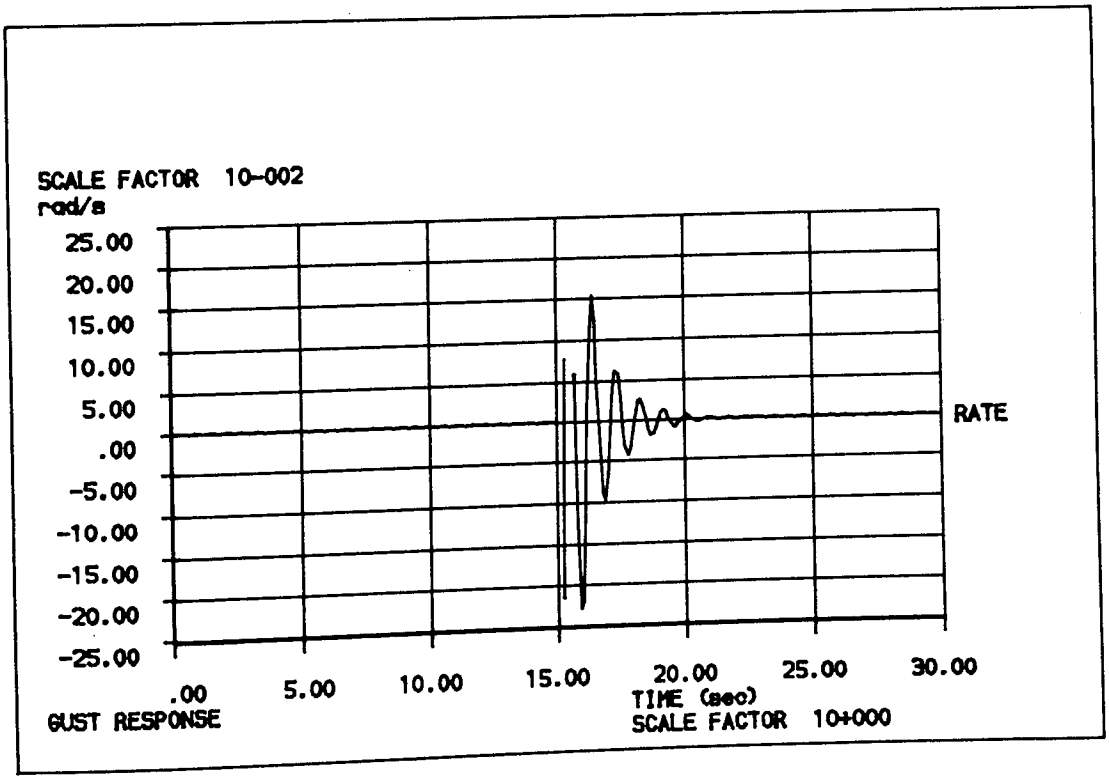

Figure 10.16 Simulation output - Pitch rate response to an x_0 wind gust of 10 m/s applied for 0.1 second duration at t = 15 seconds

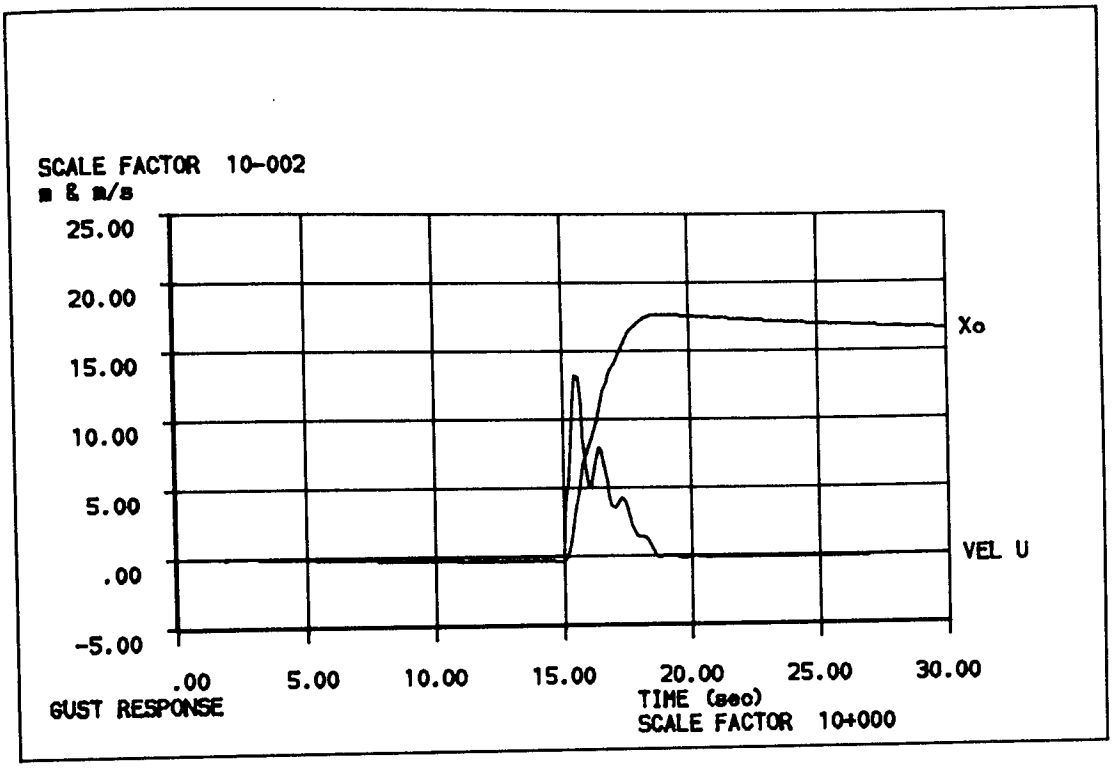

Figure 10.17 Simulation output - x_0 positioned rate response to an x_0 wind gust of 10 m/s applied for 0.1 second duration at t = 15 seconds

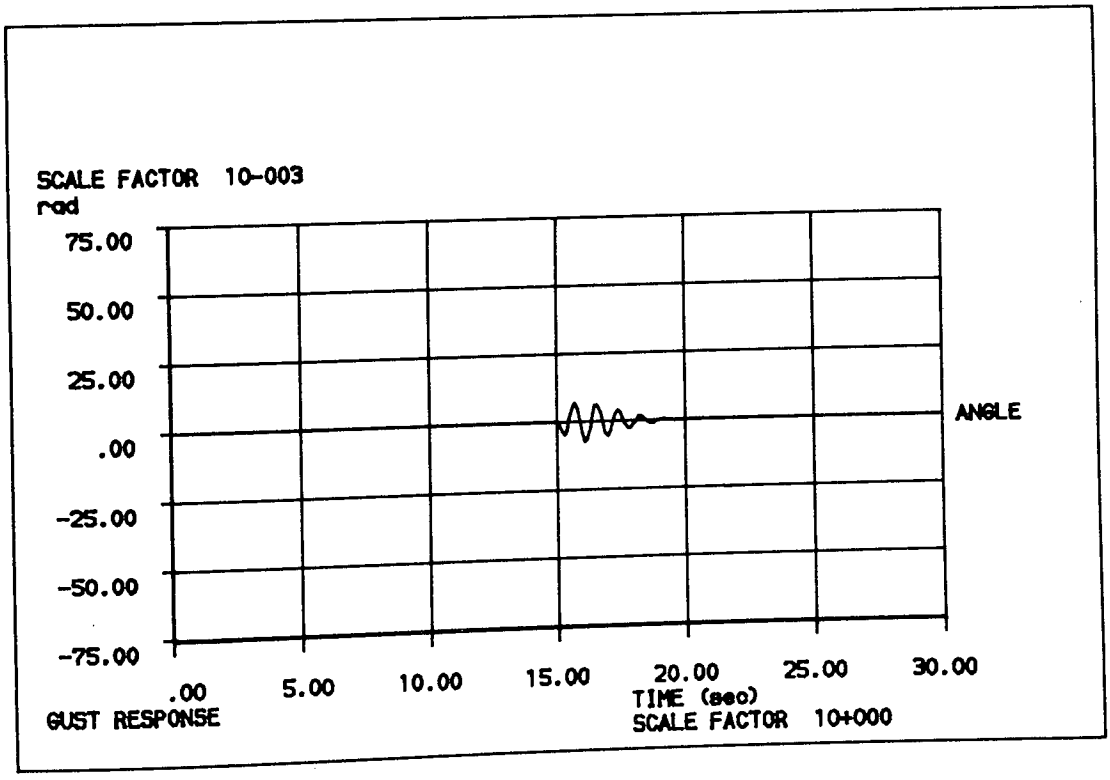

Figure 10.18 Simulation output - Roll position response to an x_0 wind gust of 10 m/s applied for 0.1 second duration at t = 15 seconds

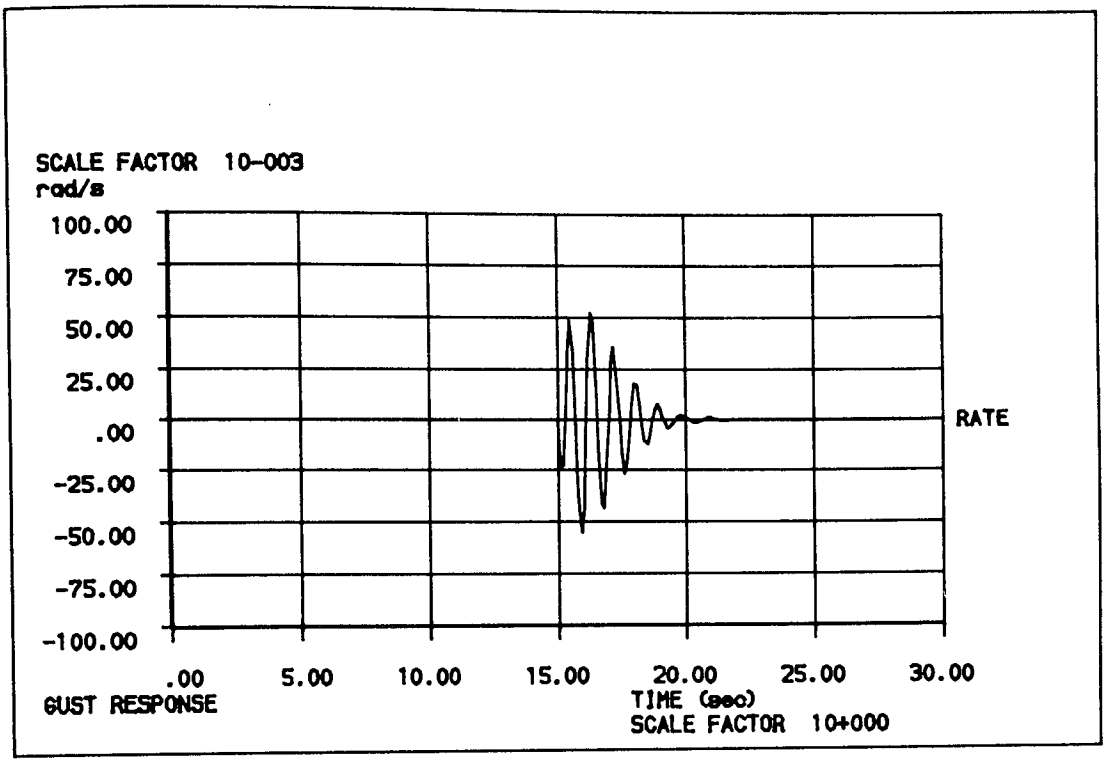

Figure 10.19 Simulation output - Roll rate response to an x_0 wind gust of 10 m/s applied for 0.1 second duration at t = 15 seconds

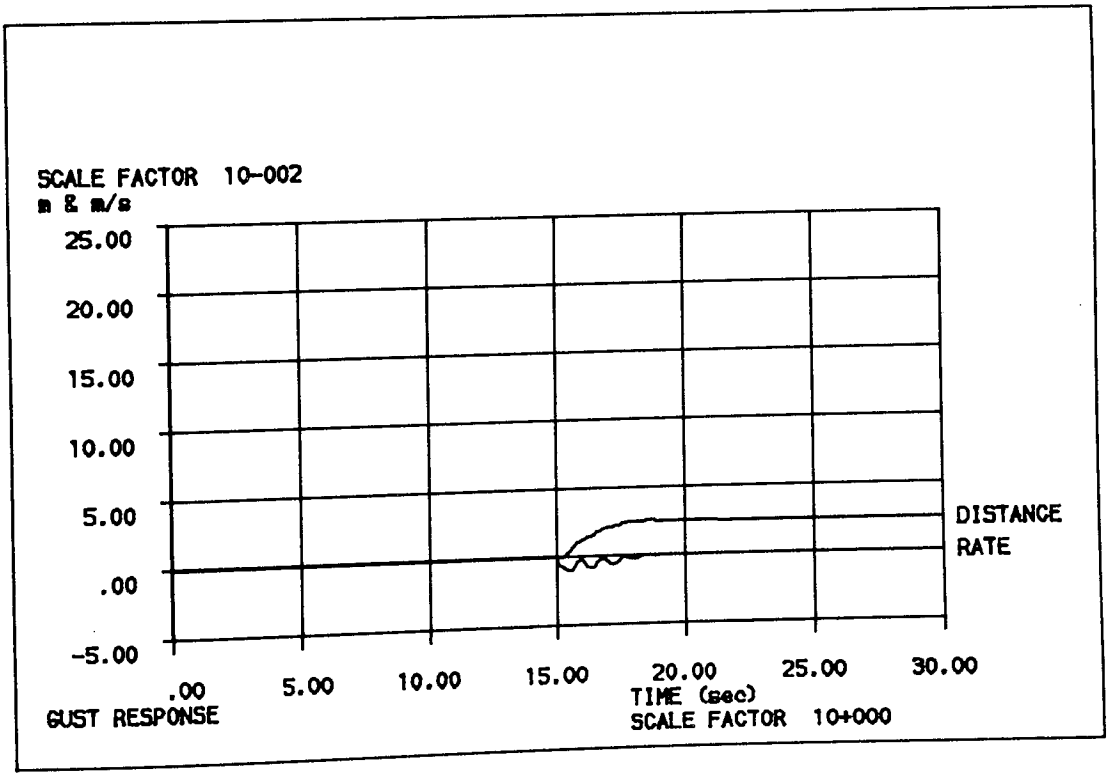

Figure 10.20 Simulation output - Y_0 position and rate response to an x_0 wind gust of 10 m/s applied for 0.1 second duration at t = 15 seconds

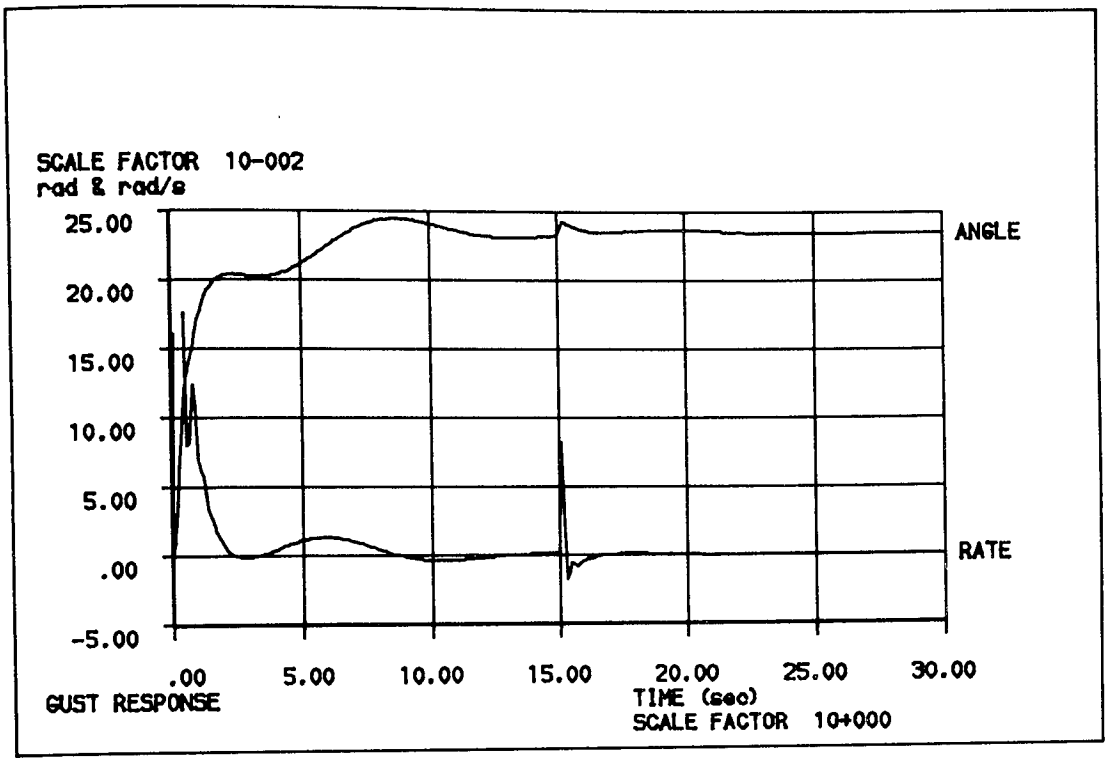

Figure 10.21 Simulation output - Heading position and rate response to an x_0 wind gust of 10 m/s applied for 0.1 second duration at t = 15 seconds

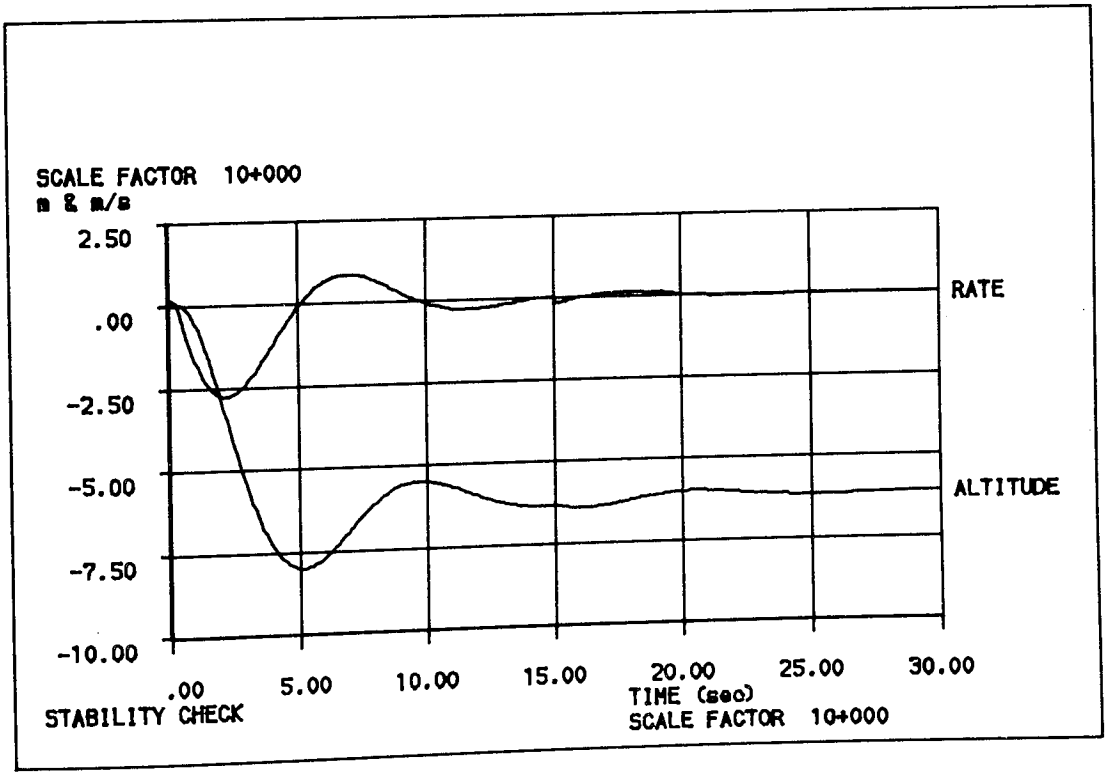

Figure 10.22 Simulation output - Altitude position and rate response to an x_0 wind gust of 10 m/s applied for 0.1 second duration at t = 15 seconds

10.5 Review

This section has presented three cases where the air vehicle simulation has made a useful contribution to the SPRITE project. Namely stability verification, comparison of control systems and gust response performance. The runs required for these investigations needed little user effort due to the design of the software package and were completed within a 2 week period.

SECTION 11

PROJECT REVIEW AND CONCLUSIONS

11 PROJECT REVIEW AND CONCLUSIONS

11.1 Introduction

This section contains a brief review of the research described in the thesis. The achievements of the project are summarised from the original broad brief which was the guideline at the commencement of the work to the final benefits which have been received by the Company.

11.2 Contributions to the Company

This project commenced at a time when ML Aviation had designed and manufactured a prototype air vehicle which could be manually flown by two pilots sharing the workload. Component and sub assembly development was proceeding but no mechanism was available for the Company to progress with the full closed loop SPRITE control system to an optimum production design. The original aim of the project was stated as 'to make recommendations to assist with the development of an optimum control system in terms of performance, cost, mass, and size constraints to satisfy specific customer requirements'.

Potential RPAV user requirements were investigated in an attempt to establish performance criteria for the control system. This work resulted in three useful conclusions.

(a) The major UK requirement for RPAV systems, embodied in PHOENIX specifications, were defined in detail but are subject to the Official Secrets Act. (However privileged discussion enabled the Company to gain this information).

(b) Other potential RPAV users could not define their requirements,

due substantially to the fact that:

(c) most potential RPAV users had little knowledge of RPAV system performance and no means of gaining that knowledge. Certainly the Company had no means of generating such information.

Parallel reviews of the Company's suite of analysis tools resulted in the identification of a need for a simulation model to provide independent assessment of alternative control systems. A dual capability requirement was identified as desirable to investigate:

(a) short term stabilisation

and

(b) long term navigation

and the following list of proposed applications was presented:

Design and Development

(a) stability verification;

(b) demand response - step inputs,

- impulse inputs;

(c) cross coupling evaluation,

roll, pitch, yaw, altitude;

(d) gust response;

(e) sensor error effect;

(f) navigation system evaluation;

(g) component failure effect;

(h) effect of: aerodynamic changes to rotors,

aerodynamic changes to fuselage,

mass changes,

cg position changes;

Operational Assessment

(i) economic flight envelope determination,

(j) flight envelope extreme condition determination,

(k) navigation updating frequency

vs

error analysis comparison,

(l) waypoint navigation evaluation.

A review of other RPAV systems and their development was provided so that the Company may assess its position compared

to competitors and more importantly so that sensors used in other RPAVs are not overlooked and can be considered for potential application to SPRITE. As an extension to this work promising sensors under development have also been identified for consideration.

Once the Company's need for a detailed SPRITE simulation was identified a strategy to develop it within strict timescale and resource limitations was defined. The development of the simulation model occupies the bulk of this work. The following criteria were raised for consideration throughout simulation development:

(a) high practical application,
(b) adequate depth and visibility of solution,
(c) acceptably quick run times,
(d) modular programme design,
(e) high emphasis on traceability and repeatability.

The simulation software package was designed with the following skeletal structure:

(a) data input file handler,
(b) simulation control and module caller,
(c) data output file handler,

with the following air vehicle specific modules:

(d) co-axial rotors,

(e) flight control system,

(f) fuselage aerodynamics,

(g) control laws,

and the following utility modules:

(h) six degrees of freedom motion,

(i) integration,

(j) axes systems transformations.

the simulation was developed and validated to meet the stated design aims. Areas of the work that made a particular contribution include the following:

(a) Euler parameter quaternion to maintain body/earth axes relationship,

(b) dynamically variable integration time step size, based on error assessment,

(c) novel co-axial rotor model,

(d) pragmatic approach to fuselage aerodynamic loads,

(e) detailed control system model,

(f) graphical output facility.

The use of the Euler parameter quaternion to maintain the angular relationship between the body and earth axes obviated

the need for monitoring for angular singularities for certain flight conditions and provided potentially low errors.

The technique adopted for dynamically adjusting the integration step size was a major contribution to the project permitting minimum run time to be used for a required solution accuracy.

The novel co-axial rotor model reduced run times significantly when compared to techniques which necessitate integration along the rotor blade.

A pragmatic approach to the aerodynamic loads was adopted in order that a solution be obtained within the given constraints. This being justified by the fact that the quality of the available data was good for extreme conditions and in any case the forces were small compared to rotor and gravitationally induced forces.

The detailed model of the control system allows the effects of configuration changes of individual op-amps to be assessed and it allows easy modification to include alternative control system designs and motion sensor effects to be included.

The graphical output facility has not only proven useful during development but will prove invaluable now the simulation is ready for use by the designer.

A strategy of using published data has proved successful and good agreement with the limited practical data available has been achieved. The modular design allowed easy expansion and the policy of pursuing a high degree of traceability has resulted in a high integrity software package. The data handling philosophy minimised keyboard entry, with its associated scope for errors. The practical engineer is provided with good visibility of intermediate and overall output.

Section 10 includes examples of stability verification, cross coupling of motion between control channels and response to demand and gust inputs. The simulation has a capability of accomplishing all proposed evaluation studies.

By optimising the simulation in terms of run time for required solution accuracy and providing interactive or batch capabilities this has resulted in a flexible and powerful addition to the designers' 'tool box'.

This thesis reports research on a truly interdisciplinary project (123) where a 'real' problem has been identified and solved in a given timescale to a depth appropriate to the needs of the Company. In the opinion of the author the most useful outcome of this project to the Company is that it now has a working simulation debugged, proven and demonstrated within the timescale required for it to make a significant contribution to the Company product.

From the Company's viewpoint the completed simulation software package is more valuable than the sum of its components, as it now not only possesses understanding accruing as a result of the development of each module of the simulation but it also has a tool which can be used for more advanced studies.

11.3 Contribution to Knowledge

Section 11.2 summarised how the Company benefitted from sponsoring this work. Additionally a contribution to the knowledge available to all researchers has also been made. These contributions can be summarised under the three categories:

(a) clarification of Euler/attitude angle definitions,

(b) new miniature co-axial rotor modelling method,

(c) derivation of a compatible system of equations for modelling a miniature PSH.

This work indentified a confusion in published work between Euler angles and attitude angles which can both be used to relate the angular orientation of one axes system compared to another. The confusion was compounded by the fact that many researchers have referred only to recent publications and are basing their work on papers which are themselves not correct. Further confusion is caused by the popular practice where American publications seem to have called 'attitude angles' 'Euler angles' for some considerable time. Definitions and

appropriate transformation matrices for both Euler angles and attitude angles are restated with reference to authoritative texts, their differences being clearly presented.

The major contribution to knowledge made by this research is the development of a model for a miniature co-axial contra rotating twin rotor system capable of running acceptably quickly for simulation purposes.

Closed loop solution models obviating the need to integrate along each blade and around the rotor disc were identified for full size single rotor helicopters. Despite rigorous searches no such models were identified for co-axial rotor systems of any size. However, detailed models based on disc integration requiring an individual blade approach based on a strip and momentum theory were identified but found to be inappropriate for simulation due to the excessive run times that would result.

An appropriate full scale single rotor model (151) was identified as a basis for the development of a co-axial model. This rotor model was extended for use by validation for small scale single rotors and a capability of modelling a clockwise rotor rotation direction was added through axes transformations. The method of inputting wind to the model was also amended so that it was more appropriate for use by engineers.

Advantage was taken of published work carried out on comprehensive co-axial rotor models in order that a simple co-axial model based on the full scale single rotor model was proposed through the definition of a rotor interaction coefficient. The result was an economic to run rotor model which showed good agreement with practical tests and published work.

The early part of this research identified a lack of means suitable for carrying out assessments of control systems and RPH system performance. In this thesis a theoretical model of a miniature twin co-axial contra rotating rotor helicopter has been derived for flight dynamics and control system studies. Confidence in the model has grown through comparison with limited test data. Further work in this area is discussed in the next section. This model has been structured to allow easy expansion and is well suited to further development in areas of a users' specific interest.

SECTION 12

FUTURE WORK

12 FUTURE WORK

The management of ML Aviation will need time to assess the work described in this thesis before they commit the company resources further in the fields of control system development and RPAV system simulation. However, the author suggests that priority should be given to the following studies. For ease of discussion the future work is separated in the following two categories:

(a) simulation enhancement and further validation,

(b) SPRITE evaluation and development using the simulation software package.

The design of the software package and the presentation of the theory in this thesis is aimed at allowing easy adaptation of the model to suit an individual user's requirements.

The current design of the simulation as described herein is appropriate to general purpose evaluation and a capability exists to satisfy studies identified as part of this work. However, for limited further work some useful capabilities could be gained. The Company may consider it worthwhile to extend the rotor model so that the effects of the control rotor can be included in the simulation. This would not be an onerous task and would allow the prototype air vehicles, as are currently being flown, to be modelled.

A second further development would be alternative rotor models. A detailed rotor model, perhaps similar to that used by Azuma (156)(170), would provide the Company with the capability of detailed rotor analysis so that the rotor may be optimised for both performance, strength and fatigue life. Investigation of alternative control systems given in Section 10 show the dangers of using analysis techniques of inadequate depth. This caveat can only be ignored by the rotor designer, when optimising the rotor, at his peril. Ill planned strategies based on minimum short term investment can prove very expensive in the longer term and would contribute significantly to longer product development timescales.

Alternative repetitive simulation runs may benefit from downloading rotor results to a look up table during the first run. Subsequent studies would benefit from faster running by use of these look up tables.

Other areas of work which may also speed up the simulation is the use of faster integration routines such as error predictor techniques*. Further consideration could also be given to separating linear and angular motions (134) as discussed in Section 5.

---

*These may give faster running at reduced accuracy which could be acceptable in some cases.

Attention to the actuator may result in a more sophisticated model. In order to achieve this, carefully designed tests will need to be carried out to provide the necessary performance data for the SPRITE actuator system. The topics raised below have not been included in the simulation at this stage. This is due to a lack of data as, in the opinion of the author, unless the performance of the SPRITE actuators is accurately quantified a more detailed model would not yield any advantages, rather, poor data may make the actuator model less accurate. The areas for consideration are:

(a) motor load torque,

(b) linkage and gearbox flexibility,

(c) load direction dependent hysteresis (blacklash) (estimated at $\pm$ 0.0175 rad, 1^{0})

(d) actuator direction dependent hysteresis (feedback potentiometer wiper stiction).

It may be advantageous to investigate the effects of the fuselage aerodynamic modelling. Before any commitment is made by the Company to wind tunnel tests a sensitivity study using the simulation would provide the following useful data:

(a) whether the effect of fuselage data on air vehicle performance warranted a wind tunnel programme,

(b) if wind tunnel tests are carried out priority test cases may be identified.

This work would assist the Company to follow a high value development programme.

Another facility which may improve the model would be consideration of inclusion of ground effects if landing and hover cases close to the ground are to be investigated.

The validation of the simulation could usefully be extended through well planned concurrent programmes of simulation runs and practical tests, the following areas are recommended for consideration:

(a) rotor lateral thrust performance,
(b) torque balance blade angles,
(c) confirmation of the relationship between geometric blade angles and angles relative to no lift conditions,
(d) dynamic response to various inputs,
(e) review of actuator and sensor models.

Several aspects of SPRITE are ripe for design or further development, indeed those listed below were partly the stimulus for this work. Three related areas of development which can progress now that the simulation software is available are:

(a) the design, evaluation and optimisation of air vehicle control laws,
(b) alternative sensor/sensor combination evaluation,
(c) navigation system design and evaluation.

As an essential part of equipping the project team for this work the software package will need to be handed over to them. Of course a PhD thesis is not an acceptable vehicle for this process. Therefore the software will be documented according to existing Company procedures and training in its use given. A presentation has already been given to the senior project staff so that they have an insight, in advance of this thesis, into the facility with which they will be provided.

There are many avenues of study now open to the Company in accelerating the development of SPRITE. In the opinion of the author one of the most useful outcomes of this work is that new doors have been opened and the Company are now in a better position to make a rational and well-informed choice of future study and development programmes.

APPENDIX A

ML AVIATION COMPANY LIMITED

A1 APPROVALS

Defence Contractors List Registration No 101M01 Approved by the Ministry of Defence to Defence Standard 05-21 for the Design, Development, Quantity Production and repair of mechanical, electro-mechanical and electrical products and equipment to aerospace standards including but not limited to:

Aircraft up to an all-up weight of 5,670 kg (12,500 lb).

Armament Equipment, Weapons Response Simulators, and associated Test Sets.

Aircrew Personal and Life Support Equipment.

Airfield, Aircraft and Weapon Servicing, Handling and Loading Equipment.

Air Conditioning, Cooling and Refrigeration Systems.

Inflatable Shelters.

Power Cartridges, supported by an explosives filling area and test site.

Specialized installations for research and development.

Design and development of specialized packaging, transit and storage equipment.

The ML Aviation cartridge filling and explosives trials facilities are registered under the Health and Safety Executive Explosives Registry No XB70/460/4.

Quality Assurance Directorates representatives from MoD(PE) are in some cases resident, and in other cases visit the Company. In the resident category are AQD (Aeronautical Quality Assurance Directorate) and DWQ(N) Directorate Weapons Quality (Naval). In the visiting category are QAD (Ord) Quality Assurance Directorate (Ordnance) and MQAD (Materials Quality Assurance Directorate).

Approved by the UK Civil Aviation Authority under the Air Navigation Order, Authority Reference No. DA1/2210/46 as a Group A1 Primary Company and Group B2 Process Company to certify the design of aeroplanes up to 5,600 kg and the design, manufacture, installation, repair and inspection of:

CLASS		RATING	
A1	Airframe/Powerplant Components, Equipment and Systems	(a)	Associated with the above aeroplanes.
		(b)	Structural, sheet metal and fibre reinforced plastics.
		(c)	Mechanical, hydraulic, pneumatic and oxygen.
	Electrical Equipment and	(a)	Associated with the above aeroplanes.
		(b)	Mechanical and electromechanical.

CLASS (Cont)		RATING (Cont)
	Instrument, Equipment and Systems	Design of installations
A3	Process	(a) Heat treatment. (b) Protective treatment. Supplementary Rating Certification of Manuals, Control of Subcontractors.

Process approvals are also held from McDonnell Douglas Corporation (MDC).

A1 COMPANY STRUCTURE

Aston University

Content has been removed for copyright reasons

APPENDIX B

AXES SYSTEMS AND SOME TRANSFORMATIONS

B1 Introduction

The model uses several axes systems each chosen in order to simplify local analyses of the sub elements of the model. All axes systems are right handed orthogonal triads. This allows advantage to be taken that the inverse of the transformation matrix is equal to its transpose (188).

B2 Body Axes

The body axes are based at the air vehicle centre of gravity with the x axis pointing forward (aligned with the camera in the horizontal x-y plane), the y axis pointing starboard and the z axis pointing downwards. Instantaneous body axes are stationary, momentarily coinciding with body axis. They possess no linear or rotational motion and may be used for calculating instantaneous body accelerations and velocities.

B3 Earth Reference (Fixed) Axes

The earth reference axes are defined as a stationary orthogonal triad positioned such that the x_0 axis points north, the y_0 axis points to the east and the z_0 axes points downwards. The earth reference axes origin may be positioned at any arbitrary point, usually for convenience it is taken as being at the starting point of flight so that the flight position is measured relative to the launch location. Sometimes researchers may choose to have the reference point at a proposed landing or target position if this is centre to the simulation.

B4 Local Earth Axes

Local earth axes x_{OL}, y_{OL}, z_{OL} are defined such that they are parallel with the earth reference axes but they move with the air vehicle such that the origin is maintained coincident with that of the body axes.

These definitions for reference and local earth axes are for a flat non-rotating earth (138)(140).

B5 Stability and Flight Path Axes

The stability axes x_{st}, y_{st}, z_{st} are obtained by rotating the body axis through an angle of $-\alpha$ (α, the incidence angle) about the y axis. This is an intermediate axes system used in the transformation to flight path axes. Flight path axes x_f, y_f, z_f are defined such that the x_f axis is aligned along the gross velocity vector. They are obtained by applying a rotation of β (the sideslip angle) about the z_{st} axis.

B6 Shaft Axes (anticlockwise rotor)

The shaft axes are aligned along the rotor shaft and centred at the shaft hub. The z_s axis points downwards along the shaft, the y_s points starboard and x_s axis points forward.

B7 Shaft Axes (clockwise rotor)

The shaft axes for a clockwise rotating rotor x_{sc}, y_{sc}, z_{sc} are obtained from the (anti-clockwise) shaft axes by a rotation of Π radians (180°) about the x_s axis.

B8 Shaft Wind Axes

The shaft wind axes share a common z axis with the shaft axes, z_{sw} but the x_{sw} and y_{sw} axes are rotated to allow the x_{sw} axis to be aligned with the resultant air vehicle velocity. This means that there will be a zero y_{sw} velocity component. This axes system is convenient for use when calculating hub moments and forces.

B9 Blade Axes

The blade axis system is positioned by rotating the shaft axes so that the x_B axis lines up with the blade line the y_B axis points to the right and the z_B axis points downwards. The blade is allowed only freedom in shaft rotation and flapping and the usual practice of using an anticlockwise (from above) rotating rotor in adopted where the datum angle is taken when the blade points backwards (in the line of the $-x_B$ axis). The blade rotation angle (anti-clockwise) is ψ.

The rotor blade will be allowed two planes of motion, rotation due to shaft rotation ψ and blade flapping (β) about a hinge perpendicular to both the shaft and the blade centrelines. Directions of rotor anticlockwise from above and blade flapping (β) up are taken as positive. The datum position for ψ is taken at the rear i.e. -x direction in order that usual convention i.e. Bramwell (112) is followed.

The transformation between blade and shaft axes systems can be stated.

$$\begin{bmatrix} \underset{\sim}{i}_H \\ \underset{\sim}{j}_H \\ \underset{\sim}{k}_H \end{bmatrix} = \begin{bmatrix} \cos\beta & 0 & \sin\beta \\ 0 & 1 & 0 \\ -\sin\beta & 0 & \cos\beta \end{bmatrix} \begin{bmatrix} \underset{\sim}{i}_B \\ \underset{\sim}{j}_B \\ \underset{\sim}{k}_B \end{bmatrix}$$

and

$$\begin{bmatrix} \underset{\sim}{i}_S \\ \underset{\sim}{j}_S \\ \underset{\sim}{k}_S \end{bmatrix} = \begin{bmatrix} -\cos\psi & -\sin\psi & 0 \\ \sin\psi & -\cos\psi & 0 \\ 0 & 0 & 1 \end{bmatrix} \begin{bmatrix} \underset{\sim}{i}_H \\ \underset{\sim}{j}_H \\ \underset{\sim}{k}_H \end{bmatrix}$$

hence the blade axis to shaft axis transformation can be written as:

$$\begin{bmatrix} \underset{\sim}{i}_S \\ \underset{\sim}{j}_S \\ \underset{\sim}{k}_S \end{bmatrix} = \begin{bmatrix} -\cos\psi & -\sin\psi & 0 \\ \sin\psi & -\cos\psi & 0 \\ 0 & 0 & 1 \end{bmatrix} \begin{bmatrix} \cos\beta & 0 & \sin\beta \\ 0 & 1 & 0 \\ -\sin\beta & 0 & \cos\beta \end{bmatrix} \begin{bmatrix} \underset{\sim}{i}_B \\ \underset{\sim}{j}_B \\ \underset{\sim}{k}_B \end{bmatrix}$$

[T1]

$$\begin{bmatrix} \underset{\sim}{i}_S \\ \underset{\sim}{j}_S \\ \underset{\sim}{k}_S \end{bmatrix} = \begin{bmatrix} -\cos\psi\cos\beta & -\sin\psi & -\cos\psi\sin\beta \\ \sin\psi\cos\beta & -\cos\psi & \sin\psi\sin\beta \\ -\sin\beta & 0 & \cos\beta \end{bmatrix} \begin{bmatrix} \underset{\sim}{i}_B \\ \underset{\sim}{j}_B \\ \underset{\sim}{k}_B \end{bmatrix}$$

B10 Blade to Body Axes Transformation

For an air vehicle where the rotor shaft is vertical in the air vehicle (parallel with the z axis), and defining the c of g position of the air vehicle with respect to the shaft axis as (x_{cg}, y_{cg}, z_{cg}) the velocities at the shaft hub can be written:

[T2]

$$\begin{bmatrix} u_s \\ v_s \\ w_s \end{bmatrix} = \begin{bmatrix} 0 & -z_{cg} & +y_{cg} \\ z_{cg} & 0 & -x_{cg} \\ -y_{cg} & x_{cg} & 0 \end{bmatrix} \begin{bmatrix} p \\ q \\ r \end{bmatrix} + \begin{bmatrix} u_A \\ v_A \\ w_A \end{bmatrix}$$

To simplify the rotor analysis it is convenient to use a slightly re-aligned version of the shaft axes system such that the x_s axis is rotated about the z_s axis until it is aligned with the resultant velocity. This axis system is notated as shaftwind (sw).

hence with a wind angle of ψ_w

$$u_{sw} = u_s \cos \psi_w + v_s \sin \psi_w$$

$$v_{sw} = 0$$

$$w_{sw} = w_s$$

The angular velocities converted to wind shaft axes become:

[T3]

$$\begin{bmatrix} p_{sw} \\ q_{sw} \\ r_{sw} \end{bmatrix} = \begin{bmatrix} \cos \psi_w & \sin \psi_w & 0 \\ -\sin \psi_w & \cos \psi_w & 0 \\ 0 & 0 & 1 \end{bmatrix} \begin{bmatrix} p \\ q \\ r \end{bmatrix} + \begin{bmatrix} 0 \\ 0 \\ \dot{\psi}_w \end{bmatrix}$$

and the angular accelerations in the wind shaft axes are found by differentiating the following equations

[T4]

$$\begin{bmatrix} p_{sw} \\ q_{sw} \end{bmatrix} = \begin{bmatrix} \cos \psi_w & \sin \psi_w \\ -\sin \psi_w & \cos \psi_w \end{bmatrix} \begin{bmatrix} p \\ q \end{bmatrix}$$

$$p_{sw} = p \cos \psi_w + q \sin \psi_w$$

$$\frac{dp_{sw}}{dt} = \dot{\psi}_w p \sin \psi_w + \dot{p} \cos \psi_w + \dot{\psi}_w q \cos \psi_w + \dot{q} \sin \psi_w$$

$$= (\dot{p} + \dot{\psi}_w q) \cos \psi_w + (\dot{q} - \dot{\psi}_w p) \sin \psi_w$$

$$q_{sw} = -p \sin \psi_w + q \cos \psi_w$$

$$\frac{dq_{sw}}{dt} = -\dot{\psi}_w p \cos \psi_w - \dot{p} \sin \psi_w - \dot{\psi}_w q \sin \psi_w + \dot{q} \cos \psi_w$$

$$= (\dot{q} - \dot{\psi}_w p) \cos \psi_w + (\dot{p} + \dot{\psi}_w q) (-\sin \psi_w)$$

This can be written using the same transformation matrix as used above as:

$$\begin{bmatrix} \dot{p}_{sw} \\ \dot{q}_{sw} \end{bmatrix} = \begin{bmatrix} \cos \psi_w & \sin \psi_w \\ -\sin \psi_w & \cos \psi_w \end{bmatrix} \begin{bmatrix} \dot{p} + \dot{\psi}_w q \\ \dot{q} - \dot{\psi}_w p \end{bmatrix}$$

APPENDIX C

VELOCITY TRANSFORMATION BETWEEN AXES

APPENDIX C - VELOCITY TRANSFORMATION BETWEEN AXES

The transformation of the cg position velocities from body to local earth axes is stated in Section 5. This brief appendix summarises an alternative approach to the result used in that section.

It is given in Section 5 that the velocity transformation is accomplished by:

$$\dot{x}_{oL} = \left[C \right]^T \dot{\underset{\sim}{x}}' = \left[C \right]^T \left[\dot{\underset{\sim}{x}} + \Omega \underset{\sim}{r} \right]$$

Consider the possible coupling between lateral motion, y, descent z, and roll p. Then figure C.1 may be drawn.

A first-order integration of z is

$$z (t + \delta t) = z (t) + \dot{z} \delta t$$

but because of the roll velocity this yields a lateral displacement component $\delta y_z = -p \, \delta t \, \delta z$ and hence an incremental velocity component $\dot{y}_z = p \, \dot{z}$. Similar steps may be used to complete the argument for the vector x yielding:

$$\dot{\underset{\sim}{x}}' = \dot{\underset{\sim}{x}} + \Omega \, \delta \underset{\sim}{x}.$$

POINT 1 - The centre of mass of the vehicle is never allowed to drift from the coordinate system origin - by definition (as stated in Appendix B).

POINT 2 - To determine the incremental lateral velocity component due to roll/decent coupling.

$$\dot{y}_z = \lim_{\delta t \to 0} \frac{\delta y}{\delta t} = \lim_{\delta t \to 0} \frac{-p\delta t \; f(\ldots t)\delta t}{\delta t} = 0$$

hence for the cg point the velocity transformation reduces to the form:

$$\underset{\sim}{\dot{x}}_{OL} = \left[C \right]^T \underset{\sim}{\dot{x}}$$

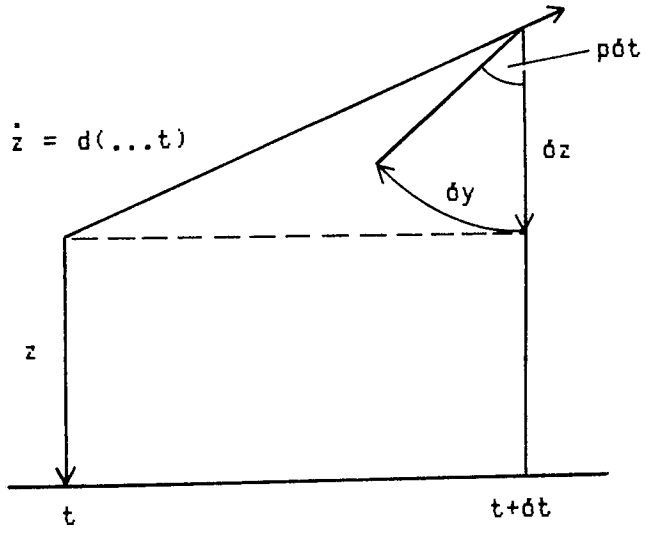

Fig C.1 Motion cross coupling

APPENDIX D

SINGLE ROTOR MODEL

D1 Introduction

This appendix is intended to give an understanding of the rotor blade flapping and rotor force and moment coefficient aspects of the single rotor model developed by Padfield (151). It is not intended to reproduce Padfield's work here, merely to whet the appetite of the reader and to briefly state the salient features of the model.

A brief summary of his derivations is presented along with the final modelling equations which are used for the simulation. These have been stated previously in Section 6.

D2 Blade Velocity and Acceleration

Expressions to determine the approximate velocity components of the blade relative to the air are given by Padfield (151) assuming the flapping angle β to be small:

$$u_B = -u_{sw} \cos\psi - w_{sw}\,\beta \qquad (151)$$

$$v_B = -u_{sw} \sin\psi - r_B(\Omega - r_{sw} + \beta W_x) \qquad (151)$$

$$w_B = -u_{sw}\,\beta \cos\psi + w_{sw} + r_B(W_y - \beta) \qquad (151)$$

Where

$$\begin{bmatrix} W_x \\ W_y \end{bmatrix} = \begin{bmatrix} \cos\psi & -\sin\psi \\ \sin\psi & \cos\psi \end{bmatrix} \begin{bmatrix} p_{sw} \\ q_{sw} \end{bmatrix} \qquad (151)$$

Further, neglecting gravitational and aircraft accelerations expressions for blade element accelerations are given as:

$$a_{xB} = r_B \left[-(\Omega - r_{sw})^2 + 2\dot{\beta}W_y - 2(\Omega - r_{sw})\beta W_x + \beta\ddot{\beta} \right] \quad (151)$$

$$a_{yB} = r_B \left[-(\dot{\Omega} - \dot{r}_{sw}) - \beta(\dot{q}_{sw} \sin\psi - \dot{p}_{sw} \cos\psi) + r_{sw}\beta W_y) \right] \quad (151)$$

$$a_{zB} = r_B \left[2\Omega W_x + (\dot{q}_{sw} \cos\psi + \dot{p}_{sw} \sin\psi) \right. \quad (151)$$

$$\left. -r_{sw}W_x - (\Omega - r_{sw})^2\beta - \ddot{\beta} \right] \quad (151)$$

D3 Blade Flapping

Blade flapping is presented by Padfield (151) in terms of the three force contributions, aerodynamicaly induced forces, inertial forces and hinge stiffness forces. The flapping behaviour is described by equating to zero the sum of these three terms. In a general form, for the i th rotor blade this is expressed as:

$$\int_0^R r_B \left[f_z(r_B) - ma_{zB} \right] dr_B + K_\beta \beta_i = 0 \quad (151)$$

Aerodynamic Inertial Hinge Stiffness

Writing the blade moment of inertia as:

$$I_\beta = \int_0^R m r_B^2 \, dr_B$$

and the normalised rotor flapping frequency as:

$$\lambda_\beta = \sqrt{\left(1 + \frac{K_\beta}{I_\beta \Omega^2}\right)}$$

Padfield (151) presents a detailed analysis to support this simple model for centrally hinged and small offset articulated, and hingeless rotors.

Rewritten in normalised form:

$$\beta_i'' + \lambda_\beta^2 \beta_i = 2\left(\left(\bar{p}_{sw} + \frac{\bar{q}'_{sw}}{2}\right)\cos\psi_i - \left(\bar{q}_{sw} - \frac{\bar{p}'_{sw}}{2}\right)\sin\psi_i\right) + 4n_\beta \int_0^1 \left(\bar{U}_T^2\,\theta + \bar{U}_T\bar{U}_p\right)_i \bar{r}_B \, d\bar{r}_B \qquad (151)$$

$$i = 1, 2, \ldots, b$$

$\beta' = \frac{d\beta}{d\psi}$ and the inertia number, n_β, is the lock number divided by 8 ie:

$$n_\beta = \frac{\gamma}{8}$$

where $$Y = \frac{\rho c a_0 R^4}{I_\beta}$$

Using the following substitution:

$$f_{\beta'} = \frac{4}{3}\mu + \sin\psi_i$$

$$f_\lambda = f_\beta = \frac{4}{3} + 2\mu \sin\psi_i$$

$$f_{\theta p} = 1 + \frac{8}{3}\mu \sin\psi_i + 2\mu^2 \sin^2\psi_i$$

$$f_{\theta tw} = \frac{4}{5} + 2\mu \sin\psi_i + \frac{4}{3}\mu^2 \sin^2\psi_i$$

$$f_W = 1 + \frac{4}{3}\mu \sin\psi_i$$

the flapping expression is expanded to the form:

$$\beta_i'' + \left(1 + f_{\beta'}\right)n_\beta\beta_i' + \left(\lambda_\beta^2 + n_\beta\mu\cos\psi_i f_\beta\right)\beta_i$$

$$= 2\left[\left(\bar{p}_{sw} + \frac{\bar{q}_{sw}'}{2}\right)\cos\psi_i - \left(\bar{q}_{sw} - \frac{\bar{p}_{sw}'}{2}\right)\sin\psi_i\right]$$

$$+ n_\beta\left[f_{\theta p}\theta_p + f_{\theta tw}\theta_{tw} + f_\lambda\left(\mu_z - \lambda_0\right) + f_W\left(\bar{W}_y - \lambda_1\right)\right] \quad (151)$$

$$i = 1, 2, \ldots, b$$

This equation is suitable for programming if integration along the blade length is required and complex aerodynamic loadings could be added at this stage. However, Padfield estimates that time

intervals giving 12 points per rotor revolution would be required, adding significantly to the computational burden.

Hohenemsar and Yin (166) recommend the use of multiblade coordinate systems for simplifying the analysis. Writing the blade flapping for the i th blade in the form:

$$\beta_i = \beta_o + \beta_d (-1)^i + \beta_{1c} \cos \psi_i + \beta_{1s} \sin \psi_i + \beta_{2c} \cos 2\psi_i + \beta_{2s} \sin 2\psi_i + \beta_{3c} \cos 3\psi_i + \beta_{3s} \sin 3\psi_i + \ldots \quad (166)$$

$$i = 1, 2, \ldots, b$$

Hohenemsar and Yin recommend that n terms be retained, where n is the number of blades on a rotor. However, for a two bladed rotor this would even neglect the first cyclic flapping frequency which would be clearly unreasonable. Therefore, for this analysis terms up to and including the first cyclic flapping frequency are included. Consequently the following analysis is similar to that for a four bladed rotor where the first four terms are retained (ie n = 4 for 4 blade positions) where β_I the flapping vector represents the blades of a rotor i.e.,

$$\beta_I = \left[\beta_1, \beta_2, \beta_3, \beta_4\right]^T$$

(where ψ_i = 0, 90, 180 and 270°)

Higher order flapping modes such as sin 2ψ, cos 2ψ are neglected as it is asserted that these give no net forces or moments over a complete rotor cycle. The fundamental modes can be considered as the rotor disc tilt in the pitch and roll planes.

Taking $\underset{\sim}{\beta}_I = \left[\beta_1, \beta_2, \beta_3, \beta_4 \right]^T$ where

β_1 to β_4 are the blade positions at 0, 90, 180, and 270° and $\underset{\sim}{\beta}_M$ as the coning vector where:

$$\underset{\sim}{\beta}_M = \left[\beta_0, \beta_d, \beta_{1c}, \beta_{1s} \right]^T$$

The transformation matrix can be written to define the blade flap at each disc location as:

$$\underset{\sim}{\beta}_I = L_\beta \, \underset{\sim}{\beta}_M \qquad (151)$$

then taking $\psi_i = \left(\psi - (i-1) \, (\Pi/2) \right)$

and $$\beta_0 = \frac{1}{n} \sum_{i=1}^{n} \beta_i$$

$$\beta_d = \frac{1}{n} \sum_{i=1}^{n} \beta_i (-1)^i$$

$$\beta_{jc} = \frac{2}{n} \sum_{i=1}^{n} \beta_i \cos j \, (\psi_i)$$

$$\beta_{js} = \frac{2}{n} \sum_{i=1}^{n} \beta_i \sin j \, (\psi_i)$$

$$L_\beta = \begin{bmatrix} 1 & -1 & \cos\psi & \sin\psi \\ 1 & 1 & \sin\psi & -\cos\psi \\ 1 & -1 & -\cos\psi & -\sin\psi \\ 1 & 1 & -\sin\psi & \cos\psi \end{bmatrix} \qquad (151)$$

hence

$$L_\beta^{-1} = \frac{1}{4} \begin{bmatrix} 1 & 1 & 1 & 1 \\ -1 & 1 & -1 & 1 \\ 2\cos\psi & 2\sin\psi & -2\cos\psi & -2\sin\psi \\ 2\sin\psi & -2\cos\psi & -2\sin\psi & 2\cos\psi \end{bmatrix} \qquad (151)$$

For i=1 to n can be rewritten in matrix form:

$$\underset{\sim}{\beta}_I'' + C_I(\psi)\,\underset{\sim}{\beta}_I' + D_I(\psi)\,\underset{\sim}{\beta}_I = \underset{\sim}{h}_I(\psi) \qquad (151)$$

Padfield transforms and expands by taking:

$$C_M = L_\beta^{-1}\left[2L_\beta' + C_I\,L_\beta\right]$$

$$D_M = L_\beta^{-1}\left[L_\beta'' + C_I\,L_\beta' + D_I\,L_\beta\right]$$

$$\underset{\sim}{h}_M = L_\beta^{-1}\,\underset{\sim}{h}_I$$

the blade flapping can be written in a similar form:

$$\underset{\sim}{\beta}_M'' + C_M(\psi)\,\underset{\sim}{\beta}_M' + D_M(\psi)\,\underset{\sim}{\beta}_M = \underset{\sim}{h}_M(\psi)$$

Padfield recommends a further simplification, of neglecting harmonics above the fundamental on the grounds that an averaging process can be applied. This gives a reduced form as:

$$\underset{\sim}{\beta}_M'' + C_{MO}\,\underset{\sim}{\beta}_M' + D_{MO}\,\underset{\sim}{\beta}_M = \underset{\sim}{h}_{MO} \qquad (151)$$

where

$$C_{MO} = \begin{bmatrix} n_\beta & 0 & 0 & \frac{2}{3}\mu n_\beta \\ 0 & n_\beta & 0 & 0 \\ 0 & 0 & n_\beta & 2 \\ \frac{4}{3}\mu n_\beta & 0 & -2 & n_\beta \end{bmatrix}$$

$$D_{MO} = \begin{bmatrix} \lambda_\beta^2 & 0 & 0 & 0 \\ 0 & \lambda_\beta^2 & 0 & 0 \\ \frac{4}{3}\mu n_\beta & 0 & \lambda_\beta^2 - 1 & n_\beta\left(1 + \frac{\mu^2}{2}\right) \\ 0 & -\frac{4}{3}\mu n_\beta & -n_\beta\left(1 - \frac{\mu^2}{2}\right) & \lambda_\beta^2 - 1 \end{bmatrix}$$

$$h_{MO} = \begin{bmatrix} n_\beta\left\{\theta_0\left(1 + \mu^2\right) + 4\theta_{tw}\left(\frac{1}{5} + \frac{\mu^2}{6}\right) + \frac{4}{3}\mu\theta_{1ssw} + \frac{4}{3}\left(\mu_z - \lambda_0\right) + \frac{2}{3}\mu\left(\bar{p}_{sw} - \lambda_{1ssw}\right)\right\} \\ 0 \\ 2\left(\bar{p}_{sw} + \frac{\bar{q}_{sw}}{2}\right) + n_\beta\left\{\theta_{1csw}\left(1 + \frac{\mu^2}{2}\right) + \left(\bar{q}_{sw} - \lambda_{1csw}\right)\right\} \\ -2\left(\bar{q}_{sw} + \frac{\bar{p}_{sw}}{2}\right) + n_\beta\left\{\frac{8}{3}\mu\theta_0 + 2\mu\theta_{tw} + \theta_{1ssw}\left(1 + \frac{3}{2}\mu^2\right) + 2\mu\left(\mu_z - \lambda_0\right) + \left(\bar{p}_{sw} - \lambda_{1ssw}\right)\right\} \end{bmatrix}$$

These matrices are described by Padfield as being the constant residues of C_M, D_M and $\underset{\sim}{h}_M$. This level of simplification has been used in a simulation by Chen and Talbot (189).

Hohenemsar and Yin (190) introduce the idea of neglecting the rotor inertia at zero rotor speed compared to the gyroscopic inertia at speed Ω. This effectively reduces the expression to first order. Wilcock (150) has simulated Lynx flight using this approximation.

Padfield's final recommended simplification is that it can be asserted that the frequency separation between the rotor modes and overall fuselage rigid body modes is high and in practice cross coupling in these modes is low therefore:

$$\underset{\sim}{\beta}_M = D_{M0}^{-1} \; \underset{\sim}{h}_{M0}$$

where

$$D_{M0}^{-1} = \frac{1}{\delta_\beta} \begin{bmatrix} \frac{\delta_\beta}{\lambda_\beta^2} & 0 & 0 & 0 \\ 0 & \frac{\delta_\beta}{\lambda_\beta^2} & 0 & 0 \\ -\frac{4\mu}{3}\frac{S_\beta}{\lambda_\beta^2} & -\frac{4\mu}{3}\frac{1+(\mu^2/2)}{\lambda_\beta^2} & \frac{S_\beta}{n_\beta} & -\frac{1+(\mu^2/2)}{n_\beta} \\ -\frac{4\mu}{3}\frac{1-(\mu^2/2)}{\lambda_\beta^2} & \frac{4\mu}{3}\frac{S_\beta}{\lambda_\beta^2} & \frac{1-(\mu^2/2)}{n_\beta} & \frac{S_\beta}{n_\beta} \end{bmatrix} \qquad (151)$$

$$\delta_\beta = S_\beta^2 + 1$$

$$S_\beta = \frac{\lambda_\beta^2 - 1}{n_\beta}$$

Padfield then presents the flapping coefficients rewritten in the form:

$$\beta_0 = \frac{n_\beta}{\lambda_\beta^2} \left[\left[1 + \mu^2, \frac{4}{5} + \frac{2}{3}\mu^2, \frac{4}{3}\mu, 0 \right] \begin{bmatrix} \theta_0 \\ \theta_{tw} \\ \theta_{1ssw} \\ \theta_{1csw} \end{bmatrix} + \left[\frac{4}{3}, \frac{-2}{3}\mu, 0 \right] \begin{bmatrix} \mu_z - \lambda_0 \\ \lambda_{1ssw} \\ \lambda_{1csw} \end{bmatrix} + \left[0, 0, \frac{2}{3}\mu, 0 \right] \begin{bmatrix} \bar{p}'_{sw} \\ \bar{q}'_{sw} \\ \bar{p}_{sw} \\ \bar{q}_{sw} \end{bmatrix} \right] \quad (151)$$

$$\begin{bmatrix} \beta_{1csw} \\ \beta_{1ssw} \end{bmatrix} = \frac{-n_\beta}{\lambda_\beta^2 \left(1 + S_\beta^2\right)} \left\{ \begin{bmatrix} \frac{4}{3}\mu\left(S_\beta + \frac{2\lambda_\beta^2}{n_\beta}\right), & 2\mu\left(\frac{\lambda_\beta^2}{n_\beta} + \frac{8}{15} S_\beta\right), & \left(1 + 2\mu^2\right)\frac{\lambda_\beta^2}{n_\beta} + \left(\frac{4}{3}\mu\right)^2 S_\beta, & -\frac{\lambda_\beta^2}{n_\beta} S_\beta \left(1 + \frac{\mu^2}{2}\right) \\ \frac{4}{3}\mu\left(1 - 2S_\beta\frac{\lambda_\beta^2}{n_\beta}\right), & 2\mu\left(\frac{8}{15} - S_\beta\frac{\lambda_\beta^2}{n_\beta}\right), & \left(\frac{4}{3}\mu\right)^2 - S_\beta\frac{\lambda_\beta^2}{n_\beta}\left(1 + \frac{3}{2}\mu^2\right), & -\frac{\lambda_\beta^2}{n_\beta} \end{bmatrix} \begin{bmatrix} \theta_0 \\ \theta_{tw} \\ \theta_{1ssw} \\ \theta_{1csw} \end{bmatrix} \right.$$

$$+ \begin{bmatrix} \mu\left(\left(\frac{4}{3}\right)^2 S_\beta + \frac{2\lambda_\beta^2}{n_\beta}\right), & -\left(\frac{\lambda_\beta^2}{n_\beta}\left(1 + \frac{\mu^2}{2}\right) + \frac{S_\beta}{2}\left(\frac{4}{3}\mu\right)^2\right), & \frac{\lambda_\beta^2}{n_\beta} S_\beta \\ \mu\left(\left(\frac{4}{3}\right)^2 - 2S_\beta\frac{\lambda_\beta^2}{n_\beta}\right), & -\frac{1}{2}\left(\frac{4}{3}\mu\right)^2 + \frac{\lambda_\beta^2}{n_\beta} S_\beta, & -\frac{\lambda_\beta^2}{n_\beta}\left(\frac{\mu^2}{2} - 1\right) \end{bmatrix} \begin{bmatrix} \mu_z - \lambda_0 \\ \lambda_{1ssw} \\ \lambda_{1csw} \end{bmatrix}$$

$$\left. + \begin{bmatrix} \left(\frac{\lambda_\beta}{n_\beta}\right)^2\left(1 + \frac{\mu^2}{2}\right), & -\left(\frac{\lambda_\beta}{n_\beta}\right)^2 S_\beta, & \frac{\lambda_\beta^2}{n_\beta}\left(1 + \frac{\mu^2}{2} - \frac{2S_\beta}{n_\beta}\right) + \frac{S_\beta}{2}\left(\frac{4}{3}\mu\right)^2, & -\frac{\lambda_\beta^2}{n_\beta}\left(S_\beta + \frac{2}{n_\beta}\left(1 + \frac{\mu^2}{2}\right)\right) \\ -\left(\frac{\lambda_\beta}{n_\beta}\right)^2 S_\beta, & \left(\frac{\lambda_\beta}{n_\beta}\right)^2\left(\frac{\mu^2}{2} - 1\right), & \frac{\lambda_\beta^2}{n_\beta}\left(\frac{2}{n_\beta}\left(\frac{\mu^2}{2} - 1\right) - S_\beta\right) + \frac{1}{2}\left(\frac{4}{3}\mu\right)^2, & \frac{\lambda_\beta^2}{n_\beta}\left(\frac{2S_\beta}{n_\beta} + \frac{\mu^2}{2} - 1\right) \end{bmatrix} \begin{bmatrix} \bar{p}'_{sw} \\ \bar{q}'_{sw} \\ \bar{p}_{sw} \\ \bar{q}_{sw} \end{bmatrix} \right\}$$

D4 Rotor Forces and Moments

The rotor forces can be expressed with reference to the shaft wind axes system as below. The in-plane and normal components of the aerodynamic forces acting on the blade at an element m dr_B (m is the mass distribution) are f_y and f_z, hence the following expressions are presented for a rotor with b blades:

$$X_{sw} = \sum_{i=1}^{b} \int_0^R \left[-(f_z - ma_{zB})_i \beta_i \cos\psi_i - (f_y - ma_{yB})_i \sin\psi_i + ma_{xB} \cos\psi_i \right] dr_B \quad (151)$$

$$Y_{sw} = \sum_{i=1}^{b} \int_0^R \left[(f_z - ma_{zB})_i \beta_i \sin\psi_i - (f_y - ma_{yB})_i \cos\psi_i - ma_{xB} \sin\psi_i \right] dr_B \quad (151)$$

$$Z_{sw} = \sum_{i=1}^{b} \int_0^R \left[(f_z - ma_{zB} + ma_{xB} \beta \right]_i dr_B \quad (151)$$

The aerodynamic force f_y and f_z can be written in terms of lift and drag coefficients $l(r_B, \psi)$ and $d(r_B, \psi)$ and the zero blade blade pitch line angle of attack ϕ (small angle assumptions):

$\cos\phi \simeq 1 \sin\phi \simeq \phi$):

$$f_y = d \cos \phi - l \sin \phi \simeq d - l\phi \tag{151}$$

$$f_z = -l \cos \phi - d \sin \phi \simeq -l - d\phi \tag{151}$$

If the velocity components of the blade along the y_B and z_B directions, relative to the air are denoted by $-U_T$ and U_p and the blade pitch angle is θ, measured from a line coincident with the y axis then the general form of the lift and drag functions written in linearised, quasi-steady, two dimensional form are:

$$l(\psi, r_B) = {}^1/_2 \rho(U_T^2 + U_P^2)\, ca_0 \left(\theta + \frac{U_p}{U_T} \right) \tag{151}$$

$$d(\psi, r_B) = {}^1/_2 \rho(U_T^2 + U_P^2)\, c\, \delta \tag{151}$$

Where δ is the blade drag coefficient assumed to be of the form

$$\delta = \delta_0 + \delta_2 C_T^2. \tag{151}$$

If it is asserted that $U_T \gg U_P$ so that

$U_T^2 + U_P^2 \simeq U_T^2$ and U_T and U_P are normalised by dividing by ΩR

i.e.

$$\bar{U}_T = \frac{U_T}{\Omega R}$$

$$\bar{U}_P = \frac{U_P}{\Omega R}$$

the normalised force coefficients can be written for a b bladed rotor:

$$\left(\frac{2C_{Xsw}}{(a_0 s)} \right) = \frac{X_{sw}}{\tfrac{1}{2}\rho(\Omega R)^2 \pi R^2 s a_0}$$

and

$$= \frac{1}{b} \sum_{i=1}^{b} F^{(1)}(\psi_i)\beta_i \cos\psi_i + F^{(2)}(\psi_i) \sin\psi_i \qquad (151)$$

$$\left(\frac{2C_{Ysw}}{(a_0 s)} \right) = \frac{Y_{sw}}{\tfrac{1}{2}\rho(\Omega R)^2 \pi R^2 s a_0}$$

$$= \frac{1}{b} \sum_{i=1}^{b} -F^{(1)}(\psi_i)\beta_i \sin\psi_i + F^{(2)}(\psi_i) \cos\psi_i \qquad (151)$$

$$\left(\frac{2C_{Zsw}}{(a_0 s)} \right) = \frac{Z_{sw}}{\tfrac{1}{2}\rho(\Omega R)^2 \pi R^2 s a_0}$$

$$= \frac{1}{b} \sum_{i=1}^{b} -F^{(1)}(\psi_i) = -\left(\frac{2C_T}{a_0 s} \right) \qquad (151)$$

where $$F^{(1)}(\psi_i) = \int_0^1 \left[\bar{U}_T^2 \theta_i + \bar{U}_P \bar{U}_T \right] d\bar{r}_B \qquad (151)$$

and $$F^{(2)}(\psi_i) = \int_0^1 \left[\bar{U}_P \bar{U}_T \theta_i + \bar{U}_P^2 - \frac{\delta_i \bar{U}_T^2}{a_0} \right] d\bar{r}_B \qquad (151)$$

where the rotor solidity s is defined as:

$$s = \frac{bc}{\pi R} \quad \text{and} \quad \bar{r}_B = \frac{r_B}{R} \tag{151}$$

The normalised velocity $\bar{U}_T$ and $\bar{U}_p$ can be written as:

$$\bar{U}_T = \bar{r}_B(1 + \bar{W}_x\beta) + \mu \sin\psi \tag{151}$$

$$\bar{U}_p = (\mu_z - \lambda_0 - \mu\beta\cos\psi) + \bar{r}_B(\bar{W}_y - \beta' - \lambda_1) \tag{151}$$

$$\bar{W}_x = \frac{W_x}{\Omega}, \quad \bar{W}_y = \frac{W_y}{\Omega}$$

$$\beta' = \frac{d\beta}{d\psi}$$

The induced inflow, positive down through the rotor, is written in a general linear form:

$$\lambda = \frac{v_i}{\Omega R} = \lambda_0 + \lambda_1 \bar{r}_B \tag{151}$$

Linear twist can be incorporated into the blade pitch by writing this in the form:

$$\theta = \theta_p + \bar{r}_B\theta_{tw} \tag{151}$$

Where θ_p is composed of common collective, differential collective and cyclic contributions.

The function $F^{(1)}(\psi)$ and $F^{(2)}(\psi)$ can be evaluated by the substitution of the expressions for $\bar{U}_T$, $\bar{U}_p$, λ and θ. For a rotor with b blades equally spaced the azimuth angles are related by:

$$\psi_{i+1} = \psi_i - i\,\frac{2\pi}{b} \tag{151}$$

also assuming $W_x\beta \ll 1$

$$\begin{aligned}
F^{(1)}(\psi) &= (1/3 + \mu \sin\psi + \mu^2 \sin^2\psi)\,\theta_p \\
&+ (1/4 + 2/3\,\mu \sin\psi + 1/2\,\mu^2 \sin^2\psi)\,\theta_{tw} \\
&+ \left(1/3 + \frac{\mu \sin\psi}{2}\right)\,(\bar{W}_y - \lambda_1 - \beta') \\
&+ (1/2 + \mu \sin\psi)\,(\mu_z - \lambda_0 - \beta\mu \cos\psi)
\end{aligned} \tag{151}$$

$$\begin{aligned}
F^{(2)}(\psi) &= \Big\{(1/3 + 1/2\,\mu \sin\psi)\,(\bar{W}_y - \lambda_1 - \beta') \\
&+ (1/2 + \mu \sin\psi)\,(\mu_z - \lambda_0 - \beta\mu \cos\psi)\Big\}\,\theta_p \\
&+ \left\{(1/4 + \frac{\mu \sin\psi}{3})\,(\bar{W}_y - \lambda_1 - \beta')\right. \\
&+ \left.(1/3 + \frac{\mu \sin\psi}{2})\,(\mu_z - \lambda_0 - \beta\mu \cos\psi)\right\}\,\theta_{tw} \\
&+ (\mu_z - \lambda_0 - \mu\beta \cos\psi)^2 \\
&+ (\mu_z - \lambda_0 - \mu\beta \cos\psi)\,(\bar{W}_y - \beta' - \lambda_1) \\
&+ \frac{(\bar{W}_y - \lambda_1 - \beta')^2}{3} - \frac{\delta}{a_0}\,(1/3 + \mu \sin\psi + \mu^2 \sin^2\psi)
\end{aligned} \tag{151}$$

The above equation can be further simplified depending on the way that the blade flapping freedom is retained in the rotor model. The equations could be used as they stand if an individual blade model is to be adopted. Having investigated various methods of reducing the equation to quasi-steady flapping models where flapping can be determined purely through the use of algebraic relationships e.g. (166), Padfield (151) recommends that it is sufficient to determine the fundamental components when flapping is written in the form:

$$\beta = \beta_0 + \beta_{1csw} \cos \psi + \beta_{1ssw} \sin \psi \qquad (151)$$

β_0 is the coning angle and β_{1csw} and β_{1ssw} are the first harmonic cyclic flapping angles in shaft wind axes. Similarly the applied blade pitch can be written as:

$$\theta_p = \theta_0 + \theta_{1ssw} \sin \psi + \theta_{1csw} \cos \psi \qquad (151)$$

The normalised force coefficients for each blade are equal and in order to derive these functions the relationships describing $F_{(1)}$ and $F_{(2)}$ are expanded as follows:

$$F^{(1)}{}_{(\psi)} = F_0^{(1)} + F_{1c}^{(1)} \cos \psi + F_{1s}^{(1)} \sin \psi + F_{2c}^{(1)} \cos 2\psi$$

$$+ F_{2s}^{(1)} \sin 2\psi \qquad (151)$$

and

$$F^{(2)}(\psi) = F^{(2)}_{0} + F^{(2)}_{1c} \cos\psi + F^{(1)}_{1s} \sin\psi + F^{(2)}_{2c} \cos 2\psi + F^{(2)}_{2s} \sin 2\psi \tag{151}$$

Padfield argues that it is advisable to include the second harmonic terms even though they are not included in the expression for flapping. The steady components of C_X, C_Y and C_Z can be reduced to:

$$\left(\frac{2C_{Xsw}}{a_0 s}\right) = \left(\frac{F^{(1)}_{0}}{2} + \frac{F^{(1)}_{2c}}{4}\right) \beta_{1csw} + \frac{F^{(1)}_{1c}}{2} \beta_0 + \frac{F^{(1)}_{2s}}{4} \beta_{1ssw} + \frac{F^{(2)}_{1s}}{2} \tag{151}$$

$$\left(\frac{2C_{Ysw}}{a_0 s}\right) = \left(-\frac{F^{(1)}_{0}}{2} + \frac{F^{(1)}_{2c}}{4}\right) \beta_{1ssw} - \frac{F^{(1)}_{1s}}{2} \beta_0 - \frac{F^{(1)}_{2s}}{4} \beta_{1csw} + \frac{F^{(2)}_{1c}}{2} \tag{151}$$

$$\left(\frac{2C_{Zsw}}{a_0 s}\right) = -\left(\frac{2C_T}{a_0 s}\right) = -F^{(1)}_{0} \tag{151}$$

where:

$$F^{(1)}_{0} = \theta_0\left(\frac{1}{3} + \frac{\mu^2}{2}\right) + \frac{\mu^2}{2}\left(\theta_{1ssw} + \frac{\bar{p}_{sw}}{2}\right) + \left(\frac{\mu_z - \lambda_0}{2}\right) + \frac{1}{4}(1 + \mu^2)\,\theta_{tw}, \tag{151}$$

$$F_{1s}^{(1)} = \frac{\alpha_{ssw} + \theta_{1ssw}}{3} + \mu\,(\theta_0 + \mu_z - \lambda_0 + \frac{2}{3}\,\theta_{tw}), \tag{151}$$

$$F_{1c}^{(1)} = \frac{\alpha_{csw} + \theta_{1csw}}{3} - \frac{\mu\beta_0}{2}, \tag{151}$$

$$F_{2s}^{(1)} = \frac{\mu}{2}\left\{\theta_{1csw} - \beta_{1ssw} + \frac{\bar{q}_{sw} - \lambda_{1csw}}{2} - \mu\beta_0\right\} \tag{151}$$

$$F_{2c}^{(1)} = -\frac{\mu}{2}\left\{\theta_{1ssw} - \beta_{1csw} + \frac{\bar{p}_{sw} - \lambda_{1ssw}}{2} + \mu\left(\theta_0 + \frac{\theta_{tw}}{2}\right)\right\}, \tag{151}$$

$$\begin{aligned} F_{1s}^{(2)} = {} & \frac{\mu^2}{2}\,\beta_0\,\beta_{1ssw} + \left(\mu_z - \lambda_0 - \frac{\mu}{4}\,\beta_{1csw}\right)\alpha_{ssw} \\ & - \frac{\mu}{4}\,\beta_{1ssw}\,\alpha_{csw} + \theta_0\left(\frac{\alpha_{ssw}}{3} + \mu\,(\mu_z - \lambda_0)\,\frac{\mu^2}{4}\,\beta_{1csw}\right) \\ & + \left(\frac{\alpha_{ssw}}{4} + \frac{\mu}{2}\left(\mu_z - \lambda_0 - \frac{\beta_{1csw}\,\mu}{4}\right)\right)\theta_{tw} \\ & + \theta_{1ssw}\left(\frac{\mu_z - \lambda_0}{2} + \mu\left(\frac{3}{8}\,(\bar{p}_{sw} - \lambda_{1ssw}) + \frac{\beta_{1csw}}{4}\right)\right) \\ & + \frac{\mu}{4}\,\theta_{1csw}\left(\frac{\bar{q}_{sw} - \lambda_{1csw}}{2} - \beta_{1ssw} - \mu\,\beta_0\right) - \frac{6\mu}{a_0} \end{aligned} \tag{151}$$

$$\begin{aligned} F_{1c}^{(2)} = {} & -2\beta_0\,\mu\,(\mu_z - \lambda_0 - \frac{3}{4}\,\mu\,\beta_{1csw}) \\ & + (\mu_z - \lambda_0 - \frac{3}{4}\,\beta_{1csw}\mu)\,\alpha_{csw} - \frac{\mu}{4}\,\beta_{1ssw}\alpha_{ssw} \end{aligned}$$

$$+ \theta_0 \left(\frac{\alpha_{csw}}{3} - \frac{\mu}{2} \left(\beta_0 + \frac{\mu}{2} \beta_{1ssw} \right) \right)$$

$$+ \theta_{tw} \left(\frac{\alpha_{csw}}{4} - \mu \left(\frac{\beta_0}{3} + \frac{\mu}{8} \beta_{1ssw} \right) \right)$$

$$+ \theta_{1csw} \left(\frac{\mu_z - \lambda_0}{2} + \frac{\mu}{4} \left(\frac{\bar{p}_{sw} - \lambda_{1ssw}}{2} - \beta_{1csw} \right) \right)$$

$$+ \frac{\mu}{4} \theta_{1ssw} \left(\frac{\bar{q}_{sw} - \lambda_{1csw}}{2} - \beta_{1ssw} - \mu \beta_0 \right) \qquad (151)$$

$$\alpha_{ssw} = \bar{p}_{sw} - \lambda_{1ssw} + \beta_{1csw} ,$$

$$\alpha_{csw} = \bar{q}_{sw} - \lambda_{1csw} - \beta_{1ssw} .$$

Due to the complexity of these expressions Padfield (151) gives physical interpretations and investigates the possible simplification which could be adopted. The terms $F_{2s}^{(1)}$ and $F_{2c}^{(1)}$ are the harmonic lift variations. $F_0^{(1)} \beta_{1c}$ and $F_{1c}^{(1)} \beta_0$ are the first harmonic components of the product of lift and flapping in the direction of the motion and represent the contribution to $C_{X_{sw}}$ from blades in the fore and aft positions. The term $F_{1s}^{(2)}$ represents the contribution to $C_{X_{sw}}$ from the profile drag and inclined lift acting on the advancing and retreating blades. $C_{Y_{sw}}$ can be described along similar lines.

Researchers have investigated simplifying assumptions such as assuming that the X and Y forces are produced simply by the tilt of the rotor thrust vector but this approximation, although

widely used, has proved considerably in error (191) for some of the flight envelope. Other approximations such as (149), (189) and (192) have been proposed but it is apparent that there is no accepted consistant simplification; therefore Padfield (151) recommends that the harmonic equations should be used as they stand. This does not present such a problem as it used to in earlier research due to the higher performance of modern digital computers.

Use is made of the inverse of the shaft to shaftwind transformation matrix to convert the rotor force coefficients from shaft wind to shaft axes.

$$\begin{bmatrix} C_X \\ C_Y \end{bmatrix} = \begin{bmatrix} T4 \end{bmatrix}^T \begin{bmatrix} C_{Xsw} \\ C_{Ysw} \end{bmatrix}$$

Taking K_β as the hinge stiffness Padfield asserts that the rotor hub pitching and rolling moments are approximately proportional to quasi-steady blade flapping and can be expressed as:

$$L_H = -\frac{b}{2} K_\beta \beta_{1s} \qquad (151)$$

$$M_H = -\frac{b}{2} K_\beta \beta_{1c} \qquad (151)$$

The rotor yawing moment can be written in the form:

$$N_H = \sum_{i=1}^{b} \int_0^R r_B \, (f_y - m a_{yB}) \, dr_B \qquad (151)$$

Padfield argues that the only significant inertial contribution results from the rotor angular acceleration term, hence using the expression for f_y, can be written as:

$$N_H \sum_{i=1}^{b} \left[\int_0^R r_B \, (d - 1\,\Phi)\, dr_B \right] + I_R \dot{\Omega} \tag{151}$$

Where I_R is the moment of inertia of the rotor (blades and other rotating mass). This can be normalised and rewritten by substitution:

$$\frac{N_H}{{}^1/_2 \rho (\Omega R)^2 \pi R^3 s a_0} = \frac{2C_Q}{a_0 s} + 2 \left(\frac{I_R}{b I_\beta} \right) \frac{1}{Y} \bar{\Omega}' \tag{151}$$

where

$$\bar{\Omega}' = \frac{\dot{\Omega}}{\Omega^2} \tag{151}$$

$$Y = \frac{\rho c a_0 R^4}{I_\beta} \tag{151}$$

$$\left(\frac{2C_Q}{a_0 s} \right) = - \int_0^1 \bar{r}_B \left(\bar{U}_P \bar{U}_T \, \theta + \bar{U}_P^2 - \frac{\delta}{a_0} \bar{U}_T^2 \right) d\bar{r}_B \tag{151}$$

Padfield further simplifies this expression by introducing the approximation:

$$\bar{r}_B \simeq \bar{U}_T - \mu \sin \phi \tag{151}$$

and hence:

$$\left(\frac{2C_Q}{a_0 s}\right) = -\int_0^1 (\bar{U}_T - \mu \sin\psi)\,\frac{\bar{U}_P}{\bar{U}_T}\,\bar{l}\,d\bar{r}_B + \int_0^1 \bar{r}_B \bar{d}\,d\bar{r}_B \qquad (151)$$

where

$$\bar{l} = \bar{U}_T^2\theta + \bar{U}_P\bar{U}_T \quad \text{and} \quad \bar{d} = \frac{\delta}{a_0}\,\bar{U}_T^2 \qquad (151)$$

This equation is rewritten to clearly identify three separate terms:

$$\left(\frac{2C_Q}{a_0 s}\right) = -\left(\int_0^1 \bar{U}_P \bar{l}\,d\bar{r}_B\right) + \left(\mu \sin\psi \int_0^1 \frac{\bar{U}_P}{\bar{U}_T}\,\bar{l}\,d\bar{r}_B\right) + \left(\int_0^1 \bar{r}_B\,\bar{d}\,d\bar{r}_B\right) \qquad (151)$$

Treating these terms separately they are expanded and simplified as below

$$\int_0^1 \bar{U}_P \bar{l}\,d\bar{r}_B = (\mu_z - \lambda_0 - \mu\,\beta\cos\psi)\int_0^1 \bar{l}\,d\bar{r}_B + (\bar{w}_y - \beta' - \lambda_1)\int_0^1 \bar{r}_B \bar{l}\,d\bar{r}_B \qquad (151)$$

Padfield argues that the second term on the right hand side can be neglected on the grounds that it contains only second order terms such as $\beta_{1s}\ \beta_{1c}$, pq.

Padfield shows that the first term can be reduced to:

$$\left(\frac{2C_Q}{a_0 s}\right)_1 = -(\mu_z - \lambda_0 - \mu\,\beta\cos\psi)\left(\frac{2C_T}{a_0 s}\right) \qquad (151)$$

Further the second component of the torque coefficient can be reduced using:

$$\sin\psi \int_0^1 \bar{l}\ \frac{\bar{U}_P}{\bar{U}_T}\, d\bar{r}_B = \left(\frac{2C_{Xsw}}{a_0 s}\right) - \left(\frac{2C_T}{a_0 s}\right)\beta\cos\psi$$

$$+ \int_0^1 \bar{d}\sin\psi\ \bar{r}_B \qquad (151)$$

The last term is neglected as harmonic components of d are not included in the analysis. Combining the two lift dependent torque coefficients:

$$\left(\frac{2C_Q}{a_0 s}\right)_2 = -(\mu_z - \lambda_0)\left(\frac{2C_T}{a_0 s}\right) + \mu\left(\frac{2C_{Xsw}}{a_0 s}\right) \qquad (151)$$

Also the third term is reduced:

$$\int_0^1 \bar{r}_B \, \bar{d} \, d\bar{r}_B = \frac{\delta}{4a_0} (1 + 2 \mu^2) \qquad (151)$$

Finally the expression for the torque coefficient is can be rewritten using the expansions and simplification above as:

$$\left(\frac{2C_Q}{a_0 s} \right) \approx - (\mu_z - \lambda_0) \left(\frac{2C_T}{a_0 s} \right) + \mu \left(\frac{2C_{Xsw}}{a_0 s} \right) + \frac{\delta}{4a_0} (1 + 2 \mu^2) \qquad (151)$$

APPENDIX E

SOFTWARE IMPLEMENTATION

E1 Example Master Code Program

```
C      #9INFLPLN  *  ROUTINE FOR INPUTING FLIGHT PLAN
C
C                      RAD 22-4-86
C
C PROG
C
$INSERT SYSCOM)KEYS.F
$INSERT SYSCOM)A$KEYS
$INSERT (TECOMP)TECHLIB)INS_BEG1
C
C
      INTEGER FLPN,FLPNC
      REAL**1 FLPLN
      DIMENSION FLPLN(100,5)
C
      LPROG=.TRUE.
C
$INSERT (TECOMP)TECHLIB)INS_DFU
      GOTO 9999
 5000 CONTINUE
      ID=0
      CALL INPI('No DEMANDS = ',13,IFUNDF,FLPN
     +,ID,EDID,CODE)
      DO 1200 FLPNC=1,FLPN
      CALL TNOUA('FLIGHT DEMAND POINT = ',22)
      CALL TNOUI(FLPNC)
      CALL TONL
      CALL INP*3('TIME = ',7,IFUNDF,FLPLN(FLPNC,1)
     +,ID,EDID,CODE)
      CALL INP*3('ROLL = ',7,IFUNDF,FLPLN(FLPNC,2)
     +,ID,EDID,CODE)
      CALL INP*3('PITCH = ',8,IFUNDF,FLPLN(FLPNC,3)
     +,ID,EDID,CODE)
      CALL INP*3('HEADING = ',10,IFUNDF,FLPLN(FLPNC,4)
     +,ID,EDID,CODE)
      CALL INP*3('ALTITUDE = ',11,IFUNDF,FLPLN(FLPNC,5)
     +,ID,EDID,CODE)
 1200 CONTINUE
      GOTO RT5000
$INSERT (TECOMP)TECHLIB)INS_END
      STOP
      END
```

E2 Change Precision Utilities Listings

COMMAND FILE

```
/* CONV.CPL - CONVERTS MASTER PROGS TO S, D OR H PRECISION
COMO -NTTY
&ARGS PROG; PREC:=H; QUE:=P
&IF %QUE% = CPL &THEN &GOTO TERM
&DATA ED
COMO CONV.COMO.%PREC%%PROG%
CPL (TECOMP)TECHLIB)$SYSLIB)SDH.CPL %PROG% %PREC%
BCHMES
LO
COMO -E
;
T
FILE CONV.%PREC%%PROG%.CPL
&END
&GOTO JOBDIS
&LABEL TERM
&DATA ED
COMO CONV.COMO.%PREC%%PROG%
CPL (TECOMP)RAD)$SYS)SDH.CPL %PROG% %PREC%
BCHMES
COMO -E
;
T
FILE CONV.%PREC%%PROG%.CPL
&END
&LABEL JOBDIS
COMO -TTY
CPL (TECOMP)TECHLIB)$SYSLIB)DISP CONV.%PREC%%PROG%.CPL %QUE%
&IF %QUE% = CPL &THEN DELETE CONV.%PREC%%PROG%.CPL -RPT
```

EDIT FILE

```
/* SDH.CPL - CONVERTS MASTER PROGRAMS TO S, D OR H PRECISION
&ARGS INAM; PREC
&IF %PREC% = S &THEN &GOTO SP
&IF %PREC% = D &THEN &GOTO DP
&IF %PREC% = H &THEN &GOTO HP
&GOTO ER
&LABEL SP
&DATA ED %INAM%
T
C/#1/4/G 9999
T
C/#2//G 9999
T
C/#3/R/G 9999
T
C/#4//G 9999
T
C/#5/R/G 9999
T
C/#6/E/G 9999
T
C/#7/E/G 9999
T
C/#8/S/G 9999
T
C/#9/S/G 9999
T
FIL S%INAM%
&END
&GOTO FIN
&LABEL DP
&DATA ED %INAM%
T
C/#1/8/G 9999
T
C/#2/D/G 9999
T
C/#3/D/G 9999
T
C/#4/D/G 9999
T
C/#5/D/G 9999
T
C/#6/D/G 9999
T
C/#7/D/G 9999
T
C/#8/D/G 9999
T
```

```
C/#9/D/G 9999
T
FIL DZINAMZ
&END
&GOTO FIN
&LABEL HP
&DATA ED ZINAMZ
T
C/#1/8/G 9999
T
C/#2/D/G 9999
T
C/#3/D/G 9999
T
C/#4/H/G 9999
T
C/#5/H/G 9999
T
C/#6/D/G 9999
T
C/#7/H/G 9999
T
C/#8/D/G 9999
T
C/#9/H/G 9999
T
FIL HZINAMZ
&END
&GOTO FIN
&LABEL ER
&LABEL FIN
```

E3 Example Build Program

BHRPH1.CO

```
CPL RPH1BLD.CPL
CP RPH1 H CPL
CPL (TECOMP)TECHLIB)$SYSLIB)PV.CPL HRPH1 CPL AE 6
COPY L_HRPH1 (TECOMP)RAD)$RPHSIM)== -NQ
COPY V_HRPH1.SEG (TECOMP)RAD)$RPHSIM)== -NQ
CO -E
```

RPH1BLD.CPL

```
&DATA ED
;
LOA RAD)$RPHPROG)MRPH1
T
N
D3
PP
B
LOA RAD)$RPHPROG)MROT3
LOA RAD)$RPHPROG)MBANG
/*LOA RAD)$RPHPROG)MDIN
/*LOA RAD)$RPHPROG)MRCF
/*LOA RAD)$RPHPROG)MRHC
/*LOA RAD)$RPHPROG)MRFC
/*LOA RAD)$RPHPROG)MRFSA
/*LOA RAD)$RPHPROG)MRFBA
/*LOA RAD)$RPHPROG)MFVF
LOA RAD)$RPHPROG)MFFCF
/*LOA RAD)$RPHPROG)MFFBA
/*LOA RAD)$RPHPROG)MTFBA
/*LOA RAD)$RPHPROG)MRTQM
/*LOA RAD)$RPHPROG)MRMBA
LOA RAD)$RPHPROG)MFMCF
/*LOA RAD)$RPHPROG)MFMBA
/*LOA RAD)$RPHPROG)MTMBA
/*LOA RAD)$RPHPROG)MNBR
/*LOA RAD)$RPHPROG)MAVEL
/*LOA RAD)$RPHPROG)MRSV
/*LOA RAD)$RPHPROG)MNRV
/*LOA RAD)$RPHPROG)MCSW
LOA RAD)$RPHPROG)MFUSFM
LOA RAD)$RPHPROG)MCON5
/*LOA RAD)$RPHPROG)MLIMIT
LOA RAD)$RPHPROG)MFLDEM
LOA RAD)$RPHPROG)MWIND
FIL RPH1
&END
```

E4 Example Data File Proformas

SIMULATION RUNFILE

ML Aviation Company Limited

RPAV SIMULATION	
FILE	DATE
SIMULATION PROGRAM	
SIMULATION CONTROL FILE	
INITIAL CONDITION FILE	
RPAV PARAMETER FILE	
PRINT FILE	
CONTROL SYSTEM FILE	
FLIGHT DEMAND FILE	
WIND VELOCITIES FILE	

[TS023A]

SIMULATION CONTROL FILE

ML Aviation Company Limited

SIMULATION CONTROL DATA (DINSICN2)			
FILE			DATE
FIELD	UNITS	VALUE	COMMENTS
GENERAL			
ENDTIME	sec		
OUTPUT TYPE	deg=0 rad=1		
PRINT INTERVAL	sec		
SPOOL INTERVAL	sec		
INTEGRATION ADJ	Y/N		
INTEGRATION INTERVAL	sec		
INTEGRATION INTERVAL T_0	sec		

[TS023D]

SIMULATION CONTROL DATA (DINSICN2)			
FILE			DATE
FIELD	UNITS	VALUE	COMMENTS
INTEGRATION INTERVAL MAX	sec		
INTEGRATION INTERVAL MIN	sec		
NO.OF STATE TEST VARIABLES	No.		
MAX ERROR ST1			
MAX ERROR ST2			
MAX ERROR ST3			
MAX ERROR ST4			
MAX ERROR ST5			
MAX ERROR ST6			
MAX ERROR ST7			

SIMULATION CONTROL DATA (DINSICN2)			
FILE			DATE
FIELD	UNITS	VALUE	COMMENTS
MAX ERROR ST8			
MAX ERROR ST9			
MAX ERROR ST10			
MAX ERROR ST11			
MAX ERROR ST12			
MAX ERROR ST13			
MAX ERROR ST14			
MAX ERROR ST15			
DOWNWASH ITERATION TOL			
COMMENTS			

REFERENCES

(1) ARONSON R B RPVs, The End of Manned Military Flight? Machine Design April 20th 1972 44 20-5.

(2) ANON Himat tries its Wings and its Remote Pilot Machine Design September 6th 1979 51 4.

(3) REED R D Flight Research Techniques Utilizing Remotely Piloted Research Vehicles Agard Lecture Series No 108 1980, (8) 1-15.

(4) BLANCHARD R W WOOD R H RPV's as Communitcations Relays Signal October 1973 28 22-4.

(5) EILERSTON W H Navel VATOL RPV in Testing Astronautics and Aeronautics June 1977 15 30-7.

(6) REKENTHALER D A World Surveillance from Space in the 1990's NATO's Sixteen Nations November 1984.

(7) ANON Tables International RPV's and Drones Aviation Weekly and Space Technology March 8th 1982 116 130-132.

(8) FRISCH B RPV's Too Cheap for Its Own Good? Astronautics and Aeronautics April 1978 16 10-11

(9) TOWNSEND J Unmanned Systems for NATO NATO's Sixteen Nations August 1985 Vol 30 No 4.

(10) SEIDEL F Prospects for Advanced Tactical RPV's Remotely Piloted Vehicles International Conference September (Bristol) Proc 3-5 September 1979 Paper 2.

(11) TOMLINS G F MANORE M J Remotely Piloted Aircraft for Small Format Aerial Photography BC Research (Vancouver, British Columbia) Publication 1984.

(12) ANON SUPERVISOR Ministry of Defence Sales Leaflet AD/SCPS 1978.

(13) AUSTIN R G The SPRITE System ML Aviation Co Ltd Bristol Report BR/R/1050 April 1984.

(14) ANON Advanced Subsonic Aeriel Target Flight Refuelling Ltd Wimborne Sales Brochure 1983.

(15) ANON STABILEYE RPV System for Surveillance British Aerospace Sales Leaflet BDS 320 1983.

(16) Israel Aircraft Industries SCOUT Mini RPV System for Real-Time Surveillance Brochure 1985.

(17) DAVIS R A Notes on a visit to Mr F Mauger AP 2 RARDE on Monday 20th February 1984 ML Aviation Co Ltd Report IHD/R10713 February 1984.

(18) YOUNG Dr P (Assistant Director Home Office Scientific Research and Development Branch) Telephone Conversation 14th March 1984.

(19) ANON 'Telecopter' - A Miniature Helicopter with a TV Camera Nachrichtentech Z Germany October 1977 30 (10) 756-7.

(20) ANON Remotely Controlled Model Airplanes Testing Military Ideas Machine Design June 28th 1973 45 12.

(21) BENJAMIN J UMA System Research in the UK International Conference Remotely Piloted Vehicles (Bristol) Proc 3-4 September 1979 Paper 5.

(22) KNACKE T W RPV Developments Plumb the Field's Potential Astronautics and Aeronautics October 1976 14 (37) 37-41.

(23) ANON The Search for Smarter and Scrappier Drones Microwaves October 1973 12 (10) 42-52.

(24) ANON RPV Technology Developments Pressed Aviation Weekly and Space Technology January 31st 1977 106 176-181.

(25) EVANS (Col) R D AQUILA, The Force Multiplier Signal April 1983 37 (8) 21-26.

(26) DAVIS R A Notes on a Visit to RAE Farnborough RN2 Dept on 27th January 1984 ML Aviation Co Ltd Report IHD/R10700 February 1984.

(27) DAVIS R A Visit to British Aerospace Filton on 22nd February 1984 ML Aviation Co Ltd Report IHD/10725 March 1984.

(28) ANON Stabileye RPV Flies Night Vision Payload Aerospace January 1985.

(29) STEPHENSON R C BAC Experience with Small Fixed Wing and Rotary PRV's Royal Aeronautical Society Symposium RPV's Roles and Technology (London) Proc January 1976 Paper 12.

(30) ANON Minimum RPV Unveiled Flight International 4th February 1984.

(31) SYMS P TURNER P S 'ASAT' The UK's First Turbojet RPV Third International Remotely Piloted Vehcile Conference (Bristol) Proc 13-15 September 1982 Paper 12.

(32) DAVIS R A Visit to Mr P Syms Flight Refueling Wimborne ML Aviation Co Ltd Report IHD/R10737 March 1984.

(33) DAVIS R A Visit to Mr M Bennet Marconi Avionics on 30th March 1984 ML Aviation Co Ltd Report IHD/R10769 March 1984.

(34) ANON Surveillance Aircraft Uses μP Ground Control Electronic Design April 1981 1972.

(35) ANON A Different Kind of Engineering Aerospace November/ December 1983 19.

(36) BIRCH S GEC Wins the £80M order for Spy-in-Sky The Engineer 21 February 1985.

(37) DICKEY A Sky Spies - Into Battle by Remote Control The Engineer 3/10 April 1986.

(38) ALLEN D W The Minimum RPV Royal Aircraft Establishment (Farnborough) Technical Memorandum Space 246 March 1977.

(39) ALLEN D BENJAMIN J A Ground Control System for UMA Third International Conference Remotely Piloted Vehicles (Bristol) Proc 13-15 September 1982 Paper 25.

(40) HAWKINS M T PCM Telecommand in the RAE Unmanned Aircraft Programme Royal Aircraft Establishment (Farnborough) Technical Report 82976 July 1982.

(41) PUTTOCK M C A Low Signature RPV Third International Conference Remotely Piloted Vehicles (Bristol) Proc 13-15 September 1982 Paper 8.

(42) ANON Vinten Military Autogyro Systems W Vinton Ltd (Bury St Edmunds) Sales Brochure 1984.

(43) PRESTON A Spy in the Sky for Small Ships Jane's Defence Weekly 3rd March 1984 321-2.

(44) FRASER W M The Autogyro as an RPV Fourth International Conference Remotely Piloted Vehicles (Bristol) Proc 9-11 April 1984 Paper 10.

(45) WANSTALL B Automated Air Support MBB's Family of Drones International Defense Review August 1984.

(46) SEIDEL F AN/USD-502 (CL289) Reconnaissance Drone System Third International Conference Remotely Piloted Vehicles (Bristol) Proc 13-15 September 1982 Paper 9.

(47) TOMLINS G F Some Considerations in the Design of Low Cost Remotely Piloted Aircraft for Civil Remote Sensing Applications The Canadian Surveyor Autumn 1983 37 (3) 157-67.

(48) DAVIS R A Notes on Visit to Dr G F Tomlins British Columbia Research (at London) on Wednesday 18th April 1984 ML Aviation Report IHD/R10800 April 1984.

(49) TOMLINS G F CONDOR: A Canadian RPA for Commercial Applications Fourth International Conference Remotely Piloted Vehicles (Bristol) Proc 9-11 April 1984 Paper 6.

(50) SEEMANN G R The SKYEYE R-4E Surveillance System Third International Conference Remotely Piloted Vehicles (Bristol) Proc 13-15 September 1982 Paper 10.

(51) ANON New RPV Impressive on First Flights Machine Design 1976 48 4.

(52) LOWE D T Mini-RPV Technology Development International Conference Remotely Piloted Vehicles (Bristol) Proc 3-5 September 1979 Paper 6.

(53) RAPAPORT I 'SCOUT' A Real Time Intelligence and Surveillance System Third International Conference Remotely Piloted Vehicles (Bristol) Proc 13-15 September 1982 Paper 13.

(54) WARWICK G 'SCOUT' Israel's Combat Proves RPV Flight International 6th February 1982 307-308.

(55) LUCAS H Marines' RPV Unit Soon Operational Jane's Defence Weekly 8th December 1984.

(56) BULLOCH C Tactical Pilotless Aircraft Do They Really Have a Future? Interavia April 1979 34 335-8.

(57) TAYLOR J W R Janes' Pocket Book 13 RPV's Robot Aircraft Today London McDonald and Jones Publishers Ltd 1977.

(58) SCHWANHAUSSER R R Remotely Piloted Vehicles Advanced Technology International Conference Proc London June 1985.

(59) WHITE A J The AERODYNE: An RPV with Multiple Capabilities The Royal Aeronautical Society Symposium RPVs - Roles and Technology (London) Proc 27th January 1976 Paper 10.

(60) RANSOM H D SKYSPY: A Ducted Fan RPV The Royal Aeronautical Society Symposium RPV's - Roles and Technology (London) Proc 27th January 1986.

(61) KLASS P J Increased Use of Mini-RPVs Foreseen Aviation Week and Space Technology 17 May 1976.

(62) ANON Into Battle by Flying Robot The Engineer 26th June 1986.

(63) GUNSTON W And Now The RPH Flight International April 1975 24 670.

(64) HYNES M K Remote Pilot Vehicles (RPV) Helicopters - Comprehensive Technical Description Performance Specification and Other Technical Data Hynes Aviation Industries Report Oklahoma US 1986.

(65) AUSTIN R G Westland Activities in Remotely Piloted Helicopters Royal Aeronautical Society Paper Presented 23rd November 1977.

(66) GRIFFIN D A Novel Rail Launcher for RPAV's Fourth International Conference Remotely Piloted Vehicles (Bristol) Proc 9-11 April 1984 Paper 20.

(67) VEAZEY G R Launch and Recovery for Airborne RPV's Fourth International Conference Remotely Piloted Vehicles (Bristol) Proc 9-11 April 1984 Paper 21.

(68) AUSTIN R G The Remotely Piloted Helocpter for Battlefield Surveillance and Other Tasks Westland Helicopters Yeovil Publication 1978.

(69) FAULKNER A J SIMONS I A The Remotely Piloted Helicopter Vertica 1977 1 231-8.

(70) BREWARD M J Westland Wisp Agard Conf Proc N233 Rotorcraft Design 16-19 May 1977 23/1-23/14.

(71) FORD T E The Remotely Piloted Helicopter Aircraft Engineering September 1977 49(9) 10-11.

(72) DAVIS R A Visit to Mr P Thickett Westland Helicopters Ltd Yeovil on 2nd March 1984 ML Aviation Co Ltd Report IHD/R10736 March 1984.

(73) CLARK A S Canadair Rotary Wing RPV Technology Development Part II Third International Conference Remotely Piloted Vehicles (Bristol) Proc 13-15 September 1982 Paper 11.

(74) AUSTIN R G ALLDRIDGE W J Now is the Time for RPH's Fourth International Conference Remotely Piloted Vehicles (Bristol) Proc 9-11 April 1984 Paper 11.

(75) DAVIS R A Visit to APRE Farnborough on 3rd April 1984 ML Aviation Co Ltd Report IHD/R10772 April 1984.

(76) HENDERSON C Sea Based Remotely Piloted Vehicles Issues and Concepts Part 1 Military Electronics/Countermeasures April 1982 61-4.

(77) HENDERSON C Sea Based Remotely Piloted Vehicles Issues and Concepts Part 2 Military Electronics/Countermeasures May 1982 45-47.

(78) FARRAR HOCKLEY A H Maj Gen A Prospect for RPVs on the Battlefield The Royal Aeronautical Society Symposium RPV's Roles and Technology (London) Proc 27th January 1976 Paper 1.

(79) CLITHEROW K Comdr RPVs in the Maritime Environment The Royal Aeronautical Society Symposium on RPV's - Roles and Technology (London) Proc 27th January 1976 Paper 3.

(80) MITCHELL J Wing Cd Remotely Piloted Vehicles, An Air Force View The Royal Aeronautical Society Symposium on RPV's - Roles and Technology (London) Proc 27th January 1976 Paper 2.

(81) HELBREN N J Use of a Simulator in the Development of an RPV System International Conference Remotely Piloted Vehicles (Bristol) Proc 3-5 September 1979 Paper 4.

(82) WADDY J L A Philosophy for the Tactical use of RPHs on the Battlefield International Conference Remotely Piloted Vehicles (Bristol) Proc 3-5 September 1979 Paper 3.

(83) MAUGER F E RPV Operational Effectiveness Assessment Methods Third Internation Conference Remotely Piloted Vehicles (Bristol) Proc 13-15 September 1982 Paper 3.

(84) PARKINGTON L V A Study into the Operability of RPV's in Bad Weather Fourth International Conference Remotely Piloted Vehicles (Bristol) Proc 9-11 April 1984 Paper 1.

(85) PARKINGTON L V Remotely Piloted Vehicles: A comparison of the Merits of Expendable and Recoverable Air Vehicles Third International Conference Remotely Piloted Vehicles (Bristol) Proc 13-15 September 1982 Paper 5.

(86) ADAMS J Race on to Build Robot Spotter Plane for Army Sunday Times 3rd June 1984 7.

(87) DAVIS R A Visit to Lt Col Toomey Infantry Trials and Development Unit Warminster on 24th February 1984 ML Aviation Co Ltd Report IHD/R10735 March 1984.

(88) DAVIS R A Control Systems for Remotely Piloted Air Vehicles - Basis for Introductory Section ML Aviation Co Ltd Report IHD/R10622 December 1983.

(89) ANON Low Cost Inertial Navigation System Passes Test Electronics 3rd October 1974 37 43.

(90) BARGERY A W ROSENBERG K W Flight Control System for Aerial Targets Second International Conference Remotely Piloted Vehicles (Bristol) Proc 6-8 April 1981.

(91) GATES R L Reviewing the Status of Inertial Sensors Control Engineering March 1971 18 54.

(92) TECHNICAL INDEXES LIMITED Electronic Engineering Index January-June 1984 Issue 33.

(93) BENDIX CORPORATION (US) True Airspeed Indicator of the Ionisation Type US PATENT 670647 11th February 1949.

(94) BEATTIE J A C A True Air Speed Sensor for Miniature Unmanned Aircraft Aeronautical Journal May 1983 87 (865) 173-5.

(95) DRAPER C S Origins of Inertial Navigation J Guidance and Control September/October 1981 4 (5) 449-63.

(96) FOGGIE Sqn Ldr P R Advances in Inertial Navigation Electronics and Power August 1978 24 582-4.

(97) COLLINSON R P G Strapped Down Navigation Flight International 6th February 1975 (107) 205-206.

(98) GARG S C MORROW L D MAMEM R Strapdown Navigation Technology: A Literature Survey J Guidance and Control May/June 1978 1 (3) 161-172.

(99) ANON Navigation System Choices Flight International 13th March 1975 401-2.

(100) MILLER B Light Compact Navigator Designed Aviation Weekly and Space Technology 9th February 1970 92 (1) 51.

(101) GILMORE J P Modular Strapdown Guidance Unit with Embedded Microprocessor J Guidance and Control January/February 1980 3 (1) 3-10.

(102) WOOLEY M Development, Flight Test and Application of RPV Control Law Concepts for Microprocessor Based Computers International Conference Remotely Piloted Vehicles (Bristol) Proc 3-5 September 1979 Paper 14.

(103) ANON Low Cost Servoed Rate Gyroscope 900 Series Smith Industries Sales Brochure SIA 502V 1983.

(104) ALLEN D W CLARKSON P H A Manoeuvre Demand Autopilot for Small Unmanned Aircraft Farnborough Royal Aircraft Establishment Technical Memorandum Space 301 March 1982.

(105) ALLEN D W An Analogue Autopilot for Small Unmanned Aircraft Farnborough Royal Aircraft Establishment Technical Memorandum Space 302 April 1982.

(106) ALLEN D W The Flight Testing of a Computer Controlled Position Fixing System for Small Unmanned Aircraft Royal Aircraft Establishment (Farnborough) Technical Memorandum Space 315 January 1983.

(107) PARTRIDGE A Flight Path Control of Unmanned Aircraft Using a Small Desktop Computer Royal Aircraft Establishment (Farnborough) Technical Memorandum Space 325 November 1983.

(108) DAVIS R A Notes on a Visit to Mr J Mortimer Marconi Avionics Rochester 12th April 1984 ML Aviation Co Ltd Report IHD/R10799 April 1984.

(109) MANT I Flight Control and Navigation System for Small RPV's Third International Conference Remotely Piloted Vehicles (Bristol) Proc 13-15 September 1982 Paper 26.

(110) ANON Strapdown Attitude and Heading Reference System Smiths Industries Sales Brochure SIA 458V 1983.

(111) KOGER O D TIETZ D E LAMONT G B Microprocessor Based Digital Autopilot Development for the XBQM-106 Mini PRV IEEE Nat Aero and Elec Con NAGCON 79 Proc 1979 157-67.

(112) BRAMWELL A R S Helicopter Dynamics Edward Arnold London 1976.

(113) STRANG W J Review of Helicopter Airworthiness Civil Aviation Authority Report CAP 491 June 1984.

(114) DRAKE J A Radio Control Helicopter Models Model and Allied Publications Argus Books Watford 1977.

(115) FINCHER S J The Control of Remotely Piloted Helicopters IEE Computing and Control Div Colloquium on Control and Operation of Remotely Piloted Vehicles 23-10-80 Proc 1980 Paper 1.

(116) FORD J PAGE S J The Design of a Simulator to Study the Human Factors of the Control of RPVs IEE Computing and Control Div Coloquium on Control and Operation of Remote Piloted Vehicles 23-10-80 Proc 1980 Paper 2.

(117) ANON Test Results of the ML Aviation 3-Axis Accelerometer STC Harlow Technical Report 1983.

(118) DAVIS R A Visit to Mr R Bowker RN2 Farnborough on Wednesday 15th February 1984 ML Aviation Co Ltd Report IHD/R10714 February 1984.

(119) DAVIS R A Notes on discussions with SPRITE Project Manager (R G Austin) with regard to modelling requirements of the SPRITE Project 17th April 1984 ML Aviation Co Ltd Report April 1984.

(120) PEARSON D P Performance, Stability and Control Analysis of SPRITE Air Vehicle ML Aviation Co Ltd Report Bristol September 1982.

(121) ALLDRIDGE W J Design Parameters Required to Ensure Stability in the SPRITE Cyclic Pitch and Roll Control Loops ML Aviation Report FSN 58 October 1984.

(122) ALLDRIDGE W J Update of the Model of the Height Control Loop for SPRITE ML Aviation Report FSN 82 January 1986.

(123) COCHRAN A J Vocational PhDs: Aston's IHD Scheme Aston University Press 1981.

(124) GREEN H S Letter of Agreement to B RASHID IHD University of Aston 13th July 1983.

(125) YOURDON E CONSTANTINE L L Structured Design Fundamentals of a Discipline of Computer Program and Systems Design Yourdon Press New York 1978.

(126) de MARCO T Concise Notes of Software Engineering Yourdon Press New York 1979.

(127) ELECTRONIC ENGINEERING ASSOCIATION Guide to the Quality Assurance of Software EEP London January 1978.

(128) BRITISH STANDARDS INSTITUTION Recommendation for the Documentation of Computer Based Systems London DD 26th February 1973.

(129) NAMAS EXECUTIVE NATLAS Software Unit Test Standard and Method National Physical Laboratory London 1985.

(130) ML AVIATION (FOSKETT A G) Technical Computer Software Company Quality Procedure 2409 Issue 5 May 1986.

(131) PARNAS D A Technique for Software Module Specification with Examples Communications of the ACM May 1972 Vol 15 Part 5 pp 330-3.

(132) TOMLINSON B N SESAME A System of Equations for the Simulation of Aircraft in a Modular Environment Royal Aircraft Establishment Technical Report 79008 January 1979.

(133) HOWE R M Coordinate Systems for Solving Three Dimensional Flight Equations WADC Technical Note 55-747 June 1956.

(134) FOGARTY L E HOWE R M Computer Mechanization of Six-degree of Freedom Flight Equations NASA Report CR-1344 May 1969.

(135) WALTERS D Flight Envelope Discussion Private Communication June 1985.

(136) McFARLAND A Standard Kinematic Model for Flight Simulation at NASA-AMES NASA Report CR-2497 January 1975.

(137) WHITTAKER E T A Treatise on the Analytical Dynamics of Particles and Rigid Bodies 4th Ed Dover New York 1944.

(138) ENGINEERING SCIENCE DATA UNIT The Equations of Motion of a Rigid Aircraft Dynamics 1 ESDU Data Item 67003 ESDU London 1966.

(139) McRUER D ASHKENAS I GRAHAM D Aircraft Dynamics and Automatic Control Princeton Press, New Jersey US 1973.

(140) MORTENSON R E Strapdown Guidance Error Analysis IEEE Transactions of Aerospace and Electronic Systems Vol Aes 10 No 4 July 1984.

(141) RUTHERFORD D E Vector Methods Oliver Boyd University Mathematic Texts Edinburgh 1944.

(142) ROBERTS C J The Efficient Computation of Trigonometric Functions in Double Precision Arithmetic Using Thiele Approximations ML Aviation Co Ltd Report No: R11112 June 1985.

(143) CLENSHAW C W Mathmatical Tables Chebyshev Series for Mathematical Functions Department of Scientific and Industrial Research Volume 5 HMSO 1962.

(144) GLAUERT H A General Theory of the Autogyro Aeronautical Research Committee, Reports and Memoranda No 1111 (Ae 285) November 1926.

(145) COLEMAN R P FEINGOLD A M STEMPIN C W Evaluation of the Induced Velocity Field of an Idealised Rotor National Advisory Committee for Aeronautics Wartime Report ARR L5E10 Langley Memorial Aeronautical Laboratory Washington June 1945.

(146) GESSOW A MYERS G C Aerodynamics of the Helicopter Frederick Ungor New York 1952.

(147) SHAPIRO J Principles of Helicopter Engineering Temple Press Ltd London 1955.

(148) BELLINGER E D Analytical Investigations of the Effects of Blade Flexibility, Unsteady Aerodynamics and Variable Inflow on Helicopter Rotor Stall Characteristics Journal of the American Helicopter Society July 1972 pp 35-44.

(149) WILCOCK T THORPE A C Flight Simulation of a Wessex Helicopter A Validation Exercise Royal Aircraft Establishment Technical Report 73096 May 1973.

(150) WILCOCK T A Piloted Flight Simulation of the Westland Lynx Royal Aircraft Establishment Technical Report 74099 July 1974.

(151) PADFIELD G D A Theoretical Model of Helicopter Flight Mechanics for Application to Piloted Simulation Royal Aircraft Establishment Technical Report 81048 April 1981.

(152) FORD J WIDEYE RPH Model Cranfield Institute of Technology Private Correspondence December 1985.

(153) CHEESEMAN I C A Method of Calculating the Effect of One Helicopter Rotor Upon Another Aeroplane and Armament Experimental Establishment Report No AAEE/Res/298 CP No 406 April 1958.

(154) HARRINGTON R D Full-Scale Tunnel Investigation of the Static-Thrust Performance of a Co-Axial Rotor NACA Report TN 2318 1951.

(155) ANDREW M J Co-Axial Rotor Aerodynamic in Hover Vertica Pergamon Press Ltd UK vol 5 pp 163-172 1981.

(156) AZUMA A SAITO S KAWACHI K KARASUDANI T Application of the Local Momentum Theory to the Aerodynamics Characteristics of Multi-rotor Systems Vertica Pergamon Press Ltd UK Vol 3 pp 131-144 1979.

(157) SAITO S AZUMA A A Numerical Approach to Co-Axial Rotor Aerodynamics Vertica Pergamon Press UK Vol 6 pp 253-266 1982.

(158) NAGASHIMA T NAKANISHI K Optimum Performance and Wake Geometry of a Co-Axial Rotor in Hover Vertica Pergamon Press UK Vol 7 No 3 pp 225-239 1983.

(159) TALBOT P D CORLISS L D A Mathematical Force and Moment Model of a UHIM Helicopter for Flight Dynamics Simulations NASA Report TM-73 254 June 1977.

(160) PRICE H L Rotor Dynamics and Helicopter Stability Aircraft Engineering pp 168-172 June 1963.

(161) BISPLINGHOFF R L ASHLEY H HALFMAN R L Aeroelasticity Addison-Wesley Publishing Corp Inc 1955.

(162) LANCZOS C Applied Analysis Sir Isaac Pitman & Sons Ltd 1957.

(163) PITT D M PETERS D A Theoretical Prediction of Dynamic-Inflow Derivatives Proc 6th European Rotorcraft and Powered Light Aircraft Forum Paper 47 Univ Bristol September 1980.

(164) HEYSON H H A Momentum Analysis of Helicopters and Autogyros in Inclined Descent, with Comments on Operational Restrictions NASA Report TN D-7917 1975.

(165) YOUNG C A Note on the Velocity Induced by a Helicopter Rotor in the Vortex Ring State Royal Aircraft Establishment Technical Report 78125 1978.

(166) HOHENEMSER K H YIN S K Some Applications of the Method of Multiblade Coordinates Journal of the American Helicopter Society July 1972 pp 3-12.

(167) BUNNISS P ML Aviation Private Communication 27th August 1986.

(168) ENGINEERING AND SCIENCE DATA UNIT Aerodynamic Characteristics of Aerofoils in Compressible Inviscid Airflow at Sub Critical Mach Numbers EDSU Data Item 72024 ESDU London October 1976.

(169) PAGLINO V M Forward Flight Performance of a Co-Axial Rigid Rotor 27th Annual Forum of the American Helicopter Society 1971.

(170) AZUMA A KAWACHI K Local Momentum Theory and its Application to the Rotary Wing J Aircraft 16 1979.

(171) PRICE J Preliminary Spin Rig Tests ML Aviation Report October 1984.

(172) PRICE J Preliminary Endurance Test Air Vehicle Data ML Aviation Report August 1986.

(173) AZUMA A Institute of Interdisciplinary Research Faculty of Engineering The University of Tokyo Private Correspondence April 10 1986.

(174) VINER P J Intermediate 'Spin Rig' Data Private Communication ML Aviation Co Ltd August 1986.

(175) WALSHAW A C JOBSON D A Mechanics of Fluids Longman London 2nd Ed 1972.

(176) PEARSON D M Wind Tunnel Tests on Potential SPRITE Airframe Shapes ML Aviation Co Ltd Report Bristol FSN 9 October 1981.

(177) POSTLETHWAITE A WARNER D L An Investigation into the Aerodynamic Characteristics of Axisymmetric Bluff Bodies of Ellipsoidal Shape with Protruberances Bristol University Dept Aeronautical Engineering Report No 209 January 1977.

(178) ENGINEERING SCIENCE DATA UNIT Mean Fluid Forces and Moments on Cylindrical Structures in Polygon Sections with Rounded Corners Including Elliptical Shapes ESDU Data Item 79026 March 1980.

(179) ENGINEERING SCIENCE DATA UNIT Pressure drag of blunt forebodies at zero incidence for Mach numbers up to 10 EDSU Data Item 80021 September 1980.

(180) JUNG W G IC Op Amp Cookbook Howard W Sams Co Inc Indianapolis 6th Ed 1979.

(181) SGS - ATES Technical Note 150 40 Industrial Application Ideas Planer House Walton Street Aylesbury Bucks 1980.

(182) SGS - ATES L292 DATA SHEET Planer House Walton Street Aylesbury Bucks 1980.

(183) DAVIS R A Notes of Visit to John Alldridge (MLA Bristol) 26.4.84 ML Aviation Co Ltd Report April 1984.

(184) OGATA K Modern Control Theory Prentice Hall Instrumentation and Control Series 1970.

(185) PRICE J Preliminary Actuator Blade Test Results ML Aviation Test Notes June 1984.

(186) ENGINEERING SCIENCE DATA UNIT The Response of First and Second Order Systems Dymanics 1 EDSU Data Item 69005 ESDO London January 1969.

(187) NODEN D PRIME Libraries and Systems ML Aviation Document June 1984.

(188) GERE J M WEAVER W W Matrix Algebra for Engineers van Nostrand Reinherd Co 1965.

(189) CHEN R T N TALBOT P D An exploratory investigation of the effects of large variations in rotor system dynamics design parameters on helicopter handling characteristics in nap-of-the-earth flight Proc 33rd Annual National Forum of the AHS May 1977.

(190) HOHENEMSER K H YIN S K On the use of first order rotor dynamics in multi-blade coordinates Proc 30th Annual National Forum of the AHS May 1974.

(191) AMER K B Theory of Helicopter damping in pitch or roll and a comparison with flight measurement NACA Report TN2136 (1950).

(192) SHAUGHNESSY J D DEAUX T N YENRI K Development and Validation of a piloted simulation of a helicopter and external sling loads NASA Tech Paper 1285 1979.